EUROPEAN ORGANIZATION FOR NUCLEAR RESEARCH
CERN –ACCELERATORS AND TECHNOLOGY SECTOR

CERN-ATS-2013-045

PROCEEDINGS OF THE 2012 EVIAN WORKSHOP ON LHC BEAM OPERATION

Evian, 17th to 20th December 2012

Edited by
B. Goddard, S. Dubourg

Geneva, Switzerland
December, 2012

LHC Beam Operation Workshop

Evian 17-20 December 2012

The aims of the 2012 workshop were to:

• review and capture 2012 LHC beam operations experience;
• review system performance;
• examine the foreseen challenges and limitations of LHC Run 2 operation (post LS1);
• examine possible running scenarios for LHC Run 2.

There were five sessions covering:

• operational availability;
• the operational cycle;
• system performance and outlook;
• performance limitations and outlook;
• scenarios for 2014/2015.

Chairman	Mike LAMONT
Scientific Secretary	Malika MEDDAHI
Editors of the Proceedings	Brennan GODDARD
	Sylvia DUBOURG
Informatics & infrastructure support	Pierre CHARRUE
Workshop Secretary	Sylvia DUBOURG

The write-ups for the December 2012 Evian proceedings were based on the JaCoW templates, for which the JaCoW team is gratefully acknowledged.

The individual authors are both thanked and congratulated for their high quality contributions, written during a very busy period.

Table of contents

Session 4: Second Part: Performance limitations: 2012 review and 2014 outlook (6.5 TeV, 25ns, higher total I...)

Chairmen: Gianluigi Arduini, Rudiger Schmidt, Scientific Secretaries: Chiara Bracco, Ghislain Roy

Special Session

Session 5: Scenario for 2014 - 2015

Chairman: Mike Lamont, Scientific Secretary: Malika Meddahi

†no written contribution

LHC AVAILABILITY AND PERFORMANCE IN 2012

A.L. Macpherson, CERN, Geneva, Switzerland

Abstract

The LHC performance and overall machine availability for the 2012 proton-proton run are discussed, as well as the factors that contributed to another excellent LHC run

INTRODUCTION

Following on from an excellent year in 2011 in which ~5.5 fb^{-1} of proton-proton collisions at 3.5 TeV were delivered to both ATLAS and CMS, the 2012 run was intended to further extend performance reach. For the 2012 proton-proton run, beam energy was raised to 4 TeV, the beta* squeeze was set to 60 cm, and the target average bunch intensity set at $1.6x10^{11}$ protons. Also, to ensure expedient luminosity delivery it was decided to continue with 50ns bunch spacing, and push back the 25ns scrubbing program to late in the 2012 run.

With this configuration, a target delivered proton-proton luminosity (based on the 2011 luminosity production) was set at 15 fb^{-1}. This was seen as an ambitious goal, given that initially a proton-Lead run, four machine development periods, and four technical stops were also scheduled for 2012. Due to the strong request by the experiments for luminosity delivery, a machine schedule was revised was put in place which allocated the entire 2012 run to proton-proton physics, and moved the proton-Lead run to early 2013. The revised 2012 schedule is as shown in Figure 1. With this schedule the revised target for delivered luminosity was set at 22 fb^{-1} for both ATLAS and CMS.

In actuality the 2012 LHC run exceeded expectations, with a final delivered luminosity of over 23 fb^{-1} for both ATLAS and CMS, and the mid-year announcement of the discovery of a Higgs-like particle based on the combined 2010-2012 data sets [1]. Indeed, this excellent result, along with a proton-Lead pilot run, a high-beta physics program [2], a 25ns scrubbing run [3] and pilot 25ns physics fill, and a vigorous machine development program [4], meant that 2012 exceeded all expectations in terms of machine performance.

The LHC Run for 2012 can be summarised as follows:

- Hardware Commissioning: 35 days
- Beam commissioning: 21 days
- Machine Operation: 257 days
- Physics Operation: 228 days
- p-p Luminosity Production running: 201 days

Within the run, the following were also included:

- 3 Technical stops
- 4 Machine development periods
- 2 Floating Machine development periods
- A 25ns scrubbing run

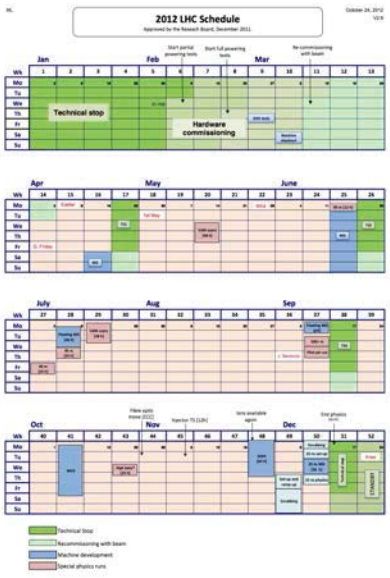

Figure 1: The final LHC machine schedule for 2012.

In terms of fill numbers, the 2012 proton-proton physics run extended from fill 2465 to fill 3457.

LHC AVAILABILITY

After short periods of hardware commissioning and beam commissioning, physics operation started on the 4th of May and continued through till the 17th of December. LHC machine availability for the 2012 proton-proton run is defined by the run period after commissioning, but excluding technical stop and machine development periods, and is shown in Figure 2. Over 36% of the run was spent in physics (stable beams) operation for a total of 73.2 days of ~1757 hours of physics, compared to 32% in 2011.

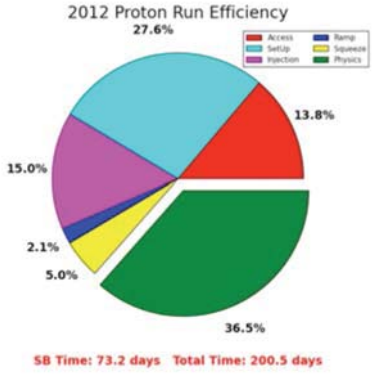

Figure 2: LHC machine availability for 2012.

If we compare the availability figures to those of the luminosity production running in 2011 [5], the difference in percentages for the 6 machine phases can be extracted, and is shown in Figure 3.

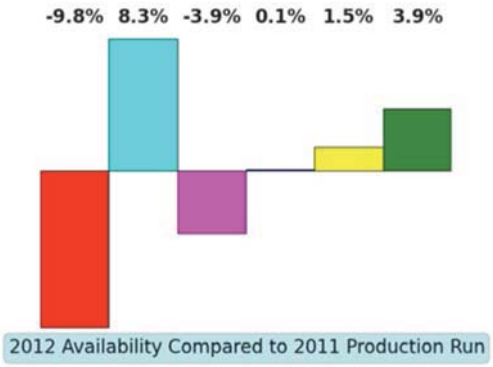

Figure 3: Comparison of 2012 LHC machine availability to that of 2011. What is shown is the difference between the 2012 and 2011 percentages for each of the 6 machine phases defined in Figure 2.

Figure 3 shows less of the available run time was spent in access in 2012 than 2011, but that this was almost completely countered by the relative increase in the beam setup phase (machine closed but no beam injected). In terms of improvements, Figure 3 shows a decrease in the percentage of time spent in injection, and an increase in the stable beams percentage. This tends to suggest that in 2012, we improved the injection procedure, and this improvement translated into more available stable beams time. It should also be noted that in 2012, the beta* squeeze was split into a two step procedure in order for LHCb to transition from a horizontal crossing angle at injection to a vertical one at physics settings (in order to improve operational conditions under polarity flips of their external crossing angle coming from the LHCb dipole).

To quantify the availability improvements it is worth comparing the 2012 Hubner factor with that of 2011. The Hubner factor is the ratio of actual delivered luminosity to the amount you could collect by running continuously at the peak luminosity, and the expected value was H=0.2, (as achieved at LEP). The Hubner factor in 2012 is H_{2012} = 0.175 which assumes a physics duration of 200.5 days, a peak luminosity of 7695 $(\mu b.s)^{-1}$ and a delivered luminosity of 23.269 fb^{-1}. The equivalent 2011 value is H_{2011} = 0.156, and so implies a clear indication of improvement of machine performance and physics availability.

LHC PERFORMANCE - LUMINOSITY

For the proton-proton 2012 run, the default filling scheme was with 1374 bunches per beam and 50ns spacing between bunches, which gave 1368 colliding bunches in ATLAS and CMS, 1262 in LHCb, and no colliding bunches in ALICE. Due to detector constraints, ALICE data taking was done with collisions generated by main bunch-satellite bunch collisions, which gave a reduced rate compatible with the ALICE detector.

With the schedule and availability as outlined above, the machine was able to deliver luminosities of 23.27 fb^{-1} for both ATLAS and CMS (see Figure 4) and over 2.1 fb^{-1} to LHCb.

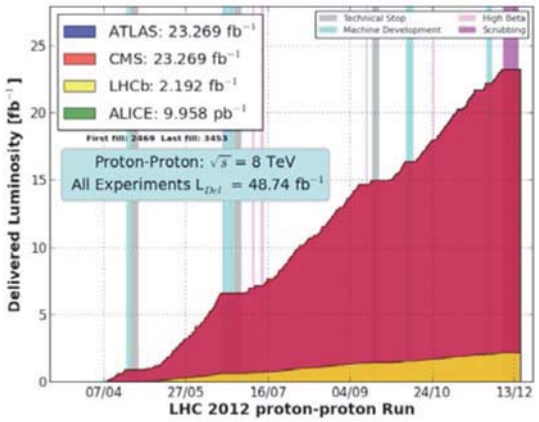

Figure 4: Delivered luminosities for the 2012 LHC proton-proton run. ATLAS and CMS delivered luminosities are almost identical, hence almost indistinguishable, while ALICE delivered luminosity is not visible due to the absolute scale.

In terms of delivered luminosity, the performance of the machine is best put in context when the target estimates are considered. Figure 5 shows both the target luminosity delivery for the run, and the actual luminosity delivery for CMS, and it can be seen that without the run extension, the machine was on target to reach the 16 fb^{-1} expected. With the run extension, the machine exceeded expectations and delivered ~1 fb^{-1} above target by the end of the run.

Such impressive performance was based not only on machine availability, but also on careful attention to the optimisation of operational parameters. This optimisation was done throughout the year, and a summary plot of the machine tuning over the year is given in Figure 6.

The target average bunch intensity at injection was set at 1.6×10^{11} protons per bunch, and Figure 6 shows that this translated into an achieved bunch charge of $\sim 1.5 \times 10^{11}$ protons at declaration of stable beams, and that only a moderate increase over the year was possible. Similarly, transverse emittance stayed relatively constant over the year despite the mid-year move from the Q26 to Q20 SPS optics[6] and other optics corrections to the injectors, which significantly reduced the transverse emittance at injection. However these improvements in injector optics can be seen in Figure 6 in terms of increased peak luminosity and transverse beam brightness, but also in the growth of the longitudinal bunch length, indicating that in terms of bunch charge, the machine was running close to its limit.

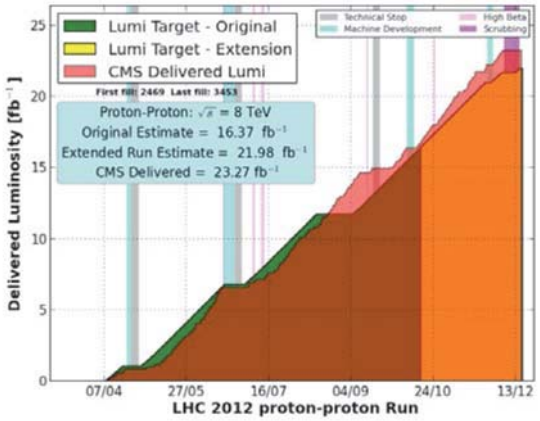

Figure 5: Comparison of target and delivered luminosities for the 2012 LHC proton-proton run. By the completion of the original run period (green) the actual and the target CMS delivered luminosities are almost identical. During the extended run period (yellow) delivered luminosity exceeds expectations.

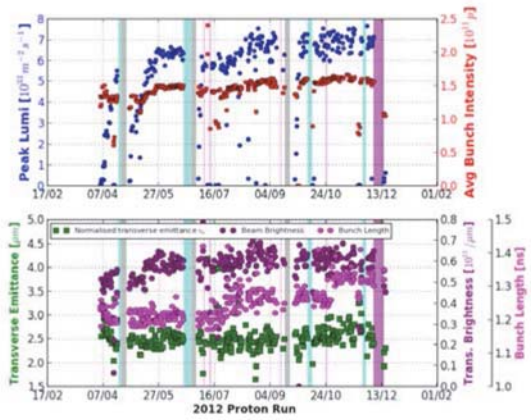

Figure 6: Beam parameter evolution during the 2012 LHC proton-proton run.

The mid-year improvement in injected beam quality, combined with enhanced satellite production in the PS enabled a significant reduction in bad background conditions in ALICE, and an increase in the rate of main bunch - satellite collisions. This had a dramatic effect on the both the ALICE data taking efficiency and their delivered luminosity, as shown in Figure 7.

For LHCb, extensive use of luminosity levelling by separation was made to ensure data taking with controlled trigger rates. Data taking efficiency was further enhanced by the two-step squeeze process that rotated the crossing angle so that it was orthogonal to the external crossing angle from the LHCb dipole. This change had the advantage that the machine operation was more transparent to the regular LHCb dipole polarity flips, and so helped improve machine turnaround. Figure 8 shows the LHCb delivered luminosity and the dipole polarity flips performed during the year. The final ratio of luminosity taken with positive and negative LHCb dipole polarities is 49.2%:50.8%, and so meets the LHCb requirements of balanced data sets, needed to reduce systematic errors in their physics analyses.

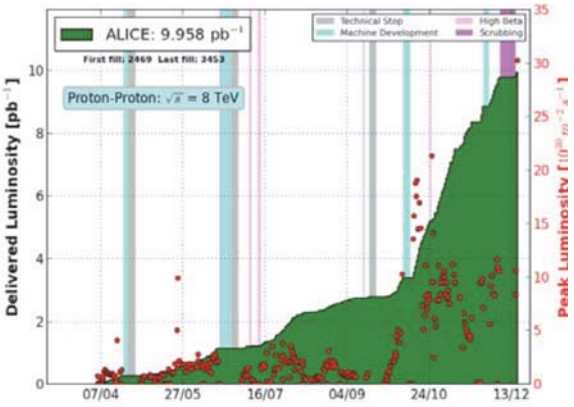

Figure 7: Delivered and peak luminosities for ALICE over the course of the 2012 proton-proton run. A clear improvement is seen after technical stop number 3, due to improvements in the beam quality from the injectors, and enhancement of the satellite population in the PS.

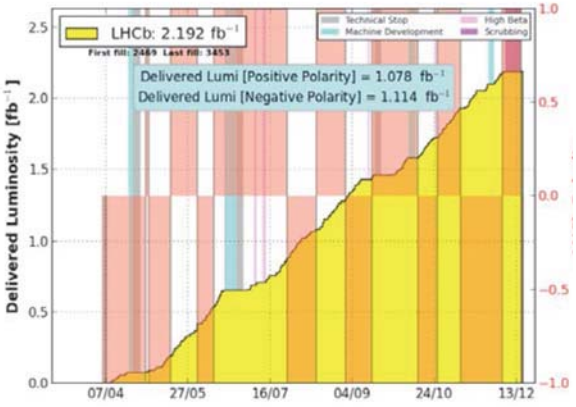

Figure 8: LHCb delivered luminosity and LHCb dipole polarity for the 2012 proton-proton run.

Finally, in terms of luminosity delivery, the weekly performance is given in Figure 9, and it shows that during the course of the year, the recovery from technical stops improved, although the statistical significance of this improvement may not be strong.

LHC PERFORMANCE - DOWNTIME AND SYSTEM FAULTS

Delivered Luminosity is not the only measure of machine performance; machine downtime and fault statistics are also key indicators that show not only performance but also the possible onset of operational issues and equipment failure modes. To examine these availability factors, both postmortem data from all beam dumps above 450 GeV and operations fault tracking data

from the e-logbook and the Technical Infrastructure Major Event tracking has been used to extract performance estimates. Unfortunately this data does not form a complete set, and it has already been identified that the fault recording and tracking mechanisms need to be revised before the LHC restart in 2015 [7].

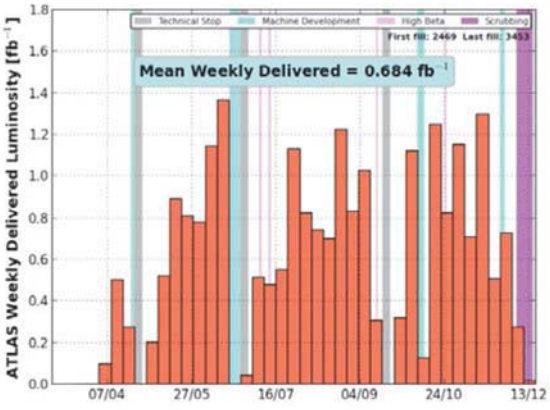

Figure 9: Weekly delivered luminosities during the 2012 LHC proton-proton run.

As a first estimate, independent of fault type, the time to recover from a beam dump until the start of ramp can be considered, and is shown here in Figure 10. Two setup time distributions are shown; the raw distribution as extracted from machine operation, and the fault corrected setup time, which for any given fill, is this setup time minus any declared fault time. This choice of setup time definition was chosen as an indicator, as it allows inclusion of both for recovery from faults in the previous fill, and the inclusion of unrelated delays from injection.

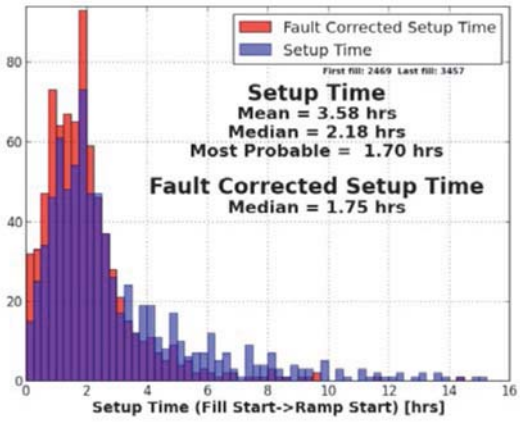

Figure 10: Machine setup time (including a 45 minute ramp down sequence). The fault corrected setup time is based on the faults logged in the LHC logbook. evolution during the 2012 LHC proton-proton run.

While the most probable setup time remains the same for both distributions, for the fault corrected setup time there is a reduction in the median setup time and a clear reduction of the tail of the distribution. Both distributions appear to follow a log-normal shape; log-normal distributions can be thought of as the multiplicative product of many independent random variables each of which is positive. The median fault corrected setup time is 105 minutes, which includes the ramp down procedure which has a minimum duration of 45 minutes. This discrepancy between actual average setup time and minimum ramp down duration, suggest that either the machine setup procedure is well away from being in the shadow of the ramp down, or that not all faults and delays have been fully accounted for.

To understand better the time delays associated with machine setup and overall turnaround, it is instructive to look at the recorded system faults, both in terms of occurrence and fault resolution time. From the data available in the e-logbook, the system faults histogram of Figure 11 can be produced. In this figure a fault is defined as any incident, hardware fault, or software failure which prevented normal operation.

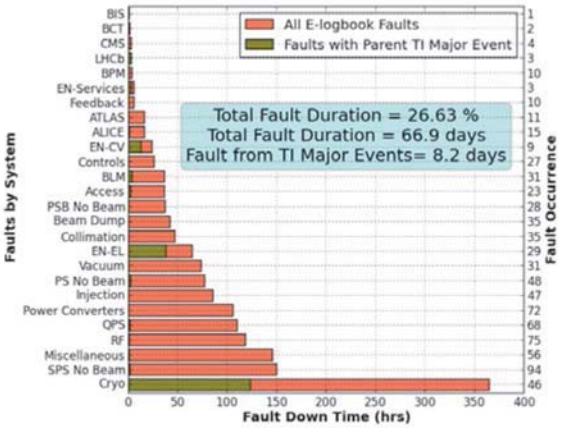

Figure 11: Breakdown of total fault time by system during the 2012 LHC proton-proton run.

From Figure 11, cryogenics is the clear leader in downtime, with a global down time of ~15 days. By comparison, detailed cryogenics availability data gives the total cryogenics availability (technical stops excluded) as 13.6 days (see Figure 12).

As noted, in terms of downtime, cryogenics dominates, but this is to be expected due to the reset procedure of the cold compressors and the thermal inertia the cryogenics system. However it is worth noting that in Figure 11, it can be seen that ~1/3 of the down time was associated to external events (as recorded in TI Major events) that triggered trips of the cryogenic sectors. A typical example of such and external event is an electrical network perturbation. Further, it is extremely encouraging to note cryogenics availability rose from 87.1% in 2011 to 94.4% in 2012. This reflects the consolidation within cryogenics, and the mitigation of communication faults which perturbed cryogenics in 2011.

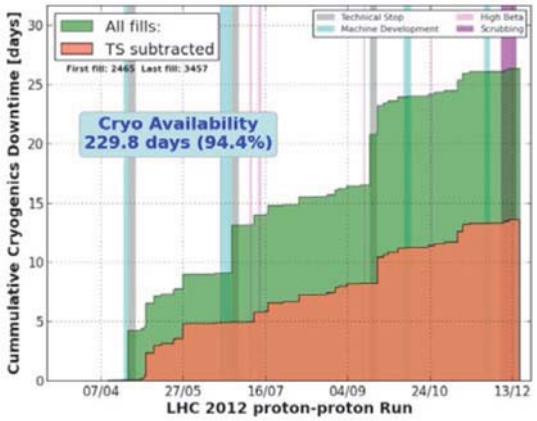

Figure 12: Cryogenics downtime during the 2012 LHC proton-proton run. The integrated downtime excluding the Technical stop periods is shown in red.

For machine performance in terms of system faults, it is also instructive to look at the beam dump statistics of fills above injection energy. Data for such statistics is taken from the LHC postmortem data base, and a breakdown by beam dump cause is given in Figure 13. As in 2011, the QPS is the most proficient, and was also the leader in terms of beam dumps triggered by radiation induced single event upsets (SEUs). This is as to be expected, as the planned QPS upgrade is not foreseen to be completed until after the 2013-2014 long shutdown. However, what is encouraging is that both the total number of cryogenics induced beam dumps and the number SEU triggered cryogenics induced beam dumps significantly decreased in 2012, and is attributed to the aforementioned consolidations and mitigations.

For an overall comparison the percentage of SEU induced beam dumps dropped from 17.5% in 2011 to 9.5% in 2012, and implies a significant improvement in performance and a validation of the R2E consolidation activities [8].

In terms of recovery time after the beam dump, Figure 14 gives the breakdown by system of the cumulative sum of recovery times from beam dump back to injection. While this distribution may be susceptible to error due to individual fills with multiple systems failing, the distribution shows, like in 2011, that the QPS system, due to both the high occurrence of faults, and the cost in terms of system recovery (LHC access or full power reset of circuits that then require precyling), is the leading system in terms of cumulative post beam dump recovery time. Indeed the top five systems are the same in 2011 and 2012, and apart from cryogenics, the other four usually involve LHC access to address the fault that triggered the beam dump. Naturally, this incurs extra downtime due to resolving of the fault, and the process of LHC machine access (especially if it has to be coordinated with the radiation piquet outside normal working hours).

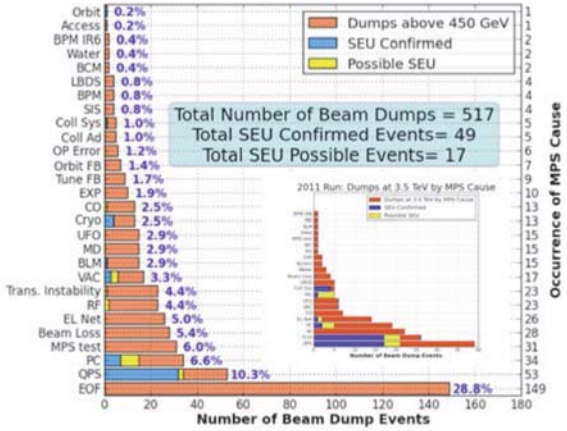

Figure 13: Beam dumps above injection energy by cause. Blue and yellow bars are stacked histograms representing SEU confirmed and SEU possible triggers, whereas the total number of beam dumps (red) is not stacked.

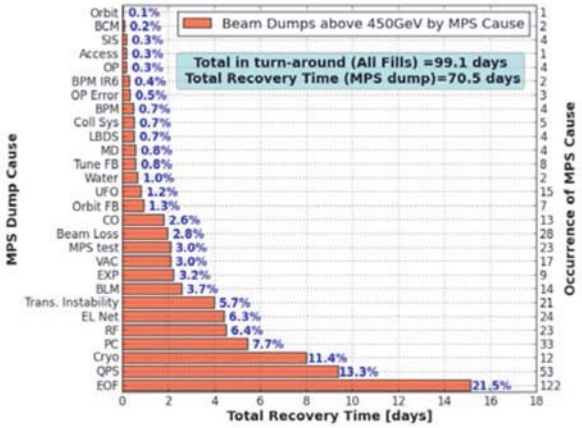

Figure 14: Cumulative recovery time by machine protection dump cause.

SUMMARY

The 2012 the LHC again completed a very successful proton-proton physics run, delivering in excess of 23 fb^{-1} to both ATLAS and CMS, which gave sufficient events for the discovery of a Higgs-like particle. As a measure of performance, the delivered luminosity was again beyond target, while the fraction of time in physics in 2012 improved by ~4% compared to 2011. This is reflected by the improvement of the machine Hubner factor from $H_{2011} = 0.156$ to $H_{2012} = 0.175$.

As this was a luminosity production run, beam quality, beam optics, and the operational cycle in both the injectors and the LHC itself were addressed, and this allowed for optimised luminosity delivery, which is perhaps best typified by the improvements made for ALICE experiment (Figure 7).

Unfortunately the fault and downtime tracking system is still not ideal, but the picture that emerges in 2012 is similar to 2011 in terms of the systems that have the biggest contribution to LHC downtime. These systems

(particularly QPS and Power Converters) are to undergo substantial upgrades in the upcoming long shutdown, which should help reduce the LHC downtime.

Yet it is very encouraging to observe both the number of single event upset related beam dumps in the cryogenics system and the total cryogenics downtime were drastically reduced. This is due to R2E mitigations and system consolidation, and offers some assurance that the overall machine availability can be further improved.

REFERENCES

[1] Observation of a new particle in the search for the Standard Model Higgs boson with the ATLAS detector at the LHC, ATLAS Collaboration. Physics Letters B, Volume 716, Issue 1, 17 September 2012. Observation of a new boson at a mass of 125 GeV with the CMS experiment at the LHC, CMS Collaboration Physics Letters B, Volume 716, Issue 1, 17 September 2012.

[2] Commissioning and operation at beta* = 1000 m in the LHC, H. Burkhardt et al., IPAC 2013.

[3] Electron Cloud and Scrubbing, G. Iadarola and G. Rumolo, these proceedings.

[4] LHC Machine Development Program, https://espace.cern.ch/lhc-md/default.aspx

[5] LHC Availability and Performance in 2011, A. Macpherson. LHC Beam Operation workshop - Evian 2011, 12-14 Deember 2011. CERN Reports Number: CERN-ATS-2012-083.

[6] Q20 in SPS, H. Bartosik, LHC Injector Upgrade 2013, 12 April 2013 https://indico.cern.ch/conferenceDisplay.py?confId=238152

[7] A Look Back on 2012 LHC Availability, B.Todd et al., these proceedings.

[8] R2E Experience and Outlook, G. Spiezia these proceedings.

A LOOK BACK ON 2012 LHC AVAILABILITY

B. Todd*, A. Apollonio, A. Macpherson, J. Uythoven, D. Wollmann, CERN, Geneva, Switzerland.

Abstract

This paper presents the conclusions of studies into the availability of LHC during 2012.

Initial and root causes of beam aborts above 450GeV have been identified and downtime associated with each event has been determined.

A comparison of operation's indications from e-logbook entries versus equipment group experience has been made for those systems having the largest indicated downtime.

Topics for further study are then introduced, including a weighting of systems by complexity, and a comparison of the observed versus predicted failure rates of the principle elements of the Machine Protection System (**MPS**).

Conclusions are drawn and proposals are made, including new approaches to information capture in the post-LS1 era to improve the quality of availability calculations.

POST-MORTEM - DUMP CAUSE

Every beam abort leads to the creation of a post-mortem event and corresponding post-mortem database entry. This contains raw information pertaining to the dump event. It is completed and a root cause is identified, by experts following investigations. These determine whether it is safe to continue LHC operations and make the post-mortem database one of the most reliable sources of information concerning LHC operation.

Post-Mortem Dump Cause Evolution 2010-2012

Considering only beam aborts that took place above injection energy, between March and November, then classifying dump cause into five categories (external, beam, equipment, operations or experiment) leads to the following distribution of beam aborts for 2010 [1]:

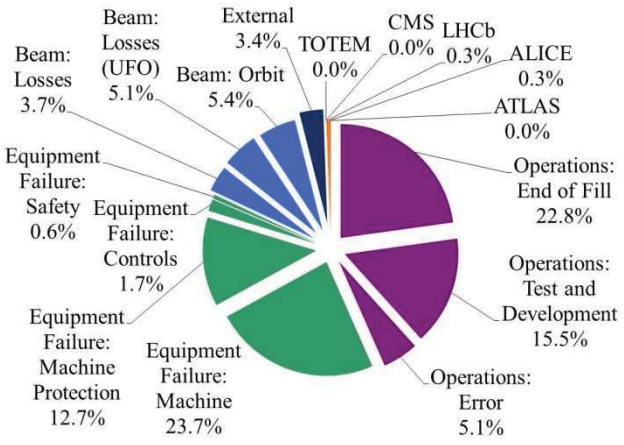

Figure 1: Distribution of Beam Aborts in 2010 (total 355)

The same analysis for 2012 [3]:

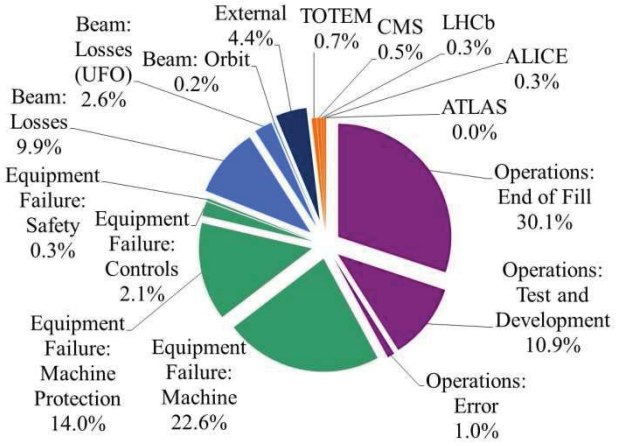

Figure 2: Distribution of Beam Aborts in 2012 (total 585)

Significant changes from 2010 to 2012 are:

- An increase in the number of fills from 355 to 585.
- An increase in the ratio of fills reaching the normal "end of fill" from 22.8% to 30.1%.
- An increase in the ratio of beam aborts due to "beam losses" from 3.7% to 9.9%.
- A slight increase in the ratio of beam aborts due to failures of the machine protection system from 12.7% to 14.0%.

Details of Dump Causes

Considering 2012 operation, excluding "Operations: End of Fill" and "Operations: Test and Development", leads to the following table of dump causes with their occurrences [4]:

Table 1: Root Cause versus Occurrence for 2012

Dump Cause	#	Dump Cause	#
Beam: Losses	58	BPM	8
Quench Protection	56	Operations: Error	6
Power Converter	35	SIS	4
Electrical Supply	26	LBDS	4
RF + Damper	23	TOTEM	4
Feedback	19	CMS	3
BLM	18	BCM	2
Vacuum	17	Water	2
Beam: Losses (UFO)	15	Access System	2
Cryogenics	14	LHCb	2
Collimation	12	ALICE	2
Controls	12	Beam: Orbit	1

DOWNTIME

The occurrence rate alone is not sufficient to determine the complete impact of each cause on the availability of

*benjamin.todd@cern.ch

the LHC. Downtime is an interpretation considering impact-on-physics. It is formed from two parts: lost-physics and fault-time.

Lost-Physics

Lost-physics (t_{lp}) indicates the length of stable-beams time lost due to a fault occurring. The calculation for this metric is to considers

1. The length of time the machine has been in stable-beams at the time the fault occurs (t_{stable}).
2. The average duration of stable-beams for physics fills in 2012, **nine hours**.
3. A pessimistic turnaround time (the time taken to get from beam abort of one fill to stable-beams of the next) of the LHC of **three hours**.

Every occurrence of a dump cause is assigned up to **three hours** of lost-physics if t_{stable} is less than **nine hours**. For example, if a water fault occurs after seven hours of stable beams, it is assigned two hours lost-physics. Table 2 indicates lost-physics due to each root cause [5]:

Table 2: Lost-Physics by Root Cause for 2012

Root Cause	t_{lp} [h]	Root Cause	t_{lp} [h]
Beam: Losses	147	Collimation	27
Quench Protection	126	BPM	17
Power Converter	80	Operations: Error	12
RF + Damper	53	LBDS	12
Vacuum	51	SIS	9
Electrical Supply	47	TOTEM	6
Feedback	45	BCM	6
BLM	43	Water	6
Beam: Losses (UFO)	42	LHCb	6
Cryogenics	33	ALICE	6
Controls	33	CMS	4

This gives a total of **812 hours** lost-physics for the LHC in 2012, due to failures.

Fault-Time

Once a beam abort has occurred, corrective action may be needed to restore operational conditions to the LHC. These actions are recorded by the operations team as faults in the e-logbook. Faults are not exclusive to the system which first caused the beam abort; they can run in parallel and can have interdependencies. Moreover, a fault can occur independently of LHC operation, not causing a beam abort, but delaying the next fill.

The time a system is unable to carry out its function, halting LHC operation (t_f) is shown in Table 3 [6].

The total fault time for the LHC in 2012 is **1524 hours**.

Downtime = Lost-Physics + Fault-Time

For each of the causes identified, t_{lp} and t_f can be combined to give downtime (t_d). Table 4 is a breakdown of downtime associated with each cause for operation in 2012, having a grand total of **2336 hours** downtime, equivalent to around 98 days.

Table 3: Fault-Time by Fault for 2012

Fault	t_f [h]	Fault	t_f [h]
Cryogenics	358	PSB	37
SPS	155	BLM	37
RF + Damper	119	Cooling & Ventilation	31
Quench Protection	112	Controls	26
Power Converter	106	ATLAS	17
Injection	86	ALICE	17
PS	82	Feedback	6
Vacuum	75	LHCb	4
Electrical Supply	70	CMS	4
Collimation	48	BPM	4
LBDS	44	BCT	2
BSRT	41	BIS	2
Access System	39	SIS	1

Table 4: Downtime by Cause for 2012

Cause	t_f [h]	Cause	t_f [h]
Cryogenics	391	BSRT	41
Quench Protection	238	Access System	39
Power Converter	186	PSB	37
RF + Damper	172	Cooling &Ventilation	31
SPS	155	ALICE	23
Beam: Losses	147	BPM	21
Vacuum	126	ATLAS	17
Electrical Supply	117	Operations: Error	13
Injection	86	SIS	10
PS	82	LHCb	10
BLM	80	CMS	8
Collimation	75	TOTEM	6
Controls	59	BCM	6
LBDS	56	Water	6
Feedback	51	BCT	2
Beam: Losses (UFO)	42	BIS	2

In this case, impact-on-physics is expressed as the number of hours of physics lost due to each cause. A more relevant metric would be the impact on integrated luminosity due to each cause.

SYSTEM BY SYSTEM

There are several shortcomings in the methods outlined for calculating downtime. The principle source of error is the use of the e-logbook for indication of fault occurrence and duration. E-logbook entries are not systematically completed, are not retrospectively corrected, do not account for multiplicity of faults and do not indicate dependency between faults.

Equipment-level fault information concerning t_{lp}, t_f and t_d for the three largest contributors to downtime was considered against operations' viewpoint. Faults were split into three categories. External – faults being outside of the control of the system in question. Internal – faults due to the system in question. Radiation Induced – faults

due to the system in question with radiation induced effects as a root cause.

Power Converters

The post-mortem database indicated **35 beam aborts** due to power converters, with operations indicating **59 faults** totalling **106 hours**. Table 5 shows equipment group records for these events, with the cause, total and average fault times given [7].

Table 5: Power Converter Operational Experience

Cause	#	Total [h]	Average [h]
External	2	2.5	1.3
Internal	38	64.8	1.7
Radiation Induced	12	25.2	2.1
combined	**52**	**92.4**	**1.8**

Equipment group experience, excluding external events, gives **50** faults for a downtime of **89.9 hours**.

Remote reset capabilities are increasingly being employed to cure faults without needing access to the machine. In addition, some faults take longer to repair than predicted due to the time needed to get piquet teams in place. Power converter problems are often linked, or in the shadow of other faults, further effecting these figures.

Quench Protection

The post-mortem database indicated **56 beam aborts** due to quench protection, with operations indicating **57 faults** totalling **112 hours**. Table 6 shows equipment group records for these events [8]:

Table 6: Quench Protection Operational Experience

Cause	#	Total [h]	Average [h]
CMW / WorldFIP	3	2.7	0.9
DFB	6	17.3	2.9
EE (600A)	6	18.9	3.2
EE (13kA)	1	4.7	4.7
QPS Acquisition Failure	10	27.4	2.7
QPS Acquisition Radiation Induced	7	11.8	1.7
QPS Detector failure	7	12.0	1.7
QPS Detector Radiation Induced	15	14.2	0.9
combined	**55**	**109**	**2.3**

Equipment group experience, excluding external CMW, WorldFIP and DFB events, gives **46** faults for a downtime of **89 hours**.

Quench protection functions during 2012 were 100% successful, Table 6 is not exhaustive however, as some faults took place in parallel.

Cryogenics

The post-mortem database indicated **14 beam aborts** due to quench protection, with operations indicating **37 faults** totalling **358 hours**. Table 7 shows equipment group records for these events. This table includes all known faults for the cryogenic system, not limited to those indicated by operations [9].

Table 7: Cryogenic Operational Experience

Cause	#	Total [h]
Supply (CV / EL / IT)	17	19
User	28	25
Internal	46	233
Radiation Induced	4	57
combined	**95**	**334**

Equipment group experience, excluding external events, gives **95** faults for a downtime of **334 hours**.

These figures represent 14 days downtime over 263 days operation, giving around 95% availability. Cryogenic downtime has halved between 2010 and 2012, however, in the post-LS1 era, recovery from a "User" fault (e.g. Quench) is expected to take 10-12 hours.

FURTHER CONSIDERATIONS

Relative Complexity

A direct comparison of failure rates leads to poor results, as system complexity has a significant influence on reliability. A large, complex system made of many components will be expected to fail more often than a smaller system with fewer components.

An example of this diversity is shown in Table 8, which details the number of channels leading to an interlock for several LHC systems [10].

Table 8: Number of Interlocking Channels by System

System	Interlocking Channels
RF	800
BIS	2000
Cryogenics	3500
Quench Detection	14000
BLM (surveillance)	18000
BLM (protection)	48000

Predicted and Observed Rates

The MPS ensures that the LHC operates with an acceptable risk, failure rates of the key LHC systems were predicted in 2005 and were used to determine the residual risk related to the operation of the LHC.

Note that it is not feasible to study unsafe events to track the safety of the MPS, as they are predicted to occur too infrequently. Instead, the MPS reliability must be well understood and closely monitored, and the safety of the MPS inferred.

Table 9 outlines the observed number of failures of key elements of the MPS in 2010, 2011 and 2012 [11].

Table 9: Downtime by Cause for 2012

System	prediction 2005	observation 2010	2011	2012
LBDS	6.8 ± 3.6	9	11	4
BIS	0.5 ± 0.5	2	1	0
BLM	17.0 ± 4.0	0	4	15
PIC	1.5 ± 1.2	2	5	0
QPS	15.8 ± 3.9	24	48	56
SIS	not studied	4	2	4

Figures shown in orange exceed predictions. These observations have not been adjusted for radiation induced effects, which were outside of the scope of the original study. Considering this, these figures show a good correlation between the predicted and observed rates. From this it can be inferred that the safety of the MPS is close to the original predictions, if it is assumed that the ratio of safe failures to unsafe failures holds.

CONCLUSIONS

On the LHC Availability

When referring to availability in the LHC context the ultimate meaning is impact-on-physics. This paper has attempted to quantify availability with impact-on-physics by determining a so-called downtime, related to lost-physics and fault time. In this case, a system referred to as high-availability should be understood as having a low impact-on-physics.

As the operations team and equipment experts have increased their understanding of the LHC and its sub-systems, so the availability of the LHC has improved. Proof of this is the evolution in the ratio of fills reaching "end of fill" between 2010 and 2012. Equally, the machine has been seen to reaching the limits of beam operation more often, shown by the increase in ratio of beam losses as a dump cause. It can be concluded that equipment is operating well enough to allow operators to spend more time exploring the physical limits of the machine.

LHC equipment has been shown to have a somewhat stable influence on availability between 2010 and 2012. This gives an indication that systems appear to be in their normal operating life, having passed the wear-in stage, before reaching the end-of-life stages. This stability is despite the increase in radiation fields which lead to higher failure rates of exposed equipment. The effort groups have made to compensate for these increased fields have successfully mitigated the impact of radiation on global machine availability between 2010 and 2012.

Equipment group records do not match operator information in the LHC e-logbook. With significant effort it has been possible to consolidate these differing opinions to a certain extent. This was made more difficult by both the variation in tracking techniques between equipment groups, and the e-logbook used for principle fault tracking. The e-logbook is not completed in a systematic manner, provides little scope for relating faults and is not retrospectively corrected. It must be noted that the primary function of the e-logbook is not fault tracking.

Comments on Future Work

If information on availability is to be used to drive investment by the organisation, it is vital that an adequate fault tracking tool be developed and implemented for the LHC restart after LS1. This tool needs to be sufficiently detailed to capture information in an unobtrusive manner yet must fit with the research and development style of running a machine such as the LHC.

To implement such a tool the fundamental definitions used must first be consolidated, as several are open to subjective interpretation.

LS1 presents an opportunity to implement new methods to improve availability studies once LHC restarts. Three recommendations (**R1-3**) emerge from this work, with two suggestions (**S1-2**):

R1. A new LHC fault tracking tool and fault database is needed.

R2. Defined and agreed reference metrics are needed to consolidate views on definitions used in availability calculations.

R3. Reliability tracking of the critical elements of the MPS is needed to ensure that LHC machine protection integrity is acceptable.

S1. A means to convert the hours of physics lost to the impact on integrated luminosity should be investigated.

S2. A metric for weighting reliability by complexity should be introduced, giving a so-called per-unit reliability.

ACKNOWLEDGMENTS

This work is a combination of information from many different sources, which took a considerable effort to consolidate, in particular the authors wish to express their gratitude for the input from the Availability Working Group (**AWG**), S. Claudet, K. Dahlerup-Petersen, R. Denz, E. Duret, V. Montabonnet, I. Romera and Y. Thurel in the completion of this work.

REFERENCES

[1] PM database. Extracted from 23rd March to 6th December 2010, only for fills >450.1 GeV, ignoring entries marked as "no input change".

[2] PM database. Extracted from 17th February to 13th December 2011, only for fills >450.1 GeV, ignoring entries marked as "no input change".

[3] PM database. Extracted from 1st March to 6th December 2012, only for fills >450.1 GeV, ignoring entries marked as "no input change".

[4] Sort [3] by MPS Dump Cause, Discarding EOF, MD and MPS Test.
[5] Calculate stable beams per fill from TIMBER, assign lost physics by dump cause from [4]
[6] e-logbook. Extracted from 1st March – 6th December 2012. Supress duplicate entries, MISCELLANEOUS is ignored, except for the BSRT related events. No correction for entries rolling-over between shifts.
[7] Courtesy V. Montabonnet, Y. Thurel.
[8] Courtesy K. Dahlerup-Petersen, R. Denz, I. Romera.
[9] Courtesy S. Claudet, E. Duret.
[10] Courtesy O. Brunner (RF), S. Claudet (Cryogenics), R. Denz (Quench Detection), C. Zamantzas (both BLM).
[11] Table 1: R. Filippini et al., "Reliability Assessment of the LHC Machine Protection System" PAC 2005, Knoxville, Tennessee May 2005, TPAP011, http://accelconf.web.cern.ch/AccelConf/p05/PAPERS/TPAP011.PDF

R2E – EXPERIENCE AND OUTLOOK

M. Brugger, M. Calviani, R. Garcia Alia, J. Mekki, G. Spiezia

CERN, Geneva, Switzerland.

Abstract

The period before 2011 and 2012 LHC operation involved several mitigation actions related to R2E ("Radiation to Electronics") project [1] aiming at keeping SEE ("Single Event Effect") failures at an acceptable rate. In this respect, 2012 very successful LHC operation has continued to provide valuable inputs for the detailed analysis of radiation levels and radiation induced equipment failures, confirming the estimates provided in Chamonix 2012. Radiation levels around LHC critical areas and the LHC tunnel were studied in detail and compared both to available 2011 measurements and previous simulation results, as well as put in perspective to future LHC operation parameters. Observed radiation induced failures were continuously analysed and addressed through early relocation measures and patch-solutions on the equipment level whenever required and/or possible. During LS1 all primary mitigation actions will be completed, involving significant relocation and shielding activities all around the LHC and aiming to allow for nominal operation and beyond. This paper will focus on the observed equipment failures, their relation to radiation levels and extrapolation to post-LS1 operation.

INTRODUCTION

Based on previous studies [2] and a respective analysis, the 2012 LHC operation was expected to be a key period for the analysis of radiation induced failures on machine equipment. The very successful LHC operation has confirmed the estimates of the radiation levels provided in Chamonix 2012 and proven valuable the early mitigation measures taken in previous years. During 2012 a strong emphasis was put in the detailed analysis of equipment failures which could possibly be linked to radiation effects and to verify if all of them are addressed throughout the LS1 mitigation measures. To study the correlation with radiation in detail, a number of criteria have been set, implying one, several and, ideally, all of the following conditions to be fulfilled:

- equipment failure occurs during periods with beam-on/collisions/losses (*i.e.*, the source of radiation being present)
- the failure(s) is/are not reproducible in the laboratory
- the failure signature was already observed during radiation tests (CNRAD, H4IRRAD and others)
- the frequency of the failures increases with higher radiation levels

For rare cases this implies remaining uncertainties which can lead to failures being incorrectly attributed to radiation. However, as shown in this paper, the performed detailed studies over the 2012 operation period limited these uncertainty cases to only a few. In addition, there is the complementary limitation that the analysis is likely to miss radiation induced failures which do not lead to a beam dump. In addition more complex events where one equipment is affected by radiation can indirectly cause a problem to another one, thus eventually leading to either longer downtimes or beam dumps.

In the following we provide a summary of the radiation levels and the induced failures regarding the 2012 LHC operation, including an estimate of the respective machine downtime. The impact of performed countermeasures is highlighted and conclusions are drawn. It is shown that the detailed monitoring of the radiation levels, as well as the detailed analysis of radiation induced failures are key ingredients to assure the successful LHC operation after the Long Shutdown 1 (LS1), and beyond. In addition to the numerous early mitigation measures performed during 2010-2012, the complete relocation, shielding activities and equipment upgrades will be carried out during the LS1 period. The goal is to reduce the failure rate to achieve a continuous LHC operation at the luminosity levels that will be reached after LS1.

RADIATION LEVELS AND PARAMETERS SCALING

The radiation levels in the LHC tunnel and in the shielded areas have been measured using the RadMon system [3]. As in 2011, the major radiation-induced failures, observed during 2012 LHC operation, are Single Event Effects (SEE) on electronic equipment. The probability of having a SEE is related to the accumulated High Energy Hadron (HEH) fluence which is reported in Table 1 for the most critical areas where electronic equipment is installed. The HEH fluence measurement is based on the reading of the Single Event Upsets (SEU) of SRAM memories whose sensitivity has been previously calibrated at various facilities [4] [5]. The results, obtained during 2012 LHC proton operation, show a very good agreement between the predictions [2] and the measurements which are given with an uncertainty factor of 2 (Table 2). It is noted that the comparison is based on a cumulated luminosity of $15 fb^{-1}$, the foreseen target of the CMS and ATLAS experiments, which has been

exceeded thanks to the efficient operation of the LHC machine. The uncertainties of the predictions of the radiation levels depend on the operational parameters because of the peculiarity of the three main categories of radiation sources at LHC: (a) direct losses in collimators and absorber like objects, (b) particle debris from beam-beam collisions in the four main experiments, and (c) interaction of the beam with the residual gas inside the beam pipe. In addition, the effect of the additional installed shielding (during 2011/2012 xMasBreak) is clearly visible for UJ14/16, the latter being the most critical areas during 2011 operation.

The most significant mismatch between predictions and measurements values arises in the areas RR53/57 and UJ76 where the radiation levels are directly impacted by the beam losses and settings of the collimators. A detailed analysis showed that the operational parameters adopted for 2012 (tight collimator settings in IR7 and closed TCL in IR1/5) are fully consistent with the observed measurements.

Another important parameter which affects the radiation levels in some of the critical areas (P4 mainly) is the interaction between the beam and the residual gas in the beam pipe. So far we only have limited experience of operating with a bunch spacing of 25 ns, which might play a role on a possible radiation levels increase due to beam-gas interactions.

Besides the critical areas listed in Table 1 and 2, there are additional zones where electronics is installed and radiations can induce failures in case radiation levels rise further due to beam-gas interactions. I.e, the HEH fluence increased by a factor 10 from 2011 to 2012 ($2x10^6$ cm^{-2} to $2x10^7$ cm^{-2}) in the alcove UX45.

It can be concluded that the present analysis nicely shows that (a) the radiation levels were correctly analysed and measured in the last two years of operation; (b) an efficient monitoring system is an important asset in order to have an online mean of verifying radiation levels in order to control a possible impact on installed equipment.

Table 1: Measured HEH fluence in critical shielded areas in 2012 and 2011.

Area	Measured 2012 (HEH/cm^2)	Measured 2011 (HEH/cm^2)
UJ14/16	$1.6*10^8$	$2*10^8$
RR13/17	$2.50*10^8$	$7.0*10^6$
UJ56	$1.50*10^8$	$3.5*10^7$
RR53/57	$2.50*10^7$	$1*10^7$
UJ76	$6.00*10^7$	$5*10^6$
RR73/77	$5.00*10^7$	$8*10^6$
UX85B	$3.50*10^8$	$2*10^8$
US85	$8.80*10^8$	$3.5*10^7$

For this, an improved RadMon system (larger sensitivity range, more accurate calibration and longer life-time) is currently in the final prototyping phase [6].

Table 2: Predicted and measured HEH fluence in critical shielded areas for a cumulated ATLAS/CMS luminosity of 15 fb^{-1} during 2012 operation.

Area	Prediction (HEH/cm^2)	Measured (HEH/cm^2)
UJ14/16	$1.1*10^8$	$1.3*10^8$
RR13/17	$1.8*10^7$	$2.1*10^7$
UJ56	$1.2*10^8$	$1.1*10^8$
RR53/57	$1.8*10^7$	$3.3*10^7$
UJ76	$5.5*10^6$	$1.6*10^7$
RR73/77	$3.0*10^6$	$2.4*10^7$
UX85B	$2.6*10^8$	$2.1*10^8$
US85	$6.5*10^7$	$4.4*10^7$

FAILURES OBSERVED IN 2012 AND CORRESPONDING MITIGATION ACTIONS

The radiation induced failures on the LHC equipment have been analysed by organizing a weekly shift within the R2E project team. The main sources of information were the LHC e-logbook and the meeting on the LHC operation follow-up, daily held at 8h30 [7]. During the year, the collaboration of all the equipment groups was highly appreciated and permitted to improve the performed failure analysis. Once a failure is suspected to be related to radiation effects, the following information is collected and stored on the web page of the RADiation Working Group (RADWG) [8]: a) equipment, b) type of failure, c) location, d) consequence of the failure, e) number of beam fill. In some cases, it is not straight forward to understand if a failure was effectively due to radiation effects. Thus, the event is marked as *to be confirmed (TBC)* if a further analysis is required to understand what happened. In addition, the number of the beam fill was used as a direct link to insert information also in the Post Mortem (PM) database and in order to track the beam dumps that were due, or possibly due (*to be confirmed*), to radiations and allow for a respective analysis operators[9]. Table 3 shows the failures due to the SEEs. Four distinct cases are reported:

a) Events leading to beam dump (Dump confirmed).
b) Events leading to beam dump which are possibly due to radiation (Dump TBC).
c) Failures which did not lead to beam dump (No Dump).
d) Failures which do not lead to beam dump and are possibly due to radiation (No Dump TBC).

The second part of the Table makes a focus on the destructive failures, i.e. failures which triggered an intervention in the machine to replace a component/system. They represent ~30% of the total number of events leading to a beam dump.

It is important to note that the number of events to be confirmed represents only a small fraction and will thus not affect the overall conclusion.

Table 3: Number of failures due to radiation. A detail view of the destructive events is given below.

Dump Confirmed	Dump TBC	No Dump	No Dump TBC
58	10	36	7

Destructive Failures

Dump Confirmed	Dump TBC	No Dump	No Dump TBC
17	1	4	0

The pie charts in Fig. 1 reports the distribution of the failures per area (a) and per equipment (b). The failures per area are almost equally distributed among the alcoves which were known to be prone to radiations (Table1).

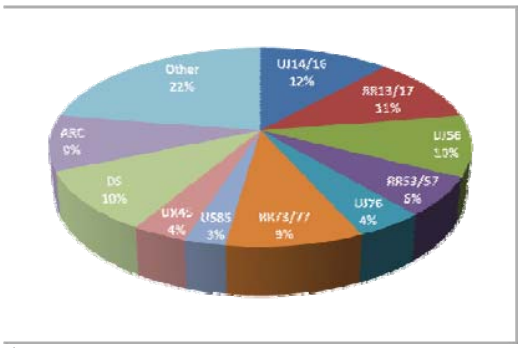

a)

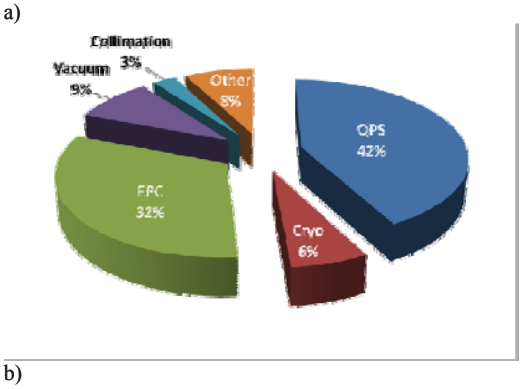

b)

Figure 1. Failure distribution per area (a) and per equipment (b).

As compared to 2011 operation and the respective observed SEE related failures, this also reflects the successful implementation of R2E countermeasures where the focus was put on the most exposed areas, thus bringing all of the critical areas more or less to the same exposure level (also visible in the reported radiation levels for 2012). I.e, the number of failures in the UJs of point 1 is not as dominant as along 2011, showing the effectiveness of the shielding that was put in place in the 2011-12 xMasBreak [2]. The majority of the failures that occurred in the tunnel was related to the Quench Protection System (QPS) electronics. The EPC equipment, installed in the RR areas, presented a recurrent failure due to a destructive event on an auxiliary power supply.

In addition to the shielding at point 1, the relocation of a few sensitive equipment (Cryogenic, Beam, Power interlocks, and UPS devices), as well as the patch solutions applied on the equipment that could not be moved yet, allowed to significantly decrease the overall number of failures with respect to 2011.

In the following subsections, the failure analysis and the envisaged mitigation actions for all the affected equipment groups are briefly summarized.

QPS

Failures on the QPS systems happened both in the tunnel and in the shielded areas. Most of the failures affected the QPS detection system which is based on a Digital Signal Processor (DSP). Other sensitive parts of the QPS system are the communication and the acquisition modules used for the protection of the magnets, the splices and the 600A converters. It is important to note that none of the observed SEE-induced failures compromised the safety of the machines. Various additional countermeasures, as the design and deployment of a data acquisition card based on a rad-tolerant FPGA and the usage of an automatic reset on the microFip, are planned for LS1 to further reduce the radiation induced failures. Moreover, the equipment in the UJ14/16 and UJ56, which caused 30% of the total number of the QPS failures, will be relocated into safe areas.

Power converters

During 2012 operation, an auxiliary power supply of the 600A Power Converters (PC) suffered 14 destructive events. A destructive event was also registered on the 120A power converter. The Function Generator Controller (FGC) was affected by 10 radiation induced failures. The events happened mainly in the UJs of Point 1, RRs of Point 1, 5, and 7, and in the ARC. The affected power supply was tested under radiation and, after several complex iterations due to the commercial nature of such power-supplies, finally the weak component could be identified. It will be replaced on the systems where it is actually installed during LS1. In addition, the new FGC is under design to be radiation tolerant. At long term, both the power stage and the controller (FGC) of the PCs will be replaced by the respective radiation tolerant version.

Moreover, already during LS1 the relocation of the PCs will be carried out wherever feasible (i.e. all areas but the RRs).

Cryogenics

The cryogenic equipment also suffered various types of failures. Both destructive and non-destructive SEU failures affected the PLC (Programmable Logic Controller) in Point 4 (UX), 5 (UJs), 7 (UJ), and 8 (US). In addition, the magnet bearing system failed due to single events at point 4 and 8. A few PLCs showed communication errors on the Profibus network. It is important to note that thanks to the mitigation actions implemented along 2011 and in the subsequent xMasBreak, the actual effective (per unit luminosity) number of failures was significantly decreased with respect to the one observed in 2011; in total only 4 failures led to a beam dump. However, each failure has a significant impact on the downtime for the machine. The group has planned and integrated several mitigation actions. The most sensitive PLCs were or will be relocated. The move of the magnetic bearing system is under study.

Collimation equipment

Abnormal communication losses affected the control equipment of the collimation system installed in UJ14, UJ16, and UJ56; only one beam dump was caused. No failure of the power supply was registered. The equipment will be removed from the critical areas during LS1.

Access system

The access doors and the iris scan systems got blocked in many LHC points, even at the surface, in 2012. As a matter of fact, the replacement of all the electronics for the access system is programmed to change obsolete systems. In addition, the failure analysis showed that the fault cases which happened at UJ14/16 and UJ56 are higher in number with respect to other areas and thus expected to be partly related to radiation effects. The relocation scheduled for LS1 should significantly reduce any failures caused due to radiations for the future operation.

Vacuum

Destructive failures of a power supply and communication losses on PLCs were registered in the UJ76 (4 events) and UX 45 (3 events). Given the radiation levels, the failures at UJ76 are most likely related to radiations and, thus, the Vacuum equipment will be relocated during LS1. The failures at UX45 are under investigation.

EN/EL equipments

The Uninterruptible Power Supply (UPS) of the electrical network exhibited a destructive event in the US85 area, the only one remaining in the currently critical areas after the relocation during the XMasBreak 2011/2012. The analysis, considering the observed failure mode, the affected location and the involved power components, demonstrated that the fault was induced by radiation. On this basis, the UPS will be relocated from US85. However, the UPS systems will remain in the REs, but exposed to much lower radiation levels as in the critical areas. Therefore, two types of UPS systems have been tested against radiations at H4irrad; the data analysis is on-going, however already indicating that no additional countermeasures are required besides the already scheduled relocation for the US85 area.

RF equipments

A few failures (3 in total) were registered on a power supply and on vacuum gauges at UX45. Those cases might not be related to radiations. However, the fact that they happened in UX45 where the radiation levels increased during 2012 by a factor 10, suggests keeping those events under investigations, and are thus noted here for completeness.

FAILURE SUMMARY AND OUTLOOKS FOR LS1

Table 4 presents a summary of the number of confirmed dumps for the 2012 operation per equipment.

Table 4. Summary of the SEU-induced beam dumps and respective downtime.

Equipment	2012 #dumps	2012 downtime (% of the total)	>LS1 #expected dumps
QPS	31	~40	5
Power Converter s	14	~20	3
Cryogenic	4	~30	1
Vacuum	4	~1	0
Collimation	1	~1	2
EN/EL	1	~6	0
Other		~2	5
Total		~250-300 hours	~10-20

A calculation of the machine downtime caused by the radiation induced failures is also reported in percentage. The latter analysis was performed by using the data collected on the RADWG website and on the PM database. A manual iteration on the data was required to take into account the downtime due to issues not related to SEEs which happened before or after the beam dump and led to longer downtimes than the radiation induced

failure itself. Although the analysis is preliminary, it gives a fair indication of the operation time loss due to radiation. The downtime for the cryogenics failures considers the recuperation of the cryogenic temperatures.
Figure 2 reports the reached objectives by the R2E project, with the important support of all the concerned equipment groups, as well as the shielding and relocation teams. The dependency on the actual radiation levels is emphasized by displaying the number of beam dumps normalized to the cumulated luminosity of the CMS and ATLAS experiments. In total, the number of dumps per fb^{-1} was reduced by a factor of almost four from 2011 to 2012.
In the long-term, and as a requirement for nominal (and beyond) LHC operation, the goal is to have less than one dump per fb^{-1} when the machine will restart operation after LS1, the latter thus being a crucial period to deploy many mitigation actions.
During LS1, all remaining possibly sensitive equipment will be moved from the critical areas (UJ14/16/56/76, US85, and UX45 partly) to safer areas; additional shielding will be installed in the RR areas; critical systems based on custom designs, such as the QPS and the Power converters will be upgraded or redesigned. On the basis of the first two years of operation, the installation of commercial devices will not be allowed in areas where the HEH fluence is expected to be higher than 10^7 cm^{-2}.
Taking into account those countermeasures, a very tentative estimation of the remaining failures for the restart of the machine on 2014 is also given in Table 4. It's important to note that the latter aims at trying to pinpoint the effectiveness of the mitigation measures, rather than aiming for accurate predictions of failures in the long-term expected to be dominated by so far rare cases, or untracked equipment changes (upgrades, etc.).
Therefore, in order to assure this result, the R2E activities will continue with the established analysis process and also follow in detail the radiation levels in the ARCs where the radiation levels will increase and also possibly imply long-term cumulative damages, as the Total Ionizing Dose (TID) effects, to be considered. In this context, the
impact of the 25 ns bunch operation will be studied in detail; areas which were so far characterized by low radiation levels, such as the UX25/45/65, the UJ/UA23, the UJ/UA87, and the RE will be observed. Finally, the upgrades as well as the new developments of custom electronics will be followed and radiation tests advised accordingly.

CONCLUSIONS

A summary of the radiation levels and the induced failures for the LHC operation in 2012 has been reported.
About 60 beam dumps were provoked by radiation effects on electronic equipments causing a downtime for the machine of about 250-300 hours. The impact of the radiation effects would have been significantly higher without the countermeasures that were already applied in the past years [2]. Furthermore, the prompt reaction of the groups to design patch solutions for mitigating radiation effects allowed throughout the year 2012 to reduce the number of failures which could have led to a beam dump. In total, the radiation induced failures were reduced by a factor 4 with respect to the 2011 operation.

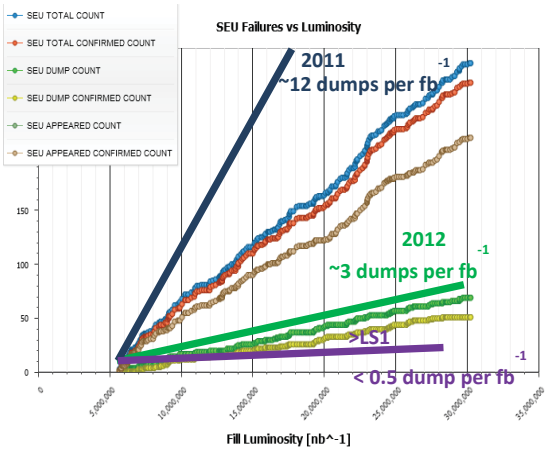

Figure 2. The number of SEU failures is reported as a function of the CMS/ATLA luminosity. The number of dumps, induced by SEUs, per fb^{-1} is extrapolated as a figure of merit for 2011, 2012 operation.

Additional mitigation actions are planned for the LS1 period to further reduce the radiation vulnerability of the equipment. Thanks to those efforts, the expected number of radiation induced dumps per fb^{-1} is expected to be <1. This objective will permit to classify the radiation induced failures as minor, and to operate the LHC smoothly without any significant number of stops related to radiation.
The monitoring of the radiation levels will be a continuous work which aims at reducing the uncertainty factors, mainly related to the beam gas effects and the losses in the collimation areas, as well as to closely monitor the long-term radiation impact on exposed electronic systems. This will allow verifying design assumptions, as well as scheduling preventive maintenance actions when required. The detailed follow-up of the system upgrades and developments remains crucial to reach the above goal.

AKNOWLEDGMENTS

The authors would like to thank all the equipment groups for their active collaboration throughout 2011-12, as well as the EN/MEF group for its continuous support in the relocation and shielding improvements. The authors would like to acknowledge M. Zerlauth for his precious collaboration to set up the SEU failure analysis in the PM database.

REFERENCES

[1] R2E website, www.cern.ch/r2e

[2] M. Brugger et al, "R2E Experience and Outlook for 2012", *Proceedings of LHC Performance workshop*, Chamonix 2012.

[3] G. Spiezia et al. "The LHC accelerator Radiation Monitoring System - RadMON" http://pos.sissa.it/archive/conferences/143/024/RD11_024.pdf.

[4] K. Røed, M. Brugger, D. Kramer, A. Masi, P. Peronnard, C. Pignard, and G. Spiezia, "Method for measuring mixed field radiation levels relevant for SEEs in the LHC", *Transactions on Nuclear Science,* pp.1040-1047, Aug.2012.

[5] D. Kramer et al. "LHC RadMon SRAM detectors Used at Different Voltages to Determine the Thermal Neutron to High Energy Hadron Fluence Ratio", *IEEE Trans. Nucl. Sci.*, vol. 58, no. 3, pp. 1117-1122, 2011.

[6] A. Masi, G. Spiezia, P. Peronnard, M. Donze, M. Brugger, R. Losito, "The new generation of LHC accelerator radiation monitoring system", *Proceedings on RT2012 conference*, May 2012.

[7] https://lhc-commissioning.web.cern.ch/lhc-commissioning/news-2011/LHC-latest-news.html

[8] http://radwg.web.cern.ch/RadWG/

[9] http://lhc-postmortem.web.cern.ch/lhc-postmortem/

MACHINE PROTECTION SYSTEMS PERFORMANCE AND ISSUES 2012

D. Wollmann*, L. Ponce, R. Schmidt, J. Uythoven,
J. Wenninger, M. Zerlauth, CERN, Geneva, Switzerland

Abstract

Operating the LHC with stored beam energies up to 140 MJ (40% of nominal value) in 2012 was only possible due to the experience with and confidence into the machine protection systems gained in the 2 previous running periods - 2010 and 2011, where the stored beam intensity was slowly increased. In this paper the performance of the machine protection system during 2012 will be briefly discussed and compared to the previous running periods. Issues, which appeared during the operation of the MP systems during 2012 are reviewed. Special attention will be given to MPS issues, which risked compromising the protection of the LHC and, therefore, lead to a stop or delay of the standard operation of the LHC. The immediate actions taken as well as the mid- and long-term mitigations in these cases will be discussed. The efficiency of machine protection procedures during intensity increase, intensity cruise and the preparation of machine development periods will be reviewed. Finally improvements of the MP systems and procedures for operation after LS1 are proposed.

INTRODUCTION

During the 2012 run of the LHC more than 1000 clean beam dumps have been performed. 585 of them have been performed at particle momenta above 450 GeV/c. Note that only dumps before the 10th December 2012 were taken into account here. The majority of these beam dumps have been performed with beam energies above 100 MJ, reaching a maximum stored beam energy of 146 MJ per beam. No beam induced quenches of superconducting magnets have been observed at a particle momentum of 4 TeV/c. Excluding the observed problems of beam induced heating, no equipment damage due to the stored particle beams was observed during the 2012 run of the LHC. The reasons and the response of the machine protection systems for all beam dumps above 450 GeV/c have been analysed in detail, validated and classified by machine protection experts. Figure 1 shows the distribution of the 585 beam dumps classified into five categories (black: external; blue: beam; green: equipment; purple: operations; orange: experiments). These categories contain further sub-classes. False dumps from the machine protection systems - including BIC, BLM, LBDS, PIC, QPS, SIS - account for about 14 % of the beam dumps. This is comparable to their share in 2011 and slightly more than in 2010. A detailed analysis of the dump causes can be found in [1].

* daniel.wollmann@cern.ch

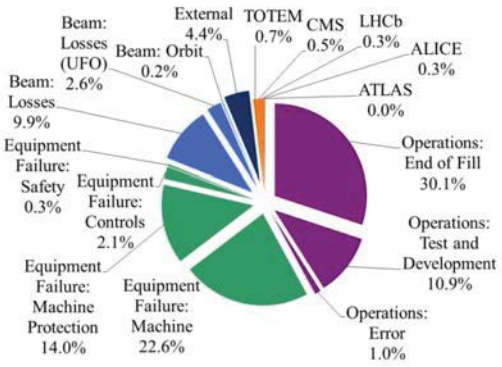

Figure 1: Distribution of Beam Aborts in 2012 (total 585). The dump causes are classified into five categories (black: external; blue: beam; green: equipment; purple: operations; orange: experiment), which contain further subclasses [1].

ISSUES 2012

During machine operation all dumps are stored and documented in the LHC post mortem database and completed with an operator and machine protection expert comment. In addition so-called machine protection check lists including all beam dumps above injection energy during the reference period concerned have been distributed regularly to the different system experts to document issues with the concerned systems. The check lists cover issues in the magnet powering system, beam interlock system, RF system, beam loss monitors, collimation, feedback systems, post mortem system, beam dumping system, issues with the beam orbit, issues during injection and with heating of accelerator equipment. The cover page of such a check list is shown in figure 2. In total 9 check lists have been distributed and filled by the system experts in 2012. During the step-wise intensity ramp up check lists were filled out before each significant step in beam intensity and after accumulating a minimum of 3 successful fills with a minimum of 20 hours operating in the machine mode stable beams with the current beam intensity. Intensity ramp check lists were completed after running with 84, 624, 840 and 1092 nominal LHC bunches per beam. During the following so-called intensity cruise with 1380 bunches per beam check lists have been distributed every 4 to 8 weeks. In total 5 intensity cruise check lists were filled out in 2012. The check lists are documented in EDMS. A list of all machine protection system issues documented in the differ-

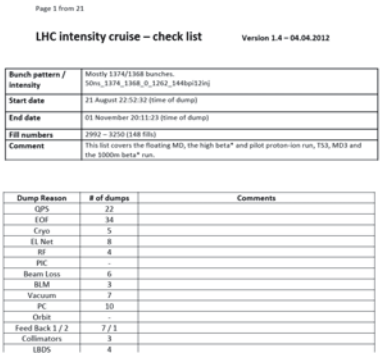

Page 1 from 21

LHC intensity cruise – check list Version 1.4 – 04.04.2012

Bunch pattern / intensity	Mostly 1374/1368 bunches. 50ns_1374_1368_0_1262_144bpi12inj
Start date	21 August 22:52:32 (time of dump)
End date	01 November 20:11:23 (time of dump)
Fill numbers	2992 – 3250 (148 fills)
Comment	This list covers the floating MD, the high beta* and pilot proton-ion run, TS3, MD3 and the 1000m beta* run.

Dump Reason	# of dumps	Comments
QPS	22	
EOF	34	
Cryo	5	
EL Net	8	
RF	4	
PIC	-	
Beam Loss	6	
BLM	3	
Vacuum	7	
PC	10	
Orbit	-	
Feed Back 1 / 2	7 / 1	
Collimators	3	
LBDS	4	

Figure 2: Screen shot of a machine protection check list during the so-called intensity cruise. The filling pattern, the reference period (time and fill numbers), and a summary table of the false beam dumps are visible here. On the following pages each beam dump above injection energy is mentioned with an operator and machine protection expert comment.

ent check lists during 2012 operation has been presented to the 71st LHC Machine Protection Panel meeting on the 9th November 2012 [2].

In the following the top five machine protection issues in 2012 and their consequences for the operation of the LHC, listed in the sequence of their appearance, are critically reviewed.

OFSU reference problem

During the intensity ramp up in the beginning of 2012 operation it was observed that the reference used by the orbit feedback system was suddenly set to zero along the whole LHC ring during the machine mode squeeze at top energy (see figure 3). This lead to orbit offsets of up to 4 mm in some of the LHC insertion regions, where the orbit feedback compensated the crossing bumps due to the wrong reference orbit. The beams were finally dumped due to particle losses in the vertical B2 tertiary collimator in IR2. Due to this problem the next step of intensity increase was postponed and a new software interlock was introduced, to dump the beam automatically, if the reference settings are not loaded correctly or zeroed. In addition checks in the LHC sequencer and by the operators were introduced to check if the correct orbit reference is loaded before starting the ramp or the squeeze. Due to these measures the problem was reduced to an availability issue. This example shows that also issues in systems, which are not directly part of machine protection can have important consequences.

Powering of the LHC beam dumping system (LBDS)

Two major problems were discovered in the LHC beam dumping system during 2012. On the 13th of April a fault in one of the two redundant WIENER power supplies caused a loss of power in the whole set of general purpose beam dump crates. This would have caused an asynchronous beam dump if beam would have been present at this time. As a short term measure one of the triggering synchronization units was connect to a second independent UPS and fast fuses were introduced. In addition a review of the LBDS UPS powering was scheduled.

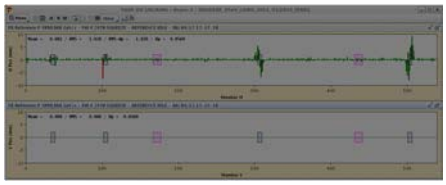

Figure 3: Screen shot of a reference orbit for beam 2 along the whole LHC ring on the 6th of April 2012 (fill 2478) for the machine mode squeeze. The top graph shows the (correct) reference orbit in the horizontal plane. In the lower graph the false reference orbit for the vertical plane is displayed. It is clearly visible that the reference has been falsely set to zero along the whole ring.

During the preparations of this review a common mode failure in the 12V DC powering of the triggering synchronization units was discovered during lab tests. This failure would have made it impossible to dump the beams in the LHC, which is considered to be the worst case failure. As any other problem could then lead to a fatal damage of the LHC. Due to the severity of the discovered common mode failure the operation of the LHC was stopped until a short term mitigation in form of a watchdog to supervise the 12V supply voltage was implemented. In case of a problem in the 12V supply this watchdog would dump the beam before the system would be off.

A fail safe and fault tolerant solution to mitigate the two problems will be implemented during LS1. In addition a redundant channel from the beam interlock system (BIS) to the LBDS re-triggering line will be installed, which will directly trigger a delayed asynchronous beam dump in case of a problem in the triggering synchronization units of the LBDS.

BSRT mirror support degradation

The transverse synchrotron light monitors (BSRT) are an important instrument to measure several critical beam parameters like the change of the beam emittance during a fill, the bunch by bunch beam intensity and information about the population of the abort gap. The latter is of importance for machine protection, as a high particle population in the abort gap may lead to high losses, magnet quenches and possibly damage of accelerator equipment in case of a beam dump.

During 2012 operation a gradual deterioration of the BSRTs due to beam induced heating was observed. On the 27th of August the deterioration suddenly increase in the B2 BSRT and the mirror, which reflects the synchrotron

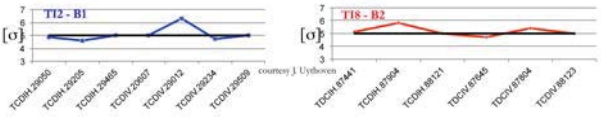

Figure 4: Deviation of TCDI gap openings from the required 5 σ due to the change in optics in the tranfer lines after the introduction of the Q20 optics in the SPS. Courtesy J. Uythoven

radiation the instrument's optical installation, threatened to drop from it's support, damage the view port and fall through the beam. Therefore, fill 3012 was dumped to allow to un-install the BSRT and avoid any risk of collateral damage due to this problem.

The BSRT of B2 was re-designed and re-installed in technical stop three. As the observation of the abort gap population was not any more possible during the period before the re-installation the abort gap cleaning was turned on frequently. In addition alternative and redundant solutions to measure the abort gap population are under investigation and should be available after LS1.

False settings of Transfer Line collimators

After the technical stop three (TS3) end of September the so-called Q20 optics has been implemented in the SPS for the injection of beam into the LHC. Therefore the optics, i.e. the quadrupole strengths, in the transfer lines to the LHC had also to be adjusted. On the 19th of November it was discovered that the settings of the transfer line collimators, which protect the aperture of the LHC against too big injection oscillations had not been adjusted accordingly. This caused deviations from the required gap openings (5 σ) of up to 1.3 σ (see figure 4), which resulted in a reduced protection.

When the problem was discovered by the injection team physics operation was stopped to re-setup the TCDIs and validate their settings with beam. For after LS1 operation it is planned to introduce additional consistency checks between TCDI settings and used optics to avoid a comparable situation with reduced protection in the future.

Injection Issues due to Timing Problems

Tests with the so-called BCMS high brightness beams from the PS lead to a problem with the timing in the SPS. This caused the injection of beam into LHC B1 instead of B2.Thus, the the injection kickers in B1 did not fire and the 20 bunches were therefore injected onto the TDI. After this the tests with the BCMS beams was stopped until the reason for this problem was identified and mitigated.

Shortly after a second problem appeared during injection, when the SPS RF-clock was not synchronized with the LHC, i.e. running on local timing. This caused a mismatch of the kicker firing and the SPS injection and therefore twice 48 bunches were hitting the TDI in IR8.

These issues were a reminder that currently there exists no active protection against timing issues during injection. The passive protection for injection problems, i.e. the correctly positioned TDI, worked as foreseen. As the TDI is currently the only protection for these type of errors it is planned to introduce additional extraction interlocks on the SPS side during LS1.

Other MP issues in 2012

Some other machine protection issues observed in 2012 are listed below. The full list of machine protection system issues documented in the different check lists during 2012 operation has been presented to the 71st LHC Machine Protection Panel meeting on the 9th November 2012 [2].

- False collimator settings of the vertical tertiary collimators in IR2 and 2 collimators in IR3. The false settings were detected on the 17th of April and corrected in LS1.
- Upper corner of the TDI in IR2 was *falling* onto the lower jaw (03.12.2012), when putting it back to injection position due to a loose splinter pin.
- Several MKI.D flash-overs in the beginning of the run. This injection kicker has been replaced during TS3.
- The tune feedback could not be used during the beam mode squeeze due to a poor tune signal, thus operation relied on a feed forward. Since the end of October an additional high gain system, which gates on the first 6 bunches is operational, which mitigated the problem.
- After technical stop two a cabling problem in the QPS instrumentation of RQX.L8 was discovered. The cables had to be changed back to the status before the technical stop.
- Different trips of power converters caused significant orbit drifts. The beams were dumped by the BLM system due to losses. During LS1 these issues will be mitigated by introducing interlocks on these power converters, which will allow to dump on the root cause of the orbit drifts.
  - Fill 3220: Removal of powering permit for the 60A corrector magnets in sector 67.
  - Fill 2985: Trip of LHCb dipole.
  - Fill 2934: Fast discharge of CMS solenoid.
- Heating of different equipment due to beam.

MACHINE PROTECTION PROCEDURES FOR MACHINE DEVELOPMENTS

Machine developments explore per definition new machine territory. Therefore, the requestors of MDs are required to prepare a machine protection document if they are

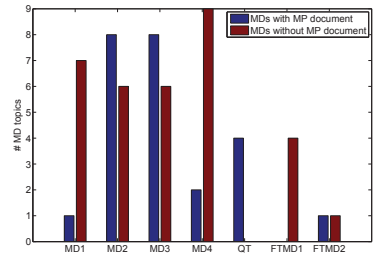

Figure 5: Comparison of the number of MD topics with and without machine protection document

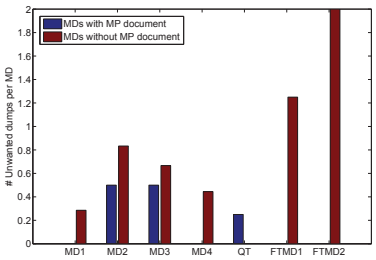

Figure 6: Comparison of number of unwanted beam dumps per MD with and without machine protection document

planning to use unsafe beam intensities with non-standard parameters and settings of machine protection devices. Figure 5 shows the comparison of the numbers of MDs with (blue) and without (red) machine protection documents during the different MD periods. In total 26 machine protection documents were prepared and approved in 2012. The discussions of the MD programs in the preparatory phase has proven to be useful for the MD and machine protection teams. It improves the safety and also the efficiency of the MDs. Figure 6 shows the number of unwanted beam dumps per MD during the different MD periods for MDs with (blue) and without (red) machine protection documents. This comparison indicates that the preparation of a machine protection document can even improve the efficiency of the MD.

Especially during MD4 a number of last minute MD program and parameter changes were requested. The short preparation and discussion time made it difficult to discover possible dangers, perform pre-tests with the requested parameter space in the LHC with safe beam intensities and go through the agreed approval process before the actual MD.

For after LS1 it is therefore proposed to request for every MD an updated program including beam parameters, thresholds and settings for machine protection relevant systems and devices. It is currently under discussion if interlocks on the specified beam parameters could be implemented for each MD in the SIS, to avoid on the spot changes of relevant beam parameters or machine protection device settings.

PROPOSED CHANGES IN THE MACHINE PROTECTION SYSTEMS DURING LS1

Following the discovered issues in the LHC beam dumping system a redundant channel from the beam interlock system (BIS) to the LBDS re-triggering line will be implemented during LS1 to create a redundancy for the triggering synchronization unit of the LBDS. Furthermore it is required to implement a measurement and interlocking on the change of the beam intensity, called DIDT, during LS1. This interlock will bring an additional redundancy for the BLM system in case of fast beam losses. Such a system has already been proposed for the LHC in 2004 and a prototype system has successfully been tested with a detection principle developed by DESY.

Due to the experienced issues with the BSRTs it is proposed to develop a redundant monitoring of the abort gap population during LS1. Studies in ALICE and with diamond particle detectors are ongoing. Furthermore it is proposed to implement automatic consistency checks for collimator settings - in the ring as well as in the transfer lines. These checks should also take the implemented optics into account. Finally it is proposed to automatically monitor the aperture in the LHC ring and transfer lines and warn the operators if defined thresholds are violated.

CONCLUSION

In 2012 more than 1000 clean beam dumps have been performed. The majority of beam dumps above 450 GeV/c have been performed with beam energies above 100 MJ. No beam induced quenches of superconducting magnets have been observed at top energy. These results are mainly due to the reliable and efficient functioning machine protection systems, the due diligence of the equipment teams, operations, (r)MPP and the coordinators.

Still weaknesses in procedures and machine protection systems were discovered during the LHC run 2012. The response of the coordinators, operations and (r)MPP to the discovered issues was adequate.

Machine protection procedures for machine developments worked in general well, but recently too many last minute program and parameter changes were requested. This can potentially put the LHC in unnecessary danger. Machine protection check lists proved their importance as prerequisite during the intensity increase and for documenting machine protection issues of the different systems during the full running period.

REFERENCES

[1] B. Todd et al. A LOOK BACK ON 2012 LHC AVAILABILITY. In *Proceedings of LHC Beam Operation workshop - Evian 2012*, 2012.

[2] D. Wollmann. Machine Protection Systems - Performance and Issues 2012, 71st MPP: http://lhc-mpwg.web.cern.ch/lhc-mpwg/.

OPERATIONAL CYCLE

Matteo Solfaroli Camillocci, CERN, Geneva, Switzerland

Abstract

The LHC has been successfully operated at 4 TeV during 2012 run. An analysis of the critical points of the standard operational cycle has been made, aiming at increasing the performance and the efficiency of the machine. An outlook at the changes that will be faced with the 7 TeV operation after LS1 is given, with particular attention at some possible scenarios. A consideration on the differences of the magnetic behavior is also made.

2012 LHC COMMISSIONING

2012 LHC commissioning was very effective. Only 2 days after the first beam injection, the first ramp at 4 TeV was carried out and only 20 days later, stable beams was declared for the first time with 3x3 proton bunches in the machine. This operation was done in perfect agreement with the planning and the physics program started on the foreseen date.

2012 operational changes

In order to increase the operational performance and diminish the time of the standard cycle of the LHC, thus raising the integrated luminosity, quite a few changes had been made with respect to 2011 operation. These major modifications had an impact on the commissioning time:

- Ramp to 4 TeV;
- B3 decay compensation at flattop separated from the ramp of the other circuits;
- ATLAS and CMS interaction points squeezed to 0.6 cm beta*;
- Further optimization of optics distribution during the squeeze;
- LHCb collision planes were tilted.

Ramp at 4 TeV

The first ramp with beam was carried out only 2 days after the first injection in the LHC; both pilots arrived at 4 TeV and B2 was dumped after few minutes at flattop due to a glitch on the safe beam flag. As well as the 2011 ramp, most of the orbit and tune changes were found around 1 TeV. Few more ramps have been performed in order to measure chromaticity, tune and orbit then calculate and feed-forward their corrections. Some minor tune spikes are still present during the snapback and they will be further analyzed during LS1.

A big time gain was obtained by the separation of the B3 decay compensation at flattop from the ramp settings. As it can be seen in Fig.1 this was achieved by separating the settings of the spool piece power converters from the others of the machine. This allowed starting the squeeze while the B3 decay compensation is still ongoing, with the result of a gain of about 15 minutes per cycle.

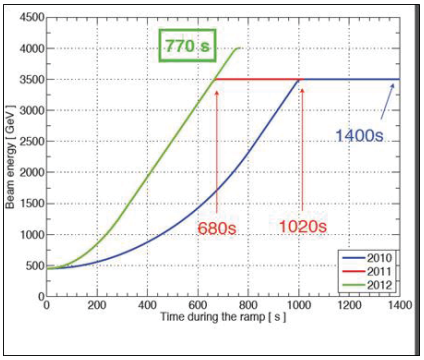

Figure 1: Comparison of the ramp power converter settings in the last 3 years of operation.

Squeeze

Two major changes in the squeeze strategy have been made in 2012.

In the light of 2011 experience the matched points distribution was optimized, by eliminating some points and by permitting different β* values in the IPs; this allowed to consistently reduce the squeeze time. Nevertheless, the global length of the squeeze passed from 475 seconds to 925 seconds due to the change in final β* from 1.5 meter to 60 centimeters.

In 2011 some orbit spikes of about 0.1mm r.m.s. were observed around the matched points. In order to increase the reproducibility of the machine and the stability of the beams, the smoothing of the K functions was changed and the amplitude of the orbit spikes strongly diminished, as shown in Fig.2.

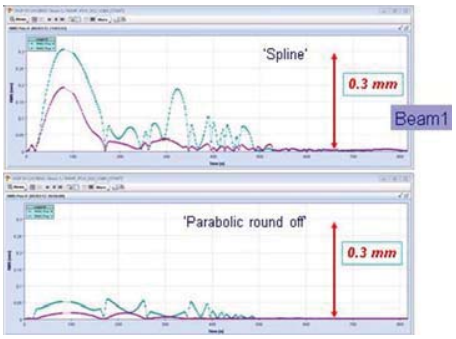

Figure 2: Amplitude of the orbit spikes with different smoothing of the K function.

Optics

Optics measurements were performed at flattop and at different matched points during the squeeze to calculate the corrections to be implemented.

Around 20% of peak beta-beating was found at 4 TeV, very well compatible with the values found on 2011 operation at 3.5 TeV.

At the end of squeeze (60 centimeters β* in IP1 and IP5), very large values of beta-beating were found, up to 100%. A very accurate correction calculation and implementation allowed reducing this value up to 7%, ensuring very high machine performance [1].

Collisions

The commissioning of the collision beam process has been a bit laborious due to the tilting process of the LHCb collision planes, which resulted in an increase of time from 56 seconds to 220 seconds. In particular, the orbit drift while collapsing the separation bumps was as large as 100 μm, but was reduced up to about 30 μm after feed-forward.

2012 LHC OPERATIONAL CYCLE

With the aim to define the best strategy to be used when operating the machine at 7 TeV after LS1, an analysis of the different phases of the cycle was done and used to estimate the expected changes.

A homogeneous set of fill was taken as sample: only physics fills with more than 1000 bunches and 60 centimeter β*. For the fills in the sample, the average of time spent for each beam mode (excluding "Rampdown" and "setup" as their declaration is not consistent from one fill to another and their length is strongly affected by the presence of hardware faults) was calculated.

The result of the analysis is shown in Tab.1

Table 1: Average beam mode time in 2012 operation

Beam mode	Theor	Mean	Comparison
INJPRO	n.a.	52 min	~0.86 h
INJPHYS	n.a.		
PRERAMP	n.a.	259	259
RAMP	770	791	21
FLATTOP	n.a.	377	377
SQUEEZE	925	996	76
ADJUST	220	513	293
RAMPDOWN	2100		
TOT		1h41	
TOT (with rampdown)		2h16m	

In Tab.1, the second column contains (where applicable) the length of the beam process settings for the hardware; the third column shows the mean value for 2012 operation (in seconds) and the last column shows the time spent in the beam mode that exceed the settings length; this last value is meant to be used for comparison with the previous years data when the settings time was different.

The comparison with the data of 2010 and 2011 shows a strong improvement. The global cycle time was reduced by almost a factor 2 between 2010 and 2011 [2] [3] and further by 21% in 2012, despite all changes implemented to increase the LHC performance.

OPERATIONAL CYCLE AFTER LS1

After the consolidation foreseen for LS1, the LHC will be operated at an energy close to 7 TeV. The settings for the machine hardware can be easily calculated; in this analysis it was assumed an operational energy of 6.5 TeV. The following cycle has been taken into account:

- Injection at 11 m;
- Ramp to 6.5 TeV;
- Squeeze to 40/45 cm β*;
- Collisions (with tilted planes in IP8);
- Rampdown.

Estimating the length of the cycle from the 2012 analysis is easy, although not fully exhaustive. The calculation shows a hypothetical increase of about 51 minutes (37%), mostly dominated by the rampdown time. This means more than 3 hours cycle, which would decrease the efficiency of the LHC.

Many different options are possible for post LS1 operation and are being considered to improve the quality of the physics production. Some of these options would also affect the cycle time like combining ramp and squeeze or performing beta star leveling as well as beam injection at a lower beta. Some other options like colliding while squeezing, flat beams or 25 ns beam would improve stability or luminosity, but do not impact the LHC cycle time.

In the view of a speculative analysis, the most aggressive scenario was considered to estimate the shortest possible cycle:

- Injection at 5 m (with collision tunes);
- Ramp & Squeeze to 6.5 TeV / 1 m;
- Collisions without LHCb tilting;
- Beta* levelling from 1 m.

The estimated time length for each beam process would result in a 29 minutes (15%) shorter length with respect to the standard scenario of post LS1 operation. Nevertheless, it is important to notice that these changes are presently under study as they have machine protection implications that might make them not suitable for operation.

Some other important aspects have to been taken into account when studying the after LS1 operation scenario. At 6.5 TeV, the dipole magnets are expected to enter a week saturation regime; the dynamics effects are expected to double; the decay and snapback of tune and

chromaticity will also have to be carefully measured and corrected. The precycle will also change: it has to be done at 6.5 TeV, which would result in about a factor 2 increase in time.
A bigger impact could come from a further squeeze to 40 centimeters β*; in this case, in fact, the precision of the model of the interaction region quadrupoles is critical. The MQM and MQY magnets are less problematic as they will go down in current; the hysteresis effect is known and can be implemented in the functions. The inner triplet magnets represent the major problem, as they will be operated in a large saturation regime and the precision of measurements and models could not be enough for operation.

CONCLUSIONS

At the end of the analysis some conclusions can be drawn.

The 2012 commissioning and operation were very effective. The machine is very reproducible and the operational time has been improved so much that it is now approaching the limit given by the hardware setting; however, some part of the cycle like flattop and rampdown can still be improved. Despite the longer settings and more complex operational envelope the LHC has been operated in 2012 on an average of 36 minutes less per fill; a big improvement was in the time spent to inject the beams from the SPS.

The post LS1 operation will be a challenge and the strategy taken can drastically change the efficiency of the machine. The higher operational energy will result in a consistent time increase that can be limited depending on the envelope chosen up to about 15%.

It is for all these reasons important to converge quickly on a strategy in order to carefully and properly prepare after LS1 operation. The analysis proposed suggests to start as a baseline with the well known 6.5 TeV standard cycle, then steer the strategy during the first year of operation.

ACKNOWLEDGMENT

The author wishes to express his sincerest thanks for the useful discussion, corrections and suggestions to the operation team, the FIDEL team and the optic measurements team.

REFERENCES

[1] R.Tomas & al. “Record low β beating in the LHC”, Phys. Rev. ST Accel. Beams 15, 091001
[2] S.Redaelli “How to improve turnaround”, 2010 LHC Beam operation workshop, proceedings
[3] W.Venturini “Turnaround - analysis, Possible improvements, combined R&S, precycles, injection”, 2011 LHC Beam operation workshop, proceedings

SQUEEZING WITH COLLIDING BEAMS

X. Buffat (EPFL, Lausanne; CERN, Geneva), W. Herr, M. Lamont, T. Pieloni, S. Redaelli, J. Wenninger (CERN, Geneva)

Abstract

There are two main reasons why performing the squeeze with colliding beams may be beneficial for the operation of the LHC after LS1. First, this procedure allows to achieve luminosity leveling in a robust way on a large range, pros and cons of this technique are being compared to luminosity leveling with a transverse offset at the interaction point. Secondly, recent observations suggest that the beams brightness is already limited by impedance driven instabilities. It may be greatly beneficial for the beam stability to profit from the tune spread provided by head-on beam-beam collision, which is significantly larger than the one provided by the octupoles. The two options have different consequences on the operation of the LHC, both are being discussed based on 2012 operational experience and MD results.

INTRODUCTION

The possibility to squeeze with colliding beam, whereas very simple from the conceptual point of view, has many implication on the operation of the LHC. Indeed, good control of the orbit at the Interaction Points (IPs) is required to maintain the beams in collision during the procedure. The current implementation of the LHC control system uses the concept of Beam Process (BP) to operate the squeeze. The BP contains functions to be played by the power converters, collimators and RF systems for a fixed sequence of optics changes defined in advance. This implementation does not allow to have the flexibility required for Luminosity Leveling (LL) independently in all IPs. Different options to overcome the difficulties of LL with β^* will be discussed.
As discussed in [1], instabilities at the end of the squeeze have been limiting the beam brightness during the 2012 run of the LHC and are linked to some tens of beam dumps due to beam losses during the squeeze and adjust [8]. The combined effect of the transverse feedback, landau octupoles and high chromaticity does not seem to be sufficient to suppress the instability. However, the instability immediately disappears when the beams are brought into collision, which indicates that the Landau damping provided by head-on collision is far more efficient to suppress instabilities [2, 3]. The possibility to overcome this limitation of beam brightness by colliding during the squeeze is discussed in this paper.

ORBIT STABILITY AT THE IP

The key to reliably operate the betatron squeeze with colliding beams is the stability of the orbit at the IPs. Indeed, it has been shown that the stability diagram from head-on collision is drastically reduced when colliding with an offset in the order of 1 σ_{RMS} [3]. A series of experiment was performed in order to demonstrate that the squeeze can be executed with the required orbit stability at the IPs.

MD results

In a first attempt, the machine was filled with two bunches per beam with intensities approximately $1.3 \cdot 10^{11}$ proton per bunch and normalized emittances around 1.6 μm, the standard operational sequence was executed up to the $\beta^*=$ 3 m step of the squeeze. The beams were then brought into collision in IP1 and 5. The rest of the squeeze BP has then been executed in steps down to $\beta^*=$ 0.6 m. The tune feedback was turn off during the procedure, while the orbit feedback was on during the execution of the squeeze steps. After each step, a luminosity optimization was performed and the resulting corrections incorporated. The specific luminosity measurement during this procedure is shown in Fig. 1. The degradation of the luminosity observed during the execution of each step is due to the drift of the orbit at the IPs. The expected luminosity is then recovered by an optimization of the collision point, as shown by Fig. 2 which compares the optimized luminosity for each step of the squeeze during the squeeze to the computed one. The separation between the beams at each IP can then be computed from the luminosity (Fig. 3a), assuming a negligible variation of the beams emittance, which is consistent with the measurement. The variation of the separation during this first attempt would not be compatible with the usage of head-on collision during the squeeze to stabilize the beams, which requires the offset to remain below $\sim 1\,\sigma$ in order to maintain a sufficiently large tune spread. This is confirmed by the observation of an instability before the last step of the squeeze. It is necessary to test the reproducibility of the corrections applied, in order to ensure smaller orbit variation at the IPs. Therefore, the same procedure was re-run three weeks later, once with a single bunch and then with a train of 36 bunches. During these tests, the maximum drift of the separation stayed below 1 σ during the squeeze (Fig. 3b-3c), demonstrating the long term reproducibility of the corrections applied. [4]

In order to get a deeper understanding of the operational options that would allow to reliably keep the beams in collision during the squeeze, it was tried, 3 months later, to go through a larger β^* range, from $\beta^*=$ 9 m down to $\beta^*=$ 0.6 m, with colliding beams. It was hoped that the corrections applied in the last part of the squeeze during the first tests will still be valid. This was however not the case, as

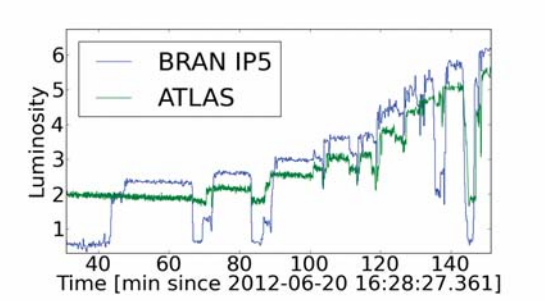

Figure 1: Luminosity during first attempt of β^* leveling

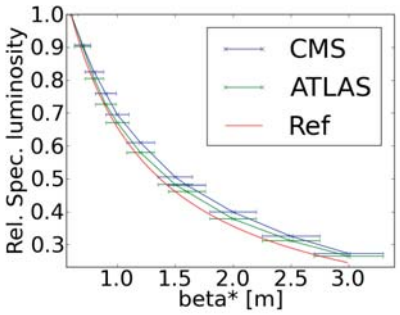

Figure 2: Measured and expected specific luminosity reduction due to β^*.

separations up to 2σ were observed during the procedure. This points out that a careful setup of the orbit has to be performed, and possibly orbit corrections cleaning have to performed from time to time, to account for the slow mechanical movement of the different element of the machine [5].
If the resolution of the Beam Position Monitors (BPMs) permits, one could use the two BPMWF located on each side of the IPs to measure the beam separation and possibly use this information in the orbit feed back. The measured beam separation during this last experiment is rather encouraging (Fig. 4).

Reproducibility in standard operation

Fig. 5 shows the orbit corrections at the IPs that had to be applied to optimize the luminosity at the end of the squeeze during physics fills of the 2012 run. One observes a slow drift over the year, even though significant, this drift is not problematic. Indeed, the average fill to fill differences mainly remain within acceptable boundaries (Tab. 1). The distribution of these differences, on Fig. 5b,

	IP1	IP2
Horz.	0.3 ± 6.7	0.3 ± 5.7
Vert.	-0.5 ± 5.5	-0.1 ± 5.4

Table 1: Average fill to fill difference of the orbit correction required to optimize the luminosity in each IP1 and 5 in μm

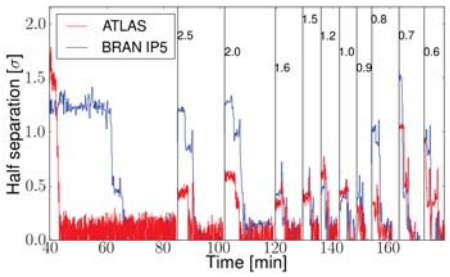

(a) 1st attempt

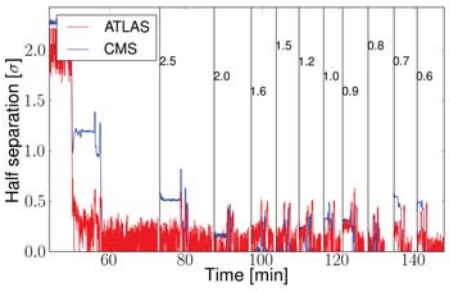

(b) 2nd attempt

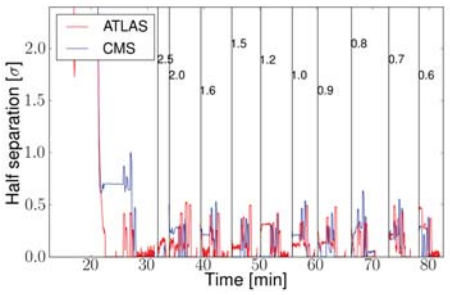

(c) 3rd attempt

Figure 3: Transverse separation at the IP from measured luminosity reduction factor.

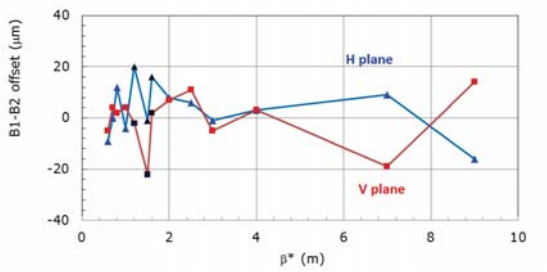

Figure 4: Beam separation at the interaction point interpolated from adjacent beam position monitors

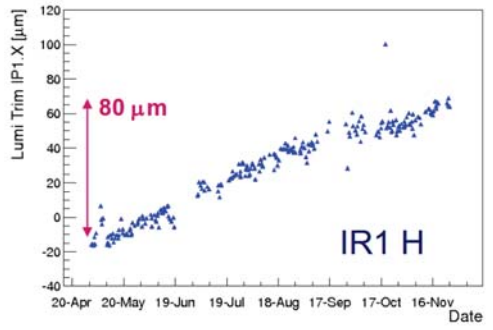

(a) Time dependence

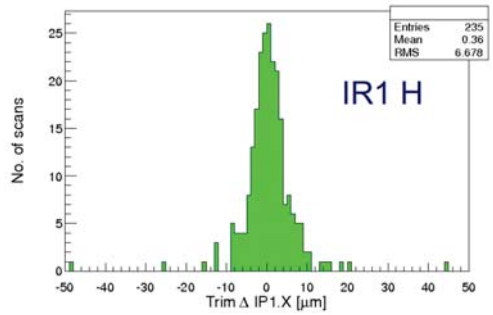

(b) Distribution of fill to fill differences

Figure 5: Correction of the orbit at the IP from luminosity optimisation during the 2012 run.

shows the existence of some outliers, during which the separation became larger than a few σ's. This implies that, whereas most of the time a feed forward procedure would be sufficient, the orbit at the IPs may not behave well during a few fills. In order to define a robust operational procedure, these cases, even though of limited amount, should not be neglected and therefore the effect of the lack of reproducibility for certain fills should be minimized.

To that purpose, one could consider the options of using an automatized luminosity optimization after each squeeze step or at least for a subset of them. This multiple optimization of the luminosity constitute a significant overhead compared to the current squeeze and may require some minor changes in the implementation of the settings management. One can however expect that practical experience will lead to a good balance between robustness and overhead. In particular, the possibility to use BPM data may be of great help in maintaining the beams in collision, in the cases where the machine reproducibility is not sufficient.

CONTROLS ASPECTS

The implications on the controls when imposing collisions during the squeeze largely depend on the aim that is targeted. Different scenarios have been sketched, they do not however represent the full set of possibilities. It is clear that a precise scenario that suits the needs of the experiments and maximizes the operational efficiency has to be worked out.

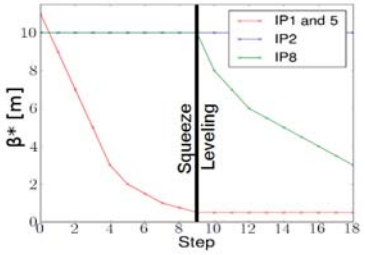

(a) β^*LL only in IP8

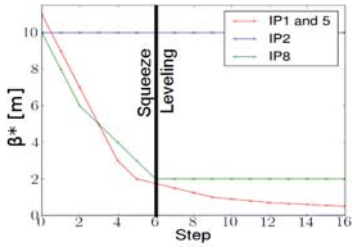

(b) β^*LL synchronously in IP1&5

Figure 6: Two examples of squeeze sequence for β^*LL with low flexibility.

Up to now, the squeeze has been operated in predefined series of step, from one Matched Point (MP) to the next, each corresponding to defined values of β^* in the different IPs, that varies towards the targeted values. The sequence of MPs defines the squeeze BP, which is being played during each fill. The BP contains both global and local machine settings and corrections along the procedure [6], its full commissioning is not trivial. Therefore, the current control system does not allow to easily change the sequence of β^* configurations. We, therefore, distinguish two cases, whether the flexibility in the choice of β^* in each IP as a function of time is required or not.

Low flexibility scenario

We are considering cases where a high flexibility in the choice of β^* in each IP is not required, e.g. if head-on collision during the squeeze is required for stability reasons or in the case where the sequence of β^*s could be defined in advance and run synchronously in the IPs. There are various scenarios in which this could be the case, two of them is pictured on Fig. 6
In this cases, the present control system is appropriate, as one can define a BP and play it in steps, as it has been done during the MDs presented above. Only minor changes have to be implemented such as to maximize the operational efficiency and robustness, as already discussed in section *Reproducibility in standard operation*.

High flexibility scenario

In the case where each IP requires to change β^* at anytime, independently from the other IPs, then the present control system is no longer appropriate. Indeed, the concept of BP is no longer applicable, since the sequence will,

a priori, be different at each run. Therefore, the global corrections defined for a specific sequence are no longer valid and a conceptual change of the control system is required. The required modifications allowing to change the optics independently in each IP are believed to be within reach. However, it is necessary to proceed with detailed studies and implementation in an early stage of the Long Shutdown 1 (LS1).

ADDITIONAL REQUIREMENTS FOR COMMISSIONING

As already mentioned, good orbit stability at the IPs is a requirement to reliably operate the squeeze with colliding beams. Based on the excellent performance of the orbit feed back system, it is not considered to operate the squeeze without it. It is possible to improve the orbit stability and in particular improve the effect of the orbit feed back by proper cleaning of the orbit corrections. Indeed, the feed back uses an SVD based method to compute the proper settings for each corrector based on the BPMs data, with specific algorithm to maximize robustness in case of noisy or faulty BPMs. These algorithm have side effects on the orbit reproducibility that can be minimized by proper correction of the orbit during the commissioning as well as regular re-correction during the year [5]. This represents an overhead of a few shifts compared to current commissioning time.
Optics corrections are now focused on the fully squeezed machine. In case β^*LL is used, the intermediate optics will require as much attention, which will cost another few shifts.

MACHINE PROTECTION

Collimator Impedance and beam stability

The LHC impedance is largely dominated by the one of the collimators [7]. The β^* reach depends on the collimator hierarchy that must be put in place to protect the triplet magnets [8, 9]. There is therefore an interest to close the collimators to the tightest achievable settings which increases the machine impedance. In 2012, the movement of the primary and secondary collimators from their settings at injection to the tight settings required at the end of the squeeze has been performed slowly during the ramp, in order to maintain the losses due to the halo scraping well below the dump threshold. This results in an increased impedance from flat top on, whereas the tight settings are strictly required only at the end of the squeeze. One could drastically reduce the beam brightness limitation due to impedance driven instabilities by moving the collimators, in particular the secondaries, to tight settings only once the beams are in collision, i.e. once the stability is ensured by the large detuning of head-on beam-beam collision. This, of course, implies that the beams are being brought into collision before the end of the squeeze, and that the scraping of the halo caused by the collimator movement is done while colliding, before or during the squeeze. Extrapolations for the experience at 4 TeV indicates that this option is in principle feasible but requires more studies. Indeed, while TCP collimators are moved into the beam, loss spikes must remain below dump and quench limits.

Collimator movement and leveling

The tertiary collimator have to be moved during the squeeze, in order to follow the modification of the crossing angle orbit bump, having important implications on machine protection in case of LL with β^*. Indeed, the full validation of the collimator settings, now only done for the last step of the squeeze, would then be required for each one of them. Moreover, collimator movement during stable beam mode were not allowed up to now. The potential machine protection issues of the transition from one step to next have to be properly addressed. If it were considered unsafe for the experiments to keep acquiring data during the leveling steps, the overhead could have a significant impact on integrated luminosity. A possible workaround is presented below, by the means of flat beams. It is however important to recall that these considerations are important only in the frame of LL, but not if colliding during the squeeze is only meant to improve the beams stability.

Flat beam option

Colliding flat beams, i.e. $\beta_x^* \neq \beta_y^*$, presents some interesting advantages when considering β^*LL. Indeed, by first fully squeezing in the crossing plane, before LL with β^* in the separation plane, one can minimize the modification of the crossing angle orbit bump, thus reducing the tertiary collimator movements during the LL procedure. Further studies are nevertheless required to fully assess the machine protection issues in this configuration. It is also important to note that this would reduce the leveling range by the square root.
There can be interests in the flat beam option from the experiments point of view, to improve detection efficiency during LL [10], which should be taken into account.
As opposed to colliding with separated beams, the separation bump is collapsed during the execution of the squeeze, leaving extra aperture in the separation plane which may be used to squeeze further, in the this plane only. The luminosity gain in the different post LS1 scenarios varies from 0 to 18% [9].
It is however important to note that, due to the lack of time, flat beam collisions were not tested in the LHC. Experience in the sp$\bar{p}$s did, however, not raise any detrimental effect from operating with flat beams [11].

CONCLUSION

Experiments have been conducted at the LHC, demonstrating the feasibility of colliding the beams during the squeeze. In particular, it has been shown that the required orbit stability at the IP can be achieved, suggesting that

the changes of the operational cycle to account for this new procedure are not out of reach. Colliding during the squeeze could improve the performance of the LHC for mainly two reasons. First, the large tune spread provided by head-on collision enhance the beam stability during the squeeze, allowing to push further the limits on beam brightness due to impedance driven instabilities. Secondly, LL with a transverse offset, while used extensively in IP8 during the 2012 run, has brought up some critical stability issues for bunches without head-on collision in any other IPs. The stability of all bunches during the LL procedure is however ensured with β^*LL. Many scenarios can be envisaged, having different implications on operation. The preferred scenario and the operational details have to be worked out, taking into account the experiments' desiderata. In order to leave appropriate time for the preparation of new software and procedures, discussions should take place early in the LS1.

REFERENCES

[1] T. Pieloni, et al., Beam stability with colliding beams at 6.5 TeV , these proceedings

[2] Presentation at LHC machine committee, `https://espace.cern.ch/lhc-machine-committee/Presentations/1/lmc_146/lmc_146e.pdf`, Aug. 2012

[3] G. Arduini, et al., Missing head-on beam-beam collisions and the effect on Landau damping, LHC project report in preparation

[4] X. Buffat, W. Herr, M. Lamont, T. Pieloni, S. Redaelli, J. Wenninger, Results of β^* luminosity leveling MD, CERN-ATS-Note-2012-071 MD

[5] X. Buffat, W. Herr, T. Pieloni, L. Ponce, S. Redaelli, J. Wenninger, MD on squeeze with colliding beams, CERN-ATS-Note-2013-002 MD

[6] S. Redaelli, et al., Betatron squeeze : status, strategy and issues, Proceedings of Evian 2010 workshop on LHC commissioning

[7] N. Mounet, The LHC transverse coupled-bunch instability, Thèse N^o 5305, EPFL, 2012

[8] B. Salvachua, Cleaning and collimator operation - outlook, these proceedings

[9] R. Bruce, Presentation at the LHC Beam Operation Commitee, `http://lhc-beam-operation-committee.web.cern.ch/lhc-beam-operation-committee/minutes/Meeting55-11_12_2012/2012.12.11--LBOC_betaStar_after_LS1.pptx`, Dec. 2012

[10] R. Jacobsson, private communication, Dec. 2012

[11] P.E. Faugeras, et al., Proposal to upgrade the luminosity of the sp$\bar{p}$s collider by a factor 2, CERN SPS/89-18 (DI)

SPECTROMETER OPERATION IN IR2 & IR8

B.J. Holzer, BE-ABP

CERN, Geneva, Switzerland

ABSTRACT

It is well known that the spectrometer dipoles of ALICE and LHCb have a considerably larger and more challenging impact on the LHC beams than the magnets in the high luminosity regions. The presentation summarises the basic layout of these devices, including the compensation of their fields and shows the theoretically expected beam orbits, envelopes and aperture needs. In addition the experience on beam will be presented for standard operation, but mainly in case of polarity flips. Possible scenarios for future operation in the context of faster and more transparent operation will be discussed. The special problem of 25ns operation together with the so-called negative LHCb polarity will be addressed as well as the latest results from aperture measurements performed during the machine development block MD#4 to decide on possible vertical crossing angle operation in IP8 at injection energy.

ALICE - IP2

The layout of the lattice of LHC in IR2 is shown in Fig.1. Ignoring for a moment the fact that the injection for beam 1 is included in the design, the layout of the straight section and the machine geometry is the same as in the other interaction regions where beam collisions take place - IR1, 5, 8 - [1]. A major difference however arises from the fact that the main magnet of the ALICE experiment is a spectrometer dipole, acting in the vertical plane and being operated during the complete LHC procedures from injection to collisions at full field. Compensator magnets, located within the drift space in front of the triplet magnets are used to counter balance the effect on the two counter rotating beams. Still the overall effect is an energy-dependent vertical crossing angle between the two beams.

At injection energy, 450 GeV, the spectrometer field creates a half crossing angle of y' = ±1089 µrad, at 4TeV (the maximum energy in the run year 2012), y'=±122.5µrad are obtained with the signs referring to the two counter rotating beams. Under usual conditions the ALICE operation requires a change of the dipole polarity once per run-mode, i.e. for standard p-p collisions in LHC once per year. Fig 2 shows the ALICE dipole before its installation into the experiment.

Fig 2: ALICE spectrometer dipole

For the operation of the machine the effect of the ALICE dipole has a number of implications that has to be taken into account. At injection and during the ramp, beam collisions have to be avoided at the interaction point (IP) and at any possible parasitic encounter. Therefore in addition to the crossing angle bump that is created by the ALICE magnets (the so-called *internal* bump) a horizontal symmetric bump is applied to separate the beams in the horizontal plane and an external vertical angle bump to guarantee sufficient separation at the parasitic encounters. Both external bumps are created by the LHC standard orbit corrector coils, located near the quadrupoles Q4...Q6.

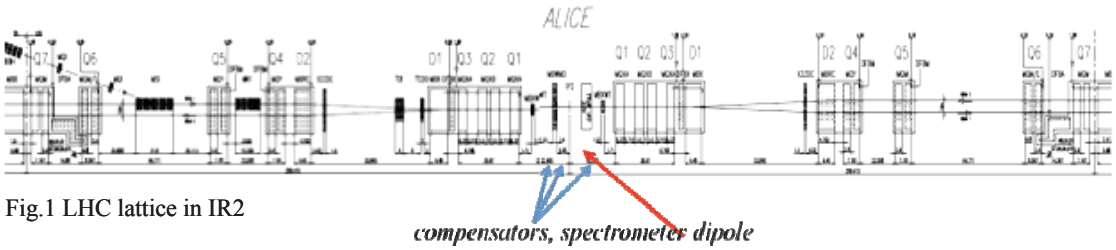

Fig.1 LHC lattice in IR2

Proton-Proton Operation

Table 1 summarises the effect of the different bumps that are applied at injection energy during the typical 2012 run. Clear enough, for any beam energy and the corresponding beam emittance a compromise has to be found between maximum possible beam separation and available aperture. The beam orbits that are created by these combined effects are plotted in Fig. 3. They refer to the standard injection optics, i.e. β^*=10m and a typical value of ε_n=2.5μmrad for the normalised emittance in both transverse planes.

Table 1: Effect of internal and external bumps in IR2 at 450 GeV injection energy

E=450 GeV		
spectr. dipole	y'	±1089μrad
ext. vert. crossing angle	y'	±170μrad
ext. hor. separation	Δx	±2mm

The vertical dotted lines in the plot show the position of the parasitic encounters for 50ns bunch spacing [2].

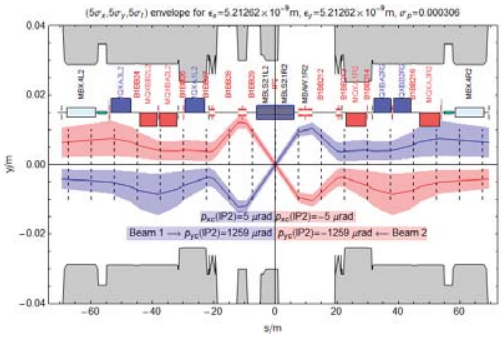

Fig 3: vertical orbit at LHC injection. under the influence of the ALICE spectrometer dipole and the external crossing angle bump.

The beam envelopes in the plot refer to 5 sigma beam size and show that a sufficient (i.e. more than 10 σ) separation is obtained at any bunch encounter.

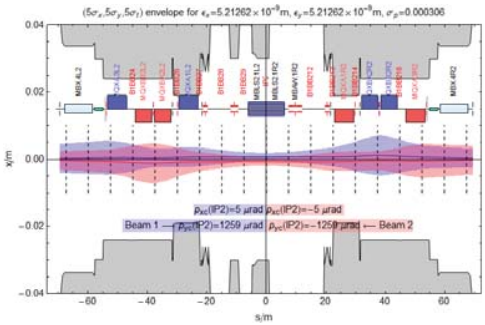

Fig 4: horizontal orbit in IR2 as result of the separation bump at LHC injection.

At 4 TeV luminosity operation the situation looks different: the hor. separation bump has to be collapsed to allow for collisions at the IP. In addition he ALICE internal bump scales down as 1/γ due to the constant magnet field and the external vertical crossing angle bump is optimised to obtain sufficient separation at the parasitic encounters, for the luminosity optics with β^*=3m and an absolute emittance of $\varepsilon_0=6.6*10^{-10}$ radm, given at that energy. It should be pointed out that in p-p operation mode, the external crossing angle bump is always chosen to support the crossing angle of the ALICE dipole.

E=4 TeV		
spectr. dipole	y'	±122.5μrad
ext. vert. crossing angle	y'	±145μrad
ext. hor. separation	Δx	0 mm

Table 2: Effect of internal and external bumps in IR2 at 4 TeV collision energy

For systematic reasons a polarity switch of the ALICE dipole is needed, to guarantee equal integrated luminosities in both spectrometer polarities. Therefore once per beam mode (p-p, Pb-Pb p-Pb or Pb-p) the polarity has to be changed and accordingly the external vertical bump. The impact on the LHCoperation is small as it leads to a quasi symmetric situation and no major impact is observed on the overall beam orbits - outside the bump regions. However - as indicated schematically by green dashed lines in Fig. 5 the tertiary collimators, TCT, have to be re-aligned for all LHC settings: injection, flat top and collision mode.

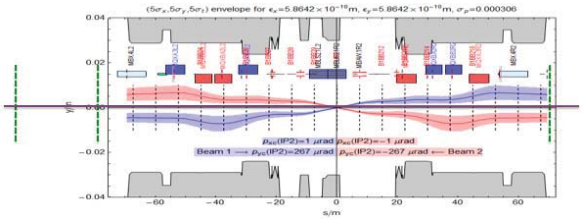

Fig 5: position of the TCT collimators: for operation with reverted ALICE polarity the beam orbits will be interchanged and the TCTs have to be re-aligned.

Proton-Pb Operation

In the run year 2013 a special operation mode using proton-lead collisions is foreseen. At injection the orbit situation is unchanged and the parameters of the separation and crossing angle bumps are the same as in table 1.

In collision however some modifications have to be taken into account: the beam optics will establish an optical function of β^*=0.8m at the IP and for reasons of

the detector acceptance the effective crossing angle has to be kept as small as possible [3]. The external vertical crossing angle bump therefore is used to counteract the internal spectrometer bump. The settings foreseen are summarised in table 3.

Table 3: Internal and external bump in IR2 at 4 TeV p-Pb operation

beam optics 4TeV	β*=80cm	
spectr. dipole	y'	+/-122.5µrad
ext. vert. crossing angle	y'	-/+ 62.5µrad

A new procedure is proposed for the polarity change of the ALICE dipole in this operation mode [4]: to save time and effort it is planned in case of a polarity switch to keep the external crossing angle at injection and during acceleration the same. The larger bunch distance of at least Δs=200ns will allow that kind of operation. Only at the end of the squeeze procedure the external vertical bump will be set to ±62.5 µrad, and as explained before counteract the spectrometer angle to keep the overall angle small. The advantage is that only in the collision mode the TCT collimators will have to be realigned, which saves time and effort. At injection and during acceleration the orbits outside the ALICE compensators will be untouched and the TCT settings are independent of the polarity. The drawback is that during the procedure of changing the external bump, a small beam separation of not more than 1σ cannot be avoided. It has been shown in machine studies with Pb-Pb in 2011 however that due to the limited bunch intensities foreseen in p-Pb mode the beam-beam effect is still small enough to be neglected.

In summary the foreseen procedure will be:

- injection: set external bump from y'=+170 to +145µrad at flat top independent of the spectrometer polarity
- collision: change external bump to ±62.5µrad with the sign chosen to counteract the spectrometer angle
- leading to an effective crossing angle of ±60µrad

LHC-B - IP8

While the accelerator lattice situation in IR8 is quite similar to the one in IR2 - a dipole spectrometer magnet and three compensator magnets that form a closed crossing angle bump (Fig 6) - there is an important qualitative difference between the two experiments: the LHCb dipole magnet deflects the LHC beams in the horizontal plane. And thus has a large impact on the beam crossing geometry, which is by the nature of the storage ring layout designed in the horizontal plane.

This in principle trivial statement has a large impact on the possible running scenarios for the LHCb experiment and therefore we dare to redraw the overall geometry of the LHC storage ring in Fig 7.

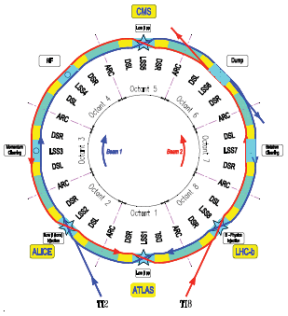

Fig. 7: LHC geometry

Under the influence of the separator / combiner dipoles D1 and D2 beam 1 is deflected in IR8 to the inner side of the ring, and accordingly will have an overall negative crossing angle. The layout of IR8, including the position of the LHCb dipole and its three compensators is shown in Fig. 6 and Fig 8 gives an impression of the LHCb spectrometer dipole magent.

As in the case of IR2, the LHCb dipole magnet is operated at constant field and so its influence is largest at LHC injection energy. However the field direction leads to a horizontal deflection of the LHC beams and the magnet strength is considerably stronger than in the case of ALICE.

Fig 8: LHCb spectrometer magnet

At injection energy and during acceleration, bunch collisions at the IP as well as at the parasitic encounters have to be avoided and thus the internal horizontal crossing angle provided by the experiment is supported by an external hor. crossing angle bump and a vertical parallel beam separation. Table 4 summarises the values.

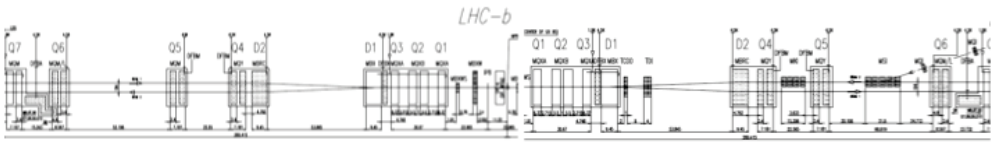

Fig 6 Lattice in IP8

Table 4: IR8 bumps at injection

E=450 GeV		
spectr. dipole	x'	±2100μrad
ext. hor. crossing angle	x'	±170μrad
ext. vert. separation	Δy	±2mm

As the LHCb dipole is powered at constant field, the deflecting effect on the beam scales down as 1/γ and at the flat top energy of 4TeV, used in 2012, we get a remaining crossing angle of x'=±235μrad.
The geometry of the beam orbits during collisions however looks quite different. While the vertical beam separation is collapsed to provide collisions at the interaction point, the horizontal external crossing angle bump is replaced by an equivalent vertical one, leading finally to a diagonal crossing plane [5]. This scheme, including the so-called diagonal levelling had been established and used routinely during the 2012 run in both LHCb polarities without problems. Difficulties arise however at LHC injection energy if the LHCb dipole is powered with "negative" polarity. Standard settings foresee a vertical separation of the beams of Δy=2mm at the IP, an internal crossing angle of 2.1mrad created by the LHCb dipole and its compensators and an additional external horizontal crossing angle of 170μrad. This combination allows for LHCb in "positive" polarity sufficient separation of the two beams at the IP and any parasitic encounter. The vertical and horizontal orbit and the beam envelopes, calculated for a normalised emittance of ε=3.0μradm and referring to 5 σ, are shown in Fig 9 and 10. The crosses in the plots indicate the location of the possible parasitic encounters for a bunch distance of 25ns - as planned for the next LHC run after LS1.

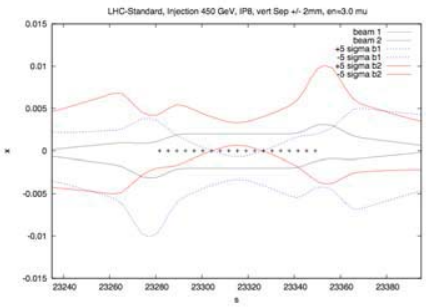

Fig 9: A parallel separation in the vert. plane delivers at injection 2mm beam separation at the IP and sufficient (more than 10σ) distance between the beams at the first three parasitic encounters

If on the contrary, LHCb is powered in "negative" polarity, the internal bump leads to a positive angle in beam 1 at IP8, deflecting the beam 1 to the outer side of the ring. This effect is balanced out by the LHCb compensator magnets, which bend the beam back to the inner side of the storage ring (Fig 11).

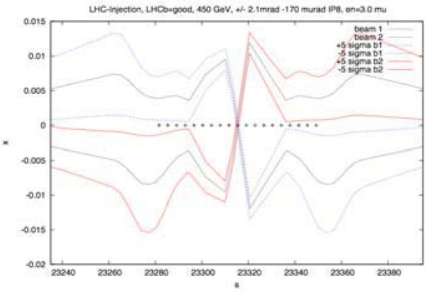

Fig 10: The horizontal beam orbits at injection are determined by the internal LHCb bump, x'=2.1mrad, and the external crossing angle bump. The net angle therefore depends on the LHCb polarity. The plot refers to the LHCb polarity that creates a negative angle of beam 1 in IP8, which corresponds to the "natural" geometry of the machine (see Fig 7).

However, due to the negative LHCb polarity, a second cross over, after the beam crossing at the IP cannot be avoided. For a bunch distance of Δs=50ns this cross over had been placed between two bunch locations.

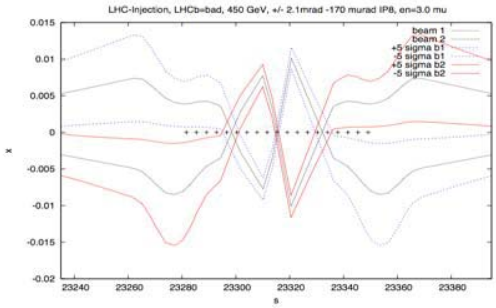

Fig 11: The horizontal beam orbits for the case of "negative" LHCb polarity. Beam 1 (blue) is deflected to the outer side of the ring, bent back by the LHCb compensators and crosses over with beam 2 before the separator dipoles D1 can take over. For 25ns operation this situation leads to detrimental collisions at injection and on the ramp.

In the case of the planned 25ns operation, this cross over will lead to beam collisions, that have to be avoided at injection and during the complete acceleration procedure. Therefore it is proposed here for injection and ramp to apply a different scheme: the unavoidable internal crossing angle bump will be combined with a horizontal separation of 2mm and a vertical external crossing angle bump. In a first step the situation had been studied with a vertical angle of y'=±170μrad, corresponding to the present horizontal situation (see table 5).

Table 5: new proposed crossing / separation scheme, the values correspond to the first test and are not applicable for the real machine.

E=450 GeV		
spcctr. dipole	x'	±2100μrad
ext. hor. separation	Δx	±2mm
ext. vert. crossing angle	y'	±170μrad

The orbits and beam envelopes are plotted in Fig. 12 - 14. As before the combination of separation and internal / external crossing angles avoid successfully bunch crossings at any encounter.

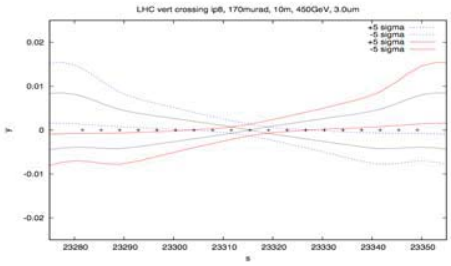

Fig 12: Beam orbits and 5σ envelopes in the vertical plane for the new proposed scheme. The applied vertical crossing angle avoids collisions already after the second parasitic encounter.

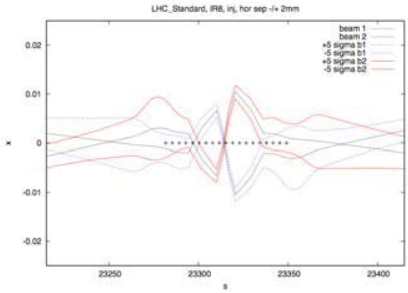

Fig 13: Beam orbits and 5σ envelopes in the horizontal plane for the new proposed scheme: the internal LHCb bump is powered in "positive" polarity. Beam separation is guaranteed by the crossing angle between parasitic encounters #2...#5. In addition the parallel horizontal separation of 2mm avoids collisions at the IP.

The plots of Figs 12-14 should directly be compared to the ones of the present scheme, Fig 8, 9. To complete the analysis of the new proposed crossing scheme for 25ns iteration, the LHC aperture model has been used to study the effect of the new bumps. Knowing, that in IP8 the beam screen in the mini beta triplets is oriented in the horizontal plane, and concluding that considerably more aperture is available in this plane compared to the vertical one, it is no surprise that the large vertical crossing angle that has been studied here as a first step, leads to considerable reduction in free aperture.

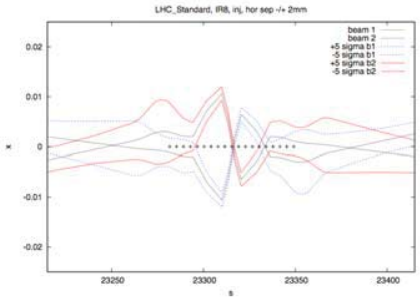

Fig 14: Beam orbits and 5σ envelopes in the horizontal plane for the new proposed scheme: the internal LHCb bump is powered in "negative" polarity, leading as before to a cross over. However due to the vertical crossing angle applied at the same time sufficient beam separation is guaranteed at that position in the vertical plane and the problem of unwanted collisions has been overcome.

The LHC beam screen that limits - inside the triplet - the free aperture to 29mm*24mm radius is shown in Fig. 15 and the result of the aperture calculations for the new proposed crossing scheme at 450 GeV injection and expressed in "n1" units is plotted in Fig 16. For comparison the LHC standard situation for the same energy and beam optics is shown in Fig 17.

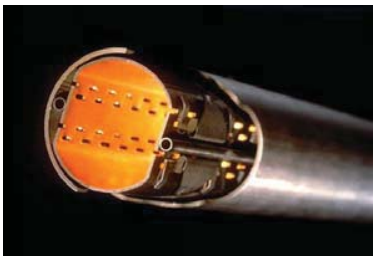

Fig 15: LHC beam screen, which is oriented in IR8 along the horizontal plane, leading to some aperture restrictions if a large vertical crossing angle is applied.

The considerable vertical angle of y'=±170μrad in IP8 leads to an aperture reduction from n1=7 to n1≈4.5, which is considered as not a marginal effect.

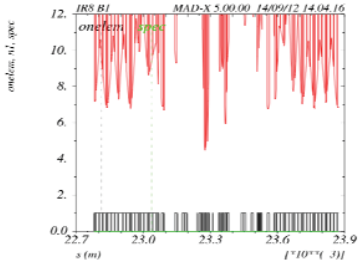

Fig 16: Aperture calculation - in units of "n1" for the new vertical crossing bump configuration

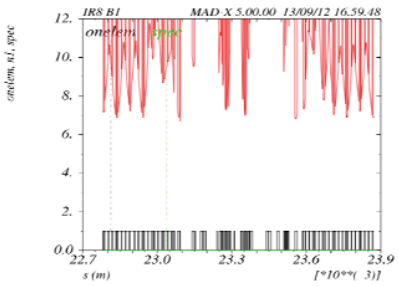

Fig 17: For comparison the figure shows - under the same conditions - the n1 aperture for the present horizontal crossing angle bump

To optimise the situation and regain free aperture, several issues have been studied:

- the use of the orbit correctors "mcbx" in the triplet magnets to flatten the crossing angle bump
- the reduction of the vertical crossing angle bump to the real needed beam separation
- a calculation of the aperture using more realistic values in the aperture model for the orbit fluctuations and beam emittances.

The effect of the first step mentioned, namely the use of the triple correctors to optimise the shape of the vertical crossing angle bump, is visualised in Fig 18. It is proposed to power the mcbx correctors in the first triplet quadrupole "Q1" in a way that - after reaching sufficient separation at the entrance of the triplet quadrupoles the beam envelopes follow a quasi parallel line, leading to nearly constant separation of 5+5 σ and avoiding too high aperture need inside the triplets. The position of the additional coils and the direction of the kick are indicated by arrows in the plot. The required normalised strength of the correctors is well within the allowed range of the magnets.

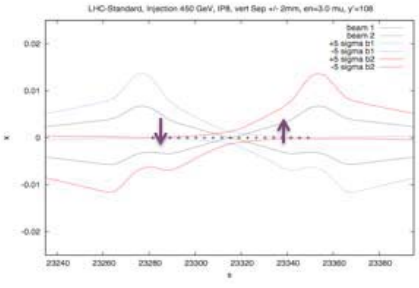

Fig 18: Optimised vertical crossing angle bump, using in addition the first orbit corrector in the triplet.

A realistic optimisation of the vertical crossing angle needed for sufficient beam separation has to be based on the actual position of the cross over. Following the results shown in Fig 14, the beams have to be separated from parasitic encounter #4 onwards.

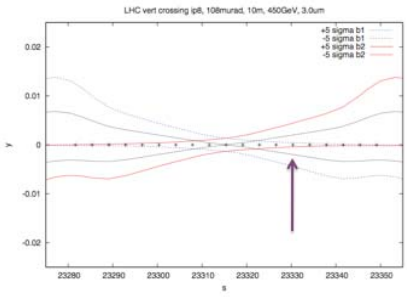

Fig 19: Optimisation of the vertical crossing angle to obtain maximum aperture and still sufficient beam separation at encounter #4.

At the encounters #1...#3, the beams are separated in the horizontal plane via the LHCb spectrometer effect. Accordingly a scan of the crossing angle bump had been performed to minimise the aperture need but still achieve this goal. The result is shown in Fig. 19, which shows a zoomed view of the beam envelopes at the first parasitic encounter locations. As before the beam envelopes refer to the standard injection optics and a normalised emittance of ε=3.0 μradm. The arrow in the picture indicates the location of the critical encounter point #4.

The third step in optimising the situation deals with realistic assumptions of the aperture model used. Mainly the maximum radial closed orbit uncertainty ("*cor*" parameter in the model) that is assumed for the simulations has a strong influence on the aperture result. For the optimised parameters explained above, Fig 20 shows the results of the aperture n1 assuming different values for the *cor* parameter. While the default value for *cor* is 4mm we compare the n1 results for a range of *cor* = 3.0mm ... 1.5mm. As expected the obtained n1 is increasing if the maximum orbit fluctuation is reduced. The dashed horizontal marker in the plots has been set to n1=8. For orbit fluctuation values of about *cor* = 2.0mm a value of n1 ≈ 7 is obtained, considered as sufficient for the machine.

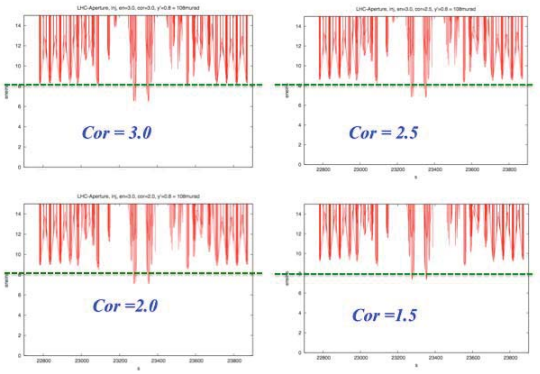

Fig 20: Aperture calculations for LHC injection optics, assuming a normalised emittance of ε_n=3.0 μradm.

Following the results summarised in Fig 20, an orbit fluctuation in the order of 2.0mm brings us back to an aperture value of n1 ≈7.

It might be worth to mention that for the real machine orbit fluctuations from fill to fill in the order of some tenth of a millimeter are observed and *cor* =2.0mm is still considered as a safe approach.

APERTURE MEASUREMENTS

During the last machine studies in the run year 2012 the actual vertical aperture in IR8 had been measured on beam and compared to the theoretically expected values. The main collimators were put to 4σ (referring the usual worst case emittance of ε=3.5μradm) and local bumps were steered until beam losses were observed in the IR8 triplet region. Fig 21 shows the measured difference orbit during the aperture scan. The difference between the two extreme values plus the beam size of 4σ (referring to ε=3.5μradm) gives the overall available aperture.

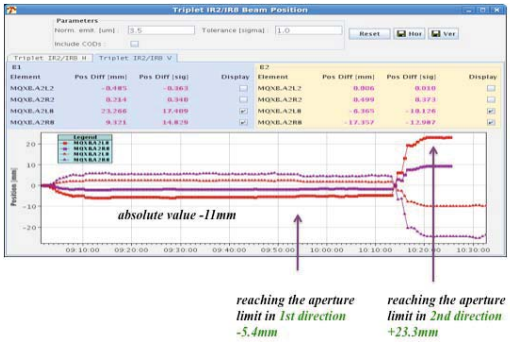

Fig 21: Orbit reading inside Q2 of the LHC triplet during the aperture scan

$$a = \Delta y + 2 \cdot 4\sigma = \Delta y + 8\sqrt{\varepsilon\beta}$$

$$a = 28.7\,mm + 8 * \sqrt{270m * 3.5\mu m} = 40.8mm$$

$$r_a = 20.4mm$$

The result obtained above is based on the orbit readings of the beam position monitors and suffers from their considerable non-linearities.

A cross check therefore has been performed based on the theoretical bump amplitudes as calculated by MADX. The aperture limits have been observed for a bump amplitude of ±11mm at IP8. Following the MADX calculation this corresponds to an amplitude of Δy=±17.8mm in Q2, which is, according to the theoretical bump shape in Fig 22, the bump maximum.

Referring to these calculations, an overall vertical aperture of

$$r_a = 17.8mm + 4\sigma = 23.8mm$$

is obtained, a little bit larger than the measurements based on the BPM readings, and in astonishingly good agreement with the beam screen dimensions (r_y= 24mm).

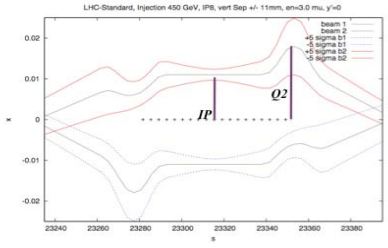

Fig 22: Bump amplitude and beam amplitudes for the bump used to measure the available aperture in IR8.

The external vertical crossing angle bump (Fig 19) needed to obtain sufficient separation at the parasitic encounters leads to an amplitude of Δy=6.8mm at the location of Q2. In other words, the remaining margin between beam orbit and the measured aperture limit corresponds to roughly 17mm or 12σ (ε=3.0μradm) at that position, which looks reasonably comfortable.

SUMMARY AND CONCLUSIONS

Spectrometer operation in IR2 does not have a big influence on the LHC operation and polarity switches are foreseen once per run mode, so in relatively rare occasions. Still a faster procedure is foreseen in p-Pb or Pb/Pb operation mode for the ALICE dipole polarity switch: the external bump will be kept constant for both spectrometer polarities, at injection and on the ramp until flat top. Only for the beta squeeze operation, i.e. going into luminosity conditions the external bump will be put to its final value and counteract the internal ALICE bump. As a consequence only in this very last file the TCT collimators have to be re-aligned. For so-called "negative" ALICE polarity this means however that during this process the bump will pass through zero crossing angle leading to very small beam separation for a moment Δy≈1σ). For the low bunch intensities foreseen during p-Pb runs it has been shown during the Pb-Pb run 2011 not to be a harmful procedure.

The spectrometer operation in IR8 is more problematic as the LHCb dipole field has a horizontal effect on the LHC beams. For the so-called "negative" polarity the deflecting effect is opposite to the natural beam geometry and leads to a second bunch cross over after the IP. Especially at 450 GeV injection energy due to the large beam emittance, this cross over cannot be avoided. In 50ns operation it is placed between two bunch positions, in 25ns however a harmful bunch collision will occur. To overcome this problem a new beam crossing and separation scheme is proposed: The internal spectrometer bump is combined with a horizontal beam separation to avoid collisions at the IP and a vertical crossing angle bump to establish sufficient separation at the parasitic encounters. As the beam screen in IR8 is oriented for horizontal crossing angles a simple swapping of the horizontal and vertical settings leads to small aperture values and the whole beam separation scheme had to be

re-optimised. Assuming not too pessimistic orbit fluctuations and using the triplet correctors to optimise the vertical bump a scenario is proposed that will give sufficient beam separation and comfortable aperture at the same time.

REFERENCES

[1] LHC Design report, CERN-2004-003
[2] R. Versteegen, priv. com.
[3] ATS-Note-2012-051
[4] CERN-ATS-Note-2012-039 MD
[5] LHCb diagonal levelling: proc. IPAC 2013, Shanghai to be published

ACKNOWLEDGEMENT

I would like to thank explicitly Reine Versteegen and John Jowett for their explanations of the IR2 geometry and for their contributions to this paper about the ALICE spectrometer operation.

BEAM BASED SYSTEMS AND CONTROLS

"What we want" a review from the operation team

Delphine Jacquet on behalf of BE/OP /LHC, CERN, Geneva, Switzerland

Abstract

This presentation will give a review from the operations team of the performance and issues of the beam based systems, namely RF, ADT, beam instrumentation, controls and injection systems. For each of these systems, statistics on performance and availability will be presented with the main issues encountered in 2012. The possible improvements for operational efficiency and safety will be discussed, with an attempt to answer the question "Are we ready for the new challenges brought by the 25ns beam and increased energy after LS1? ".

INTRODUCTION

2012 has been another amazing year for the LHC [1], with a good availability and total delivered luminosity beyond expectations. This was achieved thanks to the good performance of the controls software and equipment, only possible with the commitment and talent of all the experts. This good result didn't come without struggle, some limitations and problems have been identified along the year, some addressed already and some other to be solved during the long shutdown. The main issues and needed improvements for each of the beam based systems are presented hereafter.

ORBIT AND TUNE MEASUREMENT AND FEEDBACK [2]

The tune and orbit feedbacks are essential to operate the LHC in the best condition, and the operation efficiency suffers a lot from each issue or bad behaviour of these very complex systems.

Tune measurement and feedback

In 2012 the quality of the tune signal was affected by :

- The ADT gain that has been doubled since 2011¨
- The octupoles strength that has been tripled
- The 50Hz and 8 kHz perturbation that is difficult to compensate.

As a consequence, it was very difficult to get a precise measurement of the chromaticity at injection, the operation team spent more time to tune it to the desired value.

At the same time, the tune feedback kept stopping as bad measurement stability was detected, or was driving tune away from the target values when the tune measurement was locked on the wrong peak. As the feedback trims couldn't be completely trusted, the operation team was relying on the current in the quadrupoles to estimate if the tune was at the right value once at flat top.

At the end of 2012, the gated acquisition was tested and put in place. Its principle is to reduce the damper gain for the first six bunches of the beams, while the tune acquisition is gated in these six bunches for which the ADT doesn't degrade the tune signal. The tune measurement was much better at injection. The chromaticity measurement and tune feedback much more efficient. But still at flat top the measurement was not fully reliable and the feedback was kept off during the squeeze.

Orbit measurement and feedback

The quality of the beam position measurement has improved in 2012, some issues are nevertheless remaining:

- Temperature dependency of the measurement
- Non linearity in the strip lines
- Beam pattern effect
- Accuracy of the measurement in and around the common vacuum chambers.

In addition, issues with the interlocked BPMs in IR6 have been source of downtime in 2012. The BPM signals were very noisy for certain ranges of intensity per bunch, giving false position readings and consequently triggering the beam dump. The LHC beams were dumped thirty-two times at injection by this spurious BPM interlocks. It was a struggle for BI to find the optimum combination of gain and attenuator to get an acceptable signal for nominal intensity, but after May these spurious beam dumps occurred rarely. The problem remains for non-standard operation with different intensity per bunch like machine development (access is required to change the attenuator when the range of intensity per bunch changes)

Linked to this problem, the interlocked BPMs trigger as soon as a single bunch sees its intensity decrease, despite there is absolutely no potential danger for the accelerator.

The orbit feedback that relies on good BPM measurement is one of the key elements of the LHC operation, it stays ON from start of ramp to collisions and no beam could survive without it. Despite an overall good reliability, many issues where encountered and not less than twenty-one beam dumps (mostly in ramp and squeeze) were triggered by a wrong behaviour of the orbit feedback.

- Orbit reference not loaded properly, the feedback corrected on the wrong trajectory.
- Optics reference not loaded, the feedback couldn't converge with the wrong optic
- Corrector mask corrupted, the feedback used the common correctors in the IPs
- There was periods were the OFSU (controller for orbit feedback) was very unstable and crashed often. As it doesn't recover properly from a crash, it was decided to dump the beam as each crash in ramp or squeeze mode to protect the machine from unexpected behaviour of the feedback.

To be noted that if the feedback doesn't behave properly, it is not possible to recover the situation once we have started the ramp and the beam have to be dumped. There is another annoying issue: the BPM status (enabled/disabled) is frequently flickering every few seconds because data is missing from some crates. This issue is due to FESA latency in sending out the BPM data paquets which should be solved if possible at the source, else at the level of the data collection algorithms of the OFC.

What we want

A solution has to be found to provide a reliable tune measurement so that the chromaticity could be controlled and the tune feedback ON along the operational cycle. The gated acquisition is a promising solution to the problems encountered in 2012.

For after LS1, the IR6 interlock BPM system has to be revisited, a solution has to be find to stay safe and not dump the beams unnecessarily.

More reliability is also needed for the orbit feedback system. Most of the time, an unexpected behaviour of the feedback is not completely understood even by the expert. This shows that the system is very complex and more diagnostics and consistency check between all the layers of the system have to be implemented. The management of the optics and references to be used by the feedback could also be simplified.

BEAM SIZE MEASUREMENT [3]

LHC is equipped with different kinds of instruments for the beam size measurement: BGI, BSRT and wire scanner for transverse beam size, LDM and abort gap monitor for longitudinal distribution. Unfortunately in 2012 operation has been often missing diagnostics for the beam size, the instruments having two kinds of problems.

Hardware robustness issues: the BSRT mirror moved toward beam because of deformation induced by the temperature. It had to be retracted completely for safety reason and no BSRT measurement was possible since end of August. The wire scanners also showed signs of weakness and OP was recommended to use it as little as possible. No wire scanner possible at all for horizontal plane of beam 1.

Calibration issues: BSRT doesn't give coherent data along the cycle: it is difficult to calibrate the data with the energy. The BGI data are difficult to analyse, it is still an expert tool. The wire scanners give different result for the same beam with different working points (filters + gain settings)

What we want

For good operation efficiency and analysis of instabilities and losses, operation needs a bunch by bunch beam size measurement that is coherent along the LHC cycle, and also along the accelerator complex. The hardware issues have to be addressed, more robust instruments are needed. To ease their usage by operation, the tools in the control room could be improve. For the BSRT a lot of effort has already been made to improve and simplify the application but it is still expert oriented. The wire scanner application should also be simplified and useful functionalities implemented. LDM is a very useful tool that would be largely used if given with a proper operational application.

BUNCH/BUNCH INSTABILITIES MEASUREMENT

In 2012, with smaller emittances and higher intensity per bunch, the bunch by bunch instabilities started to be a limitation for the LHC performance. If better observation tools were available for the beam/beam effect experts, these instabilities could have been better understood and appropriate solutions put in place.
The existing tools in the control room for bunch by bunch measurement all have limitations and need to be improved. For example the ADT pick-ups give an accurate measurement of the bunch/bunch position, however one can acquire only 8 bunches for 6 seconds or 1374 bunches for 72 turns because the memory is limited. The BBQ peak-up could also give bunch by bunch tune and position measurement if another signal processing was implemented. The instruments like shottky monitors and diamond detector are promising but are not yet fully operational.

What we want

For bunch by bunch measurement, there are common requirements for all types of instrumentation:

- High measurement resolution because the instabilities are fast and appear within a few hundred turns.
- Large data buffers to acquire a maximum of turn for all bunches.
- A triggering system that would detect instabilities and trigger the acquisition of the appropriate instruments.

For a complete analyses of the instabilities, the following bunch/bunch measurements are required:

- Bunch by bunch position
- Bunch by bunch tune
- Bunch by bunch emittance
- Continuous chromaticity measurement along the cycle.
- Transverse motion inside a bunch to identify the type of instabilities

INJECTION AND DUMP SYSTEMS [4]

IQC and Steering

It is difficult for the operation team to evaluate what is acceptable or not for an injection in term of trajectory and beam losses. The IQC (injection quality check)[5] is the tool that helps for this evaluation by analysing several key parameters and comparing the measured values with pre-defined references and tolerances. The injection process is stopped when the quality as analysed by the IQC is not good enough to let the operation team take corrective actions. In 2012, it was not rare to have the IQC complaining on losses or trajectory errors that were judged acceptable by operation (i.e. only one bunch out of the tolerance at a single BPM), no special action was then taken and the injection process continued. The IQC should only stop the injection when correctives actions are absolutely necessary. Otherwise not only does it slow the injection process, but it also increase the risk that a real problem is involuntarily discarded. Therefore, the thresholds and tolerances for the IQC have to be reviewed.

It is a general feeling of the operation team that too much time is spent with the steering of the lines. First, the steering process itself is long because with time the trajectory diverged from the golden trajectory references established at the beginning of the run. So instead of just trying to reach the reference that would not be possible without huge kick on some correctors, steering the lines meant compromising between minimal beam losses and acceptable trajectories. Secondly, the stability of the lines degraded after the change of optics from Q26 to Q20 and the frequency of the steering increased. The reasons of this degradation are still being investigated. Due to this instabilities and out of date trajectory references, even specialists could not be 100% sure when the trajectory was good or not. As a consequence, several important steering campaigns were put in place to try to minimize injection losses without success because the trajectory was already very good and the losses came from longitudinal plane (satellites from the injectors or unbunched beam in the LHC). In this case, also a training of the operation team on the interpretation of injection losses is needed.

TDIs

The TDI has known several hardware problems in 2012 and was responsible for 26 hours of downtime. Two significant examples are presented.

Heating problem for TDI IR8: the LVDTs of the TDI in IP8 drifted outside the limits position due to the deformation of one jaw. This deformation is due to the heating induced by the beam.

Mechanical problem for TDI IR2: a pin broke and one jaw of the TDI fell across the beam aperture while preparing for injection.

In addition to the time needed recover from a failure, in some cases the TDIs needs to be re-aligned. This beam based alignment is time consuming but necessary to guarantee the protection in case of MKI failure.

MKIs

The MKIs have been a source of downtime mainly because of the heating induced by the beams during physics. The strength of the injection kickers is guaranteed only if the temperature in the tank is below a given thresholds and any injection is forbidden otherwise. As a consequence, after long physics fill, injection was not allowed before several hours after the beams had been dumped. In total, eighteen hours were spent waiting for the temperature to decay. To mitigate this problem, the hottest tank has been replaced during TS3. This implied conditioning and scrubbing for several days that was incompatible with physics.

Another limitation of the MKIs impacting operation was the vacuum interlock in place to prevent flashovers. As it is defined now, this interlock level is incompatible with the 25ns beam. As a consequence, the 25ns run has been pushed to the end of the run so that the vacuum thresholds could be increased without compromising the proton run in case of serious MKI failure.

LBDS

42 hours of downtime has been assigned to the LBDS systems. The main problems have been:

- Offset in the energy tracking system due to the failure of a power supply, power supply replaced but set point to be adjusted.

- A machine protection issue was discovered, the lack of redundancy of a 12V power supply could have led to a situation where dumping the beam where impossible. Immediate corrective actions were put in place.

As the LBDS systems are critical for machine protection, the quality control after a failure requires time consuming testing and revalidation.

What we want

With better trajectory reference, appropriate position and beam losses thresholds, the time spend at injection could be reduced: IQC shouldn't stop the injection process when not necessary and steering would be easier and faster if trajectory stayed closed to the reference. Of course improving the line stability would also help a lot.

LS1 will be the occasion to improve the hardware for the TDI and MKIs that has shown worrying limitations during the run. The LBDS systems also need some consolidation to reduce the source of downtime.

RF SYSTEMS [6]

The performance of RF systems, hardware and low level, have much improved in 2012 with respect to 2011. Nevertheless it remains one of the major sources of downtime for the LHC. Sixty-height hours of downtime have been assigned to the RF hardware, mostly due to crowbar problems. These faults came in waves and there also were several weeks passed without any recorded RF fault. On the low level side, the thirty-one hours of downtime came mostly from some crates to be rebooted or replaced. All in all, the RF performance has been very good, despite an increased intensity per bunch and new challenges like the batch by batch blow-up and the preparation for proton-lead run.

What we want

The operation team has nevertheless identified several points that could be improved. Of course the reliability of the hardware needs further improvement, as operating with more power and at higher beam energy may also impact the availability. More diagnostics on RF interlocks would also be needed; especially in case of low level problem it would ease the diagnostic of a fault and help the operation team to call the right experts. Now the injection phase measurements give the average phase of all bunches in the machine, a batch/batch measurement is needed to see the injection phase error at each injection. The bunch longitudinal profile measurement is now available only for expert, it would be useful also in the control room. The batch by batch blow-up recently made operational still needs diagnostics and control for the operation team.

TRANSVERSE DAMPER SYSTEMS [7]

The transverse damper has shown lots of flexibility and has been used for many different applications: injection oscillations damping, injection area cleaning, abort gap cleaning, transverse blow-up that has simplified a lot the loss maps procedure. The ADT pick-ups are also used to measure beam instabilities and the tune measurement with transverse dampers is almost operational. The ADT hardware has been quite reliable with only 12 hours of downtime assigned.

What we want

With the new functionalities implemented along the year came a lot of new parameters and settings. Some of these settings belong to function beam processes, some other to discrete beam processes that are different for the type of the beam and along the LHC cycle. At the end it becomes difficult for the operation team to manage this parameters and settings and still rely a lot on the experts. This will have to be reviewed and an attempt has to be made to simplify the parameter space. At the same time a better solution has to be found for the intensity dependent settings that have now to be set manually by experts.

CONTROLS SOFTWARE [8]

Main issues

A total of 21h of downtime has been assigned to the control systems, mainly pieces of hardware to be rebooted or replaced. Some other problems impacted the operation efficiency:

- The CMW middleware is unable to manage bad client, the server gets stuck and doesn't send update to the good clients, the major consequence being that the software interlock system triggered several time the beam dump because of subscription timeout.
- The CBCM (timing system that orchestrate the injection requests and beam production and destination in the injectors) has shown potentially dangerous issues with the dynamic destination management: twice the destination has not been updated as it should and the beam has been injected in the wrong ring.
- The LSA database becomes very slow when accessed by several processes (i.e. during database back-up) and the incorporation and regeneration of beam processes takes too much time. This problem has already been addressed during the run but further improvements are foreseen.

What we want

Some improvements have already been requested by the operation team since 2010 [9]. They have not yet been addressed either because considered as low priority or by lack of manpower. They are still valid today:

- Diamon: Clearer information is needed on the connection between applications, proxy, middletiers, front-end… The display of the server status in diamond still doesn't reflect the real status of the server that could have perfect behaviour with a red status or be completely stuck and happily displayed in green.
- Alarms: the alarm system will never really been used in operation until it becomes mode dependent: i.e. some alarms are important at injection but can be ignored during physics.
- Sequencer: the sequencer should allow for automatic parallel execution of sub-sequences. It should be possible to pass arguments to a sub-sequence, offline and at the execution time by the user.
- Timing sequence edition: more and more flexibility is requested to the injectors with the edition of the sequence of cycles to be played by the timing. Even if the situation has already much improved thanks to the use of spare cycles for intermediate intensity, lots of time is spent with the edition of the sequences. This time could be reduced by improving the timing manager application. In addition switching from one sequence to another takes several supercycles, it has to be investigated if time could be gained at this level.

The last years of LHC operation brought also other requirements to improve the efficiency:

- The console manager could propose more user friendly tools for the edition of the menus and an automatic periodic refresh of the menu configuration from the database should be implemented to avoid using old application versions by mistake.
- Fidel (process that compensate for the magnetic field decay at injection [10]) worked very well, but the existing fixed display that indicates the LSA trims performed by the process needs to be improved. It has to be investigated how to improve Fidel behaviour in case of hypercycle change: now in some cases it requires a precycle to "reset" the Fidel trims that has been done with the previous hypercycle active (often the case during MDs)
- RBAC is a powerful tool to keep control of what is done during the physics run [11]. The drawback is that it becomes painful and inefficient to enter login several times in all operational consoles. An alternative solution could be investigated, like biometric identification methods. In addition, LS1 would be a good occasion to rationalize the roles distribution and review the roles management.
- The state machine has been fully used and has shown a lack of flexibility, especially during MDs. It has to be reviewed to propose two levels of checks and distinguish between what is absolutely necessary whatever the type of operation (i.e. main magnets being at injection when going to inject state) and what should simply be checked, like the state of the tune feedback. After LS1, the action "force without check" should be exceptional as it has the risk to change state when the machine is not fully ready.
- The FESA navigator tool has been used a lot in the control room and shown very useful to check some settings directly in the FESA classes. This application that was first designed only to be used as an expert tools would need to be improved, made operational and user friendly.

DATA MANAGEMENT

The demand for bunch by bunch and turn by turn data is increasing rapidly with the need to track and understand the beam instabilities in the LHC. Presently, lots of data are stored with individual ad-hoc solution instead of going to the official logging database.

What we want

A common system is needed to log this large amount of data. This data could be automatically deleted after a configurable time period with the possibility to keep the interesting data.

There is also a need to do fill by fill data analysis. It should be possible to extract predefined set of key parameter for a given fill to analyse these parameters along the fill or from one fill to another with tools for easy comparison. It would have the advantage to immediately see the effect of one parameter change from one fill to another and give a common tool for fill analysis that would allow to follow long term evolution of given parameters.

CONCLUSION

Issues, weakness and needs for improvement has just been presented for the beam based systems. This shows that the great performance of the LHC during 2012 run has not been achieved easily. Huge work has been done by all these equipment's experts to push the performance

and availability of their systems, and the operation team had the luck to rely on their help, involvement and reactivity. LS1 will be the occasion to consolidate and improve all the systems and controls to have them ready for the new challenges that will have to be faced in 2015.

ACKNOWLEDGMENTS

The author would like to thanks the following persons for their help in the preparation of this paper: the whole LHC operation team for the collection of issues and new requirements, Gianluigi Arduini, Vito Baggiolini, Xavier buffat, Tatiana Pielonni, Chris Roderick, Benoit Savant and Ralph Steinhagen.

REFERENCES

[1] Alick Macpherson "Introduction and review of the year", these proceedings.
[2] Thibaut Lefèvre "What you get- orbit and tune measurement and feedback", these proceedings.
[3] Frederico Roncarolo "What you get- beam size measurement", these proceedings.
[4] Chiara Bracco "What you get- injection and dump systems", these proceedings.
[5] Verena Kain "Injection beam loss and beam quality check for the LHC", proceedings of IPAC'10, Kyoto, Japan.
[6] Themistoklis Mastoridis "What you get- RF systems", these proceedings.
[7] Daniel Valuch "What you get- Transverse damper system", these proceedings.
[8] Steen Jensen "What you get- Controls software", these proceedings.
[9] Delphine Jacquet "Software and control issues", proceedings of LHC Beam operation workshop, Evian, 7-10 December 2010.
[10] Nicholas Sammut ""FIDEL – The field description for the LHC", EDMS doc nbr LHC-C-ES-0012 v2.0
[11] I.Yastrebov "Status of the RBAC infrastructure and lessons learnt from its deployment in LHC" CERN-ATS-2011_210

WHAT YOU GET: ORBIT AND TUNE MEASUREMENTS AND FEEDBACK

M. Andersen, C. Boccard, S. Bozyigit, E. Calvo, M. Favier, J. Fullerton, M. Gasior, S. Jackson, L. Jensen, R. Jones, T. Lefevre, A. Margiolakis, A.A. Nosych, J.J. Savioz, R. Steinhagen, M. Wendt, J. Wenninger, CERN, Geneva, Switzerland

Abstract

The Large Hadron Collider (LHC) has now been operated successfully for 3 years relying on the good performance of its beam instrumentation, including position and tune monitors and their respective feedback systems. This contribution gives an overview of the performance and limitations of the current orbit and tune systems. The major hardware and software modifications performed in 2012 are presented as well as the developments and improvements planned during the Long Shutdown 1 (LS1). The last part of the paper discusses the expected performances of both systems with 6.5TeV beams after LS1.

INTRODUCTION

With its 1070 monitors, the LHC Beam Position Monitor (BPM) system is the largest BPM system worldwide [1]. Based on the Wide Band Time Normalizer (WBTN) [2], it provides bunch-by-bunch beam position (and intensity) over a wide dynamic range (~50dB). Despite its size (3820 electronic cards in the accelerator tunnel and 1070 digital post-processing cards in surface buildings) and complexity the performance of the system during the last three years has been excellent, with 97% availability.

The tune monitoring system is based on direct diode detection [3] allowing operation with nanometres beam oscillation. Both the BPM and the tune monitors are used for feedback [4] to stabilise the orbit and tune around their optimal values throughout whole LHC fill.

Nevertheless, after three years of operation, the performance of the existing systems has been investigated in detail and several limitations were found and partially mitigated. This paper will discuss the status of the BPM and tune related monitors with an emphasis on the planned upgrades foreseen during the long-shutdown and the expected performance of the systems with >6.5TeV beams.

BEAM POSITION MONITOR

For the BPMs, in the arcs, the position resolution was measured to be better than 150µm in bunch/bunch mode and 10µm in averaged orbit mode [5]. In 2012, an automatic configuration of the digital signal processing system was successfully tested in order to adjust the settings of an averaging filter with respect to number of bunches circulating in the machine. This functionality will be deployed after LS1 and should push the orbit resolution down to 5µm. The main limitation to the orbit stability is caused by long-term drifts due to temperature variations in VME integrator mezzanine causing position errors. The typical temperature drift behaviour is shown in Figure 1. The drift effect is known since 2010 and has shown orbit errors of millimetres over one fill. In order to mitigate this effect, an online temperature correction algorithm was established: the temperature dependence of the integrator mezzanine is measured with the BPM calibration mode, controlling the VME crate fan's speed to vary the ambient temperature. A linear, online correction of the BPM data is thus performed depending on the measured temperature. However, this technique turned out to work reliably only for small temperature drifts. An improved long-term solution was therefore initiated in 2010 investigating the use of water-cooled racks to keep the temperature of the electronics constant.

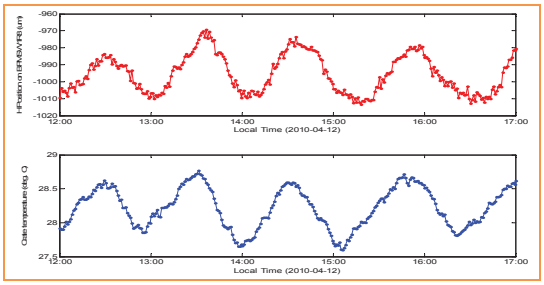

Figure 1: Time of evolution of the horizontal beam position in a selected BPMSW (top) and the temperature in the corresponding mezzanine (bottom)

Test and installation of thermalized racks

As Figure 2 shows, water-cooled racks have been evaluated for one year at LHC Point 1 on a test system, and proofed the temperature can be well controlled over long periods better than 0.05°C rms resulting in orbit drifts smaller than of 3µm.

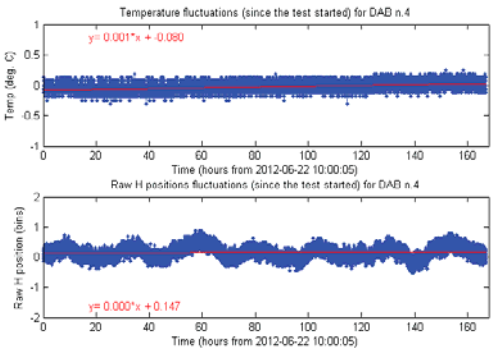

Figure 2: Temperature in water-cooled rack, (top) Corresponding horizontal position in adc's bins (bottom)

Water-cooled racks will be installed during the long-shutdown on all BPM and BLM surface racks.

Non-linearity correction of BPM

A potential limitation to the accuracy of buttons and strip-line BPMs arises from their non-linear response to off-centred beam position [6]. This effect comes directly from the physical geometry of the pick-up and can be precisely simulated and thus corrected. For most cases in LHC, like in the arcs, this is not an issue since the beam position remains close to the beam axis. However larger errors occur for large off-centred beams, like for example in the dump lines or for some BPMs around the interaction points where the pick-up electrodes had to be tilted by 45degrees for integration reasons.

Electro-magnetic simulations [6] have been performed using CST Particle Studio to characterise the non-linear effects for all types of LHC BPMs and determine the parameters of the polynomial fit to be used for corrections Figure 3 illustrates as example, the BPMD type, a 130mm aperture strip-line BPM located in the dump line, is presented. Based on the simulations, the difference between non-linearity corrections using either a 1D or a 2D correction scheme with cross term is considerable. The average absolute calibration error in the beam allowed area (1/3 of the BPM aperture) could be reduced from 1.1mm to 30µm and the maximum error for diagonal beam from 6mm down to 100um.

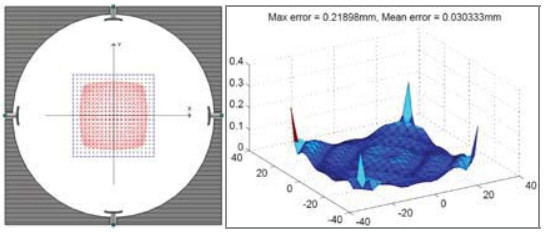

Figure 3: (left) Sketch of a BPM with the beam allowed area visible and typical errors made without correction in red (right) Residual error after 2D correction using cross-terms polynomials

In the LHC, non-linearity corrections based on single-term (1D) corrections have been implemented since the beginning of the beam operation. A more complete set of software corrections including cross-terms polynomials (2D) have been tested in machine developments and have demonstrated the potential improvements [7]. They will be put in place in the Front-end software systems during LS1 to provide better corrections for all BPMs. It is worth noting, however, that the algorithms will require testing with beam.

Orbit measurement with diodes

Originally developed to process signals from BPM buttons embedded in LHC collimator jaws [8], orbit measurement using a compensated diode detector scheme [9], named DOROS, has already demonstrated to be robust, simple and in addition providing an excellent position resolution. One prototype was tested in the SPS for two years on a LHC collimator prototype equipped with buttons BPMs. A second prototype was installed on LHC BPMs and has shown resolution in the nanometre range [9]. A comparison of the orbit measured, during a Van der Meer scan, simultaneously by WBTN and DOROS is presented in Figure 4. The resolution of DOROS is at least 50 better than for the WBTN. On this plot, there is a visible scaling error between the two systems, which is still under investigation. For this plot, the DOROS data were scaled without any non-linearity corrections of the BPM nor the electronics.

During LS1, the development of DOROS is moving from prototyping to final engineering production. This electronics will be installed on LHC collimator BPMs and on few BPMs in the LSSs region where their excellent resolution is expected to improve the LHC performance during squeeze. It is important to note that DOROS does not provide bunch-by-bunch measurements. However, if required, the electronic could be equipped with a gating circuitry, allowing the selection of single or group of bunches.

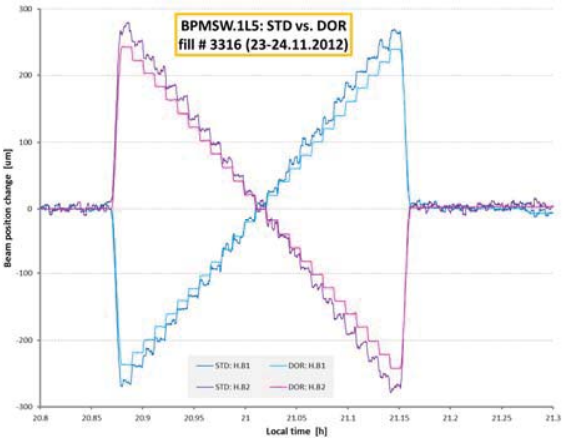

Figure 4: LHC orbits - diode system versus normaliser positions

Status of Orbit Feedback

The LHC would not have performed so remarkably well without its orbit feedback system. The current correction quality limits are not yet a real problem. In the arcs and for most of the LSS, the fill-to-fill reproducibility of the beam position is of the order of 50µm. In the common regions in points 1, 2, 5 & 8, the reproducibility is degrading with an rms value of 200 µm, mainly due to the limited directivity of strip-line BPMs.

To illustrate the performance of the orbit feedback, Figure 5 shows the evolution of the orbit correction at

IP1 to bring beams into head-on collisions (here B1H correction) over one year. There is a clear slow drift developing over the year, which is not corrected but the fill-to-fill difference is very small and sufficiently good.

At 7TeV, with tighter collimator settings and the lowest achievable β*, the orbit stability must be improved. During the long shutdown, several actions highly beneficial for OFB are foreseen to overcome the known limitation. Most of them are directly related to improvements in hardware, like the installation of water-cooled racks and the deployment of DOROS wherever possible. In parallel, software improvements are also under investigation. This includes a better handling of response matrix, better filtering of bad elements and improvements in the data transfer. A lot of modifications and improvements were made already since 2010 and the long shutdown will give the occasion to review in details the system architecture and improve the in-depth knowledge.

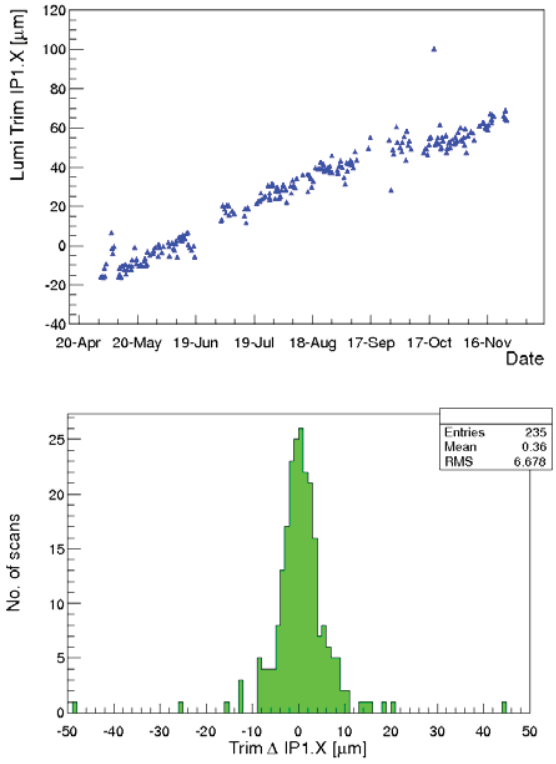

Figure 5: (top) Horizontal orbit stability in IP1 along the year (bottom) Corresponding fill to fill orbit shift in um over the year

Status of interlock BPMs

In order to ensure a safe extraction trajectory into the dump lines, the beam orbit around the extraction septum must stay within ±4mm. A set of 4 BPMs per beam was installed on both sides of the septum, 2 redundant BPMs near TCDQ and 2 near preceding quadrupole, Q4. Their positions have a 90° phase advance to minimise the possibility of a sudden unforeseen orbit bump. The system must be capable of reacting on a bunch-by-bunch basis since a single high intensity bunch at high-energy can cause damages to the septum. The read-out electronic is based on standard LHC BPM analogue electronics (WBTN), however a dedicated FPGA firmware is used and counts the number of bunches with off-centred positions outside the pre-set limits. The system will trigger a beam dump interlock if the beam conditions match the following scenarios working on two different time scales: a single bunch instability defined as 70 readings outside limits over 100 turns and a fast full beam instability with 250 readings outside limits over 10 consecutive turns. The beam abort is automatically triggered once one of the BPM channels has detected either of these errors.

Unfortunately, the WBTN electronics has a limited dynamic range in terms of bunch intensity as illustrated in Figure 6. As for the standard LHC BPMs, the system operates with 2 sensitivity ranges: High and low sensitivity modes covering respectively the corresponding bunch intensity ranges [2×10^{9} - 5×10^{10}] and [4×10^{10} to 3×10^{11}]. The system shows signal quality issues when single bunch have intensity close to either end of the dynamic range. For too low intensity, the WBTN diverges rapidly and provides false BPM readings. For high bunch intensity, the system becomes sensitive to signal reflections and a false bunch count occurs. In both cases the interlocked BPM triggers a dump.

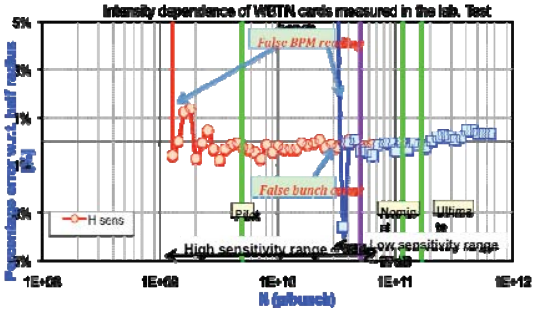

Figure 6 : Bunch intensity dependency of the WBTN

In 2012, the system suffered from several false dumps. Removing cable attenuation has allowed the system to reach 2×10^{10} in low sensitivity, which was an acceptable scenario to optimize for the proton-proton physics fill integrated luminosity. However, for heavy ions, the current settings were not adequate and required modifications. Finally non-linearity effects systematically dumped the ion fills once a single bunch reached ~3×10^{9}.

During the long shutdown, several actions have been initiated to address these issues. We are studying the possibility to cover an extended dynamic range by

reducing spurious reflections. To improve the tuning of the two sensitivity modes and provide the best flexibility for operational reasons, a DAC would be implemented to remotely control the threshold of the comparators.

Alternative acquisition electronics are also under investigation (e.g. analog divider scheme for normalization). An improved version of the firmware will be commissioned to provide more diagnostics for the system.

TUNE AND TUNE FEEDBACK

Since the very early beams in 2010, the tune monitor and feedback have been fully operational. They have however encountered several limitations due to their interaction with other systems like the transverse damper operating at very high gain and the sensitivity of the quench protection system to (too) large trim request [4]. The latter one was partially addressed by reducing the speed and the gain of the tune feedback.

Gated tune monitor

The incompatibility between the transverse damper operating at high gain and the tune monitor has been a serious limitation for the beam operation. During the fill, one has to choose between high damper gain to control beam instabilities or reliable tune signals.

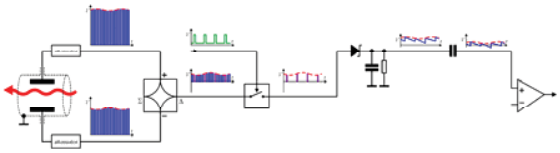

Figure 7: Schematic of the Gated BBQ system

A solution was found during summer 2012 based on the development of a new tune front-end, which enables gating on bunches for which the damper operates at lower gain. The system, as depicted in Figure 7, processes the electrodes signals using a hybrid to reduce the signal amplitude, an RF switch for gating and a normal BBQ front end [3] as a peak detector. After the success of the first prototype, the system was quickly made operational as shown in Figure 8.

Figure 8: Picture of the Gated BBQ and its implementation in LHC Tunnel

During the long shutdown, two additional strip-lines will be installed to extend the current operational system, providing measurements in parallel in order to fulfil the different functionalities as required by operation: like pilot and high intensity bunches, the gated BBQ and coupling measurement. Some operational software development is required to exploit the full functionality of nominal and gated BBQ, with a GUI for bunch selection and bunch scans display.

Status of Schottky monitor

During the last 3 years, the LHC Schottky monitors [10] were able to provide high-level Schottky signals on all ion fills, for B1H, B1V and B2H, providing reliable single bunch measurements for the tune [11] and with some limitations also for the chromaticity measurements as visible on Figure 9.

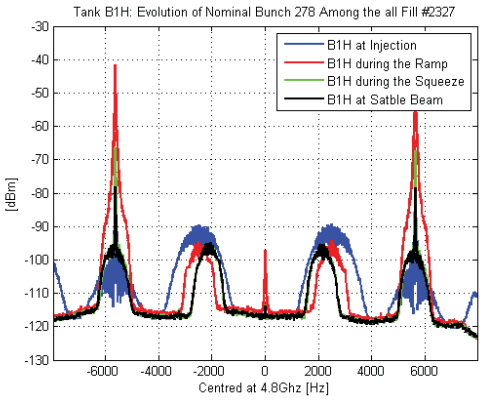

Figure 9: Schottky signals with ions

With Protons, the Schottky transverse signals are still acceptable on the B1H system, for single and multi-bunch measurements at injection and at stable beam. However, the too large coherent signals saturate the pre-amplifiers on the other systems. On one monitor, (B2H), the pre-amplifiers was damaged. A modification on the gating scheme of the B2V pick-up has led to a significant reduction of the coherent signal peaks, but no improvement of the transverse Schottky signal bumps was observed.

During the long shutdown, an overhaul of the pick-ups has been organised and all Schottky tanks will be removed from the beam line. Preliminary RF simulations demonstrate a reduction of the signal reflections with the pick-up system is necessary. This includes a better matching between the slotted and un-slotted waveguide, as well as for the waveguide-to-coaxial transition. New RF mechanics have to be manufactured and mounted on the monitors. Systematic RF measurements on a test bench with stretched wire measurements will be performed with the aim of controlling and improving the symmetry of opposite electrodes, e.g. lowering the tolerances. All internal SiO2 coaxial cables will all be replaced as some are found to be not vacuum-tight.

The RF signal processing will also be redesigned with modifications of the gating and a new RF input filter to better cope with 25 ns bunch spacing, while improving the S/N ratio.

The control and software requires some development as well. The RF attenuators and phase shifters must become remotely controllable. Requirements for the operational java GUI, which requires a complete redesign, is being specified.

DETECTION OF TRANSVERSE INSTABILITIES

Observation of instabilities in 2012 relied mainly on BBQ spectra and transverse damper (ADT) activity.

The LHC head tail monitors using fast sampling oscilloscopes (8-bits ADC) are limited to the detection of 100um oscillation amplitudes and limited in on-board memory. During summer 2012 a Multi-band Instability Monitor (MIM) was developed. It is using a set of RF band-pass filters and high sensitivity diodes, similar to the one used in BBQ. A prototype, as presented in Figure 10, was realized and tested successfully on the SPS and LHC. The monitor is processing the position signals coming from a Δ-hybrid mounted on a strip-line BPM. The signal is split into 5 frequency bands, each measured simultaneously by diode detectors: no filter and respectively 0.4GHz, 0.8GHz, 1.2GHz and 1.6GHz filters.

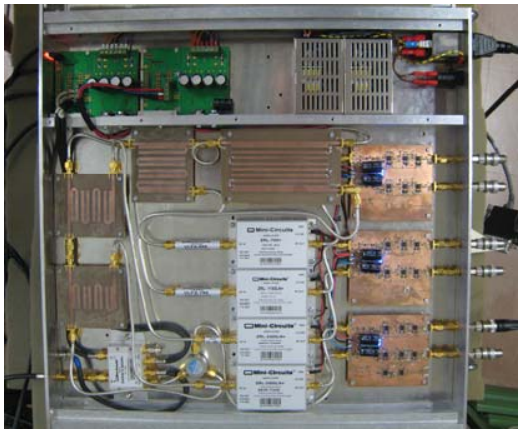

Figure 10: MIM tested in 2012 on SPS and LHC

When a beam instability occurs, the MIM provides the relative amplitude of the beam position oscillations in the different frequency bands, which then can be related to a specific instability mode. In Figure 11, data acquired with MIM clearly shows a strong activity at 400MHz, not visible in the unfiltered channel, which would indicate the presence of a head-tail instability mode with m≥1.

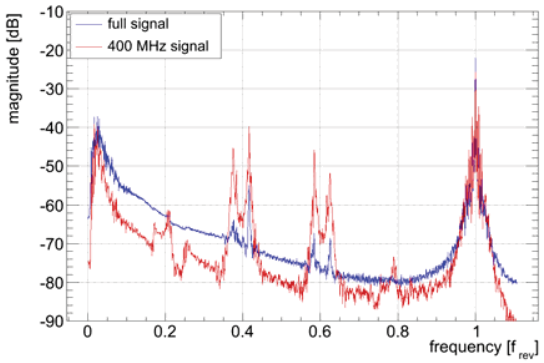

Figure 11: RF signals measured by the MIM in two frequency bands: full bandwidth and using a 400MHz band-pass filter

CONCLUSION AND PERSPECTIVES

The LHC BPM system has operated very reliably over the last 3 years. Several modifications are however under implementation to improve the performance of the system. Water-cooled racks will be installed to control the temperature in the VME crate and to provide a better long–term stability of the resulting position data. A new non-linearity correction algorithm will be implemented to minimize the errors caused by for off-centred beams. The interlocked BPM system will be revisited with the aim of increasing its dynamic range. Finally, the high-resolution diode orbit observation system will be deployed for some critical BPMs in the LSSs.

The orbit and tune feedback system will be reviewed during the long shutdown with the aim of improving its reliability and knowledge base.

The recently developed tune monitors based on gated BBQ have overcome most of the operational limitations of the previous system. After the long shutdown the tune system (hardware and software) will be made fully operational with multiple tune monitors adapted to the operational needs (pilot bunch, gated tune for feedback, coupling measurement and single bunch tune scan).

The Schottky monitors will undergo a complete system overhaul with improvements planned on pick-ups, front-end electronics and software. The goal is to make them operational with protons after the long shutdown.

The observation of beam instabilities in the LHC is crucial and clearly requires new hardware/software developments. A discussion is currently on-going to define the needs in terms of beam instruments and look into what is technically achievable (BBQ, HT monitor, MIM, ADT monitor). A coherent plan will be proposed ensuring that, when operation resumes, adequate monitors are made available.

REFERENCES

[1] E. Calvo et al, “The LHC Orbit and Trajectory System”, Proceeding of DIPAC, Mainz, Germany, 2003, 187

[2] D. Cocq, “The Wide Band Normaliser: a New Circuit to Measure Transverse Bunch Position in Accelerators and Colliders”, Nucl. Instrum. Methods Phys. Res. A 416, 1998, 1.

[3] M. Gasior, "Faraday cup award: High sensitivity tune measurement using direct diode detection", CERN-ATS-2012-246. Proceeding of BIW, Newport News, Virginia, USA, 2012.

[4] R. J. Steinhagen, "Real-time Beam Control at the LHC", Proceeding of the PAC Conference, NewYork, USA, 2011, 1399

[5] E. Calvo et al, “The LHC Beam Position System: Performance during 2010 and Outlook for 2011”, Proceeding of DIPAC, Hamburg, Germany, 2011, 323

[6] A. Nosych et al, “LHC BPM non linearity corrections”, Private communication

[7] R. Bruce et al,” IR8 Aperture Measurements at Injection Energy”, CERN-BE-2013-003

[8] A. Nosych et al, “Electromagnetic Simulations of an Embedded BPM in Collimator Jaws”, Proceeding of DIPAC, Hamburg, Germany, 2011, 71

[9] M. Gasior, J. Olexa, R.J. Steinhagen, "BPM electronics based on compensated diode detectors - results from development systems", CERN-ATS-2012-247. Proceeding of BIW, Newport News, Virginia, USA, 2012.

[10] F. Caspers et al, “The 4.8GHz LHC Schottky pick-up system”, Proceeding of the PAC Conference, Albuquerque, NM, USA, (2007) pp.4174

[11] M. Favier, et al, « Capabilities and Performance of the LHC Schottky Monitors », Proceeding of the DIPAC Conference, Hamburg, Germany, (2011) pp.44

WHAT YOU GET? TRANSVERSE AND LONGITUDINAL DISTRIBUTIONS

F. Roncarolo*, W.Andreazza, S.Bart-Pedersen, A.Boccardi, E.Bravin, B.Dehning, J.Emery, A.Goldblatt, J-J. Gras, A.Guerrero, M.Kuhn, L.Jensen, R.Jones, T.Lefevre, A.A.Nosych, M.Sapinski, G.Schneider, G.Trad, R.Veness, M.Wendt
CERN, GENEVA, SWITZERLAND

Abstract

The transverse beam emittances of the LHC proton and ion beams can be inferred by measuring the beam sizes with Wire Scanner (WS), Synchrotron Radiation (BSRT) and Beam Gas Ionization (BGI) monitors. The Abort Gap Monitor (AGM) and the Longitudinal Density Monitor (LDM) are used to characterize the longitudinal distributions. This paper covers at first all aspects related to the use of such devices in 2012. Achieved performances, reliability and operational limitations, like system failures due to high intensity beams or ageing are covered. A particular emphasis is given to the planned system upgrades for improving accuracy and robustness, while coping with both the operational limits and the LHC energy and intensity upgrades after LS1. This includes the impact of the 25 ns bunch spacing on the bunch per bunch measurements and the need for resolving smaller beam sizes at 7 TeV.

TRANSVERSE DISTRIBUTION MEASUREMENTS

Wire Scanners (WS)

The LHC is equipped with eight WS systems. Four are kept operational (one per plane per beam) while four spares can be connected remotely without interventions in the machine. They act as a reference (cross-calibration) for other devices, but can be used only below a threshold intensity that depends on energy (see Table 1). Above the threshold, wire damage and/or dumping the beam due to downstream BLM interlocks can occur, as verified through simulations and experiments. The corresponding BLM thresholds are set to minimize to possibility of a superconducting magnet quench. Failures/issues during 2012 were related to bellow vacuum leaks, wire breaking and beam dumps due to downstream BLMs.

The WS bellows are designed to withstand about 10000 scans. Indeed, in 2012 there was only one system failure, after about 10200 scans. Since each system's history is logged, the probability of such a failure is predictable and switching to the spare scanner should be the baseline when the number of executed scans approaches the design limit.

* federico.roncarolo@cern.ch

Beam Energy $[TeV]$	Intensity Threshold $[protons]$	Dominant Reason
0.450	$2.7 \cdot 10^{13}$	Wire damage
4	$3.6 \cdot 10^{12}$	BLM threshold
6.5	$1 \cdot 10^{12}$	BLM threshold

Table 1: Beam intensity thresholds above which WS measurements are software interlocked.

Concerning wire damages, in 2012 there was no evidence of wire breakage due to beam induced effects (RF coupling or direct energy deposition) during normal operation. However, there was evidence of wire diameter reduction (34 μm Carbon wires are used for the LHC WS) due to sublimation, as shown in Fig. 1.

On two occasions (Nov 14, 2012 and Jan 20, 2013), while the operator requested scans on both beams at the same time, the WS systems failed, the wires remained stuck in the IN position with circulating beam and consequently broke. In both cases the FESA server crashed after the IN movement. In the first occasion, the sever crash followed a failure of the WS actuator power supply, while for the second occasion the crash reason is not yet understood despite several attempts to simulate the behaviour without beam in the machine.

Concerning the dumps due to BLMs detecting the losses downstream the WS systems, it must be noted that during the year the intensity thresholds mentioned above were tuned to allow the scan of the maximum possible intensity in a safe way with respect to quench probability. The BLM thresholds were adjusted by measuring losses induced by a scan. In some cases, it turned out that the losses depend on the wire ageing, i.e. to the wire actual diameter. As evidenced in the examples of Table 2, this led to beam dumps after replacing a broken wire, since the new wire induced higher losses than the previous (aged) one.

During 2012 it was possible, especially during MD

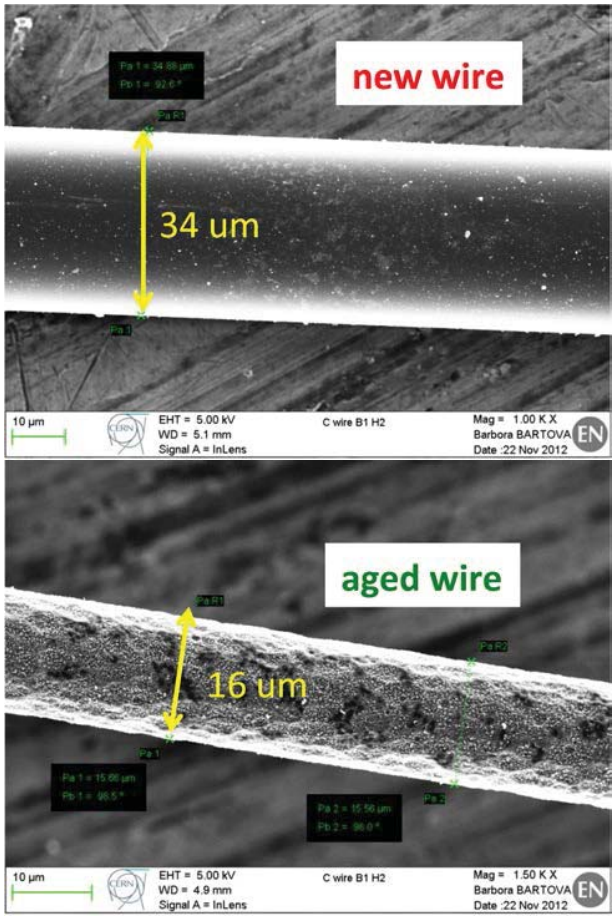

Figure 1: Microscopic inspection of a new (top) and a used (bottom) carbon wire, evidencing the wire diameter reduction due to sublimation.

	22-Aug	12-Oct	22-Nov
System	B1 H	B1 H	B1 V
Wire age	aged	new	new
Beam Intensity	$4.3 \cdot 10^{12}$	$4.2 \cdot 10^{12}$	$3.5 \cdot 10^{12}$
BLM [Gy/s]	0.0091	0.0218	0.0335
Losses [Gy/p]	$5.4 \cdot 10^{-19}$	$2.7 \cdot 10^{-17}$	$2.4 \cdot 10^{-17}$
Dump	NO	YES	YES

Table 2: Effect of a WS measurement on the BLM signals in three different occasions, with aged and new wire

periods, to study the effect the detectors' working point (determined by the photo-multiplier voltage and the optical filter settings) on the beam size determination accuracy. This is discussed in another paper included in these proceedings [1].
In general, as an outcome of the LHC Run 1 experience, the WS application is judged inefficient by OP: the bunch selection is sometimes tricky, the results display difficult to handle and interpret and the request for automatic scans at given times is pending.

Concerning WS upgrades/improvements, the situation at the moment of writing is the following:

- During the 2012 TS#4 a 7 μm carbon wire was installed on one system. The tests foreseen in February 2013 could not take place and will be done after LS1. They aim at characterizing the wire robustness, the signal and the induced losses with respect to the 34 μm wires. This will be compared to literature [2] predicting the thinner wire's higher robustness (even though smaller diameter means less material to sublimate before breaking) and faster cooling due to the higher surface/volume ratio.
- During LS1 it is foreseen to
  - investigate the possibility of slightly increasing the scan speed (of a maximum 10 % with respect to the nominal 1 m/s)
  - change the bellows, with the aim of gaining a factor 5 in lifetime
  - deploy a new, more efficient, operational GUI
- During LS2 it is foreseen to:
  - possibly install faster devices (20 m/s), following the SPS prototype tests after LS1. This would allow increasing the energy/intensity limits
  - possibly install new detectors (e.g. diamonds) at the place of the scintillator - photo-multiplier chain, in order to increase the detectors linearity range.

Beam Gas Ionization Monitor (BGI)

The BGI systems provide continuous beam size measurements averaging over all bunches circulating in the machine. The principle is based on imaging the residual gas electrons following the beam induced gas ionization (after their collection on an MCP intensifier glued to a phosphor that converts them into visible photons).
During early 2012 both the horizontal and vertical BGI MCPs on Beam 1 (exchanged during the winter technical stop) were damaged due to operational/technical failures (wrong high-voltage settings). This was the consequence of two different issues:

1. too large signal on the MCP because of electron cloud, for an extended period of time
2. abrupt shutdown of high voltage due to a hardware reading error.

Following the second issue, the automatic high-voltage shut-down procedure was improved to provide a smoother ramp down rate. To avoid the first problem, To avoid the first problem, an automatic feedback should be put in place. During the year, several problems with the camera remote control occurred, which compromised the continuous recording of the beam size measurement and the consequent understanding of the whole system.
Considering the above issues, in addition to the lack of suitable beam intensity overlap between WS and BGI during p-p runs, it can be concluded that the BGI results interpretation and its calibration remains difficult.
An example of BGI measurements compared to WS is shown in Fig. 2. This refers to the ion beam during a p-Pb MD period [5] with only 13 ion bunches and $7 \cdot 10^9$ charges per bunch. Despite the low BGI signal, it was possible to find a good calibration w.r.t. WS at both 450 GeV and 4 TeV. As mentioned above, calibration was much more difficult with protons, for which there was also evidence of BGI beam size measurement dependence on the beam space charge
During LS1, it is foreseen to

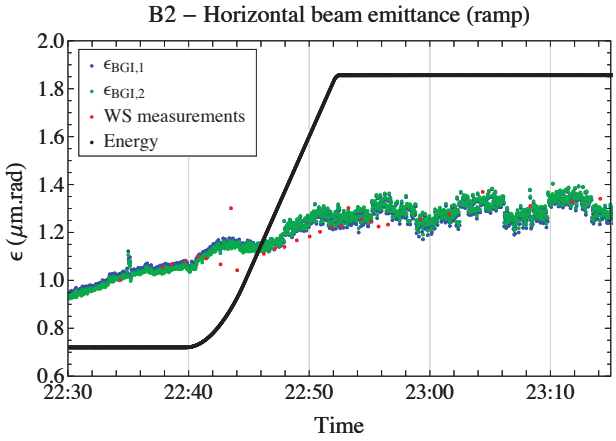

Figure 2: Horizontal BEAM2 emittance as measured by BGI and WS during a whole p-Pb fill.

- Review the low level software, taking into account the lessons learned during 2012
- Dismantle the BGI tanks and re-machine the vacuum sealing surfaces to minimize the risk of leaks
- The cameras' MCP will be repaired. In addition, the imaging optical system will be adapted to
- Ensure the optics compatibility with the smaller beam sizes at 7 TeV
- Upgrade the HV system to ensure a more stable detector operation
- Launch discussions concerning the allowable gas budget (i.e. investigate the possibility to run continuously with gas injection)

Synchrotron Light Monitor (BSRT)

The BSRT systems provide continuous bunch per bunch beam size measurements by imaging the synchrotron radiation emitted by a superconductor undulator (for beam energies below 1.5 TeV) or the D3 dipole (above 1.5 TeV). The 2012 BSRT performances were heavily affected by heating of the extraction mirror and mirror support due to electro-magnetic coupling with the circulating beam. This effect was enhanced in 2012 by the beam total intensity and intensity per bunch. The thermal cycles caused a permanent deformation of the clamps holding the mirror and a blistering of the mirror reflective coating, as can be seen in the pictures of Fig. 3, taken after the B2 system removal during TS#3. The B1 mirror was found in a very similar state after its removal in TS#4. More information about the BSRT heating effects can be found in the LHC Machine Committee minutes [3, 4].

Both systems were originally equipped with silicon bulk mirrors with dielectric coating. TS#3 and TS#4 were used to test other mirror types for investigating the best option to minimize the heating effects with the present tank design, while ensuring enough reflectivity. The outcome can be summarized as follows:

1. A silicon bulk, uncoated mirror showed a reduced heating (as measured with temperature probes outside the BSRT tank), but resulted to be unusable for imaging, given the distorted recorded images.
2. A glass bulk, metallic coated mirror resulted in a reduced heating effect at low beam intensities, but suffered coating deformation (evidenced by the beam spot image deformation) at high intensities
3. A glass bulk, dielectric coated mirror resulted in a reduced heating (w.r.t. the original silicon bulk, dielectric coated mirror) and did not show any coating deformation according to the recorded images, also at high intensity.

The extraction mirror coating damages compromised considerably the BSRT accuracy in the beam size determination. Not only did the blistering caused the image smearing, but the calibration with respect to the WS had to be

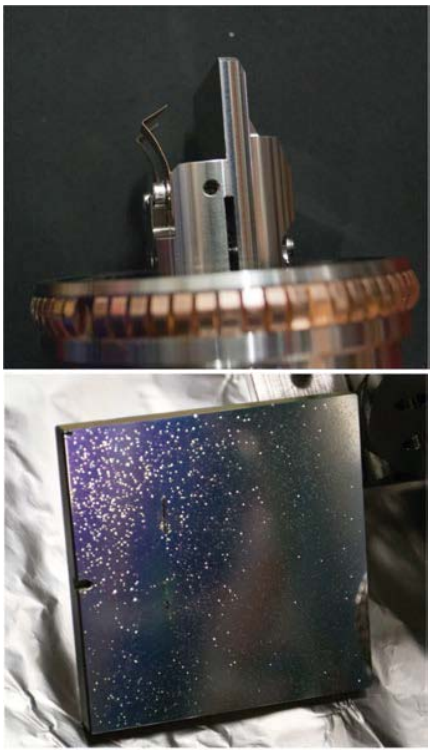

Figure 3: BSRT mirror holder clamps deformation and coating blistering, as evident after the B2 system removal in September 2012.

changed continuously following the coating ageing. Nevertheless it was possible during the year to recalibrate the system regularly and log useful data.
The analysis of the 2010 and 2011 data showed a higher than expected point spread function of the imaging system. As an improvement, towards the end of the 2012 run, the BSRT optics was changed from a layout based on focusing mirrors to focusing lenses. Due to the different focal lengths, this allowed simplifying meaningfully the optical line, by reducing the number of components and thus the image smearing due to vibrations and air flows.
A BSRT-WS comparison (B1, vertical) after the telescope upgrade is shown in Fig. 4. The example refers to a 450 GeV fill during which different bunches were blown-up with the ADT system and then scraped. Considering the BSRT calibration according to

$$\sigma = \sqrt{\sigma_{meas}^2 - \sigma_{psf}^2} \ , \qquad (1)$$

in the shown example a unique $\sigma_{psf} \approx 0.8\,mm$ correction was applied to all BSRT data, for a measured $\sigma_{meas} \approx 1.3\,mm$. This is still higher than expected from simulations, but is 20-25 % smaller than what normally found

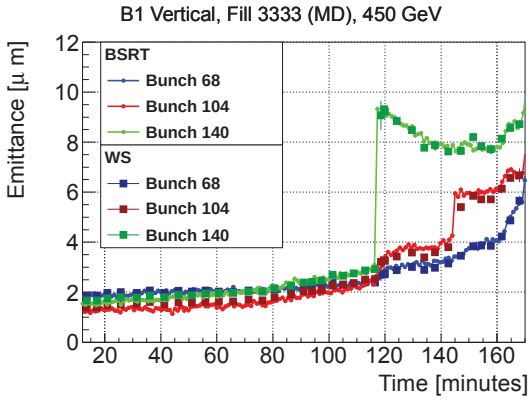

Figure 4: Example of emittance measurements with WS and BSRT at 450 GeV (B1 Vertical), while having bunches with different beam sizes and applying a single calibration factor to the BSRT.

with the old telescope. Preliminary results at 4 TeV also confirm the point spread function reduction after changing to the new optics.
A new control server, managing the BSRT system's gain and light steering as well as the bunch per bunch scans, was deployed at the end of 2012 and validated during the ion-proton run in 2013. This improved the system reliability and availability (previously BI-expert interventions were often needed to recover the proper light steering or control settings) and increased the bunch scan speed from 1 to about 10 Hz.
Concerning the BSRT upgrades foreseen for LS1, a first step was to install during TS#4 temperature probes in vacuum (B2 system only) in strategic locations (close to the mirror holder clamps, to the ferrite tiles and the bellow at the outer edge of the mechanism shaft. The temperature data recorded during a high intensity test in February 2013 are being analyzed and are meant to complement electro-magnetic and thermo-mechanical simulations in order to characterize the amount of power transferred from the beam to the equipment and the heat propagation mechanisms.
For after LS1 it is foreseen to start with:

- mirror and mirror holders minimizing RF coupling while maintaing reflectivity in the appropriate spectral range. This may imply modifying the BSRT tank, at first according to the outcome of the RF and thermo-mechanical studies.

- a telescope optics (including the extraction mirror coating and the camera sensor) suitable for a low wavelength imaging system to reduce diffraction effects at 7 TeV.

In addition, the telescopes will be equipped with a new light shielding designed to minimize parasitic light and air flows. This was motivated to diminish the Longitudinal Density Monitor and the Abort Gap Monitor background, but will be beneficial for the BSRT as well.

LONGITUDINAL DISTRIBUTION MEASUREMENTS

Abort Gap Monitor (AGM)

The AGM has been designed to monitor the particles population inside the 3 μs abort gap, needed almost empty by the dump kickers to perform clean beam dumps. The system is based on the detection of synchrotron light by a gated photomultipier and shares with the BSRT the light extraction and part of the focusing system.
During 2012 the system reliability was affected by the problems with the BSRT extraction mirror heating described above (no BSRT spot on the cameras always meant no proper AGM signal). Software issues (both on the BSRT and BSRA) also caused some AGM unavailability periods requiring the intervention of an expert, especially in the first part of the run.
The AGM accuracy relies on the energy dependent protons per photon calibration and the overall error on the abort gap population is about 50 %. The uncertainty is dominated by:

- Alignment and steering, affecting the light collection efficiency
- Attenuation of light in optical components, that can change due to dust, radiation etc.
- PMT gain versus voltage stability and HV control
- PMT Photocathode ageing
- Electromagnetic noise in the signal

For these reasons, in 2012 the AGM monitors needed frequent re-calibration by gating the PMT on a filled RF bucket and cross-calibrating with respect to the Fast Current Transformers.

The new BSRT telescope optics (after TS#3 for B1 and after TS#4 for B2) resulted in a simplified optical line to the AGM and no movable elements before the PMT. This improved the AGM calibration stability, at first by eliminating the need to compensate for light losses at the moment of inserting the old optics delay line.
During LS1, it is foreseen to improve the AGM reliability by introducing software self-checks and self-calibration procedures that should be performed systematically with circulating beam. During the self-calibration the abort gap population cannot be monitored, but this represents less than 1% of a fill. The exact details should be discussed with the MPP committee.

Longitudinal Density Monitor (LDM)

In addition to the camera for transverse beam size measurements and to the PMT for the abort gap monitoring, the BSRT telescope delivers the extracted synchrotron radiation to an avalanche photo-diode for the Longitudinal Density Monitor (LDM). At the cost of a relatively long integration time, the LDM allows measuring the intensity of satellite and ghost bunches down to about 10^{-4} of the main bunches. Despite its 50 ps resolution, it is not designed to verify the bunch shape at a fine level.
During 2012, the LDM remained an expert tool and the related operational software was still under development. Artifacts linked to the detector behavior still required a BI expert to properly setup the system during normal LHC operation. This had no impact during the Van Der Meer scans, for which the LDM proved to be an important tool to determine the absolute luminosity calibration.
Issues were related to the detector dead time and after pulse dependence on the filling pattern, for which the correction algorithms were not always effective. In addition, the measurement accuracy and interpretation was affected by internal light reflections in the telescope.
After LS1, the LDM will still start in a development mode, at first to study the filling pattern dependence and to deploy operational software. The new telescope optics (already tested in 2012) and a new light shielding will certainly diminish the internal reflections.
An example of LDM measurements during a Van Der Meer scan fill is shown in Fig. 5.

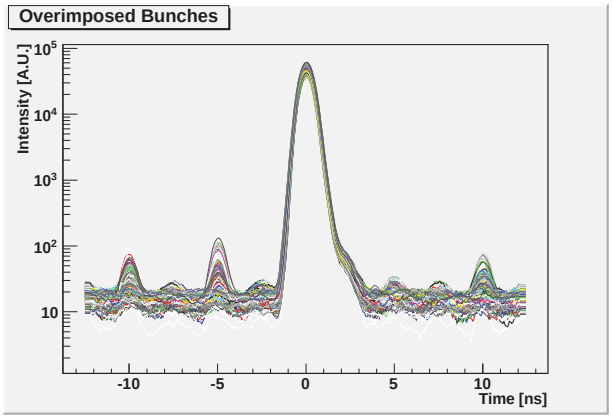

Figure 5: 25 ns slot population as measured by the LDM during a Van Der Meer scan with ions at 1.38 TeV (Fill 3540). Different colors correspond to different (superimposed) slots.

FROM 4 TO 7 TEV

Moving from 4 to 6.5 or 7 TeV, given the present beam optics (with almost constant betatron functions in IR4 as function of energy), will imply having smaller beam sizes at the transverse profile monitors.
For the WS, this will result in fewer data points per sigma. Since it is not convenient to reduce the wire speed and consequently the intensity thresholds, to increase the resolution it could be necessary to use the overlap of several data sets:

- either multiple scans on the same bunch (with different acquisition delays w.r.t. to the bunch passage through the wire)
- or the profiles from multiple bunches during a single scan (for which at each turn, the acquisition is slightly delayed from bunch to bunch according to the bunch spacing)

This second technique is already successfully used for the SPS WS at 450 GeV.
At higher energy the WS operation will be limited up to about 10^{12} circulating protons (see Table 1) in order to cope with lower BLM thresholds for protecting superconductor magnets.
For both the BGI and the BSRT, it is foreseen to adapt the optical imaging system in order to have about the same mm/pixel resolution as at 4 TeV.
The BSRT will also suffer of a higher relative contribution of diffraction to the point spread function. This is due to both the smaller beam size and the reduced synchrotron light emission cone angle. Since quantifying the absolute value of diffraction (in order to exactly correct for it) has been difficult until now, as already mentioned above, it is foreseen to design a new telescope optics working in the low wavelengths (i.e. $\leq 300\,nm$) in order to anyhow reduce the effect.

At higher energy, both the AGM and the LDM signals will result in higher photon rates. This will be easily managed by properly dimensioning the optical filters attenuations in front of the detectors.

FROM 50 TO 25 NS

The LHC WS are equipped with 40 MHz acquisition electronics allowing bunch per bunch acquisition with 25 ns sampling resolution. However, tests with 25 ns spaced bunches showed a cross-talk between consecutive bunches of about 10 %. This will be studied during LS1.
Concerning intensity thresholds, the possibility of scanning 288 bunch trains at injection will depend on the decision for going to smaller diameter wires (i.e. lower losses downstream, decision not taken yet) and of course on the actual bunch population for 25 ns beams.
For the BGI, presently averaging over multi-bunches, there is no evident difference between 50 and 25 ns beams.
Concerning the BSRT, the camera intensifiers can be gated to 25 ns and the only impact will be longer periods to scan over all bunches.
For the AGM and the LDM there is no evident impact.

REFERENCES

[1] M.Khun, *LHC Emittance Preservation during the 2012 Run*, These Proceedings .

[2] Donnet, J.B. and Bansal, R.C. , *Carbon Fibers*, M.Dekker (International fiber science and technology series), isbn:9780824778651, 1990.

[3] F.Roncarolo et al., *Update on the BSRT*, LMC-146 Minutes

[4] F.Roncarolo et al., *Update on the BSRT*, LMC-151 Minutes

[5] R. Versteegen et al., *First proton-nucleus collisions in the LHC: the p-Pb pilot physics*, CERN-ATS-Note-2012-094 MD, 2012.

LHC RF: 2012 PERFORMANCE AND PREPARATIONS FOR POST LS1 OPERATION

T. Mastoridis*, P. Baudrenghien, O. Brunner, E. Shaposhnikova,
reporting for the RF group

Abstract

This paper presents the lessons learned through the RF system performance in 2012, the RF improvements in 2012, the RF plans for LS1, and the possible limitations on RF performance past LS1. An emphasis is placed on expected operation limits for operation with 25 ns bunch spacing, at 6.5 TeV, and/or with higher beam currents. Studies performed to improve understanding (single bunch and multi bunch intensity limits, beam spectrum and relation to heating) and to evaluate mitigation techniques for these limits are described. Development plans on new equipment are discussed. Of particular importance are the cavity set-point modulation technique, which significantly reduces the klystron forward power requirements, the longitudinal damper, batch-by-batch blow-up at injection, and the RF frequency cogging, essential for p-Pb operation.

2012 PERFORMANCE

The RF performed very well during 2012. The RF system did not limit the evolution of peak or integrated luminosity. The increased single bunch intensity (up to $\approx$ 1.65e11) did not introduce longitudinal instabilities or lead to klystron saturation. Klystrons were routinely operated with up to 165 kW per klystron at flat top (V_{RF} = 12 MV). Capture losses were negligible (below 0.5%) with the injection voltage at 6 MV (Figure 1). The abort gap and injection gap cleaning were on during injections.

The RF system was also readily available to varied modes of operation: manipulations of bunch length, RF gymnastics for p-Pb operation, and the 25 ns spacing run. A test was also conducted with lower RF voltage (6 MV) during the squeeze, with no noticeable improvement on transverse stability. RF phase modulation was also used to create longitudinally flatter bunches.

RF fault summary

The system reliability was improved over 2011. During the 2011 run there were 78 faults (2.08 per week in protons, 6.5 per week in ions). During the 2012 proton run there were just 43 faults (1.34 per week) as shown in Figure 2. Most of the faults were concentrated in short time periods, since they had a common cause. For example, the crowbar related issues in weeks 20 and 27-31, and the issues with the RF amplifier for station 4B1 in weeks 43-45. The related causes have been identified and cured. Outside these time periods, there were several weeks with no faults.

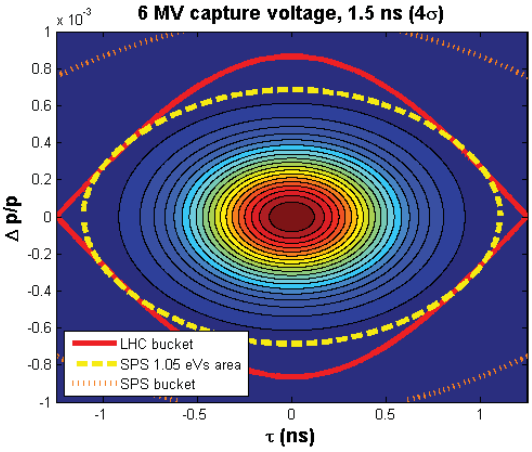

Figure 1: Comparison of SPS/LHC buckets and estimated bunch area at LHC injection (1.05 eVs). 4σ bunch length of 1.5 ns at injection.

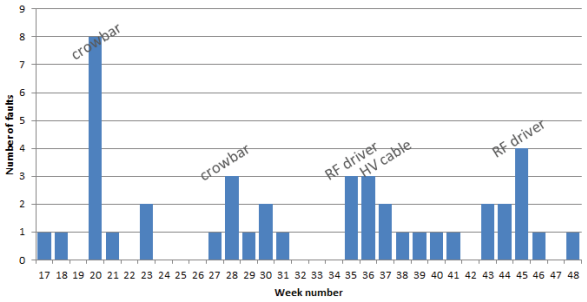

Figure 2: RF faults in 2012 (Courtesy D. Glenat).

In 2011 it was realized that cavity 3B2 cannot be operated reliably at 1.5 MV and above. Consequently, the cavity was operated with lower voltage in 2012, leading to a significant reduction in quenches, that contributed to the improved reliability.

There was also a rack recabling campaign in UX45 during the winter shutdown. All SMC cables were replaced by better quality cables. Since then, there were no more cabling related issues.

The RF system now employs about 800 interlocks. As a result there was only one serious debunching incident this year (5 in 2011).

On the other hand, there was a significant increase in crowbar inducing faults (from 11 to 20). Half of these faults took place in the first five weeks of the 2012 run

* themistoklis.mastoridis@cern.ch

and were attributed to one faulty solid state crowbar and one faulty thyratron. The rest are "real" crowbar events triggered by vacuum activity (arcing) in klystrons. There is some correlation of these events with klystrons being left at standby mode for extended periods of time. These events could be reduced after LS1 if the RF system is switched off when not in use.

The rest of the faults were separated into "unavoidable" faults and trips related to bad High Voltage contacts. The latter were either due to defective High Voltage connectors or to a damaged High Voltage cable (in September). The High Voltage cable has since been replaced and no more faults were observed. The High Voltage connectors have been upgraded, but due to the lengthy replacement process, they were only exchanged as needed. The upgrade campaign will be completed during LS1.

The good availability/reliability allowed us to make significant progress on our post-LS1 preparation during 2012.

NEW ITEMS FOR 2012

Batch-by-batch blowup

The batch-by-batch blowup was tested and commissioned during 2012 [1]. Its goal is to reduce the transverse emittance growth rates due to IBS by selectively blowing up the longitudinal emittance of the incoming batch at each injection. The technique worked well (Figure 3), but unfortunately, there was no measurable effect on luminosity. There are two explanations under investigation. First, it

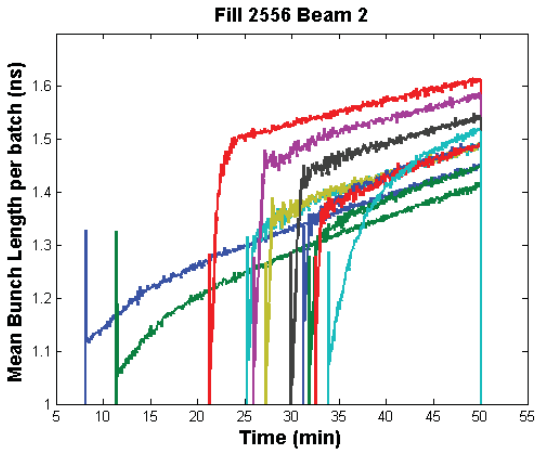

Figure 3: Mean bunch length per batch, fill 2556, Beam 2. First two batches are not blown up.

is possible that the IBS contributions to emittance growth are smaller than expected. Alternatively, it is suspected that smaller transverse emittances are achieved at flat top due to the action of the batch-by-batch blowup, but they are not preserved to physics. It was hard to test the latter explanation, since the BSRT was not available and there were no transverse emittance measurements. Operation with the Batch Compression, Bunch Merging and Splittings (BCMS) scheme beam and the corresponding higher brightness, or with higher single bunch intensities could show a more clear improvement.

Cogging/Rephasing

Cogging/rephasing of the two rings at flat top is necessary for the p-Pb run. A technique was developed, tested, and used for a p-Pb physics fill and for MD purposes (two-beam impedance MD). The process starts by accelerating (decelerating) one beam to an off-centered orbit. After time t, the relative phase of the beam has drifted by $\Delta\phi = 2\pi\Delta f t$. If only one beam is moved, the crossing azimuth drifts by half that value. When the desired position is reached the beam is decelerated (accelerated) back to the centered orbit. Figure 4 shows the results during a p-Pb

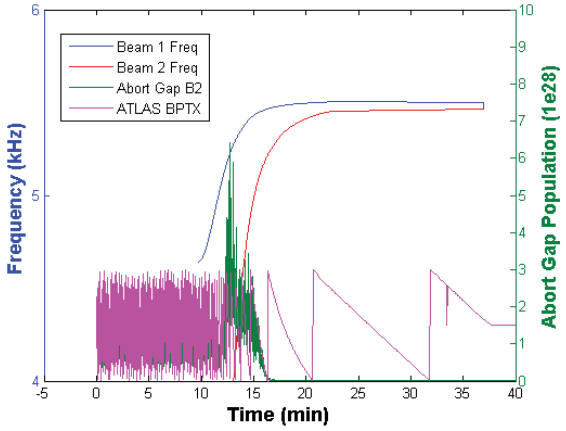

Figure 4: RF frequencies for the two rings during p-Pb ramp. ATLAS BPTX and abort gap population for Beam 2 also shown.

ramp. The difference of the two RF frequencies is evident during the ramp. The frequencies are kept apart until flat top, then the beams are rephased to make buckets 1 cross in IP1 and IP5 (as shown by the ATLAS BPTX signal). There is no evidence of an increase in the abort gap population during this process. Improvements were implemented to make the process more adiabatic for the 2013 p-Pb run.

New Diagnostics

During 2012 new RF diagnostics were made available to the CCM (fixed displays for CCC) and/or TIMBER. These include the average beam spectra which are particularly useful to analyze the effect of bunch spectrum on heating (Figure 5), individual bunch profiles (Figure 6), and the cavity sum phase noise which can help identify the cause of debunching incidents (Figure 7). Finally, an implementation of the Beam Quality Monitor (BQM) with faster sampling rate (≈1 second between samples, down from 4 seconds/sample) was tested at flat bottom.

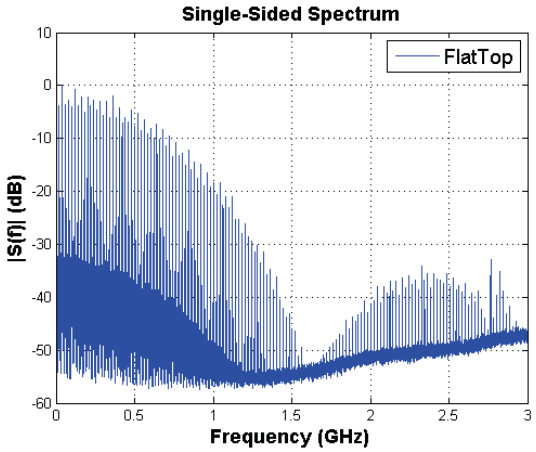

Figure 5: Average beam spectrum at flat top.

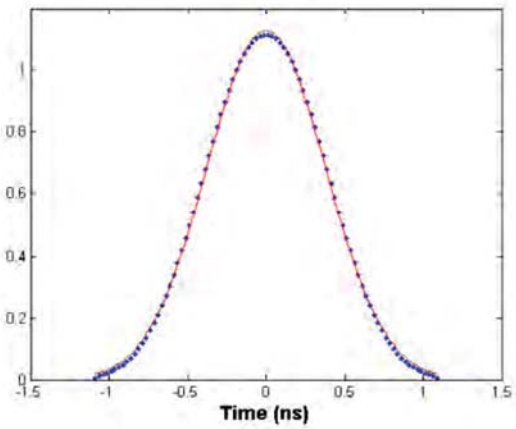

Figure 6: Single bunch profile with high sampling rate scope in UX45 (40 GSamples/second).

ANTICIPATED LIMITATIONS AFTER LS1 AND ACTIONS TAKEN

25 ns, 6.5 TeV implications

The higher beam energy implies lower thresholds for longitudinal single and multi bunch instabilities [2]. As a result, the longitudinal emittance blowup is absolutely necessary to guarantee stability. As long as the same operational scheme of a constant bunch length during the ramp is used, the stability margins will be maintained [3], [4].

The higher beam energy also implies a significantly reduced synchrotron radiation damping time, which might result in bunch shrinking at flat top. For 7 TeV operation, a 63-hour IBS growth time and a 12.9-hour radiation damping time have been estimated [5], resulting in a total emittance damping time of 16.2 hours. If this becomes an issue, it should be possible to modify the existing blowup algorithms for use at flat top.

The RF system is more affected by the possible increase in beam current due to 25 ns spacing. Such an increase implies higher demanded klystron power and reduced margin for coupled-bunch instabilities. If the higher beam current is reached through a single bunch intensity increase, thresholds for single-bunch longitudinal instabilities should be investigated.

During 2012, various actions have been taken, studies conducted, and new algorithms developed to either confirm sufficient margins of operation or adapt the RF system appropriately for higher beam current.

Power limits: Cavity Voltage Setpoint Modulation

The RF/LLRF systems are currently setup for extremely stable RF voltage (minimize transient beam loading effects). Less than 1° (7 ps) cavity phase variation along the turn is achieved as a result (Figure 8). If this scheme

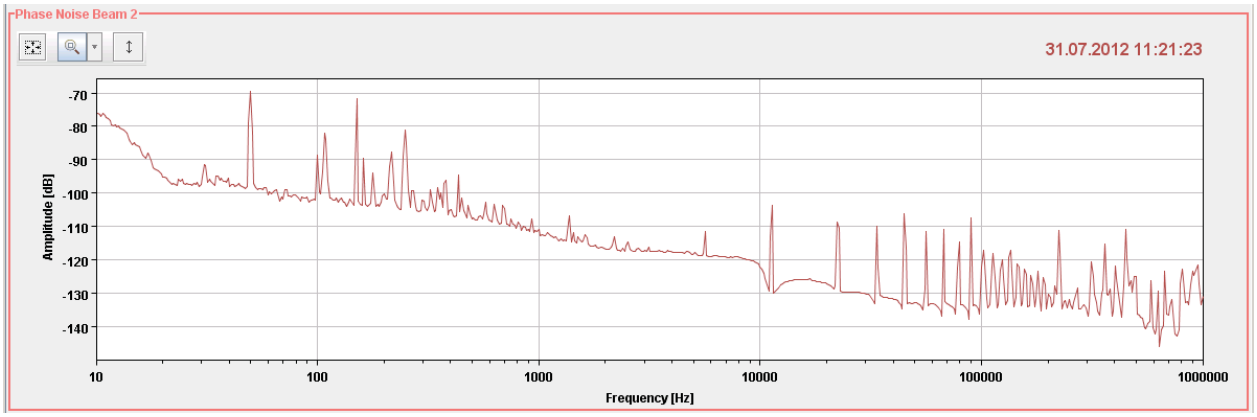

Figure 7: Cavity Sum Phase Noise in stable beams (Beam 2). The lines at the revolution frequency harmonics are a result of the small residual uncompensated beam loading. Also visible are the 50 Hz line and its harmonics, as well as the mechanical resonances of the cavity tuner.

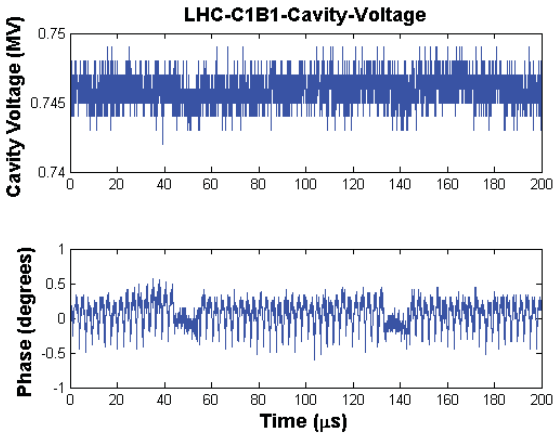

Figure 8: Cavity amplitude and phase with 2100 bunches, 25 ns spacing ($\approx$ 0.4 A DC). The gaps between batches and the abort gap are visible in the phase plot.

is preserved, more than 200 kW of klystron forward power would be required for 25 ns operation with nominal bunch intensity ($\approx$ 0.58 A DC). Even though the klystrons are rated to 300 kW, this scheme cannot be extended beyond nominal due to the reduced margin of operation, variations among the stations, and transient behavior between the beam and no-beam segments of the turn [6].

The reduced margins were evident during the short 25 ns run in 2012, when to cope with the first two ramps of 72 bunch trains at 25 ns spacing, the tuners and couplers had to be fine adjusted and the RF voltage at flat top reduced to deal with arcs in two different circulator loads during the first two ramps. It is also possible that this equipment is simply in need of conditioning at this higher power; either way, an alternative scheme for operation with beam current above nominal (and possibly earlier) would be helpful and absolutely necessary for the High Lumi LHC upgrade (2.2e11 protons/bunch, 1.1 A DC, 25 ns spacing).

With this new scheme, the beam induced cavity phase modulation in physics will be included in the cavity voltage setpoint for each bunch using an adaptive algorithm. As a result, the strong RF feedback and One-Turn feedback systems will not act on transient beam loading, but still continue regulating the cavity voltage, reducing the cavity effective impedance, and compensating for unwanted perturbations.

The trade-off of this scheme is that it results in a modulation of the bunch phase over a turn. This modulation though will only be $\approx$ 65 ps over a turn in physics, for ultimate beam (1.7e11 protons/bunch, 0.86 A DC, 25 ns spacing), compared to a 1.25 ns long bunch. Furthermore, the collision point shift will be much smaller in IP1 and IP5 due to the symmetrical phase modulation in the two rings.

The phase modulation would be more significant at 450 GeV. To avoid injection complications, the current scheme will be used during injection and then the adaptive algorithm will be switched on during pre-ramp. Since the RF voltage setting at injection is much lower, there is sufficient power available for transient beam loading compensation at 450 GeV.

The algorithm was tested during MD sessions in 2012 with very encouraging results [7], [8]. Figure 9 shows the significant reduction in klystron forward power achieved during the test. The power increases at injection with the

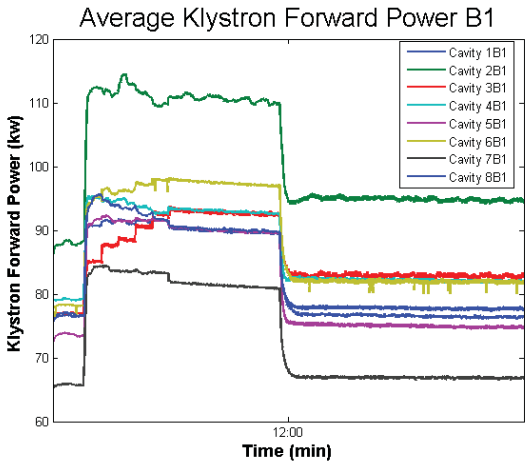

Figure 9: Average klystron forward power during cavity phase modulation MD. 144 bunches.

old scheme (single 144 bunch batch). A few minutes later the algorithm is switched on and the power returns close to the pre-injection levels. Figure 10 shows the resulting cavity phase modulation during a similar test with a half-full machine (654 bunches). This filling scheme actually

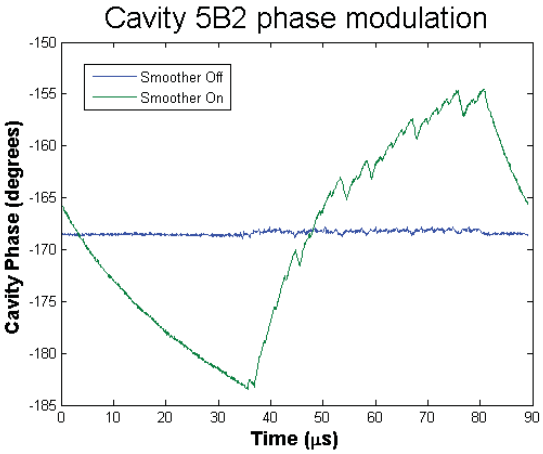

Figure 10: Cavity phase over a turn during cavity phase modulation MD. 654 bunches.

results to the highest possible phase modulation ($\approx 30^\circ$ or 210 ps).

It is important to note that with this scheme the klystron forward power requirements are independent of beam current. As a result, the existing RF system will be sufficient even for High-Lumi LHC. A further positive side effect of the new scheme and higher cavity detuning is the reduced reflected power and beam induced voltage in the case of a klystron trip [6].

Longitudinal Single-bunch Stability

As mentioned above, as long as the bunch length is kept constant during the ramp through the emittance blowup action, the stability margin is similar at flat bottom and flat top [2]. Dedicated MDs and observations during the High-pile MD were used to estimate the single-bunch stability threshold. In the latter case, two bunches per ring with intensities up to 3e11 and emittance from $\approx$ 0.6 eVs at flat bottom to 2.6-2.9 eVs at flat top (bunch dependent) were stable throughout the cycle, as shown in Figure 11 [9]. The beam

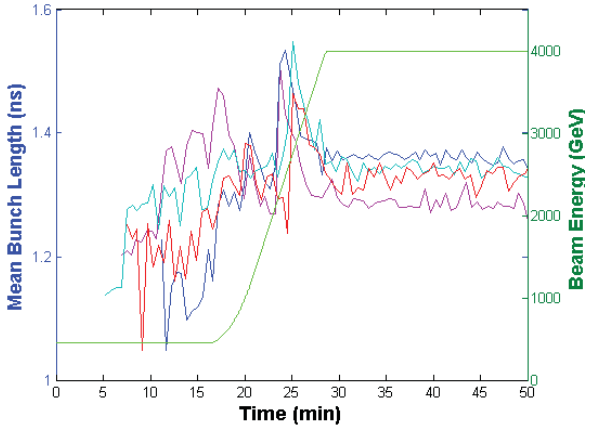

Figure 11: Bunch lengths during the ramp to 4 TeV. 4 bunches. High-pileup MD.

phase loop was on for this test. Even though the action of the beam phase loop is limited to mode zero motion, some coupling to other modes is possible with a small number of bunches. Consequently, this result is encouraging, but not necessarily reproducible with longer bunch trains.

During dedicated MDs, bunches of up to 2.4e11 and $\approx$ 0.6 eVs were stable at 450 GeV. Longitudinal instabilities developed during the ramp with the beam phase loop off [10], [11]. Bunches with residual oscillations from injections were more unstable during the ramp. The longitudinal damper acting on the injection oscillations should help. Figure 12 shows the emittance and energy of the bunches when the instabilities appear. Not surprisingly, they approximately follow the emittance curve for a bunch of constant bunch length.

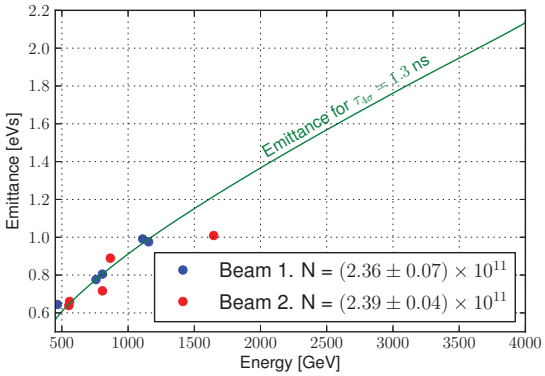

Figure 12: Loss of Landau damping as a function of emittance during the ramp. Courtesy J. Esteban Muller [11].

Longitudinal Coupled-bunch Instabilities

A factor of four stability margin on longitudinal coupled-bunch instabilities (CBI) due to the fundamental impedance of the 400 MHz cavities has been estimated, even with ultimate LHC beam (1.7e11 protons/bunch, 0.86 A DC, 25 ns spacing) [6]. An MD at 450 GeV was conducted to validate these estimates and prove that longitudinal CBIs due to the cavity fundamental impedance are not an issue for higher beam currents. To achieve this, the RF feedback gain was reduced and the most unstable coupled-bunch mode n was excited by injecting narrow band phase noise in the cavity, centered at $nf_{rev} \pm f_s$ (dipole mode). Even after an 18 dB RF gain reduction (1/8 linear) and turning the 1-turn feedback off (comparable to a situation with more than 10 times higher beam current), the beam was stable. Figure 13 shows the Fourier decomposition of bunch-by-bunch phase acquisitions over 73 turns, repeated every 10 seconds. During the beginning of these acquisitions, mode $n = \pm 3$ was excited for 30 seconds. Based on previous estimates, this is the most unstable mode for the given reduced RF feedback settings used for this measurement. The excitation and subsequent damping are evident.

During normal operation, the beam was also stable when due to a LLRF fault, a cavity was in open loop (December 1^{st} 2012), in agreement with the above observations.

It should be noted that these estimates and measurements only consider the effect of the cavity fundamental impedance on coupled-bunch instabilities. Other structures could contribute to the narrowband longitudinal impedance.

Bunch Length vs. Longitudinal Distribution

In 2012, tests were conducted to check the feasibility of operation with shorter/longer bunch lengths. No show-stopper was discovered from the RF system. There were also no limitations in terms of heating, *assuming* the beam spectrum does not deviate much from the one during the

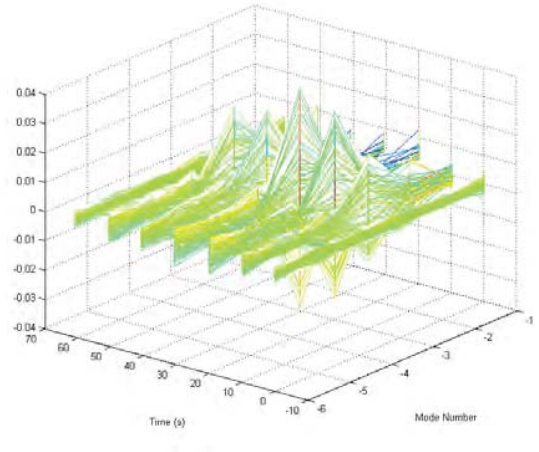

Figure 13: Modal decomposition of bunch phases. Growth and damping of mode -3 is evident.

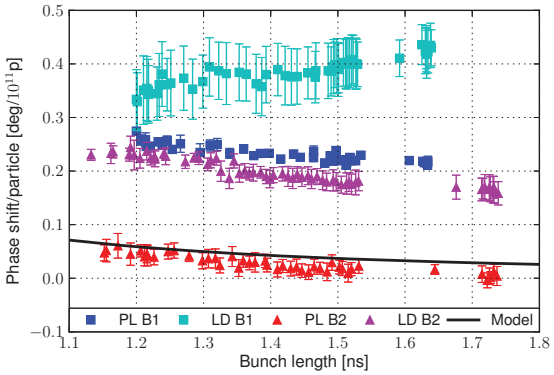

Figure 14: Stable phase shift for estimate of resistive broadband longitudinal impedance. Courtesy J. Esteban Muller [11].

test [12]. It should be noted though that the bunch length target has been slowly increased during 2011-2012 from the nominal 1 ns value to 1.25 ns. Reference [12] also reports on the tested "flat bunches" effect on heating.

An important lesson from 2012 operation was that the bunch length is a very useful and important, but sometimes limited metric: significant variations in the longitudinal distribution have been observed from fill to fill and from flat bottom to flat top (mostly due to the emittance blowup). These variations are often important; for example during heating exercises and longitudinal stability MDs. These variations should be taken into consideration before drawing conclusions on the heating of structures with narrowband impedances.

Longitudinal Broadband Impedance Estimation

An effort was made to estimate the longitudinal broadband impedance through peak-detected Schottky [13] and stable phase shift measurements [14], as well as observations during the "flat bunches" test and the single-bunch stability MDs.

The stable phase shift measurements (resistive part of impedance) measured higher broadband impedance than expected. It is suspected though that systematic measurement errors are comparable or even higher than the actual phase shift contribution from the impedance (estimated to 0.05° per 1e11 protons for a bunch length of 1.4 ns). It might be possible to increase the resolution of these measurements through post processing the data. Figure 14 shows the stable phase shift with bunch length through two different acquisition modules for each ring, as well as the predicted behavior from the impedance model. Systematic errors seem to be present and to be different among modules.

During the "Flat bunches" MD, it was possible to estimate the reactive part of the broadband impedance to ≈ 0.2 Hz per 1e11 protons, through the varied reaction of different bunches on the very narrow and slowly changed phase modulation.

The Peak-detected Schottky measurements – useful for reactive broadband impedance estimates – were limited by the very small resulting quadrupole tune shift, especially for long bunches: 0.2 Hz per 1e11 protons at f_s for a bunch length of 1.4 ns. As a result, it is very difficult to distinguish such a shift in the Schottky spectra and to decouple it from longitudinal distribution effects. Figure 15 shows the

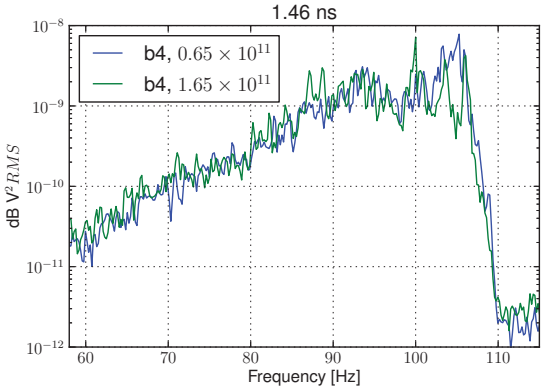

Figure 15: Peak-detected Schottky measurement, 1.4 ns bunch lengths, bunch intensities of 0.65e11 and 1.65e11 respectively. Courtesy J. Esteban Muller.

peak-detected Schottky measurements for two bunches of comparable bunch length, but significantly different bunch intensities.

Through these estimates, it seems that the reactive impedance is comparable with and definitely not larger than the estimated and budgeted values ($\approx 0.06\ \Omega$ in Design Report, $\approx 0.09\ \Omega$ with later collimator design). It is

harder to reach a conclusion on the resistive part.

Estimates based on the loss of Landau damping during the ramp with beam phase loop off seem to provide the highest resolution [4]. Simulations and estimations of the instability threshold during the ramp are necessary before a conclusion could be drawn though.

THE FUTURE: ACTIONS TO BE TAKEN

Module Replacement

The most significant intervention to the RF system during LS1, will be the replacement of the RF cryomodule M1B2. Since cavity 3B2 has been operating with a lower voltage since the start-up and to improve future reliability and availability, it was decided to replace the faulty cryomodule with the spare (Figure 16). Testing of the spare

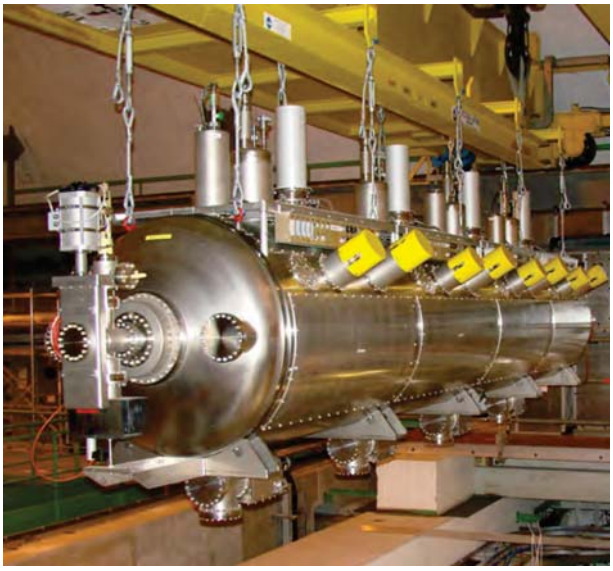

Figure 16: RF cryomodule (four cavities).

module was completed in August 2012. No quench was observed below 2.6 MV and the x-ray emissions around the module were an order of magnitude lower than for the faulty module. There is still some risk of degradation during transportation and mounting. To mitigate the risk of affecting machine operation, the replaced module will not be dismantled for repair before the new module is restarted and fully validated in the machine. New LHC spare cavities are being produced.

Further Diagnostics, New Systems

Injection oscillations with very slow damping times (≈15 minutes) have been observed in the LHC since 2011 with 1.2e11 protons/bunch [15]. The situation has not degraded with the intensity increase to 1.6e11. Further studies are necessary to explain them. The Longitudinal Damper (under development) should help reduce the injection oscillations though. The new system has been tested in the lab and once with beam in the last day of 2012 operations. Analysis is in progress and further tests and commissioning are planned for the short 2013 operation. If emittance blowup is not sufficient to achieve longitudinal stability in the High-Lumi era, the Longitudinal Damper could also be of help with low order mode coupled-bunch instabilities, whereas a higher harmonic RF system could be used for other modes.

Tests of a faster BQM system are also planned for 2013.

During LS1, "Fast diagnostics" for amplitude and phase observations/logging for each cavity will be deployed. These modules will immediately point to the "noisy" cavity in case of a problem (such as saturation due to non-moving coupler, an issue that happened a few times in 2012) and help with RF debugging. A bunch-by-bunch phase fixed display should be developed during that time too. The data are already available, but some software work will be necessary. Finally, all RF VME front-ends will be moved to LINUX. This change will require rewriting and recompiling of software drivers.

Luminosity Leveling

In the later part of 2012, the RF voltage target for the end of the ramp was reduced from 12 to 10 MV. A few hours into the physics coast, the RF voltage was increased to 12 MV in one step, with a small (≈2%) increase in luminosity.

Following this scheme, the longitudinal stability margin could be exploited for luminosity leveling. The RF voltage at the end of the ramp could be further reduced – as long as some stability margin is maintained – and then slowly increased during the physics coast, providing some amount of luminosity leveling.

CONCLUSIONS, ACKNOWLEDGMENTS

In conclusion, 2012 was a very successful year for the RF system, with improved performance and increased flexibility for new modes of operation, MD requirements, and the p-Pb run.

RF preparations for post-LS1 operation are well under way. During LS1, the RF emphasis will be on the cryomodule replacement.

Many people have contributed with material for this paper. The reported work though would not have been possible without the dedication and hard work of all RF group members.

REFERENCES

[1] T. Mastoridis, P. Baudrenghien, A. Butterworth, M. Jaussi, J. Molendijk, "Batch By Batch Longitudinal Emittance Blowup MD", CERN-ATS-Note-2012-050 MD, June 2012.

[2] E. Shaposhnikova, "Longitudinal beam parameters during acceleration in the LHC", LHC Project Note 242, December 2000.

[3] P. Baudrenghien *et. al.*, "Longitudinal Emittance Blowup in the LHC", Proc. IPAC 2011, 4-9 September 2011, San Sebastian, Spain.

[4] E. Shaposhnikova *et. al.*, "Loss of Landau damping in the LHC", Proc. IPAC 2011, 4-9 September 2011, San Sebastian, Spain.

[5] J. Tuckmantel], "Synchrotron Radiation Damping in LHC and Longitudinal Bunch Shape", LHC Project Report 819, June 2005.

[6] P. Baudrenghien, T. Mastoridis, "Proposal for an RF Roadmap Towards Ultimate Intensity in the LHC", Proceedings of Third International Particle Accelerator Conference 2012, New Orleans, Louisiana, USA, 20 - 25 May 2012.

[7] T. Mastoridis, P. Baudrenghien, A. Butterworth, J. Molendijk, J. Tuckmantel, "Cavity Phase Modulation MD", ATS-Note-2012-075 MD, 27 September 2012.

[8] T. Mastoridis, P. Baudrenghien, A. Butterworth, J. Molendijk, J. Tuckmantel, "Cavity Phase Modulation MD part II", CERN-ATS-Note-2013-013 MD, March 2013.

[9] T. Mastoridis, P. Baudrenghien, "RF Observations during High Pile-up MD", ATS-Note-2012-099 MD, December 2012.

[10] E. Shaposhnikova, T. Argyropoulos, C. Bhat, T. Bohl, P. Baudrenghien, T. Mastoridis, J. Esteban Muller, G. Papotti, J. Tuckmantel, W. Venturini Delsolaro, "Longitudinal single bunch stability in LHC with phase loop on", ATS-Note-2011-056 MD, July 2011.

[11] J. Esteban Muller *et. al.*, "Probing LHC Impedance with Single Bunches", ATS-Note-2013-001 MD, January 2013.

[12] B. Salvant *et. al.*, "Beam induced RF heating", these proceedings.

[13] T. Bohl, "Single bunch peak detected Schottky measurements in LHC", CERN Internal Note 2012-24 and 2012-04-31.

[14] T. Argyropoulos *et. al.*, "Studies of the LHC impedance at injection energy", ATS-Note-2012-060 MD, April 2012.

[15] P. Baudrenghien et. al., "Longitudinal Oscillations with Batch Injection in the LHC", CERN ATS-Note-2011-031 MD.

"WHAT YOU GET" INJECTION AND DUMP SYSTEM

C. Bracco, M.J. Barnes, W. Bartmann, E. Carlier, L.Drosdal, B. Goddard, V. Kain, M. Meddahi, V. Mertens, J. Uythoven, G. Vanbavinckhove, CERN, Geneva, Switzerland,
E. Gianfelice-Wendt, Fermilab, Batavia, USA.

Abstract

The performance of the LHC injection and extraction systems and the main problems encountered during 2012 operation are described. Special attention is dedicated to the stability of the transfer lines, steering frequency, sensitivity to beam and machine changes, injection protection collimators setup and the consequent impact on operation and possible machine protection issues. The improvements foreseen for operation with injection of up to 288 bunches after LS1 in terms of stability, availability and safety are explored. The modifications foreseen to strengthen the reliability of the LHC Beam Dumping System and the new TCDQ hardware for operation at 6.5 TeV with high intensity beams are introduced.

INTRODUCTION

Following the 2011-2012 winter stop the reference trajectories in the LHC Transfer Lines (TL) were re-established on March 25^{th}. The TL collimators (TCDI) were centred around the new reference and initially set to $\pm 4.5\ \sigma$ (nominal beam size) aperture. The "golden" trajectory, defined in March, remained valid for the full year of operation (r.m.s. deviation from reference < 0.2 mm for TI 2 and < 0.4 mm for TI 8 in both planes), also for injections with 288 bunches spaced by 25 ns. However, the need for transfer line steering became more frequent and lengthy towards the end of the run, in particular when moving to the SPS Q20 optics [1] (once/twice per week until the end of September, every 1-2 days in October and November). Observations and TL stability studies performed to explain the reason for the described degradation are presented.

Several issues, mainly caused by beam induced heating and frequent cycling, were encountered at the TDI both in IR 2 and IR 8. After the main failures the position of the TDI with respect to the beam had to be re-checked and validated. This required on average a shift of eight hours each time. The correct positioning of the TDI is vital to protect the machine in case of failures of the injection kickers (MKI) which happened several times during the year, as shown in the following. An intense consolidation campaign, involving the MKIs and TDIs, is foreseen for LS1: for both elements new beam screens will be installed, the TDIs will be completely dismounted and re-assembled with new parts as replacement, spares will be produced and the possibility of adding a thin layer of copper to reduce the heat load at the jaws is considered [2]. A new TDI design is under study and will be ready for operation after LS2.

The LHC Beam Dumping System (LBDS) [3] performance was excellent: the total downtime induced by the LBDS was about 14 hours and no asynchronous dump with beam occurred during the entire run. Nevertheless critical weaknesses were discovered in the powering logic of the system. Mitigation measures were put in place during the year and important improvements are foreseen for LS1 to allow safe operation at 6.5 TeV.

TRANSFER LINES

Ideally, the steering of the lines to the reference trajectory should minimise losses at the TCDI and injection oscillations at the same time. Large injection oscillations were the main reason for the repeated steering, while the setup procedure was slowed down by the difficulty in reducing the losses in the LHC injection region. The injection losses come from two main sources:

- Cross-talks induced by losses at the TCDI due to high tail population or mis-steering in the collimators region (transverse losses);
- Losses from de-bunched or un-captured beam from the SPS and/or in the LHC (longitudinal losses).

Only the first kind of losses can be mitigated with the TL steering while it has no effect on the longitudinal losses. Previous studies [4] showed that the Beam Loss Monitors (BLM) in the injection region can give an indication on the origin of the injection losses: high signals at the BLMs located close to the quadrupoles Q7 and Q8 indicate losses from the TL, while losses at the TDI injection protection collimator and downstream of it are mainly due to uncaptured beam. ln May the TCDIs were opened to $\pm 5\ \sigma$ to be less sensitive to injection losses induced by shot-to-shot trajectory jitter (losses reduced by a factor of 4, the validation tests were performed with the collimators at $\pm 5\ \sigma$ [4]). A detailed analysis showed that the injection losses recorded towards the end of the run were mainly longitudinal; this explained the reason for the lengthy and inefficiency of the steering. The Injection Quality Check (IQC) application will be upgraded to clearly indicate when TL steering is need to reduce injection losses (highlighting Beam Position Monitors (BPM) in the collimators region

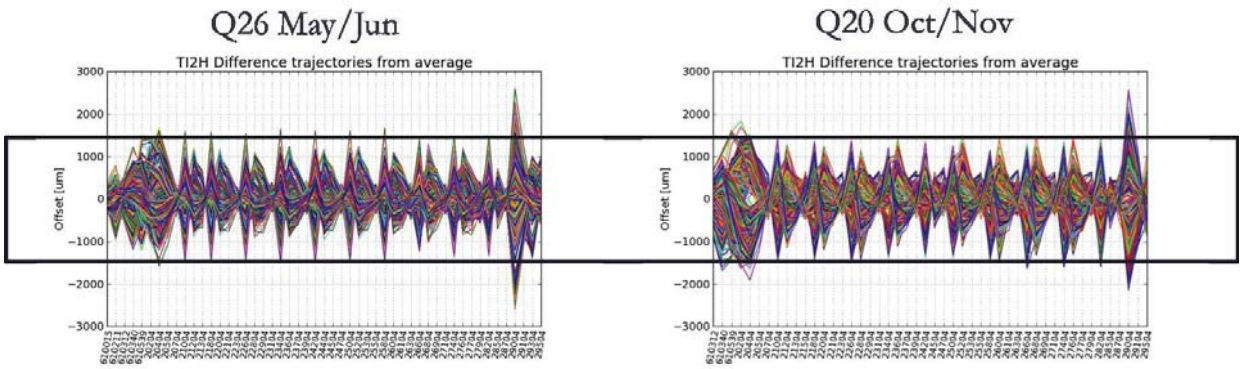

Figure 1: TI 2 uncorrected horizontal trajectories for 144 bunches injection in May/June (Q26 period, left) and in October/November (Q20 period, right).

and BLMs pointing to losses from the TL plus revision of the warning thresholds).

The steering of the lines is performed with a train of six nominal bunches. During the LHC re-commissioning period studies were carried out to define the best position of the six bunches on the waveform of the SPS extraction kicker (MKE), to be representative for the nominal injection of 144 bunches (50 ns bunch spacing) [5]. A discrepancy between the six and the 144 bunches trajectory was observed towards the end of the run. The corrections for the steering had to be calculated on the 144 bunches trajectory and, for safety reasons, any correction had to be followed by a six bunches injection. This required a frequent change of the beam in the SPS and had a relevant impact on the time spent for the injection setup. The reason for this discrepancy is not yet understood.

Stability Studies

Dedicated studies were performed to investigate the reason for the frequent drift of the lines and the resulting requirements for steering when moving to the Q20 optics. The uncorrected trajectories for the injections with 144 bunches were compared for two months of operation with the Q20 and Q26 optics. A Model Independent Analysis (MIA) was used to define the strongest Eigenmodes of the oscillations observed and to identify the most probable source of shot-to-shot variations. Two main sources of instability were identified:

- Current ripple in the SPS extraction septum (MSE) [5];
- Orbit variations in the SPS.

Only a negligible worsening of the trajectory variations was observed for the Q20 optics (Fig. 1). The MSE currents were changed by 5-8% to match the Q20 optics but the ripple remained at the same level as for Q26. The orbit variations in the SPS were monitored only for the Q20 optics; it is therefore impossible to say if any worsening was introduced. No clear conclusions could be drawn from these studies; a campaign of orbit measurements in the SPS with the Q26 optics should be performed.

Losses from De-bunched and Un-captured Beam

The LHC was operated, for three short periods (Q20 optics), with an enhanced level of 25 ns satellites to produce collisions with the main bunches in ALICE. The injection

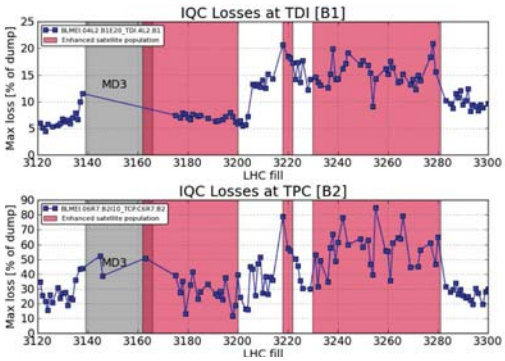

Figure 2: Maximum injection losses (in % with respect to the BLM dump thresholds) at the TDI during operations with (in red) and without satellites enhancement are plotted for several fills, for Beam 1 (top) and Beam 2 (bottom).

losses at the TDI (longitudinal losses) doubled only during the last two runs with satellites (red zones in Fig. 2). Moreover, for Beam 1, these losses remained higher than for the Q26 optics (before MD3, Fig. 1), even after removing the satellites' enhancement. Further elements (i.e.

batch-by-batch blowup, injection cleaning, etc.) must have contributed to the increased rate of de-bunched and uncaptured beam but it was not possible to disentangle the different contributions and understand the reason for the observed degradation.

Two beam dumps (fill number 3278 and 3281) were induced by the losses recorded by the LHCb Beam Conditions Monitor (BCM) at injection. These losses were due to the presence of two unwanted 50 ns bunches at the end of the 144 bunches train. The trailing bunches were removed by shortening the pulse length of the PS extraction kicker and no new similar dump re-occurred.

25 NS SCRUBBING RUN

A scrubbing run with 25 ns beam was carried out just before the Technical Stop 4 (TS4). The trajectories in the TLs were steered with respect to the "golden" reference defined for the 50 ns beams allowing a straightforward injection of up to 288 bunches with low injection losses (maximum loss in percentage from dump threshold:15.3 % for Beam 1 and 10.8 % for Beam 2). As expected, the losses from the TLs scaled linearly with the injected intensity while the longitudinal losses remained almost unchanged. Several consecutive injections of trains of 288 bunches were performed with maximum losses of $\sim$50 % of the dump threshold for both beams.

Several mitigations were put in place to reduce the sensitivity to injection losses at a number of BLMs in the LHC injection region (including the TDI): implementation of RC electronic delays at the BLMs [4] (sensitivity reduced by up to a factor 180) and TCDI relaxed apertures ($\pm 5\ \sigma$ instead of $\pm 4.5\ \sigma$). Ideally, all the electronic delays at the BLMs should be removed and the TCDIs should be set at nominal aperture to provide a better protection and allow more margin for orbit variations in the LHC. Alternative solutions have to be put in place for a safe operation after LS1 without being limited by the injection losses. The BLM team is evaluating the option of substituting the critical BLMs with Little Ionisation Chambers (LICs) which are less sensitive and have a wider dynamic range.

TDI HARDWARE PROBLEMS

TDI in IR8

Two spurious glitches occurred on the Right-Upstream (RU) end-switch of the TDI lower jaw when moving to parking position before the start of the energy ramp. As a consequence of the glitch, the switch was activated and the RU motor stopped while the motor at the other corner (Right-Downstream, RD) continued moving; this introduced a tilt of up to 22 mrad at the jaw and a suspected plastic deformation. The jaw position controller revealed the fault and reacted correctly: the collimator went into a "warning" state without triggering any beam dump (in one occasion the beam was dumped by the losses induced by the RU corner moving into the beam). As a follow-up of these accidents, the control module of the RU switch was exchanged and the TDI beam based alignment was re-checked and validated. An additional interlock was implemented to limit the maximum tilt of the jaw to 5 mrad. A task was added in the LHC operational sequencer, before the start of the energy ramp, to check the TDI position with respect to the settings and eventually stop operations in case of anomalies.

During the 25 ns scrubbing run the interplay between the beam induced heating and the frequent cycling of the jaw from injection to parking position (to reduce the heat load at the jaw) caused a mechanical degradation of the motorisation system and the blockage of the upstream axis of the upper jaw. The current of the motor was increased to augment the motor torque; the full motorisation system of the faulty axis will be replaced during TS4.

TDI in IR2

The LVDT position sensor used for the controls of the upstream corner of the TDI upper jaw (LU) in IR2 broke. The controls were moved to the second LVTD, normally used for redundancy, and the position and energy interlock thresholds were re-setup around the new LVDT readings. This introduced an offset of $\sim$200 μm between the settings and the LVDT readouts.

Figure 3: Picture of the unscrewed "goupille" which caused the fall of the TDI upper jaw in IR 2.

The LU side of the TDI jaw fell across the beam axis onto the lower jaw because of the failure of a "goupille" (Fig. 3) when moving from parking to injection position; no beam was in the machine at the time of the accident. The jaw was put back into the correct position and the system was consolidated. Both jaws were re-aligned and no

significant change was measured with respect to the previous settings. An additional offset of $\sim$100 μm was introduced between settings and readings and the LU corner approached the inner position interlock limit. This, plus a further slow mechanical drift of the LU corner, brought the LVDT beyond the inner dump limit and blocked the jaw (as by design). A new beam based alignment was required to compensate the mechanical drift and new positions and thresholds were defined. A total offset of 530 μm persisted between settings and readings.

MKI ERRATICS AND FLASHOVERS

The TDIs provide the only protection in case of MKI failure. Normally the MKIs have a pulse length of $\sim$8 μs to fit the full train of 144 or 288 injected bunches (depending on the bunch spacing) on the waveform flattop. Three main types of failures can occur:

- A flashover during injection: the pulse length is reduced so that part of the beam is mis-kicked and hits the;
- A Main Switch (MS) erratic: the circulating beam is kicked towards the lower jaw of the TDI;
- MKIs do not pulse when injecting beam (timing issues, previous erratic).

In Table 1 the failures which happened during the 2012 LHC run are summarised. All the problems occurred at the MKIs in IR8 and mainly on MKI8-D. This kicker was exchanged during the Technical Stop 3 (TS3) by a new hardware (MKI8-D* in Table 1, more details in the following) that still experienced three additional flashovers.

In all listed cases the TDI provided the required protection and no damage was provoked to the machine.

No MKI flashovers occurred during the 25 ns scrubbing run, vacuum was continuously monitored and the anti-e-cloud solenoids were always kept on.

MKI Heating

When the temperature of the MKI ferrite exceeds the Curie temperature the strength of the kicker reduces [6] and the injected beam could be mis-kicked and induce high losses and a quench of several magnets. For this reason, an interlock exists to inhibit injections if the measured temperature at the MKI is above threshold (Fig 4). At about ten occasions, after a series of long fills, it was required to wait longer than one hour before injecting to allow the cool-down of the MKI8-D kicker. A new hardware, equipped with an increased number of screen conductors (19 instead of 15), was installed during TS3 to reduce the heating [2]. The temperature of the new MKI8-D was amongst the lowest measured temperatures. On the basis of this result, all the MKIs will be upgraded during LS1 to a system with 24 screen conductors (as by design); no delays in operations for kickers cool-down are expected after LS1.

Table 1: List of MKI failures occurred in 2012.

Problem	**Magnet**	**Effect**
MS erratic during PFN charging	MKI8-C	1 nominal bunch on TDI
Flashover, 4.4 μs pulse length	MKI8-D	12 inj. bunches correctly kicked
Flashover, 3 μs pulse length	MKI8-D	108 bunches on TDI, quenches, vacuum valves closed, lost cryo conditions
Flashover during UFO MD (anti-ecloud solenoids off)	MKI8-C	MKI pulsing in empty gaps, no beam kicked
Flashover during Q20 inj. test, 1.3 μs plus length	MKI8-D*	No beam extracted from the SPS
Flashover, 6 μs plus length	MKI8-D*	6 inj. bunches correctly kicked
Flashover, 4 μs plus length	MKI8-D*	No beam extracted from the SPS

WRONG TCDI SETTINGS

The transfer lines had to be re-matched to the new SPS optics when moving to Q20 [7]. The change in the β-functions propagated until the end of the TLs in the region where the TCDI collimators are installed. The change was expected to be negligible and not to have a significant impact on the collimator settings but no explicit check was made. The trajectories could be steered to the nominal reference used with the Q26 optics so that a new centering of the TCDIs with respect to the beam was not needed. About 1.5 months after the change to Q20, the β variation at the collimators was quantified and, for two TCDIs (one per line), an half gap of 6.3 σ instead of 5 σ was measured with a consequent loss of protection. The TCDIs were moved to the correct settings and the protection level provided by the system was validated with the beam. Even if the machine was never in a real danger, this event raised a real concern about the possibility of having wrong settings and not being able to detect them except through manual checks. Discussions are ongoing on the possibility to automatically calculating the expected settings from the optics in use (current of the quadrupoles) and compare them with the applied settings to point out potential problems. Moreover, a tool for the automatic setup of the TCDIs is under development and will be ready for operation after LS1. This tool will not

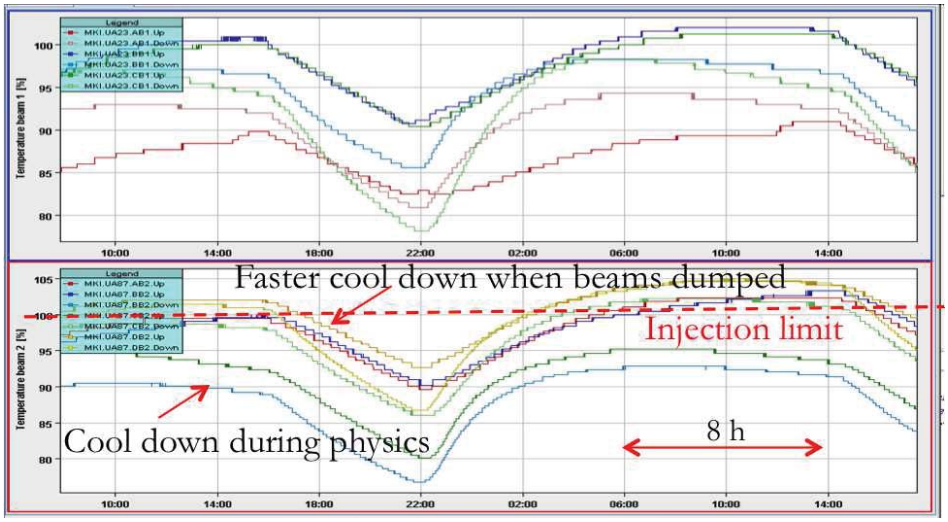

Figure 4: Temperature of the Beam 1 (top) and Beam 2 (bottom) MKIs during the LHC cycle. Injection is inhibited when the temperature is above the Curie limit (dashed red line).

make the setup and validation procedure faster (at least one shift of eight hours per line has to be considered) but will be safer since the settings will be automatically transferred to the "TRIM" application eliminating the human error factor.

LHC BEAM DUMPING SYSTEM

No major operational problems or long downtime were induced by the LBDS. The longest intervention (about eight hours downtime) was caused by the failure and the consequent replacement of a compensation power supply; this required a low level re-calibration of the power supply (gain and offset correction) and the re-validation of the Beam Energy Tracking System (BETS) through two test ramps. Two main weak points were nevertheless identified during the last year of operations:

- Issues with the powering logic of the general purpose crates (lack of redundancy) and unreliability of the WIENER power supplies used within the front-end computer; this caused the conditions (without beam) to generate two asynchronous dumps;
- A common mode failure possibility in the VME +12 V DC power feed line of the TSU crate which, if occurring, would not allow dumping the beam when requested neither synchronously nor asynchronously.

The LBDS cabling and powering logic was re-defined in order to power the Time Synchronisation Unit (TSU) and the Beam Energy Tracking System (BETS) in a fully redundant and independent way. The WIENER power supplies were equipped with additional protection (2 A fast fuses) in order to improve the electrical selectivity in case of failure. An external fast monitoring of the VME +12 V line was implemented which would trigger an asynchronous beam dump to a different way, bypassing the normal triggering lines (which would not work if the VME +12 V line had a short), in case of failures. Finally a slow surveillance of the VME +12 V line has also been added to forbid arming the system if the failure had occurred while the system was not armed. Further consolidation works are foreseen for LS1. The UPS electrical distribution will be modified to make the LBDS powering system completely redundant, the circuit breaker technology will be upgraded; the WIENER crates will be replaced by ELMA crates with internal protection and the two TSUs will be lodged in two different VME crates. The Beam Interlock System (BIS) will be connected to the re-triggering lines. The BIS, after each dump request, will trigger a delayed asynchronous dump as ultimate protection; the impact of the increased probability of asynchronous dump has to be evaluated.

Operation at 6.5 TeV, after LS1, will augment the risk of switch spontaneous firing for the extraction (MKD) and dilution (MKB) kickers. All the MKD and MKB generators of part of the GTO switches will be overhauled to increase reliability and reduce the sensitivity to radiation.

TCDQ Upgrade

The present TCDQ collimator, whose purpose is to provide protection in case of asynchronous beam dumps, will be substituted by an upgraded and more robust system during LS1. The new TCDQ will be constituted by three, instead of two, 3 m long jaws made of Carbon Fibre Com-

pound (CFC) to withstand the nominal energy deposition in case of asynchronous beam dumps at 6.5 TeV with 25 ns beams.

SUMMARY

Clean injections with 144 and 288 bunches (scrubbing run) could be performed using the same reference trajectory during the full 2012 LHC run. No intensity limitations came from injection losses but a solution has to be provided, for operation after LS1, to remove RC filters from the BLMs and operate with the TCDI at their nominal aperture of $\pm 4.5\ \sigma$. TL steering became more frequent and lengthier after moving to Q20 optics but no evident explanation could be found for this worsening (SPS orbit, MSE ripple, losses from de-bunched and un-captured beam, enhanced satellites, injection cleaning, etc.). Clearer references will be implemented in the IQC to give indications for steering and facilitate operation. A tool for automatic setup of the TCDI will become operational after LS1; studies are ongoing to calculate the expected settings from the optics in use, compare them with the applied settings and spot eventual anomalies.

Work will be done on the TDI hardware to reduce the beam induced heating, make the system more robust and avoid the failures which happened during the last run. The TDI provided the needed protection in case of MKI failures (six flashovers and one erratic) and confirmed its vital importance for machine protection.

The beam induced heating at the MKI8-D has been reduced by increasing the number of screen conductors to 19. All kickers will be equipped with 24 screens and no waiting time for cooling is expected after LS1.

Some weak points were identified in the LBDS and the system will be upgraded and made safer for operation at 6.5 TeV. The foreseen changes might increase the probability of asynchronous beam dumps; the impact on operation has to be evaluated.

ACKNOWLEDGMENT

Special thanks to M. Di Castro, G. Le Godec, A. Lechner, R. Losito and A. Masi for the fruitful exchange of information and the collaboration.

REFERENCES

[1] H. Bartosik et al., “SPS Q20 - Low Transition Energy Optics” talk presented at LIU-2011 event, November 2011, CERN, Geneva, Switzerland.

[2] B. Salvant et al., “Beam Induced RF Heating”, these proceedings, 2012, Evian, France.

[3] O. Bruning et al.,“LHC Design Report, Volume I: The LHC Main Ring”, Chapter 17 “Beam Dumping System”, pp. 441-464, CERN, 2004.

[4] W. Bartmann et al., “Injection Losses and Protection”, LHC Beam Operation Workshop - Evian 2011 proceedings, 2011, Evian, France.

[5] L. N. Drosdal et al., “Transfer Lines - Stability and Optimisation”, LHC Beam Operation Workshop - Evian 2011 proceedings, 2011, Evian, France.

[6] C. Bracco et al., “Injection and Lessons for 2012”, LHC Beam Operation Workshop - Evian 2011 proceedings, 2011, Evian, France.

[7] E. Gianfelice-Wendt, “Matching of TI2 and TI8 for Q20 SPS Optics”, CERN-ATS-Note-2012-095 TECH, November 29, 2012, CERN, Geneva, Switzerland.

"WHAT YOU GET" – TRANSVERSE DAMPER

F. Dubouchet, W. Höfle, G. Kotzian, D. Valuch
CERN, Geneva, Switzerland

Abstract

The transverse damper (ADT) operation in 2012 was very smooth, routinely switching between different modes and operating the feedback during the entire LHC cycle. We present the new features developed and commissioned in 2012, the selective blow-up, gain gating within the turn and increased bandwidth operation. Several methods were proposed and tested concerning the ADT vs. BBQ cohabitation in order to find the best compromise for machine operation. Performance scaling from 4 TeV to 6.5 TeV, potential limitations at high energy as well as the consolidation and upgrade activities for the long shutdown starting in 2013 (LS1) will also be presented.

PEFORMANCE AND SETTINGS MANAGEMENT FROM CCC

Each of the four ADT systems (one per plane and beam) [1] take signals from two pick-ups located at the Q7 and Q9 magnets in LSS4 on that side of IP4 where the betatron functions are high for the respective plane and beam. For reasons of redundancy each of the two pair of kickers with two amplifiers, is driven by a dedicated LLRF module for the signal processing as depicted in Fig. 1.

Settings to adjust for the per bunch intensity are processed by the Beam Position module (Beam Pos) [2] while all other controls of the feedback loop and processing is carried out within the DSPU module [3]. This includes the signal processing for the normalized bunch-by-bunch position as well as all gain control and additional excitation signals such as for abort gap cleaning and transverse blow-up as shown in Fig 1. An analogue input "chirp" permits the addition of an excitation signal provided by the Beam Instrumentation Group Systems in UX45.

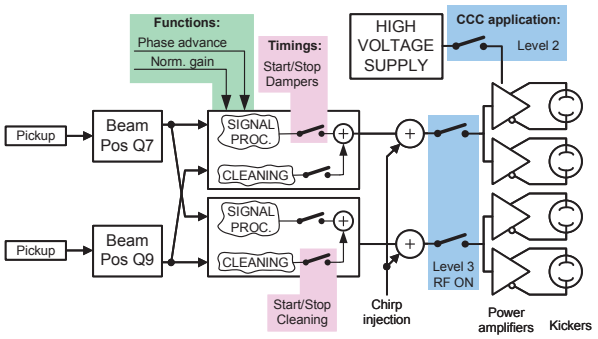

Figure 1: Layout of ADT damper feedback loop.

Operational Performance and Downtime

Thanks to the regular maintenance of the power system during the technical stops the overall downtime in 2012 has been very small. A total of 18 hours downtime affecting machine operation has been recorded. The power system comprises a total of 16 power amplifiers employing 32 tetrodes of 30 kW. During 2012 a total of 20 tetrodes were exchanged, identifying tetrodes at their end-of life by regular checks of the emission curves. The tetrode exchanges were carried out during the technical stops and thanks to the redundancy with four power amplifiers per beam and plane, machine operation could continue once a defective amplifier had been put in stand-by and the cables feeding the high voltage were disconnected.

Faults of the power system in 2012 included:

- tetrodes reaching their end-of life
- PT100 temperature probes defective
- attenuators and HV load defective in amplifiers
- water flow meters indicating insufficient supply of cooling water
- faults in the HV power converter due to damaged cables and a fault on the electronics controlling the thyristors (gate control failure)
- TPG 300 fault (vacuum gauge)

All the power amplifier faults could be quickly fixed by installing one of the two spare amplifiers held available in the LHC tunnel for this purpose. During LS1 the vacuum pumps and gauges and the water flow meters for the damper will be upgraded making these systems more robust against false measurements.

LLRF and controls faults include two FESA server crashes, the exchange of a faulty PLC (Beckhoff) module, a problem with the cabling for a GigaBit data link and a configuration issue following a technical stop which resulted in an invalid sampling clock (40 MHz).

Not counting the tetrode exchanges during the technical stops the average fault time has been 1h20min (18 hours for 13 faults counted). This can be considered small taking into account that the hardware faults required intervention in SR4, UX45 or the LHC tunnel. The short intervention duration is due to an efficient stand-by service team, backed up by experts, as well as the availability of spare material on site. A continuous effort is necessary to replenish spare material, in particular for the power system and consolidate the electronics where required.

A test lowlevel electronics system in SR4 is fed with true beam signals and has been extensively used to validate new firmware and software before deployment on the four operational VME crates. Software errors and

teething issues with new features could be kept to a minimum thanks to this test system.

Settings Management

With respect to damper configuration settings and control functions one has to distinguish between beam type or beam parameter dependent settings and functions and operational settings that are permitted for any kind of beam. In order to assure equipment protection some of the settings still required a manual intervention by an expert to load or change and are not fully integrated into the LSA system. In particular this includes the settings for the bunch intensity for which the injection of a high intensity bunch can damage the electronics when configured for low intensity bunches. Interlocking with the SPS bunch intensity interlock was successfully tested in preparation of the automation of the intensity settings management.

The less critical adjustments such as for the bunch spacing and parameters for the new wideband mode and gain modulation within the turn have already been implemented in LSA and were driven by the sequencer using Discrete Beam Processes. For the transverse blow-up a fully integrated application has been used. Further improvements to the control of the damper are planned for after LS1.

NEW FEATURES IN 2012

In the following the new features of 2012 are presented:

- selective transverse blow-up
- gain modulation within the turn for improved ADT-BBQ cohabitation
- increased bandwidth operation towards 25 ns bunch spacing
- R&D in the framework of a future tune measurement using the ADT system

Selective transverse blow-up

Following the successful tests of transverse blow-up using the ADT system in 2011 [4], a user application has been developed which is now fully integrated into the CCC control system. It permits to select individual bunches or groups of bunches to which a transverse excitation based on noise internally generated on the FPGA is applied. This facility became the standard way of checking the aperture and validating the collimation system by loss maps in 2012. It has been used at all beam energies from injection through the ramp and squeeze up to 4 TeV. Due to the selectivity of the blow-up (gating on individual trains of bunches) the efficiency of loss maps has been greatly improved.

As an example of efficient collimation system validation Fig. 2 shows the time line for the p-Pb setting-up in September 2012. 12 bunches were accelerated of which two were used for loss maps once collisions were found. A first Physics run could be carried out using the remaining ten bunches which were left untouched thanks to the gated excitation during the loss maps.

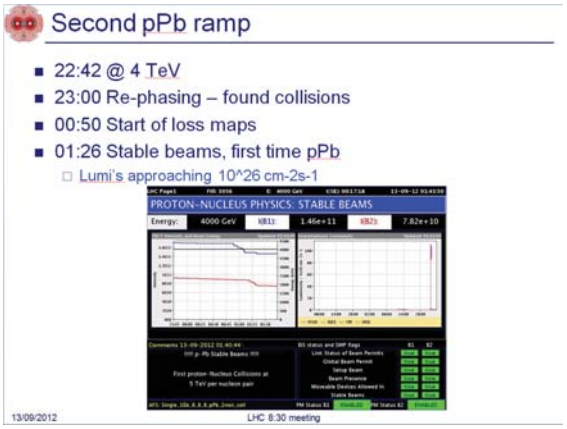

Figure 2: Efficient generation of loss maps (example from the p-Pb set-up).

Gain modulation within the turn

As proposed in 2011 a modulation of the damper gain within the turn was introduced in 2012 and operationally used. It permits to run with high gain during the ramp and the prepare-for-ramp process, while keeping the gain for the leading bunch train, six "witness" bunches at 50 ns spacing for the operational Physics beam, very low. In combination with a gating on these six bunches in the BBQ system the performance of the tune feedback system was improved even with high damper gain on the remaining bunches.

The gain modulation is implemented in the digital part of the feedback loop on the FPGA multiplying the feedback signal by a function that can be programmed to be between 0 and 127 in steps of 1 unit. A sample function accessible via LSA is depicted in Fig. 3. The horizontal axis is the bunch index, the vertical axis the gain modulation function. It should be noted that for small gains the digital multiplication and subsequent conversion to the analogue domain results in a loss of resolution, i.e. the signal-to-noise ratio for the leading bunches with low gain is reduced with respect to the rest of the beam. This loss in resolution and the limitations from having a single function controlling the output gain via the DAC have inspired the planned upgrade whereby multiple DACs are used to convert the individual signals, maintaining independent control and resolution.

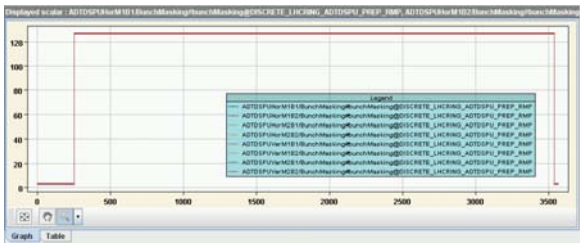

Figure 3: Gain modulation function within the turn.

Increased bandwidth operation

The appearance of instabilities in LHC in particular when running at 25 ns spacing, but also at 50 ns during the squeeze and adjust beam process, has triggered measurements and developments aimed at increasing the bandwidth of the ADT system.

The gain versus frequency characteristics of the ADT system is essentially determined by its power system, which is driving a capacitive load. The ideal low pass characteristics given by the RC time constant of the driving circuit and the kicker capacitance is plotted in Fig. 4. For comparison measured curves are also shown in Fig 4. Up to 10 MHz, the maximum frequency of coupled bunch modes with 50 ns bunch spacing, all curves perfectly agree, while in practice between 10 MHz and 20 MHz more gain is available than predicted by the ideal low pass characteristics. It should be noted that the phase response of the power system is compensated by digitally pre-distorting the signal [3] such that different coupled bunch modes are correctly damped, however with a damping time that depends on frequency.

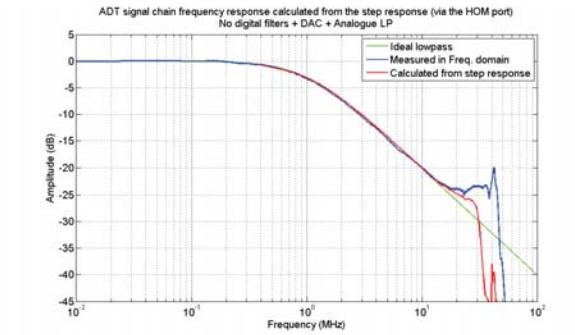

Figure 4: Gain versus frequency characteristics of ADT system without correction.

Viewed in time domain the decrease in gain for higher frequencies will spread out an initial oscillation from one bunch to adjacent bunches: Bunch oscillations appear to be coupled by the damper which may not be the optimum when individual bunches become unstable. Such single bunch instabilities call for a bunch-by-bunch damper with truly independent action on each bunch.

In theory such an independent treatment can be achieved if the transfer function exhibits a certain symmetry of the roll-off at half the bunch repetition frequency: The real part of the amplitude response at half the bunch frequency must be 0.5 and point-symmetric and the imaginary part can be arbitrary as long as it is symmetric with respect to half the bunch frequency. The resulting time domain impulse response then features zeros at adjacent bunch positions. This condition was first formulated by Niquist [5] and is today commonly known as the condition to achieve inter-symbol-interference free transmission in communication theory.

As the phase response of the ADT system had already been successfully compensated in the past it was sufficient to correct the amplitude response. Because drive power is available up to 25 MHz an FIR filter was designed to shape the roll-off of the ADT gain from 15 MHz to 25 MHz to achieve a fast time domain response for bunch-by-bunch operation.

Fig. 5 shows the step-response of the uncorrected system (blue curve), the phase compensated system (green) with its symmetric characteristics and the increased bandwidth response with tapered gain to 25 MHz (black). The responses are measured on an actual system integrating the raw signal from an HOM port with capacitive coupling to the kicker plates. It can clearly be seen how the signal processing has made the response faster (black curve).

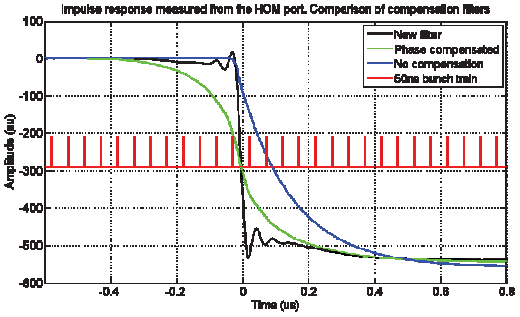

Figure 5: Measured step response of ADT with different pre-distortion filters.

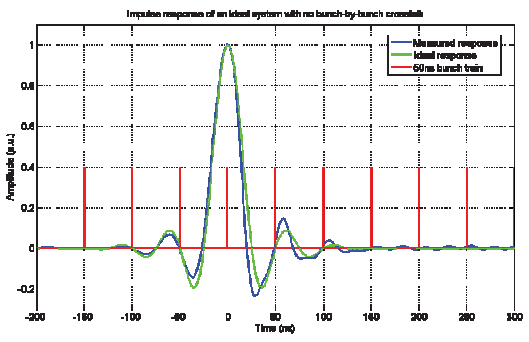

Figure 6: Comparison of measured impulse response and an optimized response for bunch-by-bunch operation at 25 ns bunch spacing.

The bunch-by-bunch properties are best checked by looking at the impulse response shown in Fig. 6. The green curve represents the ideal response with zeros spaced at 25 ns and the blue curve the actually achieved response. This measured response has perfectly spaced zeros at 50 ns spacing, the operational bunch spacing used in 2012. The leading part of the impulse response also has zeros at the intermediate positions of possible bunches for 25 ns bunch spacing but in the trailing part some residual kicks remain for bunches spaced at an odd multiple of 25 ns.

These so called “wide band” or “high bandwidth” settings have been used for the 25 ns tests and for the 50 ns operation in the second part of the 2012 LHC run

during the squeeze which was the most critical part of the cycle with respect to the instabilities.

Tests during Physics have indicated that the wideband settings lead to an increased emittance blow-up. This is a result of the large tune spread in collision in combination with the increased noise when the wide band settings are used. The low pass filter characteristics with the standard settings cuts off contributions of the noise spectrum well above 1 MHz, while the wideband settings let these noise spectral components pass through onto the beam. Improvements in the electronics foreseen for the LHC run after LS1, the use of double the number of pick-ups and an improved signal processing are expected to reduce the overall noise of the bunch oscillation detection, so that the effect of the wideband settings on the emittance are reduced.

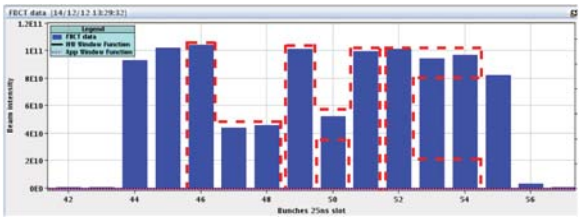

Figure 7: Beam intensity reduction after blow-up of individual bunches within a train with wide band settings.

An additional benefit of the wideband settings can be seen in Fig. 7. Using these settings for the transverse blow-up permits to target individual bunches in a train of 25 ns spaced bunches. The figure shows the bunch intensity after bunches number 47, 48 and 50 have been targeted by the blow-up and lost about half of their intensity while adjacent bunches have not been affected.

For the run after LS1, transfer functions of the damper will again be carefully measured, and the pre-distortion by the signal processing adapted to improve the bunch-by-bunch performance for the 25 ns bunch spacing.

R&D in the framework of a future tune measurement using ADT

R&D work on extracting the tune from the ADT data continued in 2012. It should be noted that the present hardware (VME crates) does not permit to extract all bunch-by-bunch data in a continuous way via the VME bus, due to the limitation of the data transfer speed of the VME bus as heavy data transfer can compromise the LLRF system operation and reliability. After LS1 additional hardware is foreseen that will process the full data available which can be streamed via GBit serial links from the VME boards without interfering with the feedback loop and its control functionalities via the VME bus.

In order to permit machine developments additional internal test buffers of a length of 16384 samples were introduced in 2012. These could be used to quasi continuously record for test purposes the oscillations of six bunches over 2730 turns with only a small interruption after each acquisition as required by the software to fetch the data over the VME bus.

The tests carried out included a passive observation of the bunch oscillations and a synchronized observation following a small excitation with the damper. The excitation kicked the leading six bunches only, for a programmable number of turns, modulated at the nominal tune. Subsequently the free oscillation of these bunches was observed using the special buffer. This way a tune measurement could be developed, however the method also suffered from spurious signals in the FFT which need further study.

An example of a passive observation without excitation is shown in Fig. 8. It shows a spectrum of horizontal oscillations of beam 2 with the data from the leading six bunches averaged. We can see in the top part the effect of cleaning during which a tune measurement seems not possible without active excitation. The dark blue vertical line represents the trench at the location of the tune, which can be used for a tune measurement during high gain operation. During the ramp at lower gain the beam is naturally oscillating and the tune can be picked-up from these oscillations. However, in this low gain regime the beam is again sensitive to external interferences such as multiples of 50 Hz, and in practice it might be difficult to separate the true tune and the spurious lines.

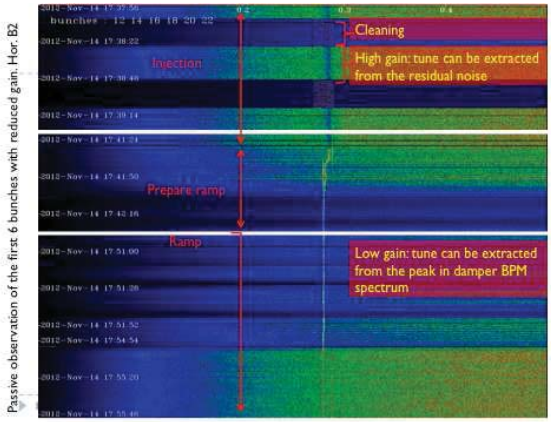

Figure 8: Result of tune observation with ADT on six witness bunches (horizontal plane, beam 2).

OUTLOOK ON OPERATION AT 6.5 TEV AND IMPORVEMENTS FOR LHC RUN 2

Outlook at 6.5 TeV operation

Measures planned to improve the signal-to-noise ratio will permit to maintain performance achieved at 4 TeV at the increased energy of 6.5 TeV planned for the LHC run 2 after LS1. Running at 25 ns with high bandwidth settings will remain a challenge due to the increased level of noise acting on the beam in this mode of operation. The strategy should be to use the wideband settings only when required and adapt the frequency response to what is needed to damp instabilities.

Maintaining a damping time of 50 turns at 6.5 TeV is feasible and the required shuffling of gains within the feedback loop to achieve it, is foreseen for LS1.

Improvements for LHC run 2

More than 25 km of new smooth wall coaxial cable will be installed to connect the existing eight pick-ups and the new set of eight additional pick-ups to the surface. The doubling of the number of pick-ups, the new coaxial cable with reduced reflections, newly built electronics with lower noise properties and improvements to the signal processing are the four measures that are expected to reduce the noise level of the feedback system.

Re-design of the VME DSPU module will permit to better integrate the different operational modes with the control of the gain, by having an independent set of DACs for the different signal contributions (feedback, cleaning, excitation).

Streaming of data via serial link to a separate stand-alone hardware is foreseen in order to fully exploit the potential of the ADT system for beam observation including tune measurement. Tests in 2012 have shown that a variety of methods are possible to extract the tune from the ADT data, with and without excitation. However, separation of the tune from parasitic beam oscillations caused by 50 Hz lines and other spurious lines is a challenge for ADT, too.

As in 2012 a train of witness bunches will be essential for the tune measurement. In addition an instability trigger to efficiently synchronize acquisitions by the damper with other instruments around the accelerator is primordial for an improved diagnostics on instabilities.

ACKNOWLEDGMENT

The excellent collaboration with the Operations Group, MD and Machine Coordinators as well as experts and users during operation and machine developments is gratefully acknowledged. Within the RF group the support by the team responsible for the exploitation of the power equipment from the BE-RF-PM section and from controls specialists from the BE-RF-CS section has been excellent.

REFERENCES

[1] E. V. Gorbachev , N. I. Lebedev, A. A. Makarov, N. V. Pilyar, V. Rabtsun, R. A. Smolkov, V.M. Zhabitsky, P. Baudrenghien, W. Hofle, F. Killing, I. Kojevnikov, G. Kotzian, R. Louwerse, E. Montesinos, V. Rossi, M. Schokker, E. Thepenier, D. Valuch, "LHC Transverse Feedback System: First Results of Commissioning", *LHC Project Report 1165*, CERN Geneva (2008), presented at the XXI Russian Particle Accelerator Conference RuPAC 2008, Zvenigorod (2008).

[2] P. Baudrenghien, D. Valuch, "Beam phase measurement and transverse position measurement module for the LHC", presented at the LLRF07 Workshop, October 2007, Knoxville TN, USA (2007), CERN EDMS document 929563, https://edms.cern.ch/file/929563/1/llrf07 poster.pdf, CERN Geneva (2007).

[3] P. Baudrenghien, W. Hofle, G. Kotzian, V. Rossi, "Digital Signal Processing for the Multi-Bunch LHC Transverse Feedback System", *LHC Project Report 1151*, CERN, Geneva (2008), presented at EPAC'08, paper THPC122, 3269-3272, Genoa (2008).

[4] W. Hofle, R. Assmann, S. Redaelli, R. Schmidt, D. Valuch, D. Wollmann, M. Zerlauth, "Controlled Transverse Blow-up of High-Energy Proton Beams for Aperture Measurements and Loss Maps", presented at IPAC'12, paper THPPR039, 4059-4061, New Orleans, USA (2012).

[5] H. Nyquist, "Certain Topics in Telegraph Transmission Theory", *Transactions of the A.I.E.E.*, Feb. 1928, 617-644 (1928); reprinted in *Proceedings of the IEEE*, vol. **90**, no. 2, Feb. 2002, 280-305 (2002).

"WHAT YOU GET" – CONTROLS SOFTWARE,

S. Jensen on behalf of BE-CO, CERN, Geneva, Switzerland

Abstract

The control system is ready for running the LHC at increased intensity at 6.5TeV and 25ns bunch spacing. Still, BE-CO will carry out a range of activities during LS1 for adding functionality and to further improve performance and availability of the controls system while meeting required security standards. This paper presents those BE-CO activities foreseen for LS1, which will have a direct or indirect impact on LHC operation.

INFRASTRUCTURE IMPROVEMENTS

A large scale renovation of low-level hardware and software will be carried out during LS1 both in LHC and the Injectors:

- LHC: 500+ CPU upgrades towards multi-core CPUs, Linux and 64 bits.
- Injectors (ACCOR project): Upgrades of some 350 CPUs, the timing system and a range of electronic modules.

In addition, a new version of FESA will be released providing:

- Support for multi-core CPUs.
- Improved thread priority management.
- Inheritance.

Comments have been reported concerning the "FESA Navigator" tool relating to its usability and functionality for OP. While this tool was intended for use by system experts, i.e. FESA class developers, BE-CO recognizes that it has become a useful tool for operators as well. The FESA Navigator tool and its usage will be reviewed during LS1 in collaboration with BI.

A new major rewrite of the middleware will be released, improving amongst others the handling of slow clients (non-blocking communication).

Finally, BE-CO will – in collaboration with BI and BE-OP – carry out a technical review of the orbit feedback system (OFSU).

BETTER DEVELOPMENT ENVIRONMENT

The following development environment improvements will be provided:

- Faster virtual machines.
- Better development platforms. BE-CO will review the development platform situation and determine whether virtual machines or office machines are preferable. In the future, almost all development shall be done on the GPN and only final validation shall be done in the TN.
- A unified commonbuild system for Java and C++ will be put in place, offering improved functionality and maintainability.
- All core software will be submitted to a rigorous Testbed system, including CMW, FESA, Timing and LSA.
- Better documentation will be put in place providing amongst others developer guidelines, quality assurance instructions and software API descriptions.
- A BE-optimized version of the Eclipse development environment is in place and ready for use.

IMPROVED CCC ERGONOMICS

- All consoles will be upgraded to more powerful machines.
- A review in 2013 will be carried out in order to determine how to improve ergonomics in the CCC. Current proposals include:
  - More mobile keyboards/mice to avoid cable cluttering.
  - Wireless phone headsets to keep hands free.
  - Review monitor size and orientation for better usability.
- Common Console Manager major rewrite.
  - A review of the CCM will be organized in order to formalize requirements.

TIMING

In addition to moving the central timing system from LynxOS to Linux, a number of reported issues will be addressed, including:

- "Time lost when requesting mastership and changing sequence" - this issue goes beyond timing and relates to PS/PSB operation as well. The situation will be reviewed, also in order to collect formal OP requirements to optimizing the Cycle Editor GUI.
- "Injection into wrong ring" (SPS timing)
  - A proposal involving changes in Timing and uses of SIS have been approved by the Machine Protection Working group and will be implemented.

A general timing review will be carried out, and this is the occasion for stating any new requirements. The Injector timing system will be renovated via the openCBCM project.

IMPROVED LSA PERFORMANCE

Concerning the regeneration of settings being too slow, this will be addressed in a number of ways:

- OP will clean up settings, i.e. reduce the number of settings to regenerate.
- CO will provide faster computers with more RAM.
- CO will provide a smarter implementation, regenerating only the settings that have changed.
- CO will provide tools to simplify the cleaning up of settings, based on OP input.

Additional LSA operations can be RBAC-protected as requested by OP.

DATA ANALYSIS

These activities were triggered by the Evian 2011 workshop, with two main work items:

- The Logging service will be improved as follows:
  - Accepting more data and data types, e.g. Bunch-by-Bunch, QPS, LHC wirescans, Statistics.
  - Month-long storage will be supported, based on a concept of data-owners who must be assigned by OP.
  - Data owners will be responsible for permitting deletion of data.
- Concerning the analysis framework:
  - A generic framework for data analysis and visualization (e.g. run statistics) will be provided.
  - The framework will be integrated with a wider range of data sources such as Post-Mortem and the eLogBook.

These solutions should facilitate minimizing ad-hoc solutions and use of SDDS. The implementation depends on continued strong collaborations with OP (A. McPherson).

SEQUENCER FUNCTIONALITY

The Sequencer functionality will be extended as follows:

- Parameterized (sub-) sequences.
- Parallelizable sub-sequences.
- Increased integration with the State Machine. Further clarification with OP is needed.
- The GUI which occasionally freezes is under active investigation. Currently, XWindows seems to be the cause, not the Java source code.

Also, the State Machine may see improvements based on further discussions with OP. Current ideas include:

- Checks can depend on cycle type, i.e. nominal vs. MD.
- Checks can be categorized as “Blocking” vs. “Performance”.

INCREASED FLEXIBILITY FOR ALARMS DEFINITION

A new implementation of LASER will offer:

- Mode-dependent alarms.
- More OP influence concerning alarms declarations.

Current alarms will be migrated by the LASER team.

It is important to note that OP effort is essential in improving alarm quality.

New tools to assist clean-up of alarms will be provided and the LASER team will actively assist the clean-up.

ACCELERATOR CONTROLS EXPLOITATION TOOLS (ACET)

The ACET project is active and aims at improving the diagnostic facilities of the controls system in preparation of the new LHC-style exploitation model in injectors. Current areas of focus include:

- Visualization of services and their relations.
- Accessible and useful documentation.
- Centralized tracing analysis.
- FEC configuration feedback and analysis.
- Process instrumentation (metrics).
- Dependency analysis and visualization.

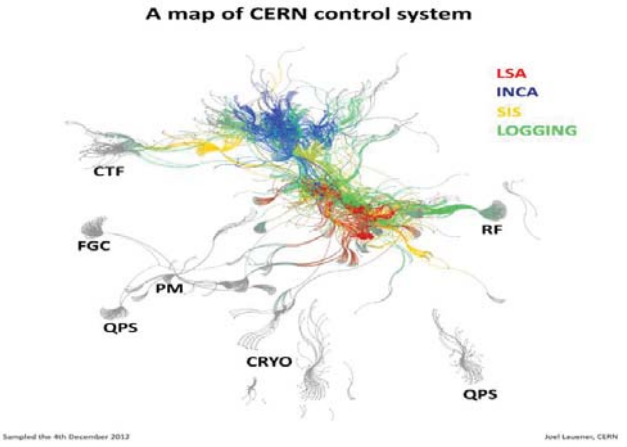

Figure 1: A view of control system dependencies.

BETTER EXPLOITATION

A number of steps will be taken to further facilitate rapid diagnostic and troubleshooting, including:

- DiaMon will become more user friendly and will provide more information and functionality, as follows:
  - A dependency view of the control system which shall help OP understand the structure of the controls system and facilitate troubleshooting.
  - OP can create custom views.
  - Easy mechanism for reporting wrong states displayed by DiaMon (feedback button).

    - More diagnostic data will be available such as dependencies, process metrics and configuration feedback.
- A pro-active exploitation approach will be taken with early detection of problems thanks to:
    - Process monitoring in DiaMon.
    - Configuration analysis.
    - Centralized trace analysis.
- Better contact information – up to date and available.

EASY ACCESS TO BETTER DOCUMENTATION

A portal will be implemented, as entry point for accessing various CO documentation, including:

- Developer guidelines.
- Useful links.
- Procedures relating to security, intervention, …
- Exploitation specific pages.
- Contact information (consistent with the OP "Web piquet" pages).

The portal can be adapted to OP needs.
In addition to the portal, the CO internal wiki structure will be improved by contribution from all major CO projects.

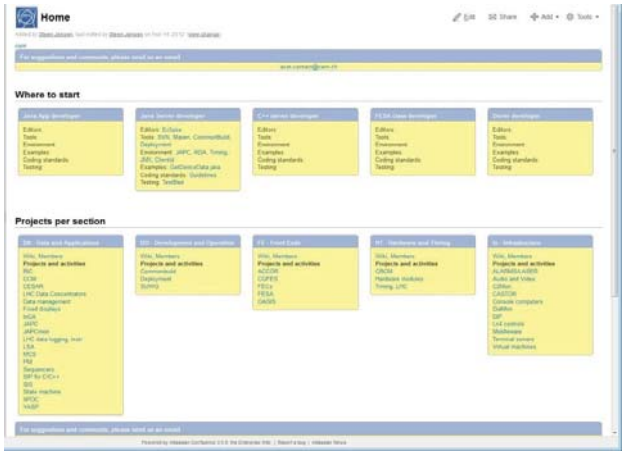

Figure 2: An example prototype page.

SMOOTH VERSUS RADICAL CHANGES

Since 2009, all high impact and importnat changes to the controls system have essentially been deferred to LS1. During Technical Stops, only backward-compatible changes with possible roll-back were implemented after careful planning and discussion in the sector-wide "Smooth Upgrades Working Group" (SUWG).

During LS1 radical, global and "big-bang" changes have to be carried out, with changes at all layers of the controls system (hardware, operating systems, Middleware, FESA3, Java and Oracle).

CO will thoroughly test software in the Controls Testbed and the core components will be validated in the Injectors, but it is important to state that OP-lead dry runs are vital for final validation.

In addition, tools for supporting smooth upgrades (showing what has changed and providing better roll-back) will be utilized.

CONCLUSIONS

- The control system is not energy/intensity dependent and therefore considered ready for 6.5TeV, 25ns and increased intensity.
- New development and consolidation work are planned both in hardware and software at all levels of the control system. Input and participation from OP is essential.
- The work planned for LS1 should bring extensive improvements and additional functionalities with evident amelioration in the availability and performance of the overall control system.
- Rigorous test procedures and tools are in place.
- OP-organized dry runs are essential.

CONTACT PERSONS

- CCM: V. Baggiolini
- Centralized tracing: S. Jensen
- CommonBuild: N. Stapley
- Data analysis: J. Wozniak, A. McPherson
- Dependency view: S. Jensen
- Development platforms: L. Gallerani
- DiaMon: M. Buttner
- Documentation portal: S. Jensen
- Eclipse: N. Stapley
- Ergonomics: P. Charrue
- FESA: S. Deghaye
- Hardware renovation: M. Vanden Eynden
- LASER: M. Buttner
- Logging: C. Roderick
- LSA/InCA: G. Kruk
- Middleware: W. Sliwinski
- Security: L. Gallerani
- Sequencer: R. Gorbonosov
- SIS: J. Wozniak
- Smooth upgrades: V. Baggiolini
- State machine: R. Gorbonosov
- Timing: J.-C. Bau
- Testbed: J. N. Xuan
- Virtual machines: L. Gallerani

BEAM LOSSES THROUGH THE CYCLE

G. Papotti, A. Gorzawski, M. Hostettler, R. Schmidt
CERN, Geneva, Switzerland

Abstract

We review the losses throughout the nominal LHC cycle for physics operation in 2012 and for a few fills in 2011. The loss patterns are studied and categorized according to timescale, distribution, time in the cycle, which bunches are affected. Possible causes and correlations are identified, e.g. to machine parameters or BBQ amplitude signal.

INTRODUCTION

In cycling accelerators it is customary to study thoroughly the beam intensity evolution in the cycle as, in case the losses show reproducible features, they might help identify which machine parameters can be modified so to improve transmission. At the LHC this kind of study has had little importance until the 2011 run as in general losses were negligible before collisions and transmission was very close to 100%, apart from few unfortunate fills.

For the 2012 run, "tight" collimator settings [1] were chosen for physics operation at the high luminosity experiments ATLAS and CMS so to guarantee protection even with β^* as low as 60 cm. Collimator jaws closer to the beam resulted in higher losses compared to previous years as more beam tails were consistently scraped away. Additionally, the increased impedance is considered one of the causes for the instabilities that were observed throughout proton physics operation [2]. These factors resulted in an overall transmission (from end of injection to start of collisions) that was appreciably lower than 100% and losses that were about a factor 10 higher than in the previous years.

In this document, we attempt a first thorough study of the losses in the LHC proton physics fills cycle. The study is mostly targeted to 2012, with an eye to 2011 for comparison. In the first part of the paper, the losses are looked at while being separated according to beam mode so that a possible correlation to major machine settings change can be highlighted. Beam modes of interest are: acceleration (separated into two: between 450 GeV and 500 GeV, e.g. capture losses; and between 500 GeV and 4 TeV, here called Ramp), Flat Top, Squeeze, Adjust, first 5 minutes in Stable Beams. Losses during injection were analysed separately [3]. Differences in bunch-by-bunch loss patterns are looked into in the second part of this paper and some reproducible structures are highlighted.

BEAM LOSSES PER BEAM MODE

Post Mortem Power Loss Module

The intensity versus beam mode data used for this part of the analysis was extracted by means of software partly already developed in the framework of the Post Mortem (PM) Analysis [4]. A PM Power Loss module has been put in place in 2012, and for every fill dumped with a PM timing event it calculates the maximum power loss per beam per mode according to

$$P = \frac{\Delta n}{\Delta t} E_{cal} \tag{1}$$

where

$$E_{cal} = \frac{64\, E_{\mathrm{TeV}}}{4\,\mathrm{TeV}\, 10^{11}\mathrm{p}} \tag{2}$$

is a calibration factor that gives the energy loss per proton at 4 TeV and $\Delta n = n_1 - n_2$ is the intensity decrease in number of protons (from DC-BCT data smoothed with a Savitzky-Golay algorithm) over the time $\Delta t = t_2 - t_1$. The maximum dissipated power is calculated by sliding the time window Δt over the duration of the beam mode under analysis. The calculation is repeated for four different time window lengths: 1 s, 5 s, 20 s and 80 s.

Another feature of the Power Loss module is that it provides the total intensity per beam at mode changes. This is the basis for the following analysis, where the intensity difference over a given beam mode is analysed over the year and correlated with settings change. The data was extracted for all proton physics fills of 2012 that reached 4 TeV (from fill number 2470 to 3341). The number of fills taken into account per beam mode is as follows: 404 fills for Ramp, 401 for Flat Top, 393 for Squeeze, 356 for Adjust and 274 for Stable Beams.

We define the transmission T as:

$$\mathrm{T} = \frac{\mathrm{I_{END}}}{\mathrm{I_{START}}} \tag{3}$$

where $\mathrm{I_{START}}$ is the total intensity for one beam at the start of the beam mode and $\mathrm{I_{END}}$ is the total intensity at the end of the beam mode. In particular, $\mathrm{T} = 1$ for zero losses ($\mathrm{I_{END}} = \mathrm{I_{START}}$) and $\mathrm{T} = 0$ if all beam is gone before the end of the mode ($\mathrm{I_{END}} = 0$). In all plots in Fig. 1 and 2, the transmission over the beam mode is plotted for each fill, in blue for ring 1 and in red for ring 2.

Capture losses (450 GeV to 500 GeV)

Fig.1a shows the transmission between 450 GeV and 500 GeV. It can be seen that transmission is generally worse for ring 1 than for ring 2. Energy matching between the SPS and the LHC was performed at fill number 2687, and it can be seen that capture losses improved then, especially for beam 1. A localized worsening of capture losses is present after the second technical stop (fill number 2780), possibly traced back to beam quality worsening at the injectors.

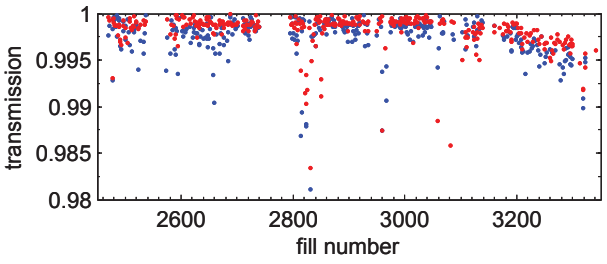

(a) Capture losses.

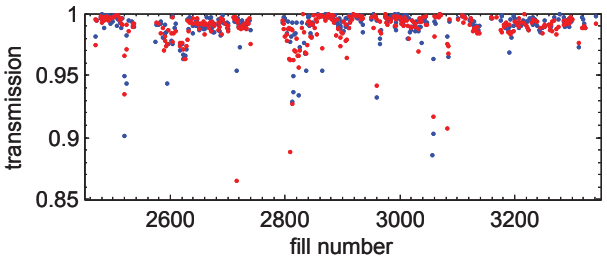

(b) Ramp losses.

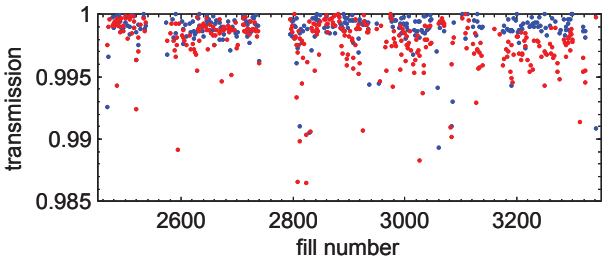

(c) Flat top losses.

Figure 1: Beam losses per mode per 2012 fill (capture, ramp and flat top). Note the different vertical scales.

The increase in capture losses towards the end of the run is apparent. A second energy matching was performed then to try and improve the situation (fill number 3271), but the effect was negligible. The increase in losses is probably rather due to the enhancement of satellite population to increase the Alice luminosity, performed after the third Machine Development block (fill number 3178).

Losses during the ramp (500 GeV to 4 TeV)

In Fig. 1b, the transmission during acceleration (between 500 GeV and 4 TeV) is shown. As a general comment, losses are non-negligible, mostly at the percent level. This pairs with the observation, often made in the control room, that the single beam lifetime decreases appreciably towards the end of the ramp, e.g. when the primary collimators close in and the transverse tails are scraped away.

The transmission improved towards the end of the run, i.e. after the third technical stop, probably when the new Q20 optics was introduced at the SPS for operational LHC beams [5], allowing the transfer of beams with smaller transverse size.

The analysis of the maximum power loss during the ramp (see Eqn. 1) highlighted that the peak losses happened for almost all fills either at the end of the ramp (20 s time window). It also showed that the highest power losses were for beam 1. For the longest time window (i.e. 80 s), the highest power loss was mostly towards 4 TeV, and peak losses were similar in amplitude for the two rings.

Flat Top losses

The time spent at the flat top was rather short for most fills (e.g. a few minutes). This time was used for manual checks on the tune trim quadrupoles and relative trims, and to load the squeeze functions on power converters and other systems. Consequently, losses were in general negligible, but it is noticeable that they are slightly higher for beam 2, for which the single beam lifetime was generally worse than for beam 1 (see Fig. 1c). The beam 2 lifetime also slightly worsened around the time at which the octupole polarity was reversed (fill number 2924, a worse lifetime could be due to the abundant increase in chromaticity that followed shortly).

Losses during Squeeze

Fig. 2a shows the transmission during the Squeeze mode. Throughout the year, the beam 2 losses are worse than the ones for beam 1, and losses get generally worse after the octupole polarity change and the increase in chromaticity.

Looking at the maximum power losses with 20 s time window, the peak is very reproducible for beam 1 ($\approx$ 10 kW), and less for beam 2 (generally $<$ 30 kW). The time in the mode at which the peak power loss happened is very reproducible for beam 2 (see Fig. 3). In fact, the peak power losses cluster around a few definite times, namely: $\approx$ 420 s (or $\approx \beta^* = 3$ m), $\approx$ 820 s (or $\approx \beta^* = 0.7-0.8$ m), $\approx$ 930 s (or $\approx \beta^* = 0.6$ m, as the total function length is 925 s).

Losses during Adjust

The Adjust beam mode is the one during which the beams are put into collisions. The main change during 2012 coincided with the use of two collision beam processes instead of one. This change had been put in place to go from one longer beam process, beginning with transverse optics gymnastics in Interaction Point (IP) 8 and followed by collapsing of separation bumps in all IPs at the same time, to two shorter beam processes in which collisions in IP1, 2 and 5 were established first, followed by the IP8 gymnastics. The double collision beam process allowed taking advantage of the stabilization properties of head-on beam-beam tune spread from IP1 and 5 as soon as possible to counteract the instabilities that had often been observed and that had caused the loss of many fills. Additionally, it resulted in more reproducible figures for transmission and peak power losses (see Fig. 2b).

Losses at start of Stable Beams

The transmission in the first 5 minutes in Stable Beams also profited by the change of the collision beam process

in Adjust: as it can be seen in Fig. 2c, the transmission generally improved and became much more reproducible. In this case, it is beam 1 that had usually higher losses than beam 2. This was also often commented on by the shift crews, highlighting that, while beam 2 used to lose more in the rest of the cycle, beam 1 lost more at the start of Stable Beams. This can intuitively be explained by the fact that the transverse tails of beam 1 were not scraped as much as the ones of beam 2 earlier on, so got scraped at start of collisions.

Comparison with losses in 2011

The difference between 2011 and 2012 proton physics operation is quantified in Table 1, where it can be seen that losses in 2012 were about a factor 10 higher than in 2011.

The 2011 peak power loss analysis was also performed and a few observations follow. Peak power losses in 2011 are generally a factor 2 to 3 lower than in 2012, with peaks < 30 kW for beam 1 and < 10 kW for beam 2 (note that beam 1 was consistently worse than beam 2). Note also that the clustering at certain times in the Squeeze beam mode was not observed.

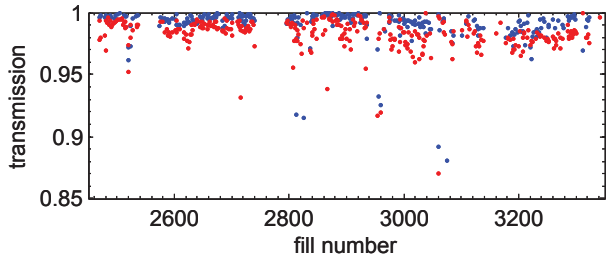

(a) Squeeze losses.

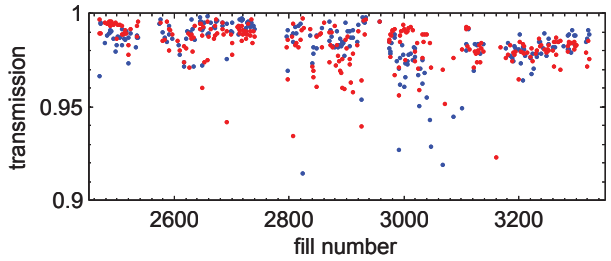

(b) Adjust losses.

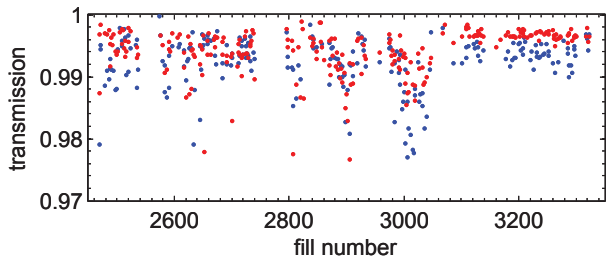

(c) Stable beams losses.

Figure 2: Beam losses per mode per 2012 fill (Flat Top, Squeeze and Adjust). Note the different vertical scales.

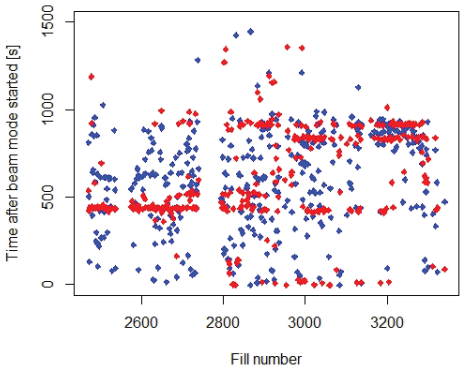

Figure 3: Time at which the maximum power loss (20 s sliding window) happened after the start of the squeeze beam mode.

BUNCH-BY-BUNCH DIFFERENCES

Two main bunch-by-bunch differences in the beam losses are explained next: one is a reproducible loss structure that develops during Stable Beams in beam 1; the other is additional losses related to transverse emittance blow up due to instabilities that developed in many fills in the second part of the run.

Other cases of punctual bunch-by-bunch differences were observed throughout 2012, but will not be expanded on here as the causes were found and rapidly corrected, e.g. different settings on the transverse damper during commissioning (e.g. fill number 2593) or insufficient beam quality from the injectors (for example, loss of proper longitudinal structure at the PS, fill number 3109).

Bunch-by-bunch loss structure in stable beams

A very reproducible loss structure developing during long physics fills was observed throughout 2012. The first ≈ 30 bunches of each SPS batch in beam 1 lose up to 10% less in Stable Beams compared to the later bunches. An example of such structure is shown in Fig. 4: the beam 1 integrated losses after 11.5 hours in Stable Beams are shown for the different SPS batches. It is also possible to see the

Table 1: Losses per beam mode, comparison between 2011 and 2012. The last line refers to the total transmission, for fills that lasted until stable beams. Statistics for 2011 are calculated over 200 fills, from fill 1615 to fill 2266.

Losses	2011		2012	
	beam 1	beam 2	beam 1	beam 2
Capture	0.14%	0.10%	0.52%	0.34%
Ramp	0.71%	0.11%	1.17%	1.22%
Flat top	0.07%	0.02%	0.57%	0.48%
Squeeze	0.08%	0.04%	1.22%	1.99%
Adjust	0.46%	0.30%	1.76%	1.65%
Total	0.81%	0.66%	3.82%	4.74%

gaps between the PS batches. A similar structure was also noticed in 2011 [6] but was never visible on beam 2 losses.

The bunch-by-bunch luminosity is known for the four main experiments and can be used to calculate the burn-off component in the total losses in collisions. Note that the luminosity production at IP2 is negligible compared to the other IPs, so only IP1, 5 and 8 are taken into account in this analysis. It is worth noting that the SPS-batch loss structure remains visible after removal of the burn-off component. The spread in beam 1 losses after burn-off removal is $\approx 7\%$ after 8 hours of collisions. A similar structure, but much smaller in amplitude ($\approx 3\%$) is also visible in beam 2.

A clear cause for this bunch-by-bunch difference has not been identified yet. Due to the asymmetry in the loss shape, no simple correlation with the beam-beam force could be identified (e.g. with number of long range encounters).

Longitudinal shaving for bunches with increased emittances

For many fills at the end of the 2012 proton physics run, it was observed [7] that bunches in beam 1 could be divided into two families, namely:

- bunches developing a shorter bunch length have higher losses and larger transverse emittance;
- bunches getting longitudinally longer have smaller losses and smaller transverse emittance.

These characteristics built up during collisions and were related to the occurrence of transverse instabilities and emittance blow up for beam 1 at the end of the squeeze, before bringing the beams into collisions. The effect was not observed on beam 2.

CONCLUSIONS AND FUTURE WORK

Beam losses through the proton physics nominal cycle were non-negligible in 2012, and the transmission was on average $\approx 96\%$ to be compared to the $\approx 99.3\%$ in 2011. Features in the losses per beam mode per ring could be highlighted: degradation of capture losses towards the end of the run, possibly related to enhanced satellite population; losses of $\approx 1.2\%$ during acceleration, mostly towards the end of the ramp when primary collimator jaws close in; peak power losses at precise moments in the squeeze function for beam 2; losses in Adjust became much more reproducible since the use of the split collision beam process.

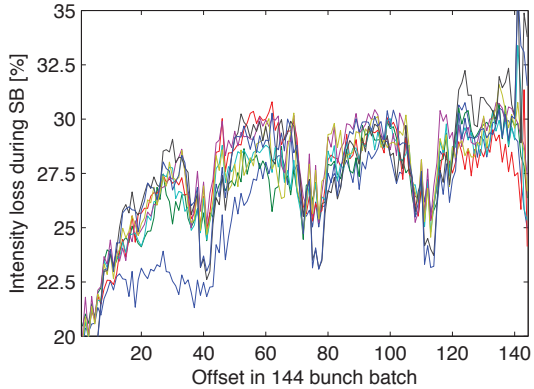

Figure 4: Integrated losses after 11.5 hours from the start of Stable Beams (SB) for beam 1 in fill 3363.

Observations of bunch-by-bunch losses in stable beams showed a reproducible SPS-batch structure (for ring 1 mostly), for which a clear cause could not be found yet. Additional losses were observed for bunches with larger transverse emittance due to instabilities that developed at the end of the Squeeze.

The authors suggest the development of a new tool for fill-by-fill data analysis e.g. to observe the evolution of the luminosity performance or of the losses on a weekly basis. This would allow a more prompt reaction to problems that might generate from the drift of parameters and a ready handle to verify the improvement of settings.

ACKNOWLEDGEMENTS

The authors would like to acknowledge the fruitful discussions with G. Arduini, C. Bracco, E. Metral, N. Mounet, T. Pieloni and G. Roy during the preparation of the workshop session.

REFERENCES

[1] R. Bruce, “Collimation settings and performance”, LHC Performance Workshop, Chamonix, 6-10 Feb. 2012.

[2] E. Metral, “Review of the instabilities observed during the 2012 run and actions taken”, these proceedings.

[3] C. Bracco, “Injection and dump systems”, these proceedings.

[4] M. Zerlauth, O. Oyvind Andreassen, V. Baggiolini, A. Castaneda, R. Gorbonosov, D. Khasbulatov, H. Reymond, A. Rijllart, I. Romera Ramirez, N. Trofimov, “The LHC Post Mortem Analysis Framework”, 12th International Conference On Accelerator And Large Experimental Physics Control Systems, Kobe, Japan, 12-16 Oct. 2009.

[5] R. Steerenberg, “Post LS1 25 ns and 50 ns options from the injectors (incl. emittance blow-up)”, these proceedings.

[6] G. Papotti, “Observations on luminosity curves”, presentation at the LHC Beam Operation Committee on 22 May 2012.

[7] M. Hostettler, G. Papotti, G. Arduini, “Observations on bunch length histogram splitting and selective emittance blow-up in LHC Beam 1”, CERN-ATS-Note-2013-003 PERF.

REVIEW OF THE INSTABILITIES OBSERVED DURING THE 2012 RUN AND ACTIONS TAKEN

E. Métral, G. Arduini, R. Assmann, O. Bruning, X. Buffat, A. Burov, W. Herr, W. Hofle, M. Lamont, N. Mounet, T. Pieloni, G. Rumolo, B. Salvant, R. Schmidt, E. Shaposhnikova, D. Valuch, J. Wenninger, S. White, F. Zimmermann

Abstract

Despite the excellent performance of the LHC in 2012, with a record peak luminosity at 4 TeV corresponding to 77% of the 7 TeV design luminosity of 10^{34} $cm^{-2}s^{-1}$, the intensity ramp-up was perturbed by several types of instabilities. All the observations (during both physics cycles and dedicated MDs) are critically reviewed, comparing them to past predictions and new findings. The lessons learned and actions taken are then discussed in detail.

INTRODUCTION AND MAIN LIMITATION AT THE END OF THE RUN

The LHC luminosity has been considerably increased in 2011 and 2012 and the peak luminosity record was ~ 7.7 10^{33} $cm^{-2}s^{-1}$, corresponding to 77% of the 7 TeV design luminosity of 10^{34} $cm^{-2}s^{-1}$, but at 4 TeV, i.e. 4 / 7 = 57% of the design energy. This great achievement led to the discovery of a Higgs-like boson, announced on July 4th, 2012, and to a total integrated luminosity of ~ 23 fb^{-1} for the two high-luminosity experiments, ATLAS and CMS. Furthermore, only half of the design number of bunches has been used (1374), using a beam with 50 ns bunch spacing instead of the nominal 25 ns bunch spacing. However, and this is the reason of the success, the bunch brightness was up to ~ 2.4 times larger than nominal, as bunches with ~ 1.6 10^{11} p/b within ~ 2.2 μm (transv. r.m.s. norm. emittance) were successfully put in collision, instead of the nominal bunches of 1.15 10^{11} p/b within 3.75 μm. Finally, tight collimators settings (collimator apertures close to nominal ones at 7 TeV) have been used in 2012, leading to larger impedances and more critical instabilities (a factor ~ 2.3 was computed for the transverse plane compared to 2011 [1]).

Despite the excellent performance of the LHC in 2012, 3 types of instabilities perturbed the intensity ramp-up, which are discussed below.

In collision: "Snowflakes"

These instabilities happened always in the horizontal plane only, for both beams and could happen after several hours of stable beam (see an example in Fig. 1). It concerned initially only the IP8 private bunches, i.e. the bunches colliding only at the Interaction Point 8. This was rapidly identified and these instabilities disappeared once the filling scheme was modified (reducing first the number of private bunches and then removing them all). The interpretation of this mechanism is that it happens on selected bunches with insufficient tune spread (and thus Landau damping) as they have no Head-On collisions in IP1/2/5 and have a transverse offset in IP8 to level luminosity.

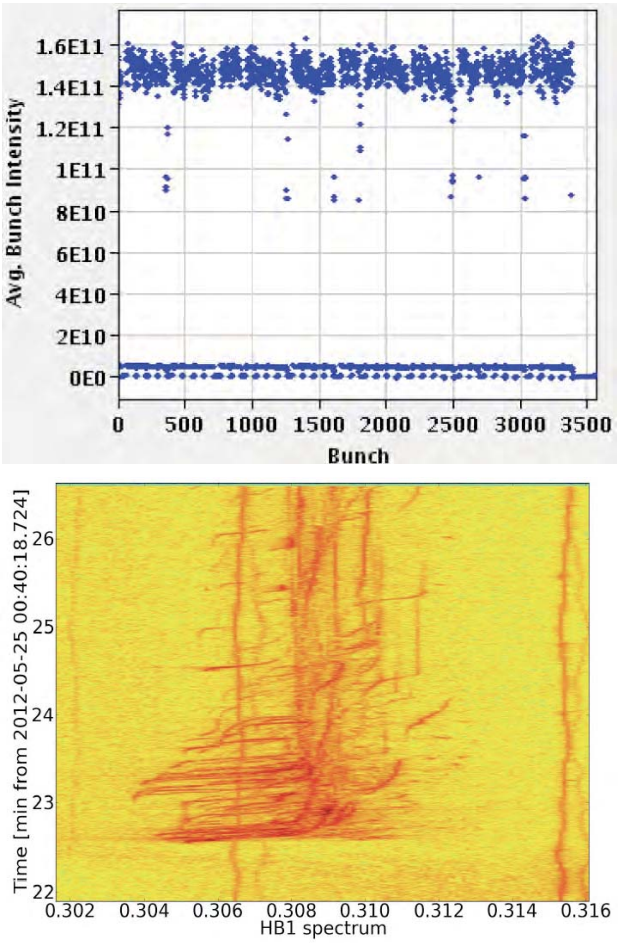

Figure 1: Example of "snowflakes" instability: (a) bunch intensity vs. number of the bunch (25 ns slot) and (b) horizontal frequency spectrum vs. time. Courtesy of X. Buffat.

During the collapsing process (putting the beams into collision)

A second type of instabilities happened at the end of the collision process when ending with residual separations of ~ 2.1 σ in IP1 and ~ 1.2 σ in IP5 (values estimated from luminosities at the moment of the dump).

These instabilities happened also in the horizontal plane and an example is given in Fig. 2.

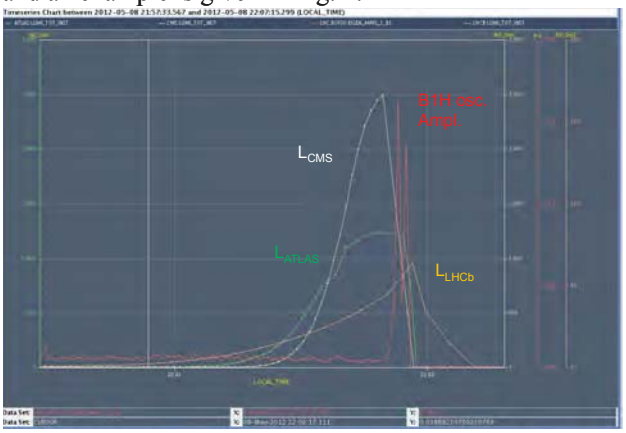

Figure 2: Example of instability during the collision process (putting the beams into collision): the luminosities vs. time are represented for the different experiments as well as the horizontal oscillations amplitude for beam 1. Courtesy of G. Arduini.

During or at the end of the squeeze process: EOSI (End Of Squeeze Instability)

A third type of instability happened during or at the end of the squeeze, called EOSI (End Of Squeeze Instability), also in the horizontal plane. A characteristic picture is shown in Fig. 3, where 3 lines spaced by the (small-amplitude) synchrotron tune can be observed.

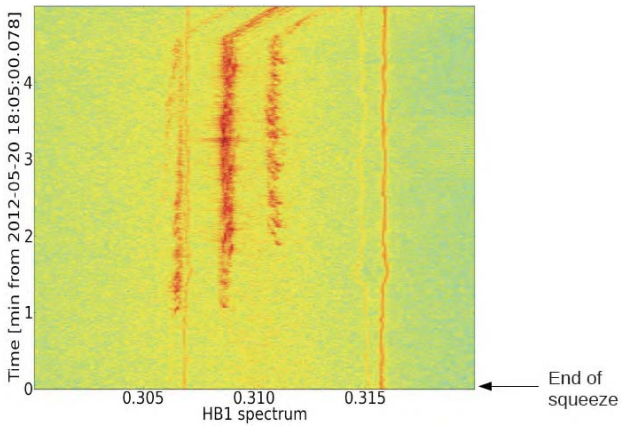

Figure 3: Example of instability observed at the end of the squeeze: horizontal frequency spectrum vs. time after the end of the squeeze. Courtesy of X. Buffat.

The first and second types of instabilities did not appear anymore after the change of the Landau octupoles polarity (moving from negative to positive detuning with amplitude) on August 7th (fill #2926) and the increase of the chromaticities and the transverse damper (ADT) gain. Unfortunately these 3 parameters have been modified more or less at the same time and it is therefore not possible to identify the main beneficial effect. The third type of instabilities could not be cured during the entire run despite the increase of the octupoles current close to its maximum value (550 A), the increase of chromaticities from ~ 2 units to ~ 15-20 units and the increase of the ADT gain to its maximum value (50 turns damping time). Note however that this instability appeared then mostly in the vertical plane of beam 1. Furthermore, it became then very reproducible at the end of the squeeze (with even more synchrotron sidebands), when β* is already at 60 cm, and after ~ 16 min from the start of the squeeze process. Examples of this instability are shown in Fig. 4.

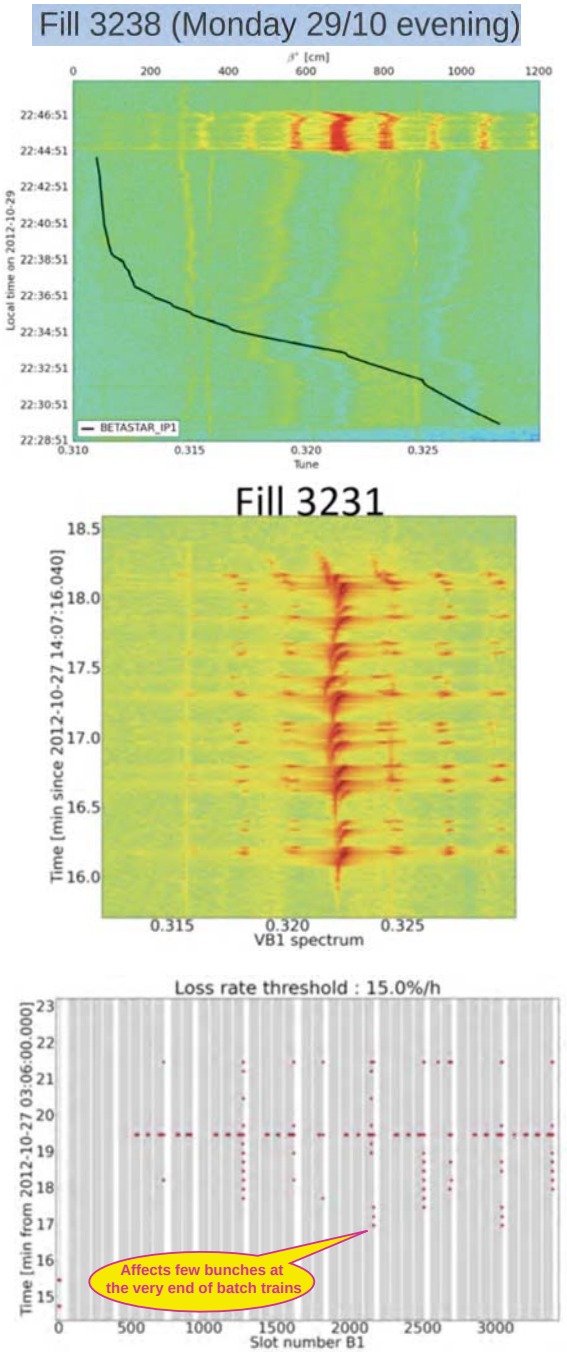

Figure 4: Examples of the EOSI instability at the end of the run, which could not be cured: (a) Courtesy of N. Mounet and (b) and (c) courtesy of T. Pieloni.

PAST PREDICTIONS, NEW FINDINGS AND ACTIONS TAKEN

Based on the past work done before the LHC commissioning [2,3], the first measurements of transverse coherent instability with a single bunch [4] and with a train of 12+36 bunches [5], the initial recommendations at the beginning of the run were the following [6]:

1) Chromaticities: ~ 1-2 units (with the wish to make some controlled studies during the run with negative values as the possibility of running with slightly negative chromaticities was proposed in the past [2]).

2) Landau octupoles current (in the focusing ones): ~ -450 A (as ~ - 200 A was used at the end of 2011 and the impedance should have been increased by a factor ~ 2.3 with the tight collimators settings).

3) Bunch length (rms): increase it from 9 cm (i.e. 1.2 ns total) in 2011 to ~ 10 cm (i.e. ~ 1.35 ns total) in 2012 for beam-induced RF heating reasons [7].

4) ADT gain: reduce it as much as we can (to minimize the possible noise introduced and the associated transverse emittance growth).

However, several issues rapidly appeared during spring and several actions were taken to continue and push the performance:

1) To avoid the beam dumps triggered during the collision process, it was proposed to change the sign of the Landau octupoles such that the tune spreads from beam-beam and octupoles add up instead of compensating each other and therefore do not fight against each other (for both Long Range - LR - and HO, IP8 and nominal bunches) [8].

2) New values for the ADT gain, chromaticities and Landau octupoles current were then suggested after a new analytical approach from A. Burov [9,10]. Figure 5 shows the latest results obtained by A. Burov for the 50 ns beam, with 1.5 10^{11} p/b within 2 μm. Several conclusions can be drawn from this figure. In the absence of transverse damper, the usual results for both single-bunch and coupled-bunch head-tail instabilities are obtained and some Landau damping is needed [3]. In the presence of the transverse damper, a valley with zero Landau octupoles current is found for negative chromaticities as discussed for instance in Ref. [11] and proposed as a possible remedy in Ref. [2]. The interpretation being that for slightly negative chromaticities, the higher-order head-tail modes are intrinsically damped and the enhanced instability of mode 0 is damped by the transverse damper. However, if the transverse impedance is twice the nominal one, the valley disappears and the best operational location seems to be at high chromaticities, i.e. ~ 15 - 20 units for a sufficiently high ADT gain (with its initial bandwidth [12]). Finally, another very interesting observation is that for sufficiently high ADT gain and chromaticities, the stabilizing Landau octupoles current is the same for both single-bunch and coupled-bunch instabilities.

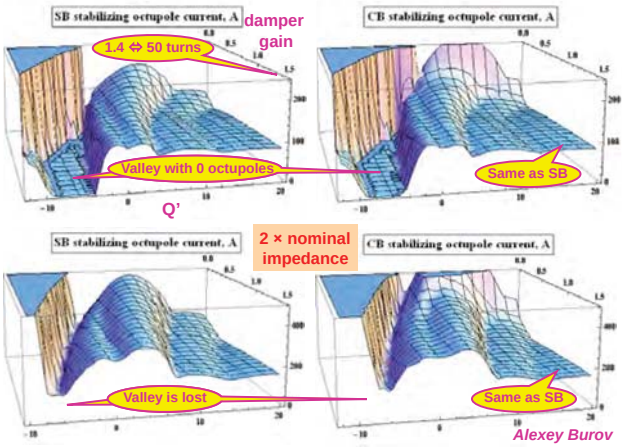

Figure 5: Stabilizing Landau octupoles current (in A) vs. chromaticity and ADT gain for (upper left) a single bunch with nominal transverse impedance, (lower left) a single bunch with twice the nominal transverse impedance, (upper right) the 50 ns beam with nominal transverse impedance, (lower right) the 50 ns beam with twice the nominal transverse impedance. Courtesy of A. Burov.

The conclusions of all the 1-beam studies are the following:

1) The current model (for the transverse impedance and the Landau damping mechanism) seems consistent and disagreements with dedicated measurements never exceeded a factor ~ 2. This is why most of the time now we consider the impedance as being a factor 2 larger than nominal. This result was already obtained in the past in several studies without ADT [5] and it seems to be confirmed this year including the effect of the ADT [10].

2) It happened several times that the situation was much better than predicted, which can be explained by larger transverse tails (for the previous negative octupoles polarity) or longitudinal tails.

The problem with the EOSI comes in the presence of 2 beams, below a β* of few m. Much more octupoles current than for 1 beam is needed, and the maximum available value was in fact not enough to completely suppress the instability. It was however sufficient in 2012 to reach the HO collisions, which then stabilizes everything but we might be limited at higher energies, and this is therefore a potential worry/showstopper for the future [13].

Therefore, the remaining question is: why is the beam unstable at the end of the squeeze? Do we understand well the ADT? Recent simulation studies are shown in Fig. 6, revealing in particular the effect of a flat gain [12] over all the coupled-bunch frequency range. Do we lose Landau damping due to the interplay with other mechanisms? Either because the stability diagram is modified (shifted, deformed, collapsing etc.) due to other nonlinearities: (i) beam-beam (LR and/or HO), but it seems it cannot explain the EOSI [14]; (ii) machine nonlinearities, but it seems also that it cannot explain the EOSI; (iii) e-cloud in IRs? This is the recent hypothesis from A. Burov, which he just started to study [15];

(iv) others? Or, because the coherent tune shift (of some modes) is underestimated: (i) a 2-beam impedance MD was performed [16], which remains without clear conclusions; (ii) beam-beam coherent modes (mode coupling), see below and Fig. 7; (iii) e-cloud in IRs? Recent hypothesis from A. Burov; (iv) others? The study of the mode coupling between the beam-beam coherent modes and the impedance-induced modes has been done by S. White by including the impedance model of Ref. [5] into the beam-beam code BeamBeam3D [17] (see Fig. 7). In case of such a problem, the solution is to introduce a tune split between the 2 beams to decouple the machine, as usual when coherent beam-beam modes are involved, as it is simply explained for instance in Ref. [18]. It is seen indeed from Fig. 7 that introducing a tune split shifts the mode coupling instability threshold to a higher number of LR interactions and that therefore the unstable bunches should move from the tail (original observed positions) to the centre of the batches. Some studies have been suggested and performed, starting with the fill #3259 (see Fig. 8), where the unstable bunches seemed indeed to move from the tail to the centre, as expected. Other studies are shown in Fig. 9. It is difficult to conclude on the effect of the tune split (and its sign) due to the small statistics and the fact that some fills with tune split behaved very similarly to other fills. It is worth noting that simulation studies show that this instability should be suppressed by the ADT (as studied by A. Burov [19] and S. White [20]) and therefore a tune split should even not

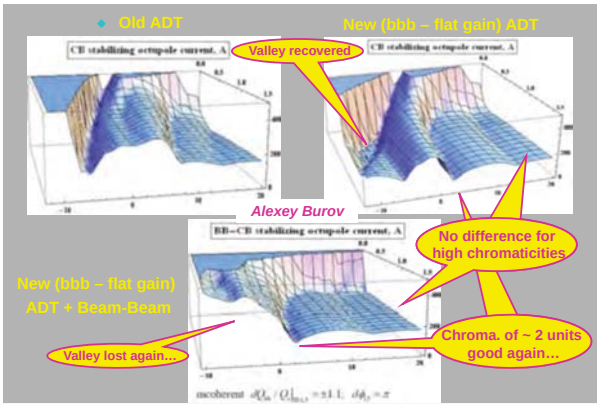

Figure 6: Recent studies on ADT with initial gain and flat gain [12]. Courtesy of A. Burov.

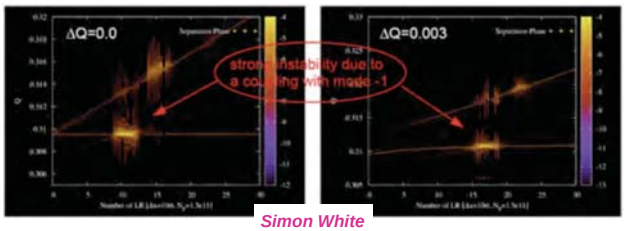

Figure 7: Interplay between the LHC impedance and beam-beam coherent modes, leading to mode coupling (a) without tune split and (b) with a tune split. Courtesy of S. White.

be needed. However, is it really true in reality in the presence of other effects such as noise etc.? This will be followed up with multi-bunch tracking studies.

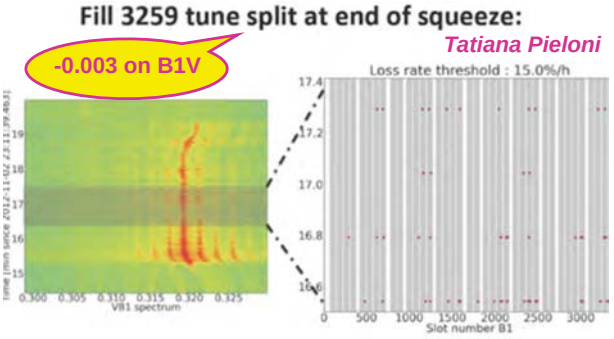

Figure 8: Measurements of the unstable bunches in the presence of a tune split of -0.003 in the vertical plane of beam 1.

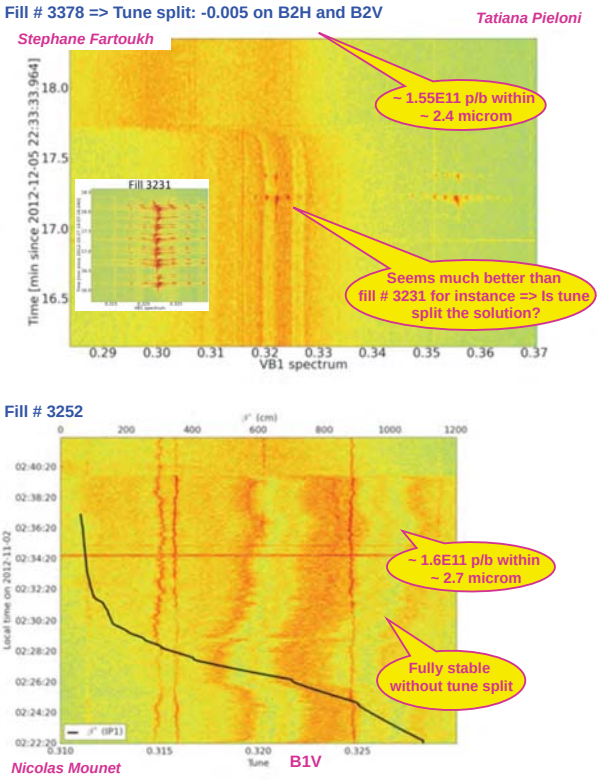

Figure 9: Other studies than in Fig. 8, (a) with and (b) without tune splits, where it is therefore difficult to conclude about the beneficial effect of the tune split.

CONCLUSIONS AND LESSONS LEARNED FROM 2012

The impedance model and Landau damping mechanism with 1 beam only is reasonably well understood as measurements never revealed a factor more than ~ 2 over the last few years. Furthermore, we have also now a new global instability model including the transverse damper, which gives us a better understanding

of the single-beam phenomena. This factor ~ 2 will need however to be better understood in the future.

The main problem concerns the 2-beam operation, for which much more octupoles current than predicted is needed and the reason has not been identified yet. Several observations have been made: some of which are clear and some of which are less clear. The clear observations are summarized below:

i) Instabilities are observed only for β* smaller than few m;

ii) Increasing the Landau octupoles current helps. As we should be limited at higher energies, could we have more octupoles current in the future? It seems that a factor ~ 2 could be gained with the spool piece correctors MCO and MCOX (the dynamic aperture should also be watched out) [21];

iii) Increasing chromaticities to ~ 15-20 units helped a lot (but according to A. Burov's theory a plateau has been reached now and no further stability gain can be expected by increasing the chromaticity);

iv) Once in collision, no instability is observed anymore due to large beam-beam HO tune spread (see also Ref. [14]);

v) No beam dumps have been observed anymore with the new (positive) Landau octupoles polarity, higher chromaticities and ADT gain, which have been modified at the same time. Note that there were also discussions to modify the collision beam process to go faster through the critical points [22], but this was implemented later.

The plan for the future is to continue the data analyses (trying for instance to identify the tunes which were lost by using the trims, the head-tail modes excited, etc.), and try and understand / work more on interplays between different mechanisms (incoherent and coherent): impedance, nonlinearities (machine and Landau octupoles), space charge (at low energy), ADT, longitudinal bunch distribution, beam-beam when the beams start to see each other, e-cloud… One needs also to understand better how the ADT works [12] and to continue and benchmark the new results [10] with tracking codes. This already started and will be continued by including the ADT in the HEADTAIL code [23] (ongoing) and including the impedance and ADT in the beam-beam COMBI code [24].

Finally, based on the 2012 experience, it is also fundamental to try and benchmark some of the main theoretical/simulation results at an early stage of the (re-)commissioning as things get then rapidly very intricate and it becomes more difficult to apply the proper corrections.

APPENDIX A

The other beam spectra of the fill #3252 (see Fig. 9c), which was fully stable without tune split, are shown in Fig. A.

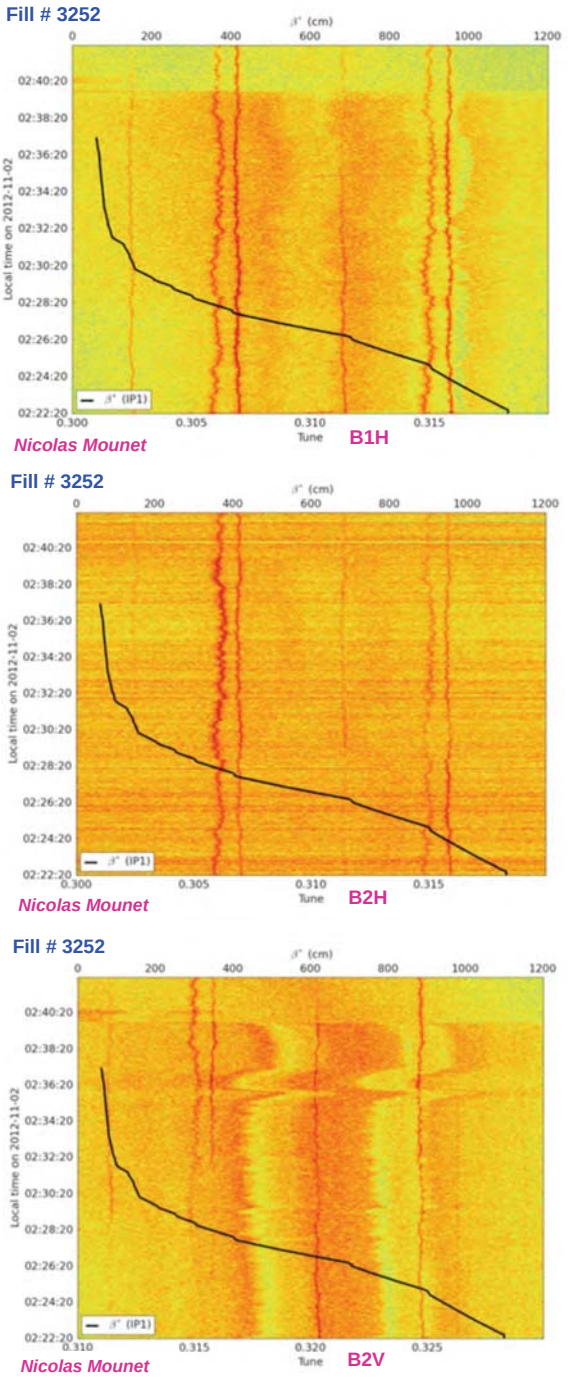

Figure A: Beam spectra for the fill #3252 in the horizontal plane for both beams and vertical plane for beam 2. The vertical plane for beam 1 is shown in Fig. 9c.

APPENDIX B

There were several examples of fills without instability with the old/previous (negative) polarity of the Landau octupoles with intensities per bunch between ~ 1.47 10^{11} p/b and 1.51 10^{11} p/b: e.g. #2717, 2718, 2719, 2720, 2723, 2724, 2725, 2726, 2728 and 2729. They all came after good chromaticities measurements all along

the cycle and proper corrections to ~ 2 units applied at all stages.

APPENDIX C

In addition to the 3 types of instabilities discussed in the paper, there were also 2 other types of instabilities:

i) A 4th type of instability was observed at injection (leading to transverse emittance blow-ups of some injected batches). This is the reason why 6.5 A in the Landau octupoles are used at injection. Note that this value has been found to work but it was not optimized and the reason why it works not yet understood. Note also that the octupoles current had to be increased even more (by a factor ~ 4) during the 25 ns scrubbing run in the presence of electron cloud. This should be followed up in the future.

ii) A 5th type of instability was also observed at flat-top before the squeeze in some cases before the re-optimization of the octupoles current as the 1-beam instability was expected to be more critical with the current (positive) sign of Landau octupoles (e.g., a factor ~ 1.6 was anticipated for a Gaussian transverse profile).

APPENDIX D

During the 2012 run, there were a lot of discussions about the crossing, during a certain time, of a zero or small tune spread: this can be the case for instance when the Landau octupoles had the negative polarity and beam-beam and octupoles fought against each other or during the collision process (whatever the octupoles current). Is crossing a zero (or very small) tune spread a problem? Yes, in principle it is a potential weakness but several other aspects should be considered at the same time. For instance, what is important in the end is the stability diagram, as the spread has to be at the correct place (with the coherent tunes inside). Furthermore, the time of the process and the most critical instability rise-time should be compared, as the instability might not have the time to develop.

For instance, the PS machine is crossing a zero tune spread every cycle at transition (see Fig. D). The solutions (if this is really a problem, i.e. above a certain intensity) are:

i) Don't cross the zero tune spread if possible. This is what was implemented in the LHC for the very small tune spread due to beam-beam and octupoles compensation by changing the sign of the octupoles. In the PS, to avoid crossing transition it would require to modify the optics.

ii) Cross faster and/or cleaner (e.g. IP1&5 first and then IP8), as it was proposed and implemented during the year. For the PS, the transition is crossed faster by using a gamma transition jump (see Fig. D) and therefore the time, during which the tune spread (proportional to the slip factor) is small, is considerably reduced and the intensity threshold is then significantly increased.

iii) Another possibility is also to try and increase the instability rise-times by reducing the impedance (opening the gaps, changing the collimators materials etc.) and/or by playing with the chromaticities and transverse damper gain (as was done also at the same time when the octupoles current was changed).

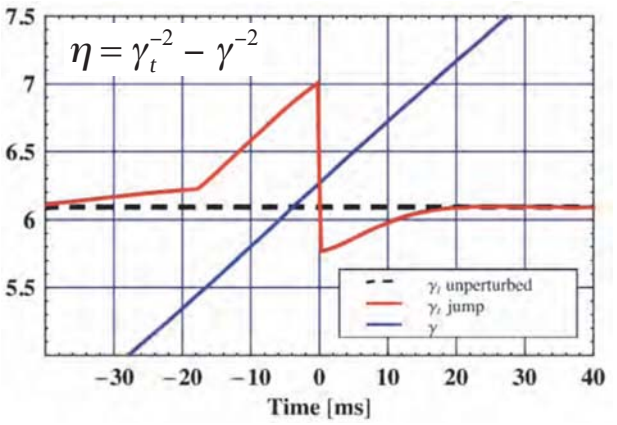

Figure D: Example of the PS transition crossing. Evolution of the relativistic gamma transition (and of the of the relativistic gamma of the beam) near transition crossing without and with the present relativistic gamma transition jump.

ACKNOWLEDGEMENTS

Many thanks to S. Fartoukh for useful discussions, Riccardo De Maria for help in measurements, to OP, BI, RF, CO (Timber), collimation teams for the close collaboration and all the fruitful discussions during this very interesting and challenging year!

REFERENCES

[1] N. Mounet at al., Impedance Effects on Beam Stability, LHC Beam Operation Workshop, Evian, France, 12-14/12/2011.

[2] (Ed.) O. Brüning et al., LHC Design Report, CERN-2004-003 (Vol. I), 4 June 2004.

[3] E. Métral, Single-Bunch and Coupled-Bunch Instability at LHC Top Energy vs. Chromaticity, CERN RLC meeting, 21/04/2006.

[4] E. Métral et al., Stabilization of the LHC Single-Bunch Transverse Instability at High-Energy by Landau Octupoles, Proc. IPAC 2011, San Sebastian, Spain, 04-09/09/2011.

[5] N. Mounet, The LHC Transverse Coupled-Bunch Instability, PHD thesis from EPFL, Lausanne, Switzerland, 2012.

[6] E. Métral, Recommendations for the Chromaticities, Octupoles' Currents and Bunch Length to be Used During the 2012 Run, CERN LBOC meeting, 13/03/2012.

[7] B. Salvant, Beam Induced RF Heating, these proceedings.

[8] S. Fartoukh, …The Sign of the LHC Octupoles, CERN LMC meeting, 11/07/2012.

[9] E. Métral, Impedances, Instabilities and Implications for the Future, CMAC meeting #6, CERN, 16-17/08/2012.

[10] A. Burov, Nested Head Tail Vlasov Solver : Impedance, Damper, Radial Modes, Coupled Bunches, Beam-Beam and More…, CERN AP forum, 04/12/2012.
[11] M. Karliner and K. Popov, Theory of a Feedback to Cure Transverse Mode Coupling Instability, Nucl. Instr. and Meth. In Phys. Res. A 537 (2005) 481-500.
[12] F. Dubouchet et al., "What You Get" – Transverse Damper, these proceedings.
[13] N. Mounet et al., Beam Stability with Separated Beams at 6.5 TeV, these proceedings.
[14] X. Buffat, Stability Considerations with Beam-Beam and Octupoles, CERN LMC meeting, 29/08/2012.
[15] A. Burov, Three-beam instability in the LHC, CERN-ATS-Note-2013-012 PERF.
[16] S. Fartoukh et al., Two-Beam Impedance MD, CERN LSWG meeting, 05/02/2013.
[17] J. Qiang, BeamBeam3D: A 3D Parallel Beam-Beam Simulation Code (http://amac.lbl.gov/~jiqiang/BeamBeam3D/).
[18] A. Hofmann, Beam-Beam Modes for Two Beams with Unequal Tunes, Proc. of the Workshop on Beam-Beam Effects in Large Hadron Colliders, 12-17/04/1999.
[19] A. Burov, ADT Suppression of Coherent Beam-Beam, CERN ICE meeting, 31/10/2012.
[20] S. White, Update on Long-Range Instabilities, CERN ICE meeting, 07/11/2012.
[21] R. Tomas, Optics and Non-Linear Beam Dynamics at 4 and 6.5 TeV, these proceedings.
[22] X. Buffat, Stability Considerations with Beam-Beam and Octupoles, CERN LMC meeting, 29/08/2012.
[23] G. Rumolo and F. Zimmermann, Phys. Rev. ST Accel. Beams, 5(121002), 2002.
[24] T. Pieloni, A Study of Beam-Beam Effects in Hadron Colliders with a Large Number of Bunches, PHD thesis from EPFL, Lausanne, Switzerland, 2008. COMBI (COherent Multibunch Beam-beam Interactions) code.

BEAM STABILITY WITH SEPARATED BEAMS AT 6.5 TeV

N. Mounet*, E. Métral, G. Arduini, T. Pieloni, B. Salvant (CERN, Geneva, Switzerland),
S. White (BNL, Upton, New York, USA), X. Buffat (EPFL, Lausanne, Switzerland),
R. Calaga, J. Esteban-Müller, R. Bruce, S. Redaelli, B. Salvachua, G. Rumolo
(CERN, Geneva, Switzerland)

Abstract

We provide here a preliminary estimate of the available parameters space in terms of collimator settings, intensity, transverse emittances and bunch spacing, in order to allow stable single-beam and flat top operation at 6.5 TeV after the 2013-2014 long shutdown (LS1), assuming the machine will operate in similar conditions as in 2012 in terms of chromaticity, damper gain and damper bandwidth. As a starting point we use the current knowledge of the machine in terms of observed limits in single-beam operation, or in physics operation up to the beginning of the squeeze, and rescale them thanks to the impedance model obtained for the possible collimator settings scenarios. We show that only the 25 ns beam with a classical injection scheme can be stable with nominal collimator settings, while tight settings allow the operation with the BCMS (batch compression merging and splitting) 25 ns beam. The 50 ns beam will on the contrary probably require relaxed settings close to those of 2011.

INTRODUCTION

Until recently, the analysis of beam stability in the LHC under the action of a beam-coupling impedance was considered separately from the action of the transverse feedback. Indeed, the feedback system, which is close to a bunch-by-bunch feedback with a flat time domain profile on the bunch length scale, in particular since the end of 2012 [1], was thought to act mainly on the rigid-bunch modes (also called headtail mode with azimuthal mode number $m = 0$), without significant impact on higher order modes which were supposed to be stabilized solely by Landau damping from lattice non-linearities (in single-beam or separated beams operation). The main purpose of the feedback was therefore to damp rigid-bunch multibunch modes present at zero chromaticity.
However, it was found during the year 2012 that a strong damper, i.e. with a damping rate comparable to the synchrotron frequency, has also an impact on higher order headtail modes, even if the damper is a low frequency bunch-by-bunch damper as in the LHC [2–5]. This damper effect on coherent modes can be beneficial or detrimental. Therefore, with such a strong damper, coherent modes can be put into several categories:

- those that can be damped with high enough damper gain: coupled-bunch rigid-bunch modes and diagonal headtail modes (i.e. the strongest headtail modes in the absence of a damper, such that the number of intra-bunch nodes matches the headtail mode number m),
- those that cannot be damped by the transverse feedback (or with great difficulty), typically modes with high order azimuthal or radial mode number, and such that bunch centroids stay close to zero. Such modes then require Landau damping to be stabilized.

Note that with a strong damper the threshold of the transverse mode-coupling instability [6] (TMCI) cannot be defined anymore according to these new findings [5].
Instability growth rates and tune shifts can be estimated thanks to

- the LHC impedance model [7]: (resistive-)wall impedance from collimators, beam-screens, vacuum pipe and broadband model from the design report, updated with the collimator half-gaps estimated for various post-LS1 scenarios,
- beam dynamics simulations (HEADTAIL [8] multi-bunch code with a bunch-by-bunch ideal damper) or analytical models (ABA [3], NHT [4, 5], DELPHI [9][1]).

In these proceedings we will first summarize the available single-beam 2012 observations in order to give a basis for the predictions at higher energy. Then we will briefly describe the various post-LS1 collimator scenarios and their implication in terms of impedance, and analyse the effect of the bunch spacing when a strong damper is on. Finally we will give preliminary estimates of the intensity limits in 2015, based on observed limits in 2012, the impedances calculated for the possible collimator scenarios and simple scaling laws. Our conclusions will follow.

CURRENT KNOWLEDGE OF THE LHC TRANSVERSE IMPEDANCE

Two kinds of beam-based impedance indirect measurements took place in 2012: single-bunch tune shifts and multibunch instabilities. Both kinds of measurements are still under analysis; we provide for each of them the first main results.

* nicolas.mounet@cern.ch

[1] The code DELPHI was developped after the presentation associated with these proceedings so is not used in the rest of the paper

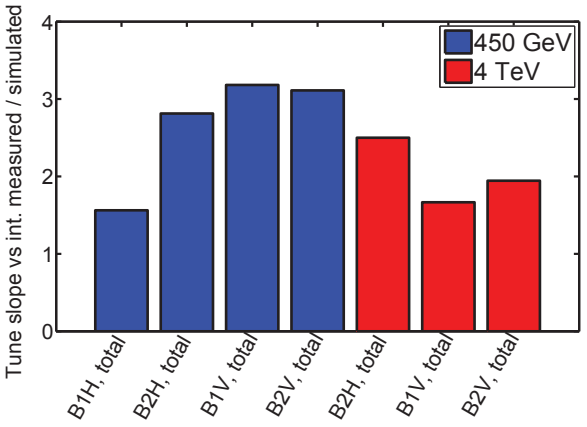

Figure 1: Discrepancy factor between measurements and simulations of the total LHC tune slopes vs. intensity, at injection and top energy, depending on the beam and plane.

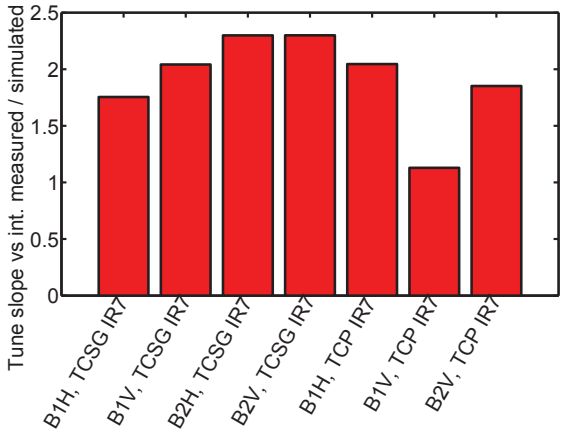

Figure 2: Discrepancy factor at 4 TeV between measurements and simulations of the tune slopes vs. intensity, for certain collimator families, beams and planes.

Single-bunch tune shift measurements

On June 20th, 2012, several measurements of the total tune shifts vs. intensity were done, at injection and 4 TeV, and for both beams and both planes [10]. Those were actually not strictly speaking single-bunch measurements since 8 bunches were present in the ring, some of them having different intensities, thus allowing the measurement of tune shifts with respect to intensity. Since bunches were equidistant in the ring, so very far apart, the influence of neighboring bunches on the tune shift was considered negligible in the analysis, which was confirmed by HEADTAIL simulations with the current impedance model.

In Fig. 1 we provide a comparison of the measurements given in terms of tune slope vs. intensity, with results from the simulation code HEADTAIL using the wake fields from the LHC impedance model. The quantity plotted is actually the discrepancy factor between measurements and simulations, which on average is around 3 at injection energy, and around 2 at flat top.

Another kind of measurement was performed on June 24th, 2012, giving the tune shifts of collimators upon moving their jaws back and forth [11]. Results, in terms of tune slope vs. intensity compared to HEADTAIL simulations, are shown in Fig. 2 for several collimator families (secondary collimators in the interaction region 7, called TCSG IR7, and primary collimators in the same interaction region, called TCP IR7), all at top energy (where the gaps are the smallest).

In the end, the values obtained for the discrepancy factors between model and measurements are ~ 3 at injection energy for the total tune shift, and ~ 2 for the total tune shifts as well as the collimators tune shifts at 4 TeV. These are consistent with most of the values obtained in 2010 and 2011 [12].

Instabilities with single or separated beams observed in 2012 with the feedback on

During the year several instabilities were observed in physics operation at flat top before the squeeze, when the beams can be considered as independent from each other [13]. In addition, dedicated measurements with a single beam were performed during the year, in particular in June 2012 [14] and October 2012 [15]. All those observations, in multibunch situation (50 ns spacing, 1374 bunches) with similar conditions of emittances, bunch length and intensity per bunch, are summarized in Fig. 3 where the octupole current (in absolute value) at which instabilites were observed is plotted as a function of the chromaticity. The two possible octupole polarities are considered: the so-called "old" polarity (negative current in the focusing octupoles, postive in the defocusing ones), and the "new" polarity (positive current in the focusing octupoles, negative in the defocusing ones). The "old" polarity is more favourable in the single beam case because it gives a tune spread centered around negative tune shifts with respect to the unperturbed tune, which is well suited to damp coherent modes from the impedance since their tune shifts are most of the time negative.

In this plot one can clearly observe the effect of the change of octupole polarity during the year, increasing the octupole current at which instabilities were seen so degrading the situation, as expected. On the other hand the increase of chromaticity to values between 10 and 20 clearly improved the situation. Unfortunately the impact of such an increase of chromaticity for the "old" polarity is not known experimentally, as the maximum chromaticity tested with the old polarity is $Q' = 7$. From Fig. 3 it is seen that with the damper on the best stability region is at high chromaticity (Q' between 10 and 20), which according to A. Burov [5] is also a region where the exact value of chromaticity matters less than close to $Q' = 0$. Then, for the highest chromaticities tested, instabilities were observed with at maximum

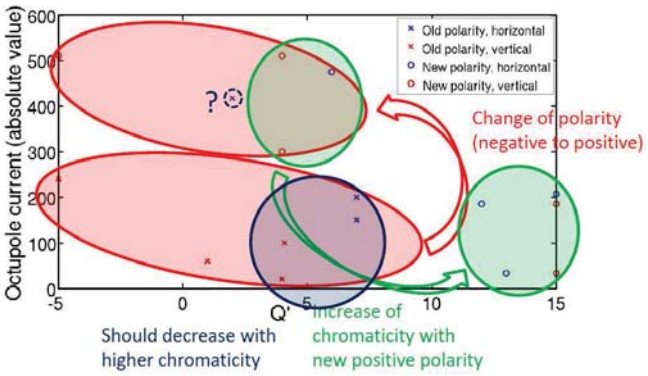

Figure 3: Octupole current (absolute value) vs. chromaticity for the separated beams instabilities observed during the year. The measurement point indicated with a question mark is very different from the others and is therefore ignored in the analysis. Note that emittances, intensity and bunch length are around 2012 operational values (respectively 2.5μm in both planes, $1.5 \cdot 10^{11}$ protons per bunch and 9.4 cm RMS) but can vary slightly between each observation.

$\sim$ 200 A in the octupoles in absolute value, for both polarities. Note that this value does not really represent an octupole threshold since at this value some instability was observed. Therefore, we prefer to take a margin and assume that the separated beams are stable with 250 A in the octupoles (in absolute value)[2].

POST-LS1 IMPEDANCE SCENARIOS

Three different impedance scenarios were considered for 2015 operation at 6.5 TeV. They are based on different collimator settings described in details in Ref. [16]:

- "nominal settings": most critical ones, where IR7 collimators are closer to the beam than now (except for primary collimators),
- "tight settings": close to 4 TeV 2012 settings,
- "relaxed settings": close to 3.5 TeV 2011 settings.

Comparison between the transverse dipolar impedances in each of these scenarios and those at 4 TeV during the 2012 run is shown in Figs. 4 to 6. For each of the three scenarios, the maximum ratio between the post-LS1 total impedance and the 4 TeV 2012 one, above 1 MHz frequency (low frequencies do not matter since we assume operation at high chromaticity), is 1.53 for the nominal settings, 1.13 for the tight ones and 0.77 for the relaxed ones.

[2]This additional margin of 50 A was not considered during the presentation associated with these proceedings, hence the slightly more pessimistic results here for post-LS1 predictions (see below).

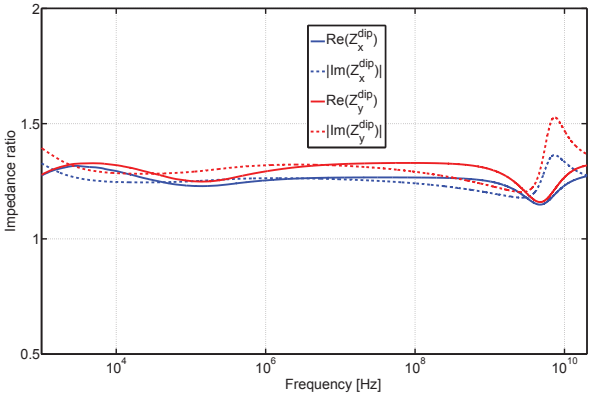

Figure 4: Ratio between the transverse dipolar impedances with the "nominal settings" post-LS1 collimator scenario and the 2012 4 TeV flat top settings.

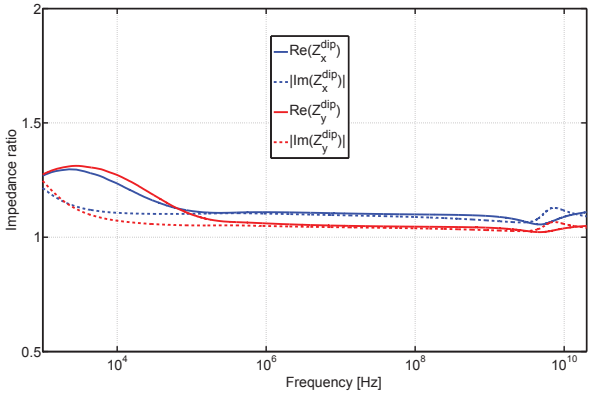

Figure 5: Ratio between the transverse dipolar impedances with the "tight settings" post-LS1 collimator scenario and the 2012 4 TeV flat top settings.

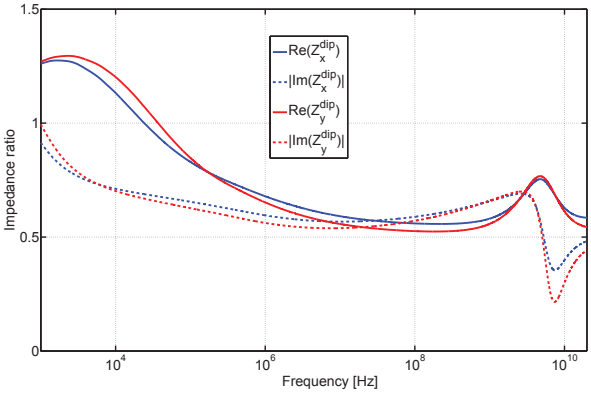

Figure 6: Ratio between the transverse dipolar impedances with the "relaxed settings" post-LS1 collimator scenario and the 2012 4 TeV flat top settings.

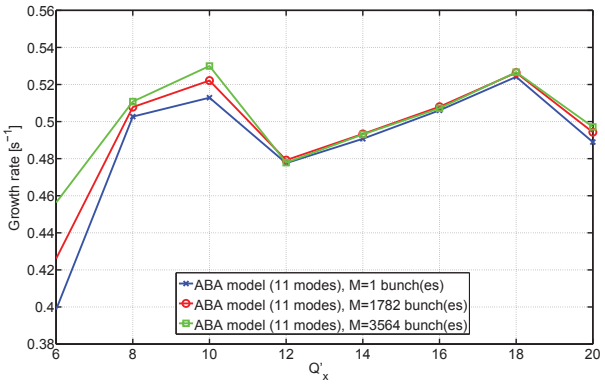

Figure 7: Effect of the bunch spacing in horizontal: comparison between single-bunch, 50 ns and 25 ns spacing (entirely filled machine), with $1.5 \cdot 10^{11}$ protons per bunch, 50 turns of damping (with a flat bunch-by-bunch damper) and 9.4 cm RMS bunch length.

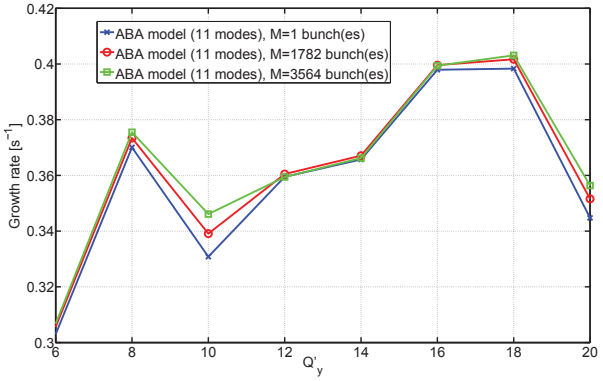

Figure 8: Effect of the bunch spacing in vertical: comparison between single-bunch, 50 ns and 25 ns spacing (entirely filled machine), with $1.5 \cdot 10^{11}$ protons per bunch, 50 turns of damping (with a flat bunch-by-bunch damper) and 9.4 cm RMS bunch length.

EFFECT OF THE BUNCH SPACING

According to recent theoretical developments [5], the bunch spacing (25 ns vs. 50 ns) should have a negligible effect on the instabilities when the transverse feedback is on and strong enough, and the chromaticity high enough. Actually, the single-beam instabilities should then be dominated by single-bunch effects. This is confirmed by the ABA model [3] (applied to the current LHC impedance model at 4 TeV) in Figs. 7 and 8 showing the growth rate vs. chromaticity of the most unstable mode for equidistant and equipopulated bunches along the ring. According to this model at high chromaticity (Q' between 10 and 20), the bunch spacing has a negligible effect on instabilities with a strong damper.

BEAM PARAMETER SPACE WITH SEPARATED BEAMS FOR POST-LS1 OPERATION

To give a preliminary estimate of the available parameters space in terms of intensity and emittance for the three different collimator scenarios foreseen (see above), we adopt here a purely empirical approach based on simple scaling laws applied to the observed limits in 2012. The assumptions on the scaling laws are the following:

- The tunespread is proportional to the geometric emittances as well as the detuning coefficient which is itself proportional to the octupolar field and inversely proportional to the magnetic rigidity [17]. Therefore [18], the stability diagram for Landau damping is proportional to the current in the octupoles and goes as $\frac{1}{\gamma^2}$ where γ is the relativistic mass factor.
- The coherent tune shifts from the impedance decrease as $\frac{1}{\gamma}$ [19] and increase proportionally to the intensity [19, 20].
- The coherent tune shifts are proportional to the impedance factor found in the previous section. This is a pessimistic assumption which is equivalent in assumming that the ratio between the post-LS1 impedance and the 4 TeV one is at all frequencies the same as the maximum ratio between the two.
- The bunch spacing (or number of bunches) has no impact in itself assuming we run at high enough Q' (see previous section).

Those assumptions are rather strong and gives here therefore only rough estimates of the final limitations for 2015 operation. This approach is justified by the lack of knowldege of the impedance of the machine in particular at high frequency as well as the lack of reproducibility of the octupole current threshold measurements, which a priori do not allow a fine estimate of the limitations. Work is ongoing to exploit and understand better the accumulated data in 2012, as well as to refine the impedance model, in order to allow a more precise determination of the limitations. Such assumptions neglect in particular mode coupling (responsible for a deviation from the proportionality between coherent tune shift and intensity), external non-linearities that may change with higher energy, and the impact of the bunches longitudinal and transverse distributions which also may vary.
Under the validity of these assumptions, one can obtain the following relation between normalized transverse emittance ε and intensity per bunch N_b:

$$\frac{I^{oct}\varepsilon}{E} = \mathcal{C} I_{fact} N_b, \qquad (1)$$

with I^{oct} the absolute value of the current in the octupoles at the stability threshold, E the particles energy at flat top, I_{fact} the impedance factor found in the previous section

(depending on the collimator scenario chosen) and C a constant multiplicative factor which is determined from the knowledge at 4 TeV, i.e. the fact that the beams are stable for $I^{oct} = 250$ A (pessimistic value with a margin taken into account, see above) with $\varepsilon = 2.5\mu$m, $I_{fact} = 1$ and $N_b = 1.5 \cdot 10^{11}$ protons per bunch. Then one can easily obtain a line describing for each collimator scenario the stability limit in terms of intensity as a function of the emittance, taking the maximum possible octupole current (550 A) at 6.5 TeV. The corresponding lines are drawn in Fig. 9, where we have also put the points corresponding to the possible post-LS1 scenarios depending on the bunch spacing chosen (25 or 50 ns) and injection scheme, namely classical or "batch compression merging and splitting" (BCMS) scheme, the latter allowing lower transverse emittances [21]. The beam parameters for these four different options are summarized in Table 1. It appears that the only possible beam parameter scenario compatible with nominal settings is the 25 ns beam with the classical scheme. With tight settings one can stabilize both 25 ns scenarios, but for any of the 50 ns scheme, one would be able to stabilize the beam only with the relaxed settings (and in the case of the BCMS scheme we would still stand quite close to the limit).

It is worth noticing that many of the assumptions made here are on the pessimistic side. In particular, with the "old" (negative) octupole polarity and with Q' higher than 10, one could probably gain in stability, but this has not been tested yet. Furthermore, we have taken a safety margin with respect to 2012 measurements, assuming that 250 A stabilize the beam at flat top (this value has been increased with respect to the presentation made during the workshop where the value of 200 A was used instead, thus the slightly more pessimistic results given here). Finally, some additional Landau damping could be gained by using the triplet octupoles to provide extra amplitude detuning [22].

We should finally stress that the stability treated here concerns only separated beams; more critical limitations might arise in the squeezed beams situation [23] where many strong instabilities were observed in 2012 [24].

Table 1: Beam parameters scenarios for post-LS1 operation, as achievable by the injectors [21] (i.e. without taking into account limitations from the LHC). A tranverse emittance blow-up of 33% was assumed in the LHC.

	N_b (p+/bunch)	ε (μm)	Nb. bunches
25 ns, classical	$1.35 \cdot 10^{11}$	3.75	2760
25 ns, BCMS	$1.15 \cdot 10^{11}$	1.9	2520
50 ns, classical	$1.65 \cdot 10^{11}$	2.2	1380
50 ns, BCMS	$1.6 \cdot 10^{11}$	1.6	1260

CONCLUSION

At 4 TeV, total single-bunch tune shifts measurements show a discrepancy factor of ~ 2 at 4 TeV with respect to the impedance model, and single-beam stability occurs for

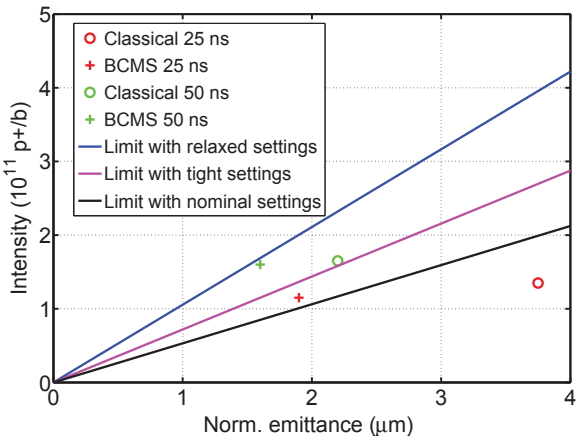

Figure 9: Intensity limit at 6.5 TeV with 550 A in the octupoles and high chromaticity, as a function of transverse normalized emittance. Beam parameters scenarios as achievable by the injectors have been indicated as well (see Ref. [21] and Table 1).

octupole currents of more than ± 250 A at high Q'. However, values above 7 for Q' were never much tested with the "old" negative polarity in the octupoles; going further in Q' could then reduce the octupole current needed.

Collimator settings scenarios at 6.5 TeV give an impedance between 0.75 and 1.5 times the 2012 4 TeV one. The bunch spacing and number of bunches have essentially no impact on the single-beam stability (when taking into account only the impedance) at high enough Q' and when the transverse damper is sufficiently strong.

Concerning beam stability in the post-LS1 era, assuming maximum octupole current (i.e. ± 550 A) we are close or above the limit for 50 ns beam parameters except with the relaxed collimator settings, and fine with 25 ns parameters except for the BCMS scheme with nominal collimator settings. Such limitations could be in principle relaxed by using additional octupolar non-linearities [22].

ACKNOWLEDGMENTS

The authors would like to thank the BI, OP and optics teams, E. Shaposhnikova and the RF team, as well as R.W. Assmann, A. Burov, M. Cauchy, D. Deboy, L. Lari, A. Marsili, G. Papotti, V. Previtali, E. Quaranta, G. Valentino and F. Zimmermann.

REFERENCES

[1] W. Höfle, G. Kotzian and D. Valuch, "Operation with ADT increased bandwidth", Presentation at the CERN LBOC meeting (30/10/2012).

[2] A. Burov, N. Mounet, "When HT Damper Drives Instability?", Presentation at the CERN ICE meeting (13/06/2012).

[3] A. Burov, N. Mounet, S. White and E. Métral, "Status of the Impedance-Damper Model and Preliminary Guidelines for

LHC Beam Operation", Presentation at the CERN LBOC meeting (14/08/2012).

[4] A. Burov and N. Mounet, "Nested HT Method: Impedance & Damper", Presentation at the CERN LBOC meeting (14/08/2012).

[5] A. Burov, "Nested Head Tail Vlasov Solver: Impedance, Damper, Radial Modes, Coupled Bunches, Beam-Beam and more...", Presentation at the CERN AP forum (04/12/2012).

[6] K. Satoh and Y. Chin, "Transverse Mode Coupling in a Bunched Beam", Nucl. Instr. Meth. 207, p. 309 (1983).

[7] N. Mounet, "The LHC Transverse Coupled-Bunch Instability", EPFL PhD Thesis (2012).

[8] G. Rumolo and F. Zimmermann, "Electron Cloud Simulations: Beam Instabilities and Wakefields", Phys. Rev. ST AB, 5, 121002 (2002).

[9] N. Mounet and E. Métral, "Effect of cavity impedance for operation at high current & low beam energy", Presentation at the 4th TLEP workshop (CERN, 05/04/2013).

[10] J. F. Esteban Müller et al, "Probing the LHC impedance with single bunches", CERN-ATS-Note-2013-001 MD (2013).

[11] B. Salvachua et al, "Results on nominal collimator settings MD at 4 TeV", CERN-ATS-Note-2012-092 MD (2012).

[12] N. Mounet, R. Bruce, X. Buffat, W. Herr, E. Métral, G. Rumolo and B. Salvant, "Impedance effects on beam stability", Proceedings of the 2011 Evian workshop on LHC beam operation, p. 143-155, CERN-ATS-2012-083 (2012).

[13] G. Arduini, "Summary of the observations on instabilities", Presentation at the CERN LMC (15/08/2012).

[14] E. Métral et al, "Octupole instability MD", Presentation at the CERN LSWG meeting (03/07/2012).

[15] N. Mounet, E. Métral, A. Burov, X. Buffat, B. Salvant and G. Papotti, "Single-beam instability MD", Presentation at the CERN LSWG meeting (26/10/2012).

[16] B. Salvachua et al, "LHC collimation cleaning and operation outlook", these proceedings (2013).

[17] J. Gareyte, J.P. Koutchouk and F. Ruggiero, "Landau Damping, Dynamic Aperture and Octupoles in LHC", CERN LHC Project Report 91 (revised) (1997).

[18] J. Scott Berg and F. Ruggiero, "Landau Damping with Two-Dimensional Betatron Tune Spread, CERN SL-AP-96-71 (1996).

[19] F. J. Sacherer, "Transverse Bunched Beam Instabilitites - Theory", 9th Int. Conf. on High-energy accelerators, Stanford, USA, p. 347 (1974).

[20] J. L. Laclare, "Bunched Beam Coherent Instabilities", CERN-87-03-V-1, p. 264 (1987).

[21] R. Steerenberg et al, "Post LS1 25 ns and 50 ns options from the injectors", these proceedings (2013).

[22] R. Tomás et al, "Optics and non-linear beam dynamics at 4 and 6.5 TeV", these proceedings (2013).

[23] T. Pieloni, X. Buffat, S. White, N. Mounet, W. Herr, E. Metral, G. Arduini and R. Bruce, "Beam Stability with Colliding Beams at 6.5 TeV: in the betatron squeeze and collisions", these proceedings (2013).

[24] E. Métral et al, "Review of the instabilities observed during the 2012 run and actions taken", these proceedings (2013).

STABILITY OF COLLIDING BEAMS AT 6.5 TeV

T. Pieloni, G. Arduini, R. Bruce, W. Herr, E. Metral, N. Mounet (CERN, Geneva),
X. Buffat (EPFL, Lausanne;CERN, Geneva), S. M. White (BNL, Brookhaven)

Abstract

In this paper we will try to propose some possible scenarios for operation of beams during the betatron squeeze, adjust and stable beam mode at 6.5 TeV energy for after the LS1. The available parameter space in term of intensity, chromaticity, octupole current, damper gain, bunch spacing and length will be explored and conclusions on possible settings for the operation will be based when possible on experience from the LHC physics runs. Different luminosity leveling scenarios will be considered. Techniques to mitigate instabilities when beam-beam effects are involved will also be discussed.

INTRODUCTION

The 2012 run of the Large Hadron Collider (LHC) has shown, despite the great physics discovery of a Higgs-like boson, several instabilities which have perturbed the accelerator performances. To achieve the required integrated luminosity several parameters had been changed and pushed compared to 2011: reduced β^*, from 1 m to 0.6 m, and higher brightness beams (approximately two times larger than nominal). To ensure protection of the triplets collimator gaps have been reduced to tight settings corresponding to apertures close the nominal 7 TeV configuration, leading to larger impedances [1]. A first type of instabilities occurred during stable beams after many hours of physics and affected specific bunches colliding only in the LHCb experiment. A second type was developing at the end of the betatron squeeze (after 3 m β^*) and while bringing the beams into collision as described in [2]. The origin of these instabilities is still not fully understood however some observations have led to considerations on the beam stability to help defining LHC possible future scenarios.

INSTABILITIES

The main beam parameters, compared to those of 2010 and 2011, are summarized in Tab. 1.

Parameter	2010	2011	2012	Nominal
$N_p[10^{11}$ p/b]	1.2	1.45	1.58	1.15
N_b	368	1380	1380	2808
Spacing [ns]	150	75/50	50	25
ϵ [μ m rad]	2.4-4	1.9-2.4	2.2-2.5	3.75
β^* (IP1/5) [m]	3.5	1.5-1	0.6	0.55
L [10^{32} cm$^2 s^{-1}$]	2	35	76	100

Table 1: LHC Operational Parameters

The LHC beams were accelerated in 2012 from injection energy (450 GeV) to a top energy of 4 TeV. The β^*s at the different Interaction Points (IPs) were then lowered (from 10 m to 3 m in IP2 and IP8 and from 11 m to 0.6 m in IP1 and IP5). This process, known as β squeeze, lasted around 15 min. At the beginning of the year at a β^* value of $\approx$ 1.5 m during the execution of the β squeeze several bunches were becoming unstable, losing their intensity in a non reproducible manner. In particular the instability was observed only during a subset of the physics fills. The bunches have become unstable one after the other for several minutes till the head-on collision was established. In some cases, the instabilities generated losses high enough to cause a beam dump. An important parameter for stability is chromaticity which might explain the non reproducibility of the instability when operating with small positive value (LHC was operating at Q' $\approx$ 2 units till the beginning of August 2012). At the beginning of August 2012 the machine configuration has been changed drastically in terms of chromaticity (changed from 2 units to 15 units [2, 6]), the polarity of the Landau octupoles (changed from negative to positive [9]) and the transverse damper (from 100 to 50 turns). The changes have been implemented within a few fills since fill number 2926, making difficult the analysis of the implications of the different parameters. As a result of these changes the instability has significantly changed. It became extremely reproducible, occurring after two minutes before the end of the squeeze and in the vertical plane only. Many bunches were affected by the instability, causing reduced intensity drops, as opposed to large losses on few bunches in the previous configuration. Two examples of the bunch by bunch intensity losses versus time during this type of instability is shown in Fig. 1.

The coherent mode is shown in Fig. 2 where several frequencies are visible all spaced by $Q_s \approx 0.002$, the synchrotron tune. Several bunches were loosing up to half their intensity while coherently oscillating. Bunches where going unstable at different moments and the instability could last till the head-on collision was established and coherent motion stopped.

The stability of the beams before going through the β squeeze and during the squeeze is given by the Landau octupoles which ensure a given stability diagram, defining a limit under which all impedance driven modes should be stabilized. In the LHC the stability diagram at the beginning of the betatron squeeze are illustrated in Fig. 3 (dashed lines) for both octupoles polarities. In red we show the stability diagram with negative octupole polarity and in blue the positive polarity effect. The negative polarity was preferred before the squeeze since it provides larger area for

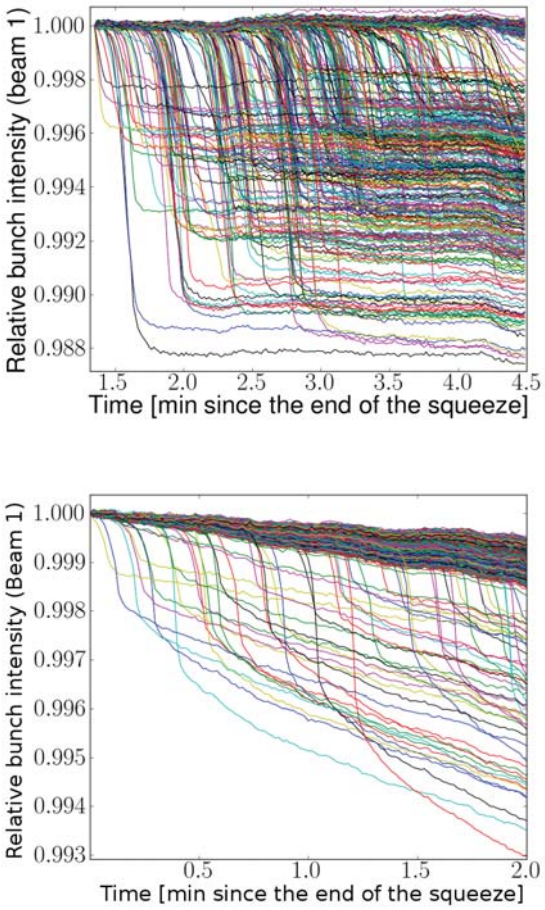

Figure 1: Bunch by bunch losses in beam 1 during an end of squeeze instability as a function of time for Fill 2648 with negative octupole polarity (top picture) and Fill 3250 with positive polarity(bottom plot).

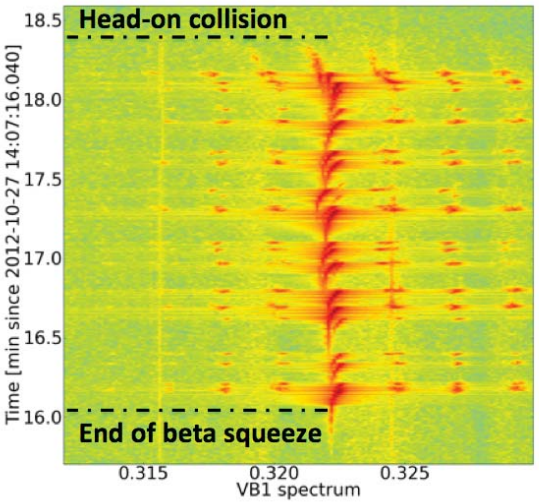

Figure 2: Beam 1 vertical frequency spectrum as a function of time during an end of squeeze instability.

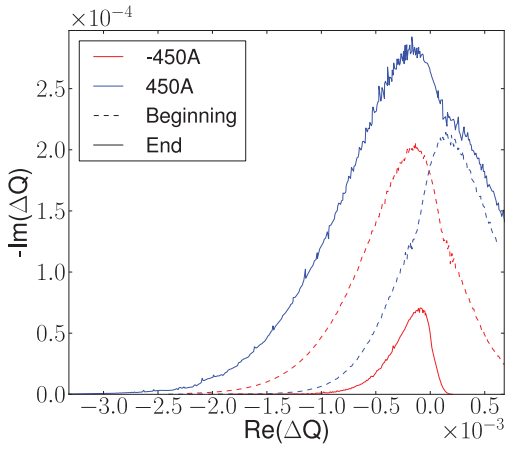

Figure 3: Beam stability diagrams for the two LHC octupole configurations: positive (blue lines) and negative (red lines) before the betatron squeeze (dashed lines) and at the end with long-range contribution (solid lines).

the expected modes, having negative real tune shift [10]. However, the long-range interactions also contribute to the non-linearities and affect the stability diagram at the end of the β squeeze (solid lines in Fig. 3). For the case of negative polarity they reduce the stability area while for the positive polarity they increase it. This was the motivation for inverting the polarity of the Landau octupoles [9] but the instabilities observed at the end of the squeeze is still present in the new configuration, despite the larger stability diagram at the end of the squeeze, increased damper gain and larger positive chromaticity, and remains unexplained.

COLLIDE AND SQUEEZE

Observations of the LHC 2012 instability have also demonstrated the head-on collision to be very efficient to stabilize the beams. Indeed, the tune spread due to a head-on collision is much larger than the one due to octupoles or beam-beam long range interactions or any other non-linearity present in the LHC. Moreover, the detuning is more important on the core particles of the beam rather than the tails, which significantly enhances its contribution to the stability diagram, as shown by Fig. 4. An observation of this effect is shown on Fig. 2 where the coherent oscillations is visible all along the end of the betatron squeeze and disappears when the beams are brought into collision. It would be therefore profitable to have the beams colliding during (part of) the squeeze in order to avoid instabilities, details on this possibility are discussed in [5].

GOING INTO COLLISION

The end of squeeze instability, as shown in Fig. 2, was lasting also during the collision beam process. At the be-

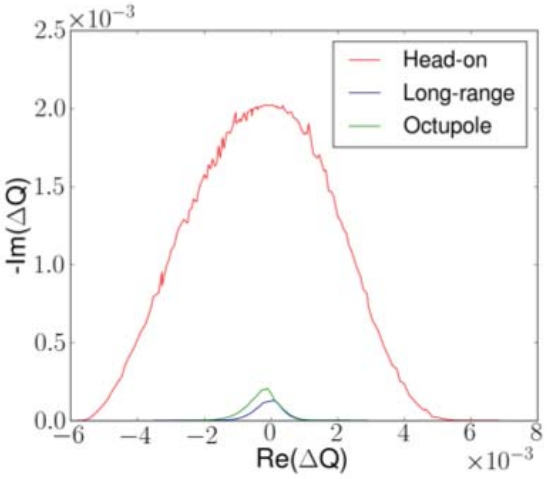

Figure 4: Beam stability diagrams provided by one head-on collision compared to octupoles and long-range.

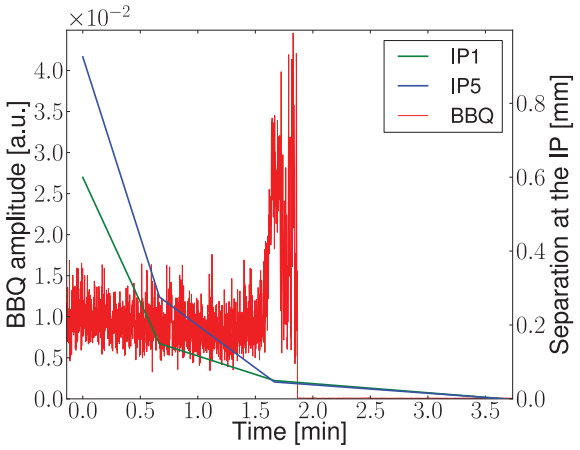

Figure 5: Oscillation amplitude of beam1 during the collapse of the separation bumps as a function of time.

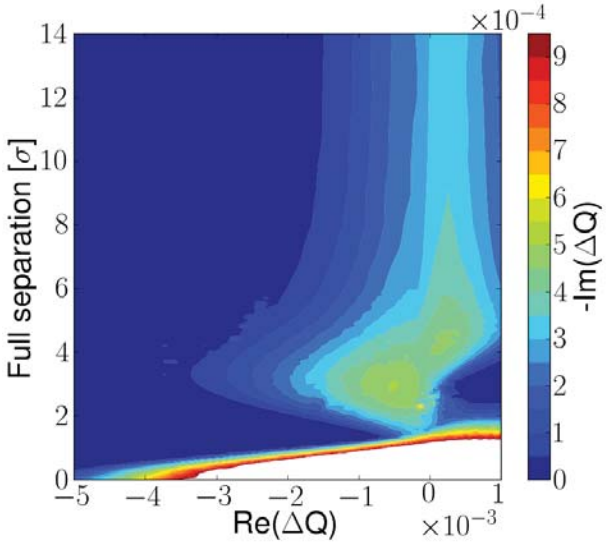

Figure 6: Evolution of the stability diagram in the horizontal plane during separation collapse in both IP1 and IP5 synchronously. In other words, the color indicates the maximum imaginary tune shift that can be stabilized for a given real tune shift and separation.

ginning of the year the process was long ($\approx$ 200 s) and was not directly going for head-on collisions in IP1 and IP5 but was slowed down to allow the tilting of IP8 crossing angle and only at the end optimized for luminosity. Several instabilities were observed while IP1 and IP5 were staying almost steady at an intermediate separation. In Fig. 5 we show the beam amplitude of oscillation and IP1 and IP5 separation reduction as a function of time. The beams are not yet in head-on collision and an exponential growth of the oscillation amplitude can be observed, causing a dump which occurred for a separation of $\approx 1-2\,\sigma$. These instabilities may be explained by the variation of the stability diagram as a function of the beams separation, as shown on Fig. 6. Indeed, there exists a minimum of stability around $1-2\sigma$ separation. A significant amount of time was spent at such separations, leaving the time for an instability to develop.

Over the year a change of the collision beam process has been proposed and implemented in the second half of the run. The purpose of the new process is to speed up the collapse of the separation bumps and to go straight to head-on collision in IP1 and IP5 to ensure stability.

However to guarantee a stronger stability several configurations have been tested with simulations and have shown that a synchronous collapse of both horizontal and vertical plane separation will lead to a minimum (magenta dots) of stability in both planes at the same time, as shown in Fig. 7 upper plot, where we show the beam footprint for different beam separations equal in both planes. The lower plot shows how one can avoid to have this minimum simultaneously in both planes by collapsing one plane at the time. The stability for this second configuration has been studied for both cases and results from multi-particle tracking simulations are shown in Fig. 8. The figure shows the amplitude of oscillation as a function of time for the different separations in either both planes at the same time (upper plot) or only the horizontal plane (lower plot). One can see that when only one plane goes through the stability minimum the other plane helps in the damping making this option more robust compared to the one going both planes together (or as for the LHC both IP1 and IP5 together) where for a defined separation of $\approx$ 1.5 σ separation in both planes the system in not stable.

LUMINOSITY LEVELING

In Fig. 9 the different luminosities as a function of the β^* at IP1 and IP5 are shown for the four beam configurations of Tab. 2. As is visible a possible 50 ns operation of

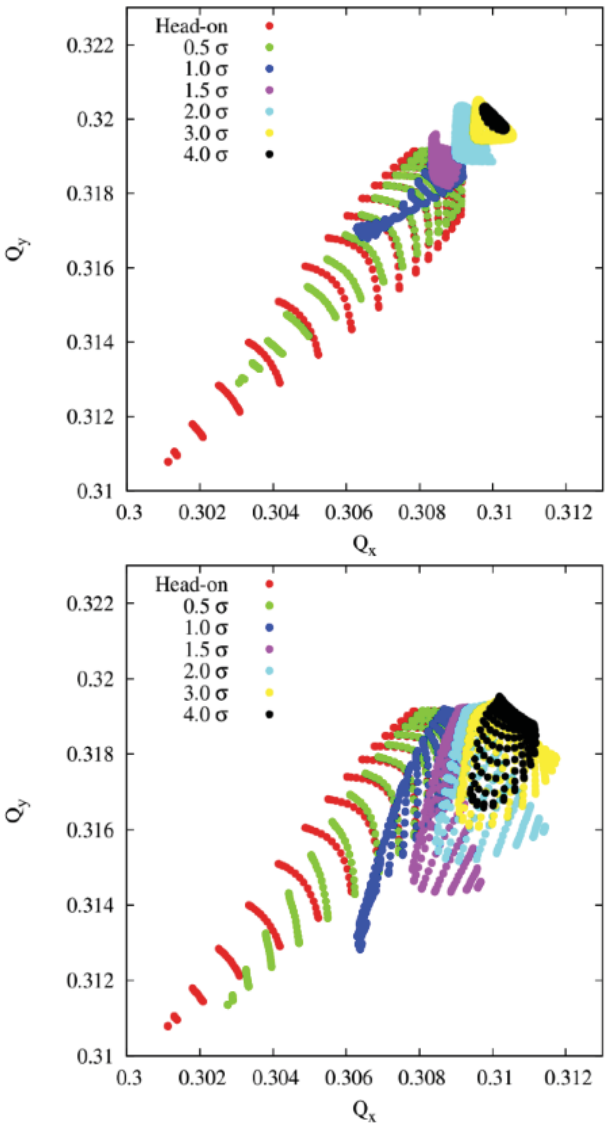

Figure 7: Footprint evolution during separation collapse in both planes synchronously (upper figure) and only in the horizontal plane (lower figure).

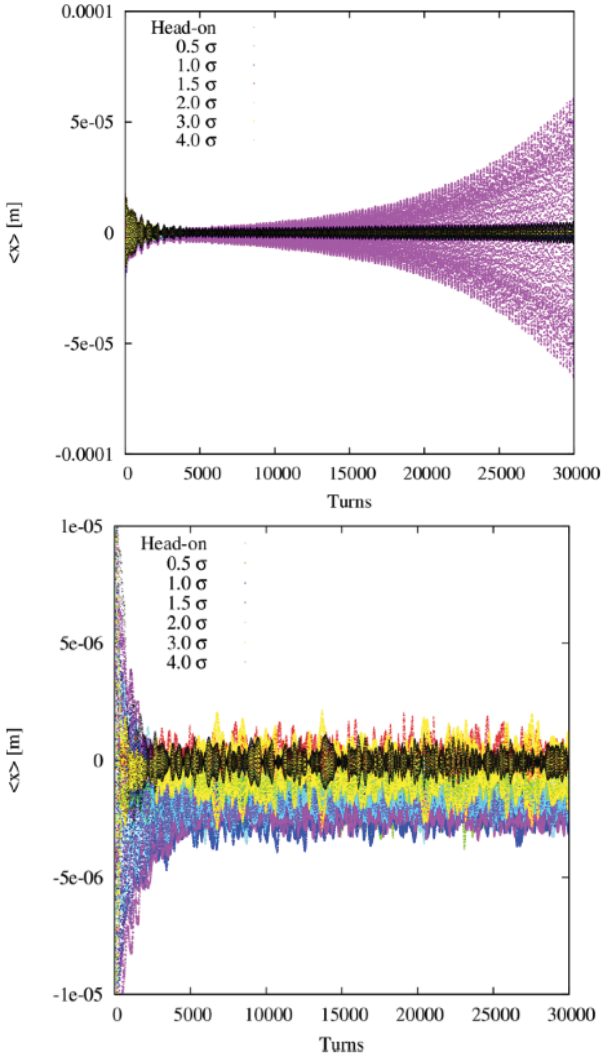

Figure 8: Beam oscillation amplitude as a function of time for different separations at the interaction point, the separation being either in both horizontal and vertical plane (upper figure) or in the horizontal plane only (lower figure).

Beam spacing	LHC emittance (SPS)	Intensity
25 [ns]	1.9 (1.4) [μm·rad]	1.15 10^{11} [p/b]
25 [ns]	3.75 (2.8) [μm·rad]	1.15 10^{11} [p/b]
50 [ns]	1.6 (1.2) [μm·rad]	1.6 10^{11} [p/b]
50 [ns]	2.3 (1.7) [μm·rad]	1.6 10^{11} [p/b]

Table 2: Possible LHC Operational Parameters after LS1.

the LHC will rely strongly on luminosity leveling since the pick luminosity is much larger than what the experiments can process. Therefore robust leveling techniques should be explored. Leveling with a transverse offset is operationally robust and flexible and has the advantage of lowering the maximum beam-beam tune shift, in case of problems due to head-on beam-beam. However, this technique may lead to instabilities during the leveling procedure due to a reduction of stability diagram, similarly to instabilities during the collapse of the separation. In this case, however, the procedure cannot be sped up. This type of instability was already observed in 2012 due to luminosity leveling with a transverse offset in IP8. Indeed, the LHC configuration included few bunches without head-on collision in IP1 and IP5, the stability diagram of these bunches was significantly reduced during the leveling procedure, leading to instabilities during luminosity production. This has enforced the usage of strong octupoles and the transverse feedback during luminosity production. There is great interest in avoiding the usage of such techniques in future scenarios since they have shown detrimental effects on the luminosity lifetime. Ensuring at least one head-on collision for every bunch would allow to reduce the need for other stabilizing technique and therefore improve the luminosity lifetime.

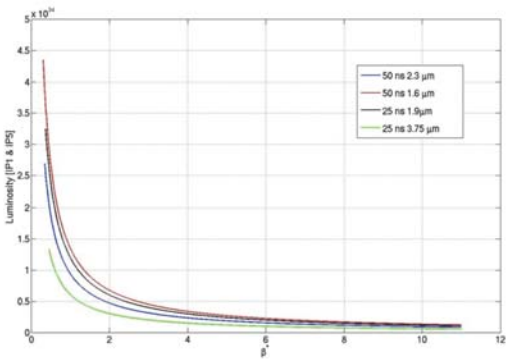

Figure 9: Luminosity as a function of β^* for the four beam parameters of Tab.2. Luminosity of calculated for IP1 and IP5 only.

TRANSVERSE DAMPER

During 2012 operation, the transverse feedback, the Landau octupoles and the chromaticity have been set to high values to ensure the beams stability. However a deep study of the different contributions is fundamental in the first commissioning period of the LHC in 2015 since few observations have shown they could act differently and that the machine luminosity can be deteriorated by using them operationally at maximum strength.

A test has been performed on single bunches separated in steps with constant chromaticity and octupoles set to their maximum strength. An instability appeared for specific separations where the stability diagram is minimum and was always cured with the transverse feedback while the octupoles were insufficient [8]. This suggests to keep the transverse feedback on when the beams are not colliding and demonstrates that it is not needed when beams are colliding head-on. Further tests are needed to identify the effect of chromaticity, set for this case to 5 units, and of different values/polarities of the octupole current.

On Fig. 10 we show the amplitude of oscillation of beam 1 in the horizontal plane as a function of time during consecutive Van deer Meer scans followed by a test during which the transverse damper gain was halved and finally turned off. After a transition period the oscillation amplitudes of the beams stayed constant. The spikes are due to few bunches not colliding which developed an instability while the rest of the beam was stable. With this observation we can state that the transverse damper is not needed if all bunches collide head-on. It is however fundamental for separated beams instabilities also without long-range beam-beam interactions.

Another important point is the feedback bandwidth which was increased in the second half of the 2012. While before collisions no detrimental effects have been visible, in collision, it is evident that the high bandwidth can be detrimental to the beams. An end of fill test has been performed where the transverse feedback at high bandwidth was turned on while the beams were colliding, the measured luminosity is shown on Fig. 11. The transverse feedback was set to high bandwidth at time 11:00 and a significant deterioration of luminosity lifetime is visible, suggesting to avoid this set-up for operation.

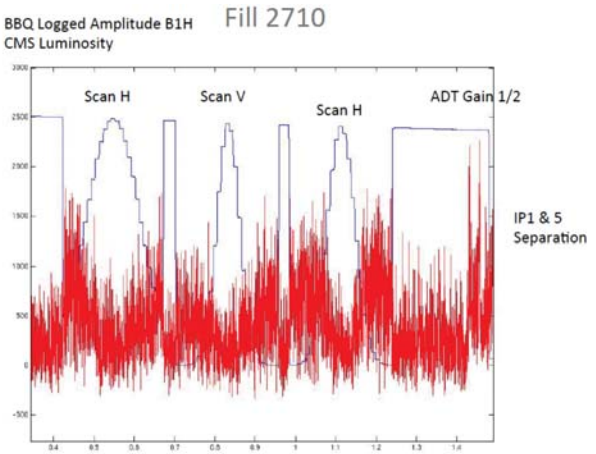

Figure 10: CMS luminosity (blue line) and BBQ logged amplitude of oscillation of beam1 horizontal plane as a function of time. The first part shows the oscillation amplitude during a Van deer Meer scans. During the second part the beams are colliding head-on, the transverse damper gain was reduced then turned off. Only non-colliding bunches start to oscillate coherently leading to an instability (high amplitude peaks at t = 1.45) the rest of the beams were stable.

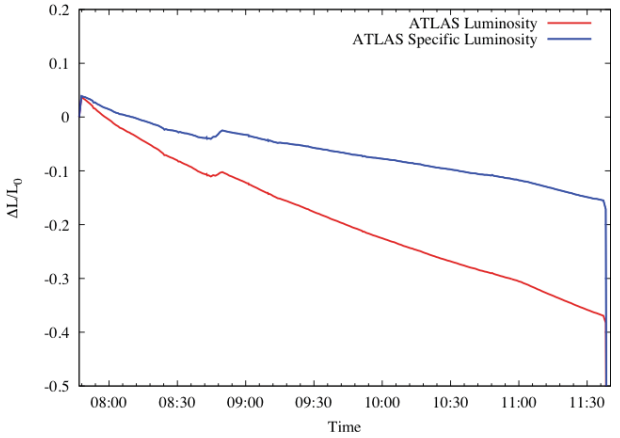

Figure 11: Atlas luminosity as a function of time while the transverse feedback was changed (at time 11:00) to high bandwidth. A deterioration of luminosity lifetime is visible and directly related to the change of bandwidth.

Moreover the lifetime deterioration is directly related to the number of beam-beam parasitic encounters as shown in Fig. 12 where the bunch by bunch deterioration of luminosity lifetime is evaluated and compared to the number of long-range encounters. It is visible that the deterioration is more important for bunches with larger number of long-range interactions suggesting an interplay between the

transverse damper and the beam-beam interactions which has to be studied in details.

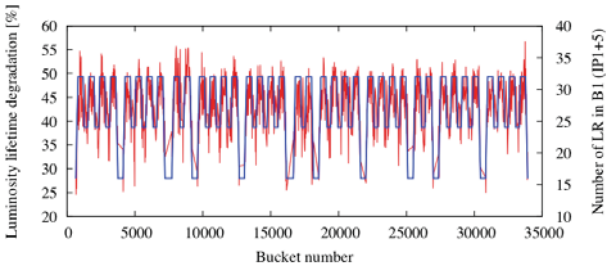

Figure 12: Bunch by bunch luminosity lifetime degradation and number of long range parasitic encounters as a function of the bunch RF bucket. The plots shows a clear dependency of the lifetime degradation with the number of parasitic encounters.

OCTUPOLES AND CHROMATICITY

In 2012, the time allocated for systematic studies on the effect of the octupoles, as well as on the effect of chromaticity was not sufficient to conclude on possible settings for 2015. An initial period of commissioning should be devoted to study the parameter space in order to properly assess potential stability issues during the run. Nevertheless, the observations described here and in [2] brings us to two possible scenarios.

The first possibility is going back to settings similar to the initial setting of 2012 where no sign of instability where observed during several fills. This configuration rely on a small positive chromaticity, around 2 units. While more stable than at high chromaticity, the stability strongly depends on the chromaticity variations [6]. Therefore a good control of this parameter is required in order to operate in this configuration. The octupole current should be minimized, not only for lifetime optimization, but also because the feed down effect leads to a strong dependency of the chromaticity on the orbit, which should be avoided to minimize chromaticity variations. The choice of the polarity results from a compromise between the stability before and after the squeeze. A lower current is required before the squeeze with the negative polarity. This option is therefore preferred, in case the stability at the end of the squeeze can be insured by colliding during the squeeze.
It is important to note that variations of the chromaticity also occur due to beam-beam interactions, as explained in [12], the variation of chromaticity along the bunch trains should be taken into account.

A second possibility, preferable in case chromaticity variations cannot be avoided, would essentially rely on a high positive values of the chromaticity, similarly to the end of the 2012 run. In this configuration the machine should be less sensitive to chromaticity variations. However, no cure for the instabilities at the end of the squeeze have been found in this configuration, at the end of 2012 run. Indeed, the end of squeeze instability was visible during all fills. The stability at the end of the squeeze will, therefore, strongly rely on colliding during the squeeze.

High chromaticity, octupole current and damper gain have potential detrimental effect on the beam and luminosity lifetime, there is therefore a great interest in finding an optimized parameter set, for which experimental time should be devoted.

CROSSING ANGLES AND LONG-RANGE BEAM-BEAM

Crossing angles in the high luminosity experiments (IP1 and IP5) are defined by setting the beam to beam separation at the first long-range beam-beam encounter equal to 10σ for the 50 ns bunch spacing and 12σ for the 25 ns, according to the following equation :

$$d_{sep} = \frac{\sqrt{\beta^*} \cdot \sqrt{\gamma}}{\sqrt{\epsilon_n}} \cdot \alpha. \quad (1)$$

The beam-beam separation is particularly sensitive to the beam emittance, any deterioration of transverse emittance (i.e. electron cloud, transverse emittances) will reduce the separation and might lead to higher losses due to several parasitic encounters at too small separation. In particular, one should remember that the separation at the first encounter is not the minimum separation the beams encounter. The separation is reduced at some encounters also by 1.5-2.0 σ. In these considerations however intensity effects are not considered, higher intensities will require larger separations at the parasitic encounters. The 2012 operation has shown that setting the separation at 10 sigma was leaving enough margin for the intensity range covered (allowing higher intensities available from the injectors without recommissioning the crossing angle). From studies of long-range interactions we have found a deterioration of 1.0-1.5σ in the on-set of losses when moving from 1.15 to 1.6 10^{11} protons per bunch [7]. Also, the separation required depends on the beams intensity. For these reasons, some margin should be kept in the initial configuration, in order to avoid delays during operation caused by the re-commissioning of procedures with new parameters.

In Tab. 2 one has the corresponding crossing angles per corresponding β^* for the four scenarios as calculated in [1].

For the low luminosity experiments (IP2 and IP8) the effect of parasitic encounters should be kept in the shadow of the high luminosity experiments. Therefore a larger separation at the long range encounters is required. These two IPs do not have passive compensation of the tune shifts and chromaticity leading to enhanced pacman effect. In particular, the difference between bunch families, in particular in term of tune and chromaticity, may become significant rendering difficult the optimization of the machine. For these two IPs we therefore suggest separations larger than 12-14 σ in all cases.

Beam [ns],[μm]	β^*_{cross} [cm]	β^*_{sep} [cm]	$\beta^*_{sep,2}$ [cm]	$\alpha/2$ [μrad]
25, 1.9	35	33	30	150
25, 3.75	31	33	30	127
50, 1.6	46	33	30	205
50, 2.3	37	33	30	163

Table 3: LHC Operational Parameters for after LS1 [1]. β^*_{cross} and β^*_{sep} are the β^*s in the crossing and separation plane respectively, during the standard squeeze. The $\beta^*_{sep,2}$ is the β^* reach in the separation plane with collide and squeeze.

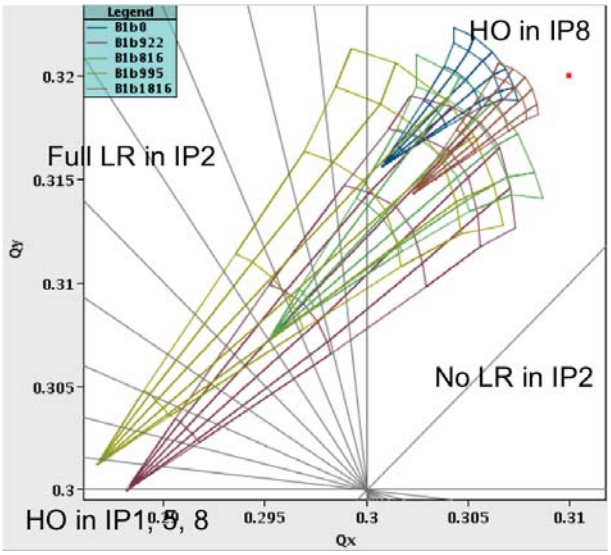

Figure 13: Footprints for extreme packman families to illustrate the separations in tune among the different bunches. The different tune shifts are due to IP8 and IP2 long ranges since for IP1 and IP5 a passive compensations cancels this effects on tunes and chromaticity.

An example of the 2012 configuration is visible in Fig. 13 where the effect of IP2 and IP8 long ranges are visible showing a larger occupancy of the tune area. Over the 2012 year moreover evidence of selective losses on bunches with long range interactions in IP2 were visible and presented in [11].

CONCLUSION

There are many unknowns concerning the instabilities observed during the 2012 run of the LHC. Models including the machine impedance, the transverse damper, Landau octupoles and beam-beam interactions are being developed to allow a better understanding of the observations. Nevertheless, some time should be dedicated for the testing of these models with beams after LS1. In particular, most stabilizing technique have shown detrimental effects on the beam, therefore finding a set of optimized parameters might be necessary to keep the luminosity lifetime under control.
The beams stability greatly depends on the chromaticity, a good control of this parameter will be required in any event. Head-on collision have shown to be an efficient damping mechanism. The stability may therefore be ensured by bringing the beams into collision during the squeeze, while ensuring at least one head-on collision for each bunch. In such configuration, the needs for other stabilizing techniques is drastically reduced.
Luminosity leveling in both the low and high luminosity experiments rises important beam stability issues that should be addressed in the early stage of the LS1 in order to find operational procedures that meet the experiments desiderata.

REFERENCES

[1] B. Salvachua, et al., "Cleaning Performance of the LHC Collimation System up to 4TeV," these proceedings.

[2] E. Métral, et al., "Review of the Instabilities Observed during the 2012 run and actions taken," these proceedings.

[3] N. Mounet, et al., "Stability of non colliding beams at 6.5 TeV," these proceedings.

[4] P.E. Faugeras, et al., "Proposal to upgrade the luminosity of the sp$\bar{p}$s collider by a factor 2," CERN SPS/89-18 (DI).

[5] X. Buffat, et al., "Squeezing with colliding beams," these proceedings.

[6] A. Burov, "Nested Head Tail Vlasov Solver," CERN AB Forum, Dec 2012.

[7] W. Herr, et al, "Results of long-range beam-beam studies - scaling with beam separation and intensity," CERN-ATS-Note-2012-070 MD.

[8] X. Buffat, et al, "Stability of beams colliding with a transverse offset," CERN-ATS-Note-2013-016 MD.

[9] S. Fartoukh, "On the sign of the LHC Octupoles," LHC Machine committee, 11th July 2012, Geneva.

[10] J. Gareyte, et al, "Landau damping, dynamic aperture and octupoles in the LHC," CERN LHC-Project-report-91 (revised), 1997.

[11] X. Buffat, W. Herr and T. Pieloni, "Beam-beam effects and the observed instability," LHC Machine committee, 16th May 2012, Geneva.

[12] W. Herr, "Features and implications of different LHC crossing schemes," LHC Project Report 628

BEAM INDUCED RF HEATING

B. Salvant, O. Aberle, G. Arduini, R. Assmann, V. Baglin, M. J. Barnes, W. Bartmann, P. Baudrenghien, O. Berrig, C. Bracco, E. Bravin, G. Bregliozzi, R. Bruce, A. Bertarelli, F. Carra, G. Cattenoz, F. Caspers, S. Claudet, H. Day, M. Garlasche, L. Gentini, B. Goddard, A. Grudiev, B. Henrist, R. Jones, O. Kononenko, G. Lanza, L. Lari, T. Mastoridis, V. Mertens, E. Métral, N. Mounet, J. E. Muller, A. A. Nosych, J. L. Nougaret, S. Persichelli, A. M. Piguiet, S. Redaelli, F. Roncarolo, G. Rumolo, B. Salvachua, M. Sapinski, R. Schmidt, E. Shaposhnikova, L. Tavian, M. Timmins, J. Uythoven, A. Vidal, J. Wenninger, D. Wollmann, M. Zerlauth (CERN, Geneva, Switzerland), P. Fassnacht, S. Jakobsen (ATLAS-ALFA), M. Deile (TOTEM).

Abstract

After the 2011 run, actions were put in place during the 2011/2012 winter stop to limit beam induced radio frequency (RF) heating of LHC components. However, some components could not be changed during this short stop and continued to represent a limitation throughout 2012. In addition, the stored beam intensity increased in 2012 and the temperature of certain components became critical.

In this contribution, the beam induced heating limitations for 2012 and the expected beam induced heating limitations for the restart after the Long Shutdown 1 (LS1) will be compiled. The expected consequences of running with 25 ns or 50 ns bunch spacing will be detailed, as well as the consequences of running with shorter bunch length.

Finally, actions on hardware or beam parameters to monitor and mitigate the impact of beam induced heating to LHC operation after LS1 will be discussed.

INTRODUCTION

The quest for higher LHC luminosity required a significant increase of the proton beam brightness in 2011[1] and 2012 [2]. In particular, both number of bunches and bunch intensity were pushed to the limits of what was available from the injectors. Increasing these intensities is known to increase beam induced heating and in 2011 indeed, several beam induced heating problems were encountered in the LHC [3, 4, 5] and are summarized in Table 1. Temperature increase in LHC devices can cause several issues (damage, delays or dumps).

This contribution deals with heating caused by the RF fields generated by the beam interacting with the longitudinal beam coupling impedance of its surrounding equipment, and is a follow-up of several reviews performed since June 2011 when heating issues started to become visible [3-10].

The equations for this beam induced RF heating have been covered in particular in [4, 5, 11]. We recall here for reference the power P_{loss} lost by a beam composed of M equispaced equipopulated bunches of N_b protons travelling in the aperture of an LHC equipment of longitudinal impedance Z_{long} is [6]:

$$P_{loss} = 2(eMN_b f_{rev})^2 \left(\sum_{p=1}^{\infty} \mathrm{Re}\left[Z_{long}(2\pi pMf_{rev})\right] \times Powerspectrum(2\pi pMf_{rev}) \right)$$

where e is the proton charge, f_{rev} is the revolution frequency, and *Powerspectrum(f)* is the power spectrum of the bunch as a function of frequency.

Table 1: Summary of LHC equipment heating in 2011 and prospects for 2012 before the run*.

equipment	Problem	2011	Expected 2012
VMTSA	Damage		replaced
TDI	Damage		
MKI	Delay		
TCP_B6L7_B1	Few dumps		
TCTVB	Few dumps		2 TCTVBs removed
Beam screen Q6R5	Regulation at the limit		
ALFA	Risk of damage		
BSRT	Deformation suspected		

* The colour code indicates the need for follow up of the considered heating problem on LHC operation after the 2011 run and what was expected for 2012. During the winter shutdown 2011-2012, 2 TCTVBs (out of 4) were taken out of the machine (including TCTVB.4R2, which was heating the most), and the VMTSA double bellow module was reinforced [10]. Black means damaged equipment; red means detrimental impact on operation (dump or delay or reduction of luminosity); yellow indicates need for follow up; green means solved.

After the first LHC power spectrum measurements at the end of 2011 [12], the beam spectra measurements became much more systematic in the second half of 2012.

In the following chapter, the observations of beam induced heating on equipment during the 2012 run are gathered.

OBSERVATIONS AND LIMITATIONS DURING THE 2012 RUN

Example of heating during physics fills

The example of temperature increase on kickers, collimators and ALFA detector for 4 fills in mid-November 2012 is shown in Fig. 1.

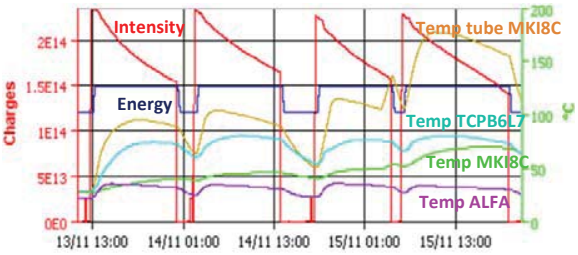

Fig.1: extraction from the logging database for the beam intensity (red) and energy (dark blue), along with the temperature of a "tube" probe of the injection kicker MKI-8C (orange), the temperature of the skew primary collimator TCP.B6L7.B1 (light blue), the temperature of a "magnet" probe of the injection kicker MKI-8C (green) and the temperature of one probe of the ALFA detector (purple).

Summary of observations in 2012

The suspected beam induced heating limitations reported by/to the impedance team in 2012 have been gathered in Table 2, and compared to the situation in 2011.

Table 2: Summary of LHC equipment heating during the 2012 run and comparison with what was expected before the run[†].

equipment	Problem	Expected 2012	What happened in 2012
VMTSA	Damage		replaced
TDI	Damage		Still problems even in parking position
MKI	Delay		MKI8D (MKI8C after TS3)
TCP.B6L7.B1	Few dumps		Interlock increased
TCTVB	Few dumps		Interlock increased
Beam screen Q6R5	Regulation at the limit		Disappeared since TS3. Correlation with TOTEM?
ALFA	Risk of damage		Due to Intensity increase
BSRT	Deformation suspected		damage

The following paragraphs will review the studies on these LHC elements in more detail.

VMTSA double bellow

At the end of the 2011 run, 8 bellows (out of 20) were found damaged.

Following studies by TE/VSC, the LRFF working group was mandated to understand the issues with LHC RF fingers. Concerning the VMTSA, the LRFF working group concluded that:

- simulations and measurements showed that there is no problem if good contact is ensured;
- consolidation of the design is needed to avoid bad contacts;
- 8 modules should be reinstalled with new shorter RF fingers, ferrite plates and reinforcement corset (see Fig. 2)

No problem of heating was observed since then (both on vacuum gauges and temperature).

The plans for LS1 are to remove all these modules and identify other modules that could fail.

[†] The colour code indicates the impact on operation of the considered heating problem on LHC operation after the 2011 and during the 2012 runs. Black means damaged equipment; red means detrimental impact on operation (dump or delay or reduction of luminosity); yellow indicates need for follow up; green means solved.

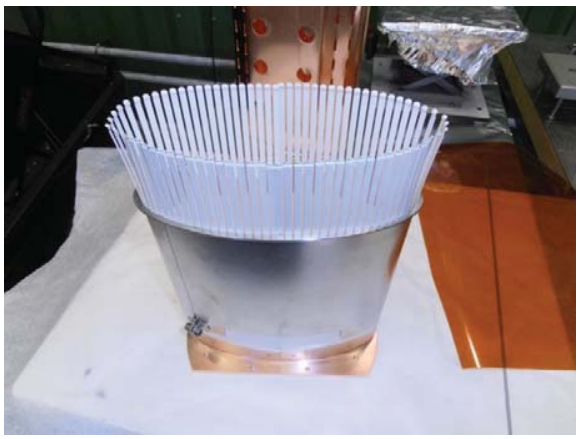

Fig.2: picture of the new shorter fingers inside the reinforcement corset (courtesy B. Henrist, TE/VSC).

TDI injection protection collimator

Abnormal deformation of the two TDI beam screens was found during the winter shutdown 2011-2012 [13]. Temperature, vacuum, and jaw deformation during the run suggested significant heating as the TDIs were not retracted to parking position. Electromagnetic simulations confirmed that the heating can be significant. It is however not completely clear that beam induced heating alone generated the damage. Both TDIs were left in that state as there was no time to prepare a new design and a reinforced spare was prepared by EN/STI.

During the 2012 run, suspicious pressure curves could indicate that additional heating occured in or close to the TDI4L2 since mid-2012 (see Fig. 3). Many mechanical issues occurred on both TDIs towards the end of the 2012 run [14], and RF heating in 2012 could potentially have made things worse.

Current plans for LS1 include reinforcing the beam screen but it is not clear if it will be enough in view of the recent problems: in particular it will not decrease the heating to the jaw.‡

‡ After the workshop, the feasibility to add a thin copper coating is now being studied to limit RF heating to the jaw, as proposed already proposed in [5].

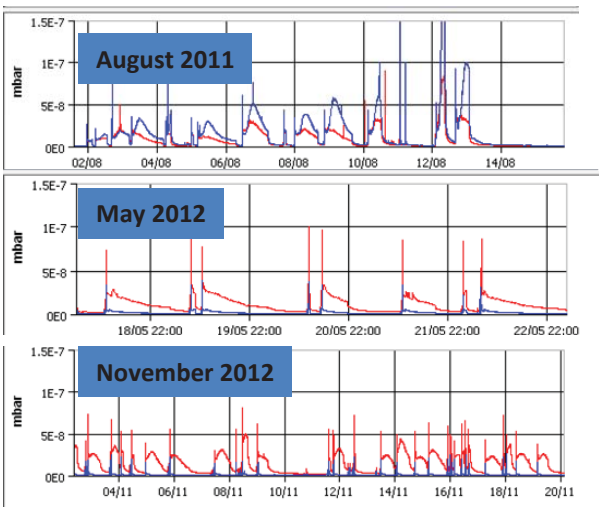

Fig. 3: pressure at TDI.4L2 (red) and TDI.4R8 (blue) in August 2011 (top), May 2012 (center), and November 2012. Even though the jaw was retracted to parking position throughout 2012, signs of beam induced heating became visible again in November 2012 on TDI.4L2.

MKI injection kickers

Some MKIs have delayed injection after a dump by up to a few hours. Electromagnetic simulations and measurements as well as thermal simulations are consistent with observations (despite the very high complexity of the device). Extensive studies have been performed within the MKI strategy meetings [15] to:

- reduce the electric field on screen conductors,
- reduce the longitudinal impedance,
- improve heat radiation from the ferrite by increasing the tank emissivity.

Selected bake-out jackets were removed and indeed reduced the measured magnet temperature by resp. 3°C to 7°C on resp. MKI8B and MKI8D: these reductions correspond to ~15% of the measured temperature rise above ambient. However it is preferred, in the future, to keep the bake-out jackets on the tanks [15].

Before the technical stop 3 (TS3) at the end of September 2012, the most critical kicker was MKI8D. Bench measurements and simulations had predicted that a new MKI design - with 19 screen conductors - would better screen the ferrite from the beam than the current MKI design – with only 15 screen conductors [16] (see Fig. 4), and would hence significantly reduce the beam induced heating. During TS3, this MKI8D kicker was replaced by a spare with 19 conductors and a clear improvement was observed for this kicker (see Fig. 5).

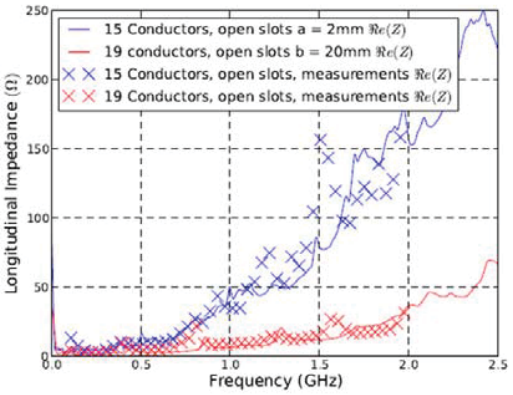

Fig. 4: Comparison between 3D electromagnetic simulations (full lines) and bench measurements (crosses) of the real longitudinal impedance of MKI kickers as a function of frequency with 15 conductors (in blue) and with 19 screen conductors (in red) [15, 16].

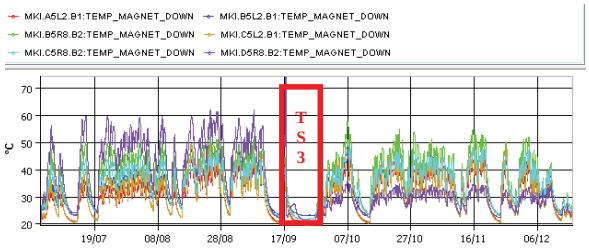

Fig. 5: Temperatures measured by the "magnet" PT100 probes of MKI kickers, before and after TS3. During TS3, magnet MKI8D (in purple)), which had 15 screen conductors prior to TS3, was replaced with a new design with 19 screen conductors, and it is observed that it moved from the hottest magnets to the coolest thanks to this change, which is very promising for the upgrade of all MKIs during LS1.

However, after this same TS3, it was realized that kicker MKI8C became limiting, and it was traced to a large temperature on the probe placed on the tube, which measures the temperature of ferrite toroids outside of the magnet yoke (up to 190°C). Analysis of kicker rise time and delay shows that the kicker performance is not affected by the increase of temperature on the probes [15]. A plausible hypothesis is that the additional source of heating is not the magnet ferrites but lies next to the "tube Up" probe. In this case the temperature increase should not directly affect the kicker performance and the interlock level for that magnet was increased accordingly.

Plans for LS1 are followed up closely by the MKI strategy meetings. All MKIs are planned to be upgraded in order to:

- Reduce the longitudinal impedance by improving the screening of the ferrite from the beam:
  - Reduce the high electric field of the screen conductors (tests are planned early January to confirm promising results from simulations) to permit more screen conductors to be installed,
  - Aim at full complement of 24 screen conductors (instead of 15 or 19 screen conductors),
  - Impedance bench measurements on a smaller scale setup to confirm promising results from simulations.
- Improve the radiation of heat by increasing the emissivity of the tank (tests of a prototype on-going). Active cooling with fluid would be a very efficient option but it is very difficult to envisage inside vacuum due to high voltage operation - however it is an option being considered for under the bake-out jacket.
- Reduce the likelihood of a spark from the beam screen conductors (by reducing the electric field. In addition a coating is under consideration [15]).
- Understand and suppress the anomalous heating presently exhibited by the ferrite toroids of MKI8C.

TCP.B6L7.B1 skew primary collimator

The TCP.B6L7.B1 collimator caused beam dumps in 2011 and 2012, and the steady increase of its jaws' temperature during physics fills with increasing intensity required increasing the interlock to 95°C.

It is important to note that the temperature of all other primary collimators (including its symmetric for B2) has increased to less than 38°C, and with a pattern that indicates that it is due to beam losses and not beam induced heating.

Joint analysis of heat deposition and measured temperatures by EN/MME and BE/ABP points to an absence of efficient cooling, and hence a suspected non-conformity of the cooling system is expected [18, 19].

It is interesting to note that beam induced heating was clearly observed but sharp heating increase was also observed to be correlated to beam losses.

Nothing wrong was seen with visual and X-ray inspections by EN/STI and EN/MME on both cooling systems and RF fingers at several occasions.

Plans for LS1 include a thorough check of the cooling system by EN/STI and the collimation working group. In addition, this collimator will be replaced with a spare for a detailed inspection.

ALFA Roman pot

The ALFA detectors' temperature reached 42°C close to the inner detector and entered the range that is expected to lead to detector damage (around 45°C), see for instance on Fig. 1. The ALFA temperature became particularly critical at the end of October 2012 on beam 2 when strong changes in longitudinal beam spectrum at flat top were observed [9].

Joint studies by BE/ABP and ATLAS-ALFA showed that the temperature increase is consistent with impedance heating of the ferrite damper ring (which is efficiently preventing more harmful heating) [19].

The TOTEM detector has a similar geometry but its inner detector structure did not suffer from temperature increase as it had been designed with efficient active cooling. In fact, during two days with stopped detector cooling, similar temperature increases as in ALFA were observed. The metallic box around the detector was however not cooled.

As emergency measures, the ALFA team removed the bake-out jackets and added some fans.

Plans for LS1 foresee the implementation of a new design with reduced impedance and active cooling in order to allow for a more comfortable operational margin in 2015.

Beam screen temperature regulation

Until TS3, the Q6R5 standalone had no margin for more cooling. This could have been an issue for 7 TeV operation.

Tests were performed (Xrays on both bellows and cooling circuit) and so far nothing special was seen that could explain the singularity of Q6R5.

Since September 2011 (TS3), the situation improved significantly. Only a few fills have been affected since then, in particular the fills following a movement of the neighbouring TOTEM roman pot, indicating a possible correlation (through vacuum or losses or both). This is under study with the TOTEM, TE/VSC and TE/CRG teams.[§]

During LS1 the valves for standalones will be replaced to allow a higher cooling flux.

BSRT synchrotron light monitor

The beam 2 synchrotron light monitor (BSRT) mirror and support suffered from damage that could be due to significant heating [20]. Indeed the reduction of B2 bunch length was observed to increase the temperature of BSRT B2 measured outside vacuum (see Fig. 6).

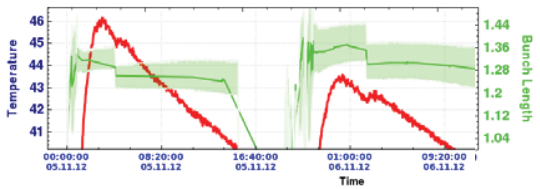

Fig. 6: temperature of the BSRT B2 (in red) and B2 bunch length (in green). The decrease of B2 bunch length on Nov. 6th generated an increase of the temperature of the BSRT B2, and can be explained by beam induced heating.

Electromagnetic simulation studies had been underway before the incident as there were signs of deformation to beam induced heating already in 2011 [4]. A combined effort between BE-BI, BE-ABP, BE-RF and EN-MME was invested to understand the heat deposition, to assess whether the Curie temperature of the ferrite has been reached, and to look for adequate solutions for the end of the run and for after LS1. There was still no clear conclusion at the moment of the workshop as the temperature probes were installed outside of the tank.[**] A BSRT working group was set up within BE/BI to find a more robust design for operation after LS1 [20].

TCTVB tertiary collimators

Despite active cooling, the 2 TCTVBs in IR8 consistently heat by around 10 degrees in most fills.

As mentioned in the introduction, the most critical IR2 TCTVB from the point of view of heating was taken out in 2011 for background reasons with the other IR2 TCTVB.

It is interesting to note that beams were dumped by TCTVB.4L8 temperature when the longitudinal blow up stopped working on May 30th 2012. This could be a worry if the bunch length is significantly reduced in physics, but the two remaining TCTVBs in IR8 should be replaced by single beam TCTPs after LS1. In any case, the bunch length reached at this occasion was much lower than the nominal bunch length: (0.85 ns instead of 1-1.05 ns).

EXPECTATIONS AFTER LS1

Beam parameters

After LS1, possible beam parameters include:

- Nominal beam at 6.5 TeV: ~1.15 10^{11} protons per bunch (p/b) with 25 ns bunch spacing
- Current beam at 6.5 TeV: ~1.6 10^{11} protons per bunch (p/b) with 50 ns bunch spacing
- New high brightness 25 and 50 ns beam with the h=9 option with batch compression, merging and splitting (BCMS), obtained so far with slightly lower intensities than the current production schemes [21].

Another crucial point for estimating beam induced heating after LS1 is the choice of operating bunch length. Before LS1, the operating full bunch length was set between 1.2 ns and 1.3 ns whereas nominal bunch length is below 1.05 ns.

Effect of bunch spacing on beam induced heating

Assuming the same bunch length and same bunch distribution for 50 and 25 ns bunch spacing, the equation in the introduction expects the same beam spectrum with 25 ns spacing as with 50 ns, but with half of the peaks.

In the frame of this assumption, switching to 25 ns for the case of a broadband impedance should yield an

[§] Other possibilities have been investigated since this workshop: in particular (1) electron cloud and (2) the consequences of the fact that the detector itself is cooled and not the metallic pot, combined with the supposed absence of high temperature bake out of the ferrite, which could lead to large outgassing when heated up.

[**] In 2013, a test was allowed after temperature probes were installed inside the vacuum and it was observed that the temperature of the ferrite reached well above its Curie temperature.

increase by a factor $M^{25}*(N_b^{25})^2/\ M^{50}*(N_b^{50})^2$ = 1.05, where M^{50}=1380, M^{25}=2808, N_b^{50}=1.6 10^{11} p/b, Nb^{25}=1.15 10^{11} p/b.

Switching to 25 ns for the case of a narrow band impedance falling on a beam harmonic line (i.e. its resonant frequency is f_{res}= *k*20* MHz with *k* an integer) should yield an increase by a factor $(M^{25}*N_b^{25})^2/(M^{50}*N_b^{50})^2 = 2$ if f_{res}= *2*k*20* MHz with *k* an integer, or a total suppression if f_{res}= *(2*k+1)*20* MHz with k an integer.

The effect of switching to 25 ns could therefore have a detrimental impact on some of the undamped narrow band resonators. Among the elements which are observed to suffer from beam induced heating, most are expected to be broadband and should not be affected by the change of bunch spacing (except the VMTSA before the 2012 run and the geometric TDI contribution, and of course all elements for which no observable has indicated issues).

Effect of bunch length on beam induced heating

Assuming the same distribution for various bunch lengths and bunch spacing, reducing the bunch length is expected to extend the beam spectrum to higher frequencies homothetically (see Fig. 7).

As a consequence, switching to lower bunch length for a broadband impedance with a resonant frequency below around 1.2 GHz leads to a regular increase of beam induced heating in general. Switching to lower bunch length for narrow band resonances enhances some resonances, damps others, and may excite higher frequency resonances.

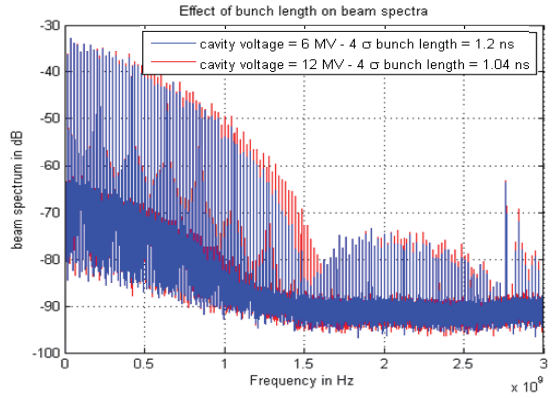

Fig. 7: effect of reducing bunch length on measured LHC beam spectrum (in dB) from 1.2 ns (in blue) to 1.04 ns (in red). The notch of the distribution is observed to shift from 1.5 GHz to 1.7 GHz. The peak at 2.7 GHz is believed to be due to a limitation in the acquisition bandwidth.

Observing the impact of changing beam spectrum and bunch length in LHC

In order to predict the situation after LS1, two tests were performed during the run: an OP test on bunch length reduction and an MD on flattening bunches.

Bunch shortening test

The bunch shortening test was performed by increasing the cavity voltage at injection, and it confirmed that shorter bunch length increases heating for most monitored devices (see Figs. 8 and 9). At this occasion, the LHC stayed 1h between 1 ns and 1.1 ns with 1380 bunches at 1.5 10^{11} p/b without detecting a major issue. It is important to note that the final distribution reached during this test should not be the same as what would be obtained if the target bunch length was decreased during the ramp.

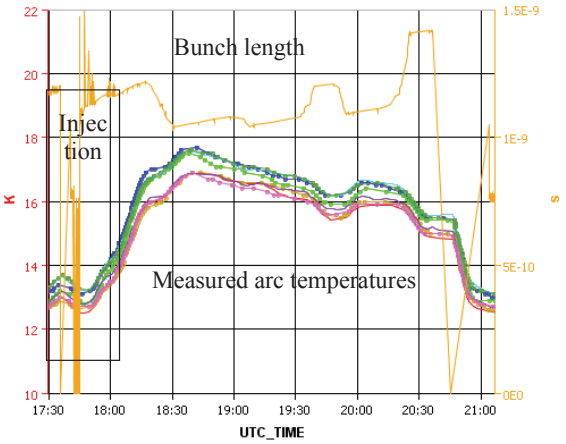

Fig. 8: Measurement of average temperature of all arcs during the bunch length reduction test. The correlation of measured temperatures with bunch length is clearly visible, in particular between 19:30 and 20:00 UTC when the bunch length was changed back and forth from ~1.1 ns to 1.2 ns.

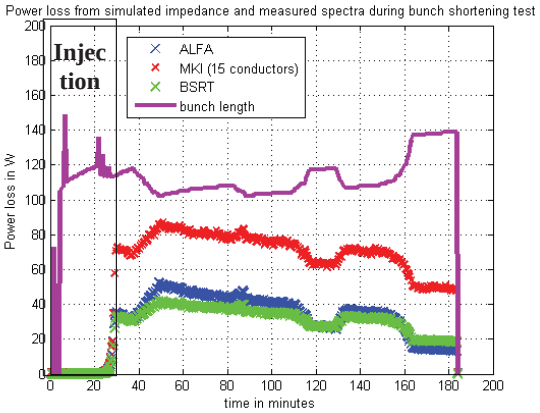

Fig. 9: Power loss predicted for the ALFA detector, MKI,

and BSRT during the bunch length reduction test. The power loss was obtained from the measured beam spectra and the simulated impedance of the respective elements.

Very different patterns were observed with bunch length (see Table 3), and these help to understand the origin of the beam induced heating. The items that heated more are planned to be upgraded (ALFA, MKI8C, TDI, BSRT) or removed (TCTVB). Finally, no hard showstopper was unveiled by this test to run at lower bunch length.

Table 3 shows a summary of the observations during the bunch length test:

equipment	Heating increases with lower bunch length?	Difference with a regular fill with ramp (3318)?
BSRT	Yes (slightly)	Similar
TCTVB	Yes	Heated more
TCP.B6L7	No (long time constants)	Heated less
MKIs (other than MKI8C)	Not observed (long time constants)	Similar
MKI8C	Difficult to see	Heated more
ALFA	Yes	Heated more
TDI pressure and deformation	Difficult to see	Seemed to be larger for TDI2
Arcs temperature	Yes	Similar
Q6R5	No (but saturated)	Heated less, indication that it may not be an RF heating issue

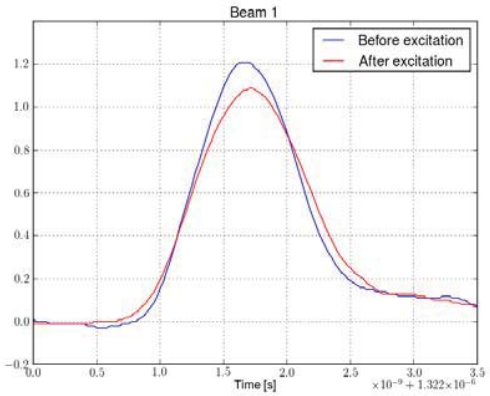

Fig. 10: bunch profile before and after RF phase modulation (courtesy J.E. Mueller et al).

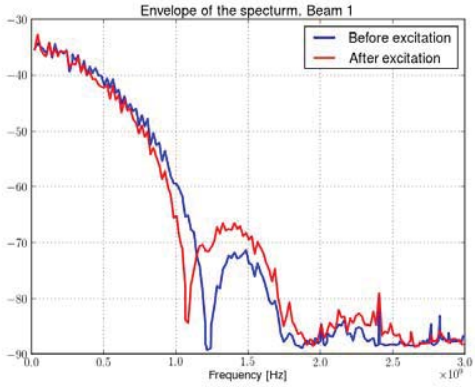

Fig. 11: beam spectrum before and after RF phase modulation (courtesy J.E. Mueller et al).

MD on flattening bunches

The MD on flattening bunches was aiming at changing the longitudinal beam spectrum by applying a sinusoidal RF phase modulation [22]. The bunch profile and the beam spectra before and after excitation are presented in Figs. 10 and 11. It can be seen that a small change of the bunch profile changes significantly the beam spectrum over a large frequency range (note that the beam spectrum is in dB scale). It is also observed that the beam spectrum is larger at frequencies above 1.2 GHz after the RF modulation, as expected. This method is hence very promising as shown in Fig. 12 but is to be used with caution if critical resonances above 1.2 GHz are present. As for the bunch lengthening test, there was no alarming sign of heating detected during this bunch flattening test.

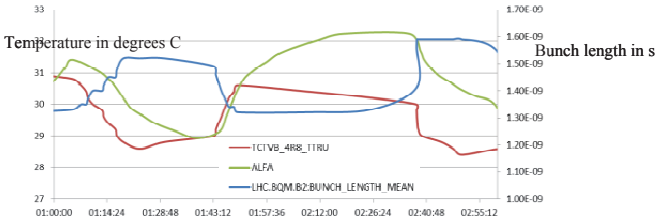

Fig. 12: measured temperatures for the ALFA detector and the TCTVB.4R8 collimator during a bunch length change at top energy with the LHC nominal physics beam (between 1:00 and 1:50) and the bunch flattening test (at 2:35). The temperatures were observed to sharply decrease after the RF modulation was applied (moment at which the measured bunch length increases sharply to 1.6 ns). It is important to note that the measured bunch length increased significantly whereas the bunch profile did not change much as seen in Fig. 10. The method used to measure bunch length therefore shows its limits in this case (courtesy J.E. Mueller et al).

Other interesting observations

Useful information was also gained thanks to unwanted issues with the longitudinal emittance blow-up from October 26th to October 28th 2012 [9]. During these fills, strong changes of beam spectra for B2 were observed (see comparison with B1spectrum in Fig. 13). The power loss expected from these measured beam spectra and simulated ALFA impedance for beam 1 (in blue) and beam 2 (in red) yielded a power loss 40% larger for beam 2 than for beam 1. The difference in beam spectrum could then explain the significant temperature difference measured at the ALFA pots and BSRT mirrors on beam 1 and beam 2 for these fills, which demonstrates the need to control the shape of the beam spectrum in order to reduce beam induced heating.

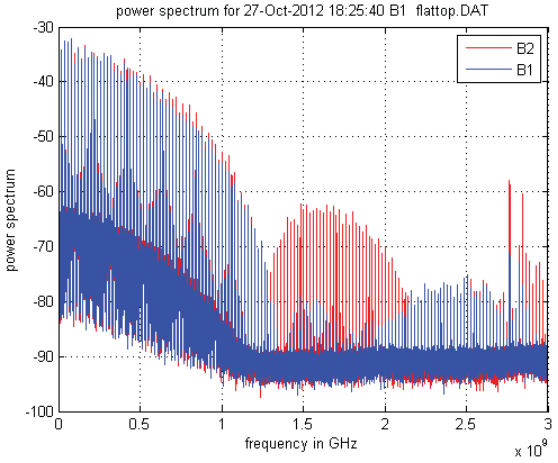

Fig. 13: comparison between beam spectrum at the beginning of flat top on October 27th for beam 1 (in blue) and beam 2 (in red). Both low and high beam frequencies are observed to be significantly enhanced in beam 2 for this fill.

All these observations show the importance of (1) keeping the bunch length large enough and (2) controlling closely the longitudinal bunch distribution in order to keep the beam induced heating to a minimum. A trade-off should however be found as increasing the bunch length also reduces luminosity through the geometric factor.

ELEMENTS PLANNED TO BE INSTALLED IN LS1

To the knowledge of the impedance team, the following changes are planned to be performed during LS1:

- Tertiary collimators replaced by new design with BPMs and ferrites replacing the longitudinal RF fingers on top of the jaws;
- 2-beam TCTVBs in IR8 will be replaced by single beam TCTVAs.
- Secondary collimators in IR6 replaced by new design with BPMs;
- New passive absorbers in IR3;
- New TCL collimators in IR1 and IR5
- Smaller radius for experimental beam pipes;
- Modifications in view of installation of the forward detectors in 2015;
- Improved roman pots (both ALFA and TOTEM);
- Improved BSRTs, TDIs, MKIs, improved cooling for TCP.B6L7;
- Maybe 1 or 2 UA9 goniometers for one beam only (to be confirmed).

Recall of general guidelines to minimize power loss

- Need to minimize RF heating already at the design stage to reduce resp. the geometric and resistive contributions of the real part of the longitudinal impedance. This optimization should be performed for all new equipment planned to be installed in the LHC, and is being performed for many project designs with the precious help of equipment groups and experiments (new collimators, new kickers, new instrumentation, new forward detectors, new LHCb VELO, new vacuum chambers, new bellows and shieldings, etc).
- Need for efficient cooling of near-beam equipment to avoid what has happened to TDI, BSRT and ALFA.
- Maximize evacuation of heat (optimize emissivity and thermal conduction).
- Need to ensure good RF contact to avoid what happened to the VMTSA double bellows (LRFF working group guidelines).
- If ferrites need to be used to damp resonant modes, use high Curie temperature ferrites whenever possible (e.g. Transtech TT2-111R or Ferroxcube 4E2 but beware of vacuum compatibility).
- Need for more monitoring of temperature inside critical equipment (e.g.: TDI, BSRT, TOTEM pot).

OUTLOOK

Many LHC devices have been heating at a faster rate in 2012 following the bunch intensity ramp-up.

Actions are/should be planned to be taken in LS1 to prepare safe and smooth running:

- Efficient cooling should be installed for all near beam equipment (in particular BSRT, TDI, ALFA)
- RF contacts should be consolidated according to the conclusions of the LRFF working group
- Suspected non-conformities should be investigated (TCPB6L7, MKI8C, and Q6R5 with its correlation with TOTEM movements).
- Logged pressure and temperatures should be systematically analysed to detect potential issues
- More temperature monitoring of critical equipment should be installed

- The longitudinal beam distribution should be controlled and optimized to reduce heating (if it is technically possible and as long as it does not impact longitudinal stability).

The summary table of the expected situation for the 2013 restart is in Table 4.

Since most heating devices have shown dominating broadband impedance, the operation with 25 ns is expected to lead to slightly larger power loss (for the same bunch length, bunch distribution and nominal bunch intensity).

TDI and maybe BSRTs which also exhibit large narrow band impedances should be monitored closely. Other devices might start suddenly heating much more if the distribution changes.

From beam induced heating point of view, the main worries for after LS1 seems to be:

- The extent of the upgrade of the TDI
- the operation with nominal bunch length (~1 ns, compared to ~1.2-1.3 ns)
- Uncontrolled longitudinal beam distribution during the ramp.

Table 4: summary of the expected situation after LS1 at the moment of the workshop.

Element	Problem	2011	2012	Hopes after LS1
VMTSA	Damage			All VMTSA will be removed
TDI	Damage			Beam screen reinforced, and the jaws?
MKI	Delay			Beam screen and tank emissivity upgrade
TCP B6L7.B1	Few dumps			Cooling system checked
TCTVB	Few dumps			All TCTVBs will be removed
Beam screen Q6R5	Regulation at the limit			Upgrade of the valves + TOTEM check
ALFA	Risk of damage			New design + cooling
BSRT	Deformation suspected			New design + cooling

ACKNOWLEDGMENTS

The authors would like to thank the Timber team, as well as the injectors and LHC operation teams.

REFERENCES

[1] M. Pojer, Introduction and review of the year including OP issues, LHC Beam Operation workshop, Dec. 2011.
[2] A. Macpherson, Introduction and review of the year, these proceedings.
[3] J. Uythoven et al, Beam induced heating and bunch length dependence, Mini-Chamonix workshop, 15 July 2011.
[4] B. Salvant et al, Beam induced heating, LHC Beam Operation workshop Evian Dec. 2011.
[5] E. Métral et al, Beam-induced Heating/Bunch Length/RF and lessons from 2012, LHC Perfromance workshop, Chamonix, Jan 2012.
[6] E. Métral et al, CERN Machine Advisory Committee, August 2012.
[7] B. Salvant et al, LHC Machine Committee 148, September 2012.
[8] E. Shaposhnikova et al, RF manipulations to reduce heating, LHC Machine Committee 152, October 2012.
[9] B. Salvant et al, LHC Machine Committee 155, October 2012.
[10] E. Métral et al, Conclusions of the RF fingers task force, LHC Machine Committee 159 and TE/TM, December 2012.
[11] E. Métral, Power spectra comparison between different types of longitudinal bunch profiles for the LHC, CERN BE/ABP-ICE meeting 23 Nov. 2011.
[12] P. Baudrenghien et al, LHC RF 2011 and beyond, LHC Beam Operation workshop Evian Dec. 2011.
[13] R. Losito et al, LHC Machine Committee 119, Jan. 2012.
[14] C. Bracco, Injection and Dump Systems, these proceedings.
[15] M. Barnes et al, CERN MKI strategy meetings (minutes and slides available on EDMS).
[16] H. Day, PhD thesis, to be published (2013).
[17] M. Garlasche, TCP.B6L7.B1: analytical and numerical evaluation of unexpected heating, LHC collimation working group 148, Sept 10 (2012).
[18] B. Salvant, TCP heating and impedance issues, LHC collimation working group 148, Sept 10 (2012).
[19] S. Jakobsen, B. Salvant et al, Update on heating and impedance studies for ALFA, ALFA collaboration meeting, Dec 4th 2012.
[20] F. Roncarolo, "What you get? Transverse and longitudinal distributions", these proceedings.
[21] R. Steerenberg, Post LS1 25 ns and 50 ns options from the injectors, these proceedings.
[22] J. E. Mueller, Bunch Flattening with RF Phase Modulation, LSWG 26, 15 January 2013.

ELECTRON CLOUD AND SCRUBBING IN 2012 IN THE LHC

G. Iadarola, G. Arduini, H. Bartosik, G. Rumolo

Abstract

During 2011, the scrubbing dose accumulated in the LHC during the tests with 25 ns beams could decrease the SEY of the chambers well below the multipacting threshold for 50 ns beams. During the Winter shut-down, the conditioning was preserved to such an extent as to guarantee smooth electron cloud free operation with 50 ns beams since the beginning of the 2012 run. However, the 25 ns injection tests that took place in July 2012 revealed that the chambers had slightly deconditioned since the last 25 ns test of 2011. Although this was not sufficient to cause electron cloud formation with 50 ns beams, this effect could noticeably impact on the quality of the 25 ns beams. A more extensive run with 25 ns beams (with stores for studies at both 450 GeV and 4 TeV and including a brief physics run) took place during December 2012 to gain experience in this mode of operation and gather more experimental information on the scrubbing process in the LHC. The outcome of this run is used to provide the guidelines to define a scrubbing strategy for operation after Long Shutdown 1 (LS1) with both 50 ns and 25 ns beams. A more general goal of the 25 ns run was also the identification of possible bottlenecks, which could prevent the safe injection and storage of the number of bunches needed to perform an efficient scrubbing process first and physics later.

INTRODUCTORY REMARKS

When an accelerator is operated with closely spaced bunches, electrons can quickly accumulate inside the vacuum chamber and fill it with a dynamic distribution dependent on both the beam structure and the properties of the chamber (i.e. geometry and maximum secondary electron yield (SEY), also referred to as $\delta_{\max}$, of the inner surface) [1]. The flux of electrons hitting the wall of the vacuum chamber is the source of both pressure rise through desorption and power deposition on the chamber wall. The presence of this electron cloud around the beam can also make the beam unstable or drive a slow process of emittance growth. The observation of the electron cloud in the LHC is for now essentially based on the direct measurement of these macroscopic effects [2]. While some of these observables are local and are mainly related to the formation of the electron cloud around specific regions of the machine (e.g. heat load in the arcs, vacuum rise at some gauges), other ones are global and give an indication of the integrated amount of electron cloud over the whole circumference of the LHC (e.g. stable phase shift, instability rise time, emittance growth, bunch-by-bunch tune shift). Both local and global indicators however include also other effects (e.g. synchrotron radiation, impedance), which need to be carefully disentangled when their contributions are comparable to that coming from the electron cloud.

Brief recapitulation of the 2011 observations

In 2011, the LHC suffered from electron cloud both at the beginning of the 50 ns run and then later, during all the machine study sessions with 25 ns beams. The electron cloud build up with 50 ns beams could be efficiently suppressed in most of the machine by means of an initial scrubbing run with 50 ns beams, which took place at the beginning of April 2011 [3]. Fitting the heat load data in the arcs (inferred from temperature and flow of helium on the beam screens) with electron cloud build up simulations, it was found that the maximum SEY in the beam screen of the dipole chambers was lowered from an estimated initial value of about 2.3 to slightly below 2.2. This was sufficient to guarantee an electron cloud free operation for 50 ns beams at both 450 GeV and 3.5 TeV. A further decrease of the maximum SEY in the arc dipoles was later achieved by injecting trains of 25 ns beams into the LHC. The first injection tests with trains of 24 bunches from the SPS were conducted on 29 June, 2011, and both heat load in the arcs and emittance growth of the bunches located at the tails of the trains were observed [4]. On a following MD session (26 August, 2011), there was an attempt to inject trains of 48 bunches, but the beam quickly became unstable after injection and was dumped after few hundreds of turns due to fast beam losses or large orbit excursions [5]. It was possible to efficiently cure a horizontal coupled-bunch oscillation with the transverse damper, while the strong single bunch instability observed in the vertical plane still affected the beam, even with the transverse feedback on. The beam instability observed on this occasion could be identified as triggered by the electron cloud. Its pattern over the bunch train could be successfully reproduced by means of combined PyECLOUD-HEADTAIL simulations, having assumed a maximum SEY of about 2.0, as it could be extrapolated from the SEY history based on reconstruction from the heat load data [6]. The next brief MD session with 25 ns beams (7 October, 2011) consisted of injection tests of up to 288 bunches (using high chromaticity settings, as opposed to the previous MD session, in which chromaticity was low at injection) and a store of few hours of 60 bunches per beam (in two trains of 24 and one of twelve bunches) at 3.5 TeV for the first data collection from experiments with 25 ns beams. It was only during the two last MD sessions, which took place on the 14 and 24-25 October 2011, that the LHC could be filled with 2100 bunches for Beam 1 and 1020 for Beam 2. A considerable amount of additional scrubbing could be achieved on these days, leading

to an estimated final value of $\delta_{\max}$ of 1.52. By the end of the MD session on the 24-25 October 2011, trains of 72 bunches with 25 ns spacing exhibited much reduced degradation with respect to the past, although both the lifetime and the emittance evolution still indicated the presence of a significant electron cloud in the LHC [7].

25 ns BEAMS IN THE LHC IN 2012

After three weeks commissioning with beam, the 2012 physics run of the LHC started in early March colliding beams with 50 ns bunch spacing. Owing to beam scrubbing from the 2011 MD sessions with 25 ns beams, which provided a safe enough margin to guarantee electron cloud free operation with 50 ns beams, the LHC quickly became productive for physics with 50 ns beams without suffering any major limitations from outgassing, heat load, or beam instabilities. The physics run successfully continued up till the 6 December, 2012, with an intensity per bunch boosted to 1.6×10^{11} ppb within transverse emittances as low as $1.6\,\mu$m at injection. This could be achieved thanks to the careful optimization and tuning in the injectors and the implementation of the low gamma transition optics (Q20) in the SPS for the production of LHC beams [8]. The MDs and physics operation with the 25 ns beams in 2012 are described in the following subsections.

25 ns beam injection tests

The first injection tests of 25 ns beams in 2012 were made on the 10 July. Trains of 72, 144, 216 and finally 288 bunches were successfully injected for Beam 1 with chromaticity Q' set to 15 in both planes. For Beam 2, only trains of 72 and 144 bunches were injected with the same high chromaticity settings. Next, it was attempted to lower chromaticity ($Q' = 5$), only for Beam 2, and repeat the injections with increasing numbers of trains. After successfully injecting a train of 72 bunches (in spite of a horizontal instability, which could be controlled by the transverse damper), the injection of 144 bunches triggered the beam dump within 700 turns due to fast beam losses. The reason was that the beam suffered an electron cloud instability right at injection because of the low chromaticity settings.

During these injection tests, the beam lifetime was found to be initially quite poor and a strong emittance growth was measured at the tails of the trains, especially in the vertical plane. Figures 1 show snapshots from the BSRT measurements when all the bunches injected with high chromaticy settings were inside the machine. Pressure rise was observed in some of the straight sections, but mainly in common areas and never above the interlock value of 4×10^{-7} mbar. The comparison between the time evolution of the relative beam losses measured during these injection tests and those mesured during the last 25 ns MD in 2012 (25 October), displayed in Fig. 2, clearly reveals a degradation of the beam quality in 2012 for the same beam parameters and machine settings. From the heat load measured during the 2012 25 ns injection tests, it could be indeed inferred that the $\delta_{\max}$ in the arc dipoles had an initial value of about 1.65 and then quickly returned to 1.55 by the end of the MD. The deterioration with respect to the last value determined from heat load data in 2011 suggests that, although the arcs were not opened to air during the Winter shut-down 2011-2012, a deconditioning of the inner surface of the beam screen occurred. However, it is encouraging that a value of $\delta_{\max}$ of about 1.55 could be quickly recovered within less than one hour store of 712 bunches for Beam 1 and 344 bunches for Beam 2, as opposed to the almost 20 hours needed in 2011 to obtain a

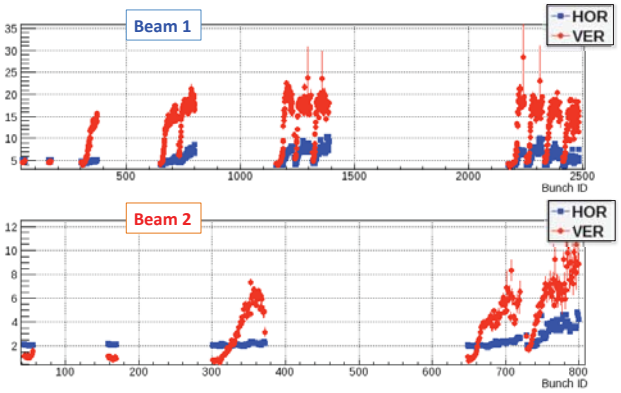

Figure 1: Snapshot of the horizontal and vertical normalized emittances for Beam 1 (top) and Beam 2 (bottom) just before the injection of the last train for Beam 2. The vertical axis is μm. Courtesy of F. Roncarolo.

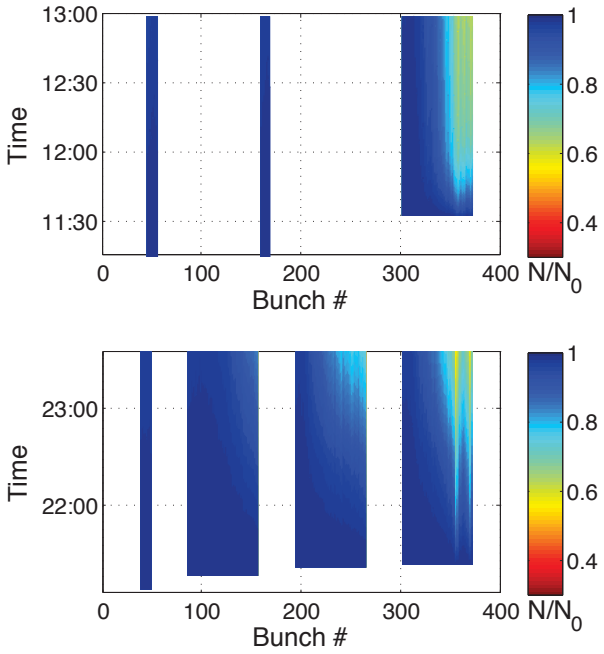

Figure 2: Comparison between the time evolution of the relative beam losses for Beam 2 during the injection test on 10 July, 2012, (top) and a store on 24 October, 2011 (bottom).

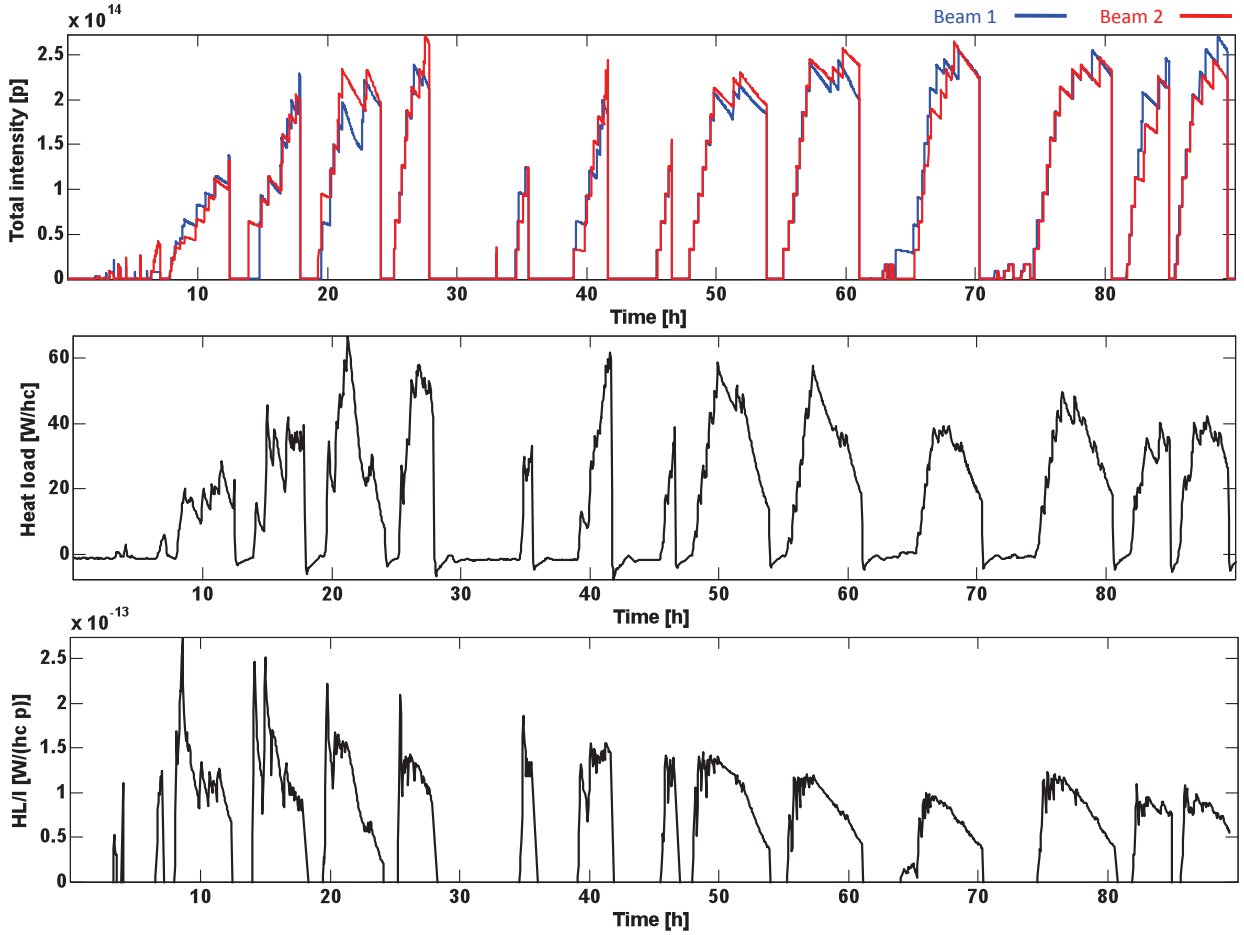

Figure 3: Beam current evolution (top), heat load in the Sector 5 – 6 (middle) and nomalized heat load in the Sector 5 – 6 (bottom) during the 2012 scrubbing run. The 0 time corresponds to the 6 December, 2012, at noon. Heat load data are courtesy of L. Tavian.

similar decrease in $\delta_{\max}$ with a larger beam filling fraction machine.

2012 scrubbing run

The 2012 scrubbing run of the LHC with 25 ns beams had the following goals:

(a) Further reduce the SEY over the whole machine by storage of 25 ns beams at 450 GeV, while monitoring electron cloud observables and beam quality evolution;

(b) Collect additional information on the evolution of the SEY as a function of the accumulated electron dose (especially in the low SEY region) and compare machine data with existing models. This is an essential step to validate and improve models, and establish strategies for the post-LS1 era;

(c) Enable LHC to be eventually ramped to 4 TeV with a few hundreds of bunches of 25 ns beams for electron cloud studies and for other studies with 25 ns beams (e.g. beam-beam, UFO) without significant electron cloud perturbations;

(d) Learn about other possible differences in 25 ns vs. 50 ns operation (e.g., equipment heating, beam longitudinal and transverse stability, UFO rates);

(e) Enable a 25 ns pilot physics run and possibly provide additional scrubbing.

Beams with 25 ns spacing were injected into the LHC and kept at 450 GeV for scrubbing purposes between the 6 and 10 December (08:00 am), 2012. Figure 3 depicts the evolution in terms of beam intensity for both Beam 1 and Beam 2 during these days (top plot). The inferred heat load in the beam screen of the arc of Sector 5 – 6 and the heat load normalized to the beam current are displayed in the middle and bottom plots.

The operation during the scrubbing run was rather smooth and no fundamental showstoppers were found. Thanks to the excellent machine availability, a significant scrubbing dose could be maintained all along the scrubbing period. During the initial stages, the overall efficiency was determined by the vacuum pressure in the MKI region. Prior to the run, the interlock levels for the MKI magnets had been increased to 4×10^{-9} mbar from 2×10^{-9} mbar, while

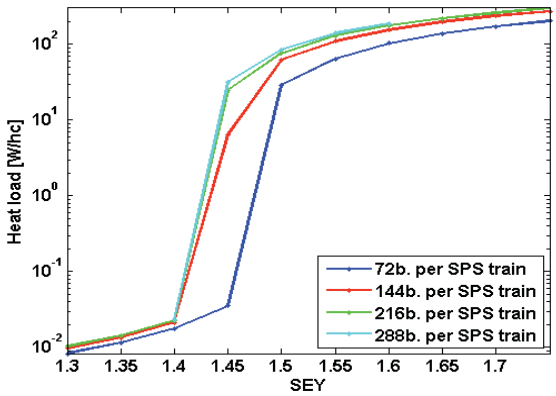

Figure 4: Heat load in the arcs (in W per half cell) as a function of the maximum SEY for different filling patterns.

those in the interconnects between the kicker modules had been raised from 5×10^{-9} mbar to 1×10^{-8} mbar. The vacuum interlocks in the interconnects between MKI2 Magnet D and Q5, between MKI8 magnet D and Q5 and between the MKI8 magnets A and B had to be further increased to 4.5×10^{8} mbar, 4.5×10^{8} mbar and 3×10^{8} mbar, respectively, during the run. Later on, when higher intensities were injected into the LHC, cryogenics slowed down the injection process requiring 10 – 15' between successive injections of 288 bunches from the SPS. This was mainly due to the limited cooling power for some of the standalone modules, while no limitation in the arcs appeared at this time. For high scrubbing efficiency, and also to avoid strong fluctuations on a 120 A current lead temperature in the matching section R8, the beams were dumped after the heat load had significantly dropped. The vacuum pressures along the ring were continuously monitored over the scrubbing period. Apart from the aforementioned MKIs and shortly ATLAS during the first night, pressure rises did not cause significant slow down. However, in order to keep temperature and pressure values below the interlock levels, heating and outgassing of the TDIs had to be avoided by retracting them after each injection. Probably because of the frequent movements, one jaw of the TDI in point 8 got blocked twice in open position and the motor had to be remotely reset. Besides, one of the LVDTs of TDI.4L2 LU had to be exchanged at the end of the scrubbing run, because its reading was found to trigger a warning/error on the lower limit due to drift while cooling down. Probably thanks to the longer bunches and smaller bunch intensities, no anomalous heating was observed during the scrubbing run on other sensitive elements (e.g. collimators, BSRT, MKIs).

The first half day of scrubbing was mainly devoted to the set up of injection (up to 288 bunches per train for both beams) and of the transverse damper. After that, there was only one fill with trains of 72 bunches, during which the quality of the beams could be seen to improve significantly from injection to injection and the chromaticity value Q' could be lowered from the initial 15 to about 7 units without triggering electron cloud instabilities. As illustrated in Fig. 4, electron cloud build up simulations for the arc dipoles suggest that, for values of $\delta_{\max}$ in the 1.40-1.55 range, it is important to use filling patterns made of longer trains than 72 bunches in order to efficiently continue the scrubbing process to lower SEY values. These simulations rely on the assumptions that: 1) the main contribution to the electron cloud remains in the arc dipoles, and 2) primary electrons are generated via residual gas ionization and 3) the SEY curve is parametrized according to [9] with 70% probability of low energy electrons to be elastically backscattered from the surface. Additionally, injection of longer trains from the SPS would allow for up to 30% more bunches in the LHC, which translates into more scrubbing power. Based on these considerations, from the second fill onwards, it was decided to switch to trains of 288 bunches per injection and maximize the scrubbing efficiency. Within the first 24 hours, the number of injected bunches reached the maximum in both rings (2748) and a record intensity of 2.7×10^{14} p was stored for Beam 2.
Several stores with full machine took then place over the scrubbing period, as visible in Fig. 3, top plot. The normalized heat load in Sector 5 – 6 during the scrubbing run, as depicted in the bottom plot of Fig. 3, indicates that the scrubbing process successfully carried on over the first 60 – 70 hours. However, the fact that the normalized heat load flattened out over the last few fills of the run also suggests that no further improvement due to scrubbing took place in the last part of the scrubbing run. Beam observations also seem to confirm this trend. While a clear improvement in the overall beam quality (lifetimes, emittances) can be observed when comparing a fill at the beginning of the run and one at the end (see, for instance, the plots of the bunch-by-bunch loss for Beam 1 displayed in Fig. 5), no

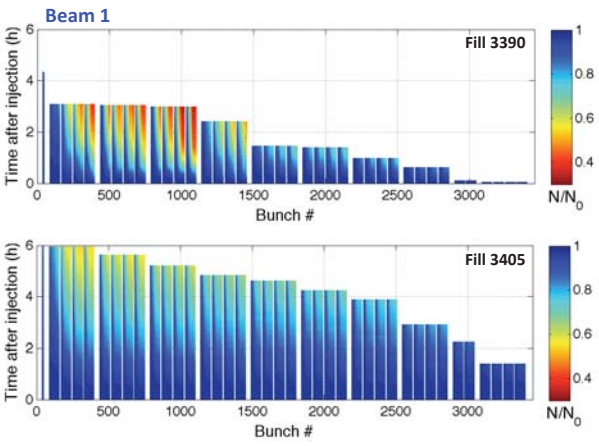

Figure 5: Bunch-by-bunch intensities for Beam 1 over the fills 3390 (top, beginning of the scrubbing run) and 3405 (bottom, end of the scrubbing run), normalized to the initial intensities. While the losses observed during fill 3390 are very strong (more than 60% in three hours), the situation looks much improved during Fill 3405 (losses below 40% in six hours).

evident progress can be observed over the last fills. This is confirmed by the evolution of the beam lifetimes during the 3.5 days of the scrubbing run (Fig. 6). The beam lifetimes shown in this figure were evaluated by averaging on the lifetimes after 1 hour store of only the last five bunches of each 72 bunch train. To be noted that, towards the end of the scrubbing run, it was necessary to increase the octupole current to 23 A (from the nominal setting of 6.5 A at injection) because it was found that this could suppress an instability affecting the first injected train of 72 bunches from the SPS and causing a "hunch" in the transverse emittance values between the middle and the tail of this train. It was suspected that the origin of this instability could be electron cloud, because it does not affect 50 ns beams and is compatible with a maximum of the electron central density seen in simulations, which is reached only along the first build up of the electron cloud in dipoles (i.e. for the first train) and becomes later suppressed by the build up of the stripes and space charge effects during the passage of the following trains.
After the tests at 4 TeV, described in the next subsection, three more fills at 450 GeV took place, two of which were made with trains of 288 bunches and one with trains of 72 bunches. The peak heat load measured during the fills with trains of 288 bunches did not exhibit any significant decrease from the values measured before the 4 TeV tests. The fill with trains of 72 bunches caused a heat load about a factor two lower than that produced by the same total intensity in trains of 288 bunches. This confirms the effect of the train structure on the amount of electron cloud in the arcs. Nonetheless, the fact that the heat load remains visibly above the resolution level also when filling the LHC with shorter trains indicates that the electron cloud in the arcs is still significant also in this configuration and, therefore, the memory between trains could be stronger than assumed in simulations.

The reasons why the scrubbing process in the arcs has sharply slowed down, or even reached saturation, after the first part of the scrubbing run still remains unclear and is presently the object of studies trying to explore different options. Possible explanations under investigation include, for instance, the existence of other regions of the arcs with much lower SEY thresholds, or model inaccuracies in the low energy part of the SEY curve. Both would be compatible with lower values of the threshold SEYs, either in the arc dipoles or in other components of the arcs, for which the rate of reduction of the SEY as a function of the electron dose logarithmically decreases (as found in laboratory measurements of SEY reduction with the electron dose).

Tests at 4 TeV

Despite a clear improvement with respect to the first day of scrubbing, 25 ns beams made of trains of 288 bunches in the LHC remained affected by quite degraded lifetime and significant emittance growth at the tails of the trains

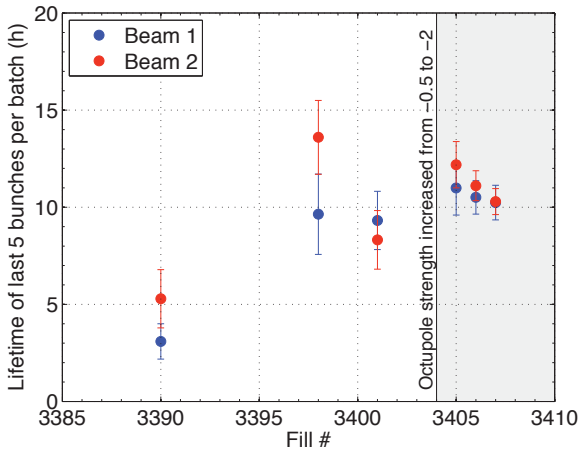

Figure 6: Beam lifetimes (after 1 hour store, averaged over the last five bunches per 72-bunch train) as a function of the fill number during the scrubbing run. The shaded region is after the change of the octupole settings.

even after the full scrubbing run. Consequently, it was decided to stick to the plan to ramp up in energy only trains of 72 bunches sufficiently spaced. This would have the advantage of limiting the beam quality degradation due to electron cloud thanks to both less electron cloud build up and shorter injection time, possible because of the reduced heat load engendered by this filling scheme. After about 60 hours since the end of the scrubbing run, mainly devoted to access, TDI alignment verification and collimator set up for $\beta^* = 1$ m, trains of 72 bunches with 25 ns spacing were finally injected into the LHC and ramped to 4 TeV during two days, 13 – 14 December, 2012. The overview in terms of beam intensity for both Beam 1 and Beam 2 during these days, together with the beam energy, is plotted in the top graph of Fig. 7, while the inferred heat load on the beam screen of the arc in Sector 5 – 6 can be seen in the bottom one (units of the heat load are Watt per half cell).
The number of bunches injected into LHC and ramped to 4 TeV was gradually increased.

1. The first fill had 84 bunches, injected in a train of 12 followed by a train of 72 bunches for both beams. This fill was used for a long-range beam-beam MD, during which the crossing angle was changed in steps;

2. Two short stores with 156 and 372 bunches took place to continue the intensity ramp up process;

3. One long store with 804 bunches (one train of 12 and 11 trains of 72 bunches) was kept for about 8 hours for scrubbing purposes and to study the evolution of the beam paramters at top energy;

4. One short store with 804 bunches with the same scheme as the previous fill and lower intensity per bunch (around 9×10^{10} ppb), aiming to investigate the heat load dependence on the bunch intensity, concluded the 4 TeV tests.

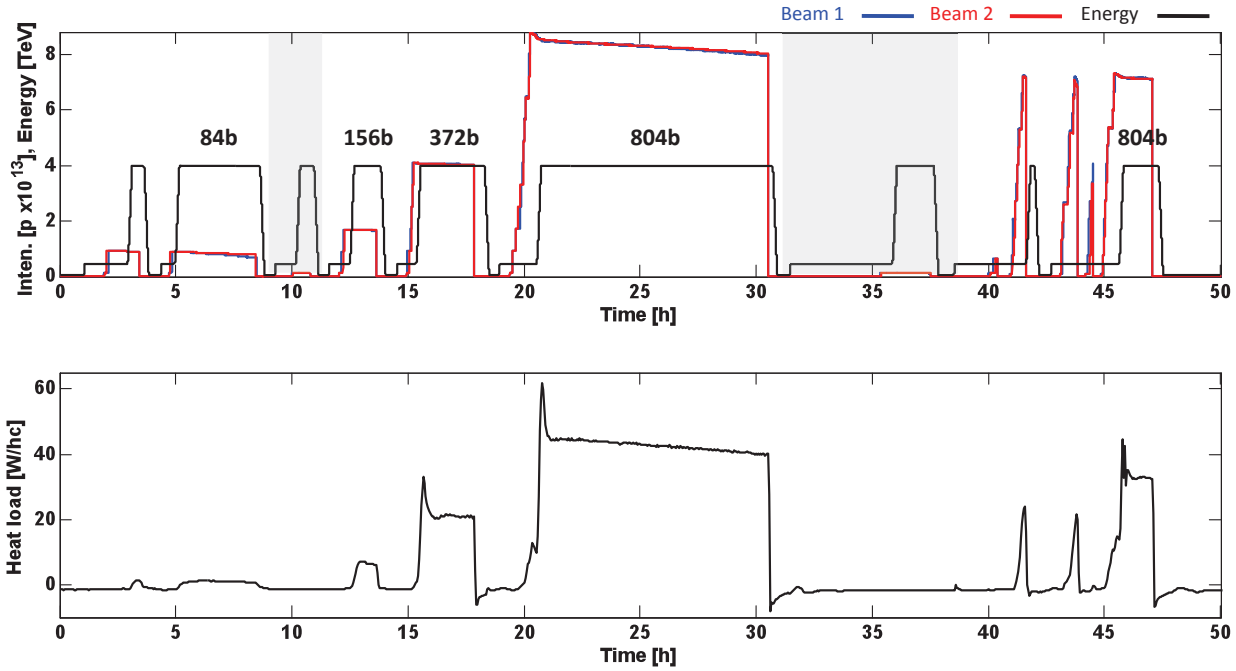

Figure 7: Beam current evolution (top) and heat load in the Sector 5 – 6 (bottom) during the test ramps with 25 ns beams (12 – 14 December, 2012). The 0 time corresponds to the 13 December, 2012, at midnight. Heat load data are courtesy of L. Tavian.

It can be noted that, during the studies, a few hours (specifically those around $t = 10$ h and then again in the time between 30 and 40 h, following the time reference as in Fig. 7) were used for further collimator verification and loss maps. A few aborted filling attempts (wrong octupole settings, software interlock due to missing BPM data) caused an additional loss of about five hours just before the last exercise of filling LHC with 804 bunches with lower intensity. The bottom plot of Fig. 7 shows the evolution of the heat load in the arcs during the two days of the tests ramps. Probably due to photoelectrons, the measured heat load was significantly enhanced at 4 TeV. For example, 804 bunches at 4 TeV were found to produce about the same heat load as 2748 bunches at 450 GeV, i.e. slightly above 40 W/half cell. The rapid increase of the heat load during the ramp required to increase the flow of helium on the beam screens before the start of the ramp. This fact caused the artificial peak observed in the heat load evolution plots, which is explained by initial overcompensation, and also limited in practice the number of bunches that could be injected into LHC. In fact, just looking at the steady values of the heat load, the cryogenic system would have allowed for at least twice the number of bunches (limited in this case by the Sector 3 – 4, which was running with approximately half the nominal cooling capacity) [10]. The increase of the heat load proportional to the number of bunches injected, as well as the flat heat load curve observed every time that the beams were kept for a long time at top energy, suggest that no further significant reduction of the SEY was achieved during these stores. Notwithstanding this, thanks to the increased

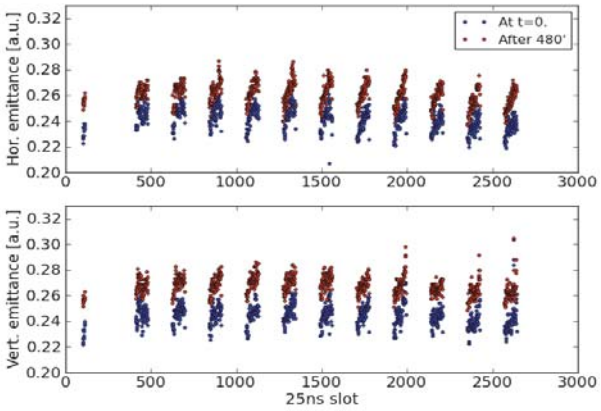

Figure 8: Snapshots of the bunch by bunch emittances from the BSRT taken at the beginning of the 4 TeV store and after 8 hours (fill with 804 bunches and nominal intensity per bunch).

beam rigidity at 4 TeV, the beam quality during the high energy stores did not exhibit any signs of degradation that could be attributed to electron cloud. Bunch by bunch losses were uniform and very small. Similarly, bunch by bunch emittances uniformly grew over the 8 hour store by less than 10% over the whole store length, as depicted in Fig. 8. Bunch by bunch stable phase measurements confirm the increase of the energy loss along the ramp also seen through the heat load measurements in the arcs, as well as the stabilization of the energy loss while the beams stayed at top energy [11].

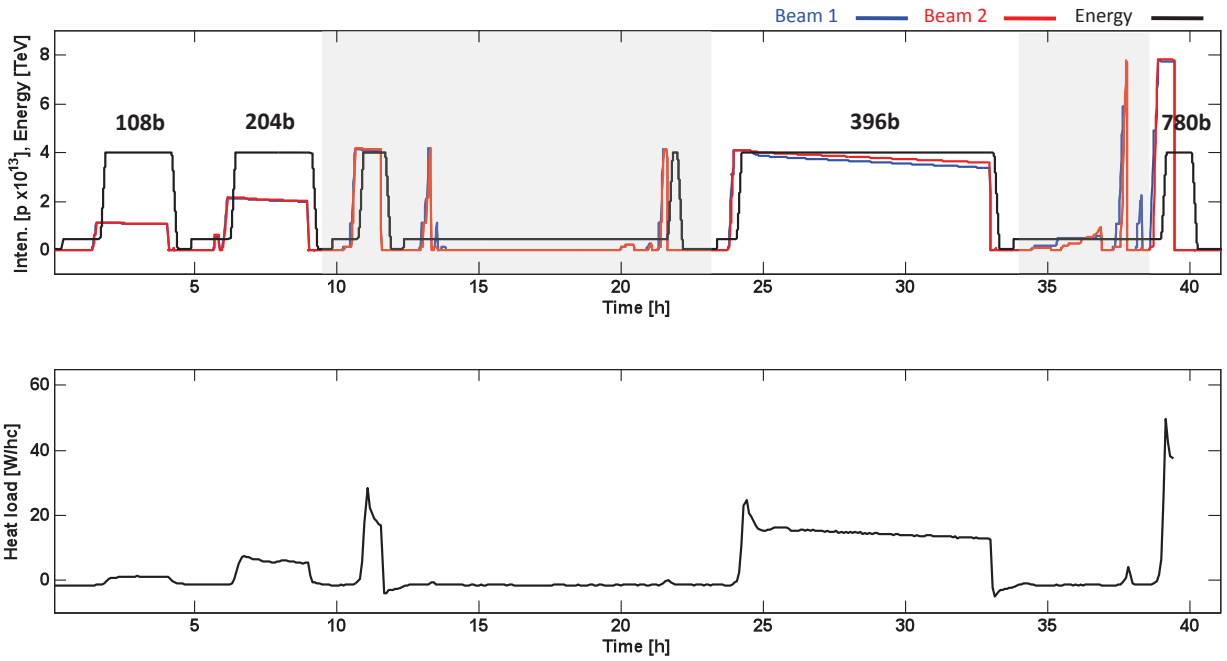

Figure 9: Beam current evolution (top) and heat load in the Sector 5 – 6 (bottom) during the pilot physics run with 25 ns beams (15 – 17 December, 2012). The 0 time corresponds to the 15 December, 2012, at noon. Heat load data are courtesy of L. Tavian.

Pilot physics run with 25 ns beams

The improvement achieved with the scrubbing run together with the experience acquired with the test ramps to 4 TeV finally enabled a short physics run with 25 ns beams just before the 2012 Christmas stop. The pilot physics run with 25 ns beams took place for about 48 hours from the 15 to the 17 December (08:00 am), 2012. During this run, in order to provide the experiments with the highest possible luminosity with 25 ns beams, it was decided to use low emittance beams from the injectors (BCMS production scheme, [12, 13] and references therein). With this scheme, the beams coming from the SPS are grouped in trains of 48 bunches (up to three trains within the same injection) and have transverse emittances of 1.4 μm at injection into the LHC. The total intensity was ramped up through three successive fills with 108, 204 and 396 bunches. The time of the third store was longer to ensure a good amount of data collection for the experiments. The last fill with 780 bunches also went successfully through acceleration and squeeze, but the beams were accidentally dumped by ALICE, due to too high luminosity. Single 48-bunch trains were used during the first two physics fills, while the third one and the final fill with 780 bunches were based on filling patterns made of double 48-bunch trains. The overview in terms of beam intensity for both Beam 1 and Beam 2 during these days, together with the beam energy, is shown in the top plot of Fig. 9. Unfortunately, due to miscellaneous RF synchronization problems and investigation, almost 15 hours were lost when first trying to fill the LHC with trains of 2×48 bunches from the SPS. In addition, on the last night before the end of the proton run, about five hours were also lost for physics, as multiband instability monitor and longitudinal damper tests with 50 ns beams had to take place and then the first attempt to ramp 780 bunches per beam was dumped by a software interlock on the orbit feedback. The evolution of the inferred heat load in the beam screen of the arc of Sector 5 – 6 can be seen in the bottom plot of Fig. 9. Comparing the measured heat load of these three fills with those in previous stores with comparable total beam currents, we can observe a decrease by about 20%. This has not yet been investigated in detail. In principle, it could be attributed to an effect of slow scrubbing, but also to the different train structures or the lower transverse emittances of the physics fills with respect to the test ramps. The beam emittances at top energy during the collisions (averaged over the two transverse planes and Beam 1 and Beam 2) could be reconstructed from the luminosity data. Figure 10 shows the emittances for the three physics fills with 108 (top), 204 (middle) and 396 bunches (bottom). The fills with 108 and 204 bunches show bunch by bunch emittances about 30% larger than their values at injection (measured with the wire scanners on the first train), but with only a faint signature of the electron cloud effect over the 48 bunch trains. The bunch by bunch emittances from the fill with 396 bunches clearly exhibit the typical electron cloud pattern along the 2×48-bunch trains. Even more interestingly, the fact that the three last trains injected are strongly affected by the electron cloud emittance growth even within their first 48 bunches shows the presence of a non-negligible memory effect between trains (over 25 μs, that is about the distance between the trains). This could be related to the fact that, unlike in the previous fill with

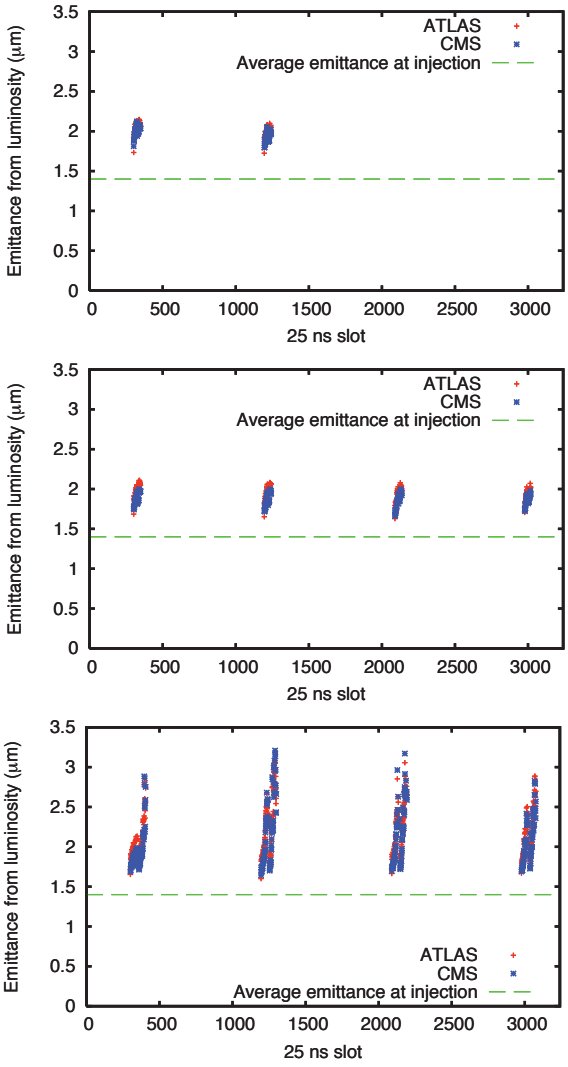

Figure 10: Snapshots of the bunch by bunch emittances from luminosity for the fill with 108 (top), 204 (middle) and 396 bunches (bottom). The line of the measured emittances at injection is also drawn. Courtesy of M. Hostettler and G. Papotti.

trains of 48 bunches, in this case the build up of the first injected train can generate a high enough electron density in the chamber that is not completely reset before the arrival of the next train. Finally, the fact that the first 48 bunches of the first train do not appear to be suffering from the same effect could be explained by the cleaning effect from the train of twelve bunches between the last and the first train. This explanation appears to be also supported both by simulations and by the stable phase shift data [11]. In fact, a first look into the bunch by bunch stable phase shift data at top energy for this physics fill reveals an electron cloud structure building up along the first train from a lower level than that of the following trains.

FUTURE SCRUBBING SCENARIO

After LS1, the situation of the beam screen in the arcs will be likely reset and, upon resuming of the LHC operation in 2015, it is reasonable to assume that the $\delta_{\max}$ in the arcs will have returned to values higher than 2.3, as it was before the 2011-2012 machine scrubbing. In these conditions, it will be necessary to envisage and schedule a period devoted to machine conditioning, or scrubbing, in order to get into physics production with 50 ns or 25 ns beams. After an initial re-commissioning with low intensity, based on the experience of 2011, five to seven days with increasingly longer trains of 50 ns beams will be needed for vacuum conditioning and for lowering the SEY in tha arcs to a value close to the threshold for electron cloud build up for 50 ns beams. At this point, in the case of 50 ns operation, this scrubbing run could be ended by one-two days with injections of trains of 25 ns beams aiming to lower $\delta_{\max}$ in the arcs below 2.0 and gain a safe enough margin to ensure electron cloud free operation with 50 ns beams. After a possible physics production period with 50 ns beams at 6.5 TeV, the 25 ns operation will require to perform a second scrubbing step with the 25 ns beam. By simply adding up the 50 hours of 25 ns MDs in 2011 and the 60-70 hours of efficient scrubbing in 2012, we obtain that 5 days of run with increasingly longer trains of 25 ns beams at injection energy should be sufficient to reach a condition in which the first ramps of 25 ns beams (shorter trains) to 6.5 TeV can be made. At this point, the LHC would be able to move into physics at 6.5 TeV with 25 ns beams. According to the 2012 experience, the scrubbing process described above will however not be sufficient to suppress the electron cloud in the LHC and further scrubbing will have to be achieved then during the physics run. It is worth noticing that the 25 ns operation of the LHC will entail the following:

- The electron cloud and its detrimental effects will be present, at least for some time (this remains to be estimated), mainly producing emittance blow-up at injection. Heat load, emittance blow up and low lifetime will slow down the process of intensity ramp up and affect the experiments because of the luminosity loss;
- As was observed in 2012, deconditioning will occur when the 25 ns beam does not circulate in the LHC for some time. This means that few hours for scrubbing could become necessary after each longer stop (i.e. certainly after every Winter stop, but possibly also after each Technical Stop);
- Other effects, like UFOs, will have to be closely monitored because there has been evidence of recrudescence with 25 ns beam in 2012 [14]. Beam induced heating did not seem to be an issue during the 2012 25 ns tests, but it will also have to be carefully controlled when the beam parameters will be pushed to higher brigthness [15].

CONCLUSIONS

During the 3.5 days of scrubbing run at 450 GeV, the LHC could be filled several times (up to 2748 bunches per beam) with 25 ns beams, reaching the record intensity of

2.7×10^{14} p stored per beam. An improvement of the heat load and beam lifetime over the first 70 hours was observed, followed by a sharp slow-down of the scrubbing process. The emittances of the bunches at the tails of the trains were blown up during the injection process, especially for long enough trains of bunches. Two days were then devoted to test ramps to 4 TeV and two days for a pilot 25 ns physics run. When performing the test ramps, fills with 84, 156, 372 and 804 bunches per beam were kept at 4 TeV for several hours in the LHC to monitor the evolution of the heat load and beam parameters. It was observed that, probably due to photoelectrons, the heat load exhibits a steep increase when ramping to 4 TeV (also confirmed by the stable phase shift data). Nevertheless, even in conditions of enhanced electron cloud, no significant blow up of transverse emittances occurs at flat top and the final bunch by bunch distribution of the emittances is mainly determined by the injectors and the blow up at injection energy. During the pilot physics run, up to 396 bunches per beam were brought into collision, while up to 780 were successfully accelerated and squeezed. Clear signs of electron cloud driven emittance blow up were observed in the fill with trains of 2×48 bunches, while the two previous fills with shorter trains did not suffer from serious beam quality degradation, except a uniform 30% emittance blow up between injection and collisions nearly independent of electron cloud.

Finally, we described a scenario to resume the LHC operation in 2015 after LS1. In particular, one week of vacuum conditioning and scrubbing will be required for the 50 ns run. After that, one more scrubbing week will be needed to get into physics with 25 ns beams. If operation with 25 ns will be chosen as standard operation after LS1, coexistence with electron cloud will be probably inevitable at least in the first part of the physics run.

ACKNOWLEDGEMENTS

Despite opening new challenging questions that require further work, research and understanding, the 2012 LHC run with 25 ns beams attained all its declared goals. Since its success has been the result of an intense interdepartmental team work involving many groups, first of all the authors would like to give big thanks to BE/OP, TE/CRG, TE/VSC, BE/RF, TE/ABT, EN/STI and BE/BI for the expert support they provided with the machine and equipment operation throughout the scrubbing run. In addition, we would like to express directly our gratefulness to V. Baglin, M. Barnes, W. Bartmann, P. Baudrenghien, C. Bracco, G. Bregliozzi, S. Claudet, M. Di Castro, B. Goddard, W. Höfle, G. Lanza, A. Lechner, T. Mastoridis, S. Redaelli, L. Tavian, D. Valuch for equipment set up, monitoring and help; N. Biancacci, X. Buffat, O. Domínguez, K. Li, H. Maury-Cuna, E. Métral, N. Mounet, Y. Papaphilippou, S. Persichelli, T. Pieloni, T. L. Rijoff, B. Salvant, S. White, C. Zannini and F. Zimmermann for their active participation in the measurements and general support; R. De Maria, J. Esteban-Müller, M. Hostettler, F. Roncarolo, E. Shaposhnikova, G. Trad for their important contributions in data acquisition and post-processing; all the EIC's, R. Alemany-Fernandez, V. Kain, A. Macpherson, G. Papotti, M. Pojer, L. Ponce, G. Roy, M. Solfaroli Camillocci, and all operators, for bearing us day and night for two weeks in the CCC and constantly following up on our requests.

REFERENCES

[1] Proceedings of the Mini Workshop on Electron Cloud Simulations for Proton and Positron Beams, **ECLOUD'02**, 15–18 April, 2002, CERN, Geneva, Switzerland, edited by G. Rumolo and F. Zimmermann, CERN-2002-001

[2] G. Rumolo *et al.*, "Electron cloud effect in LHC in 2011", in Proceedings of the LHC Beam Operation Workshop - Evian 2011 (12-14 December, 2011, Evian, France)

[3] G. Arduini *et al.*, "50 and 75 ns operation in the LHC: Vacuum and Cryogenics observations", CERN-ATS-Note-2011-046 MD (2011)

[4] B. Goddard *et al.*, "Injection into LHC of bunches at 25 ns spacing", CERN-ATS-Note-2011-050 MD (2011)

[5] H. Bartosik and W. Höfle, "Analysis of bunch by bunch oscillations with bunch trains at injection into LHC at 25 ns bunch spacing", CERN-ATS-Note-2012-027 MD (2012)

[6] H. Bartosik, W. Höfle, G. Iadarola, Y. Papaphilippou and G. Rumolo, "Benchmarking of Instability Simulations at LHC", in Proceedings of ECLOUD12 (5-9 June, 2012, Isola d'Elba, Italy)

[7] G. Rumolo *et al.*, "LHC experience with different bunch spacings in 2011 (25, 50 & 75 ns)" in Proceedings of LHC Performance Workshop Chamonix 2012 (6-10 February, 2012, Chamonix, France)

[8] H. Bartosik, Y. Papaphilippou *et al.*, "Increasing instability thresholds in the SPS by lowering transition energy", CERN-ATS-2012-177 (2012)

[9] R. Cimino *et al.*, "Can Low-Energy Electrons Affect High-Energy Physics Accelerators?", Physics Rev. Lett. **93**, 014801 (2004)

[10] L. Tavian *et al.*, "Performance limitations: 2012 review and 2015 outlook – Cryogenics", elsewhere these proceedings

[11] J. Esteban-Müller and E. Shaposhnikova, private communication.

[12] R. Garoby, "New RF Exercises Envisaged in the CERN-PS for the Antiprotons Production Beam of the ACOL Machine", IEEE Transactions on Nuclear Science. **Vol. NS-32. No. 5** October 1985

[13] C. Carli *et al.*, "Complementary/alternative possibilities", in Proceedings of LHC Performance Workshop Chamonix 2011 (24-28 January, 2011, Chamonix, France)

[14] T. Baer *et al.*, "UFO's: Observations, statistics and extrapolations", elsewhere these proceedings

[15] B. Salvant *et al.*, "Beam induced RF heating in LHC in 2012", elsewhere these proceedings

PERFORMANCE LIMITATIONS OF THE LHC CRYOGENICS: 2012 REVIEW AND 2015 OUTLOOK

L. Tavian, CERN, Geneva, Switzerland

Abstract

Dynamic heat loads are deposited in the LHC cryo-assemblies through several processes, in particular by the circulating and colliding proton beams themselves. Measurements of beam-induced heating were performed on the cryogenic system during the 2012 beam operation, mainly on the beam screens and magnet cold masses. Analyses of the measurements have allowed to correlate the beam-induced heating with the beam parameters, to review the heat deposition scaling laws, to extrapolate data for post-LS1 beam operation for different bunch spacing and to identify cooling limitations and consolidations of critical cryo-assemblies, including the continuous cryostats, the stand-alone magnets and the inner triplets.

INTRODUCTION

Scaling laws have been defined to calculate the dynamic heat loads deposited in the LHC machine mainly on the beam screens and on the magnet cold masses. During the 2012 LHC operation, measurements have been performed at reduced beam energy and beam current allowing verifying the scaling laws, identifying possible local or global cooling limitations and recommending related consolidations.

SCALING LAWS OF DYNAMIC HEAT LOADS

Beam-induced heating on the beam screens

The beam-induced heating on the beam screen circuits are coming from:

- synchrotron radiation *Qsr* from the bending magnet,
- resistive dissipation *Qic* of beam image currents induced in the resistive walls and geometrical singularities of the beam channel,
- impingement of photo-electrons *Qec* accelerated by the beam potential ("electron clouds"),

The corresponding scaling laws are given by the following equations:

$$Qsr = Qsr_{nom} \cdot \left(\frac{E}{E_{nom}}\right)^4 \cdot \frac{Nb}{Nb_{nom}} \cdot \frac{nb}{nb_{nom}} \quad (1)$$

$$Qic = Qic_{nom} \cdot \left(\frac{Nb}{Nb_{nom}}\right)^2 \cdot \frac{nb}{nb_{nom}} \cdot \left(\frac{0.60 \cdot E + 2.80}{E_{nom}}\right)^{0.5} \cdot \left(\frac{\sigma}{\sigma_{nom}}\right)^p \quad (2)$$

where:

- Qsr_{nom}= 0.165 W/m per beam,
- Qic_{nom}= 0.180 W/m per beam,
- *E*, the beam energy with E_{nom}= 7 TeV,
- *Nb*, the bunch population with Nb_{nom}= $1.15 \cdot 10^{11}$ protons per bunch,
- *nb*, the number of bunch with nb_{nom}= 2808 bunches per beam,
- σ, the bunch length with σ_{nom}= 1.06 ns,
- *p*, the bunch length dependence factor with *p*= -1.5 in the LHC Design Report (DR)

The third term of the Equation 2 corresponds to the magneto-resistance effect.

Concerning *Qec*, a scaling law is given after efficient beam cleaning and beam scrubbing, which was not the case during the measurement campaign. Consequently, the corresponding scaling law is not used.

The total beam-induced heating *Qdbs* deposited on the beam screens is given by Equation 3:

$$Qdbs = Qsr + Qic + Qec \quad (3)$$

Dynamic heat loads on the cold-masses

The dynamic heat loads on the cold-masses are coming from:

- nuclear inelastic beam-gas scattering *Qbgs* corresponding to a continuous distributed loss of particles from the circulating beam,
- losses of secondary particles *Qsec*, mostly absorbed at 1.9 K in the magnet cold-mass helium bath close to the high-luminosity experimental areas,
- resistive heating *Qrh* occurring in the non-superconducting sections of the magnet excitation circuits, essentially in splices of the superconducting cables.

The corresponding scaling laws are given by the following equations:

$$Qbgs = Qbgs_{nom} \cdot \frac{Nb}{Nb_{nom}} \cdot \frac{nb}{nb_{nom}} \cdot \frac{E}{E_{nom}} \quad (4)$$

$$Qsec = Qsec_{nom} \cdot \frac{E}{E_{nom}} \cdot \frac{L}{L_{nom}} \quad (5)$$

$$Qrh = Qrh_{nom} \cdot \left(\frac{E}{E_{nom}}\right)^2 \quad (6)$$

where:

-
- $Qbgs_{nom}$= 0.024 W/m per beam
- $Qsec_{nom}$= 182 W per high-luminosity half-insertion
- Qrh_{nom}= 0.10 W/m
- *L*, the luminosity with L_{nom}= 10^{34} Hz/cm^2

The total dynamic heat loads *Qdcm* deposited on the cold masses is given by Equation 7:

$$Qdcm = Qbgs + Qsec + Qrh \quad (7)$$

MEASURMENT OF BEAM INDUCED HEATING ON BEAM SCREENS

A measurement method has been implemented in order to assess the heat loads *Qdbs* deposited on the beam-screen circuits. This method is based on enthalpy balance using the outlet control valve characteristics to assess the cooling-loop mass-flow [1].

Bunch length dependence in the arcs

Two specific runs (run3133 and run3345) have been dedicated to study the bunch length dependence on the beam induced heating. During these runs with 50-ns bunch spacing, the photo-electron impingement is negligible. By making the assumption that the synchrotron radiation *Qsr* follows the scaling law given by Equation 1, *Qic* can be deduced from:

$$Qic = Qdbs - Qsr \quad (8)$$

Figures 1 and 2 show for the 2 runs the corresponding *Qic* evolution in the arcs deduced from equation 8 with *Qdbs* measured and *Qsr* calculated by using Equation 1. For the run3345, as the beam energy remains at injection energy (450 GeV), the *Qsr* is definitely negligible (*Qic*= *Qdbs*). On these Figures, the magenta line corresponds to the average measurement of *Qic* in the arc; the green line corresponds to the best fit of the *Qic* using the scaling law (Equation 2) with:

- *p*= -2 (to be compared with -1.5 in the DR)
- Qic_{nom}= 0.135 W/m per beam (to be compared with the DR value of 0.180 W/m per beam, i.e. 25 % lower than expected).

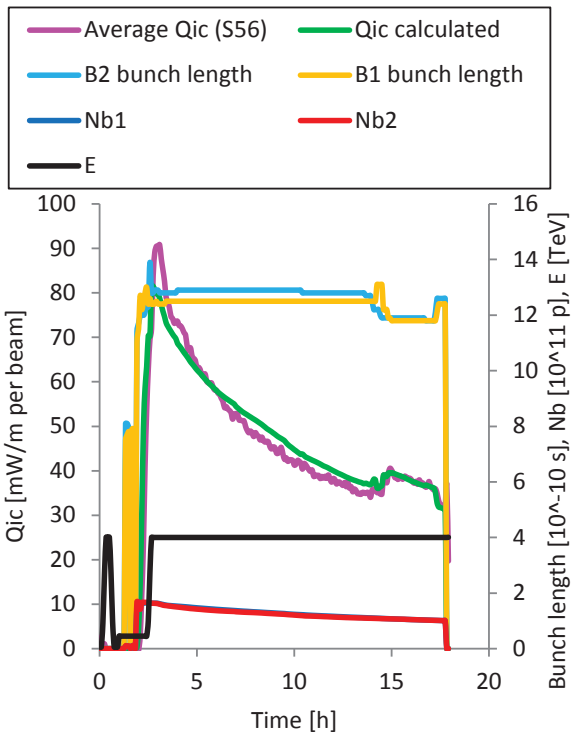

Figure 1: *Qic* evolution in the arcs for run3133

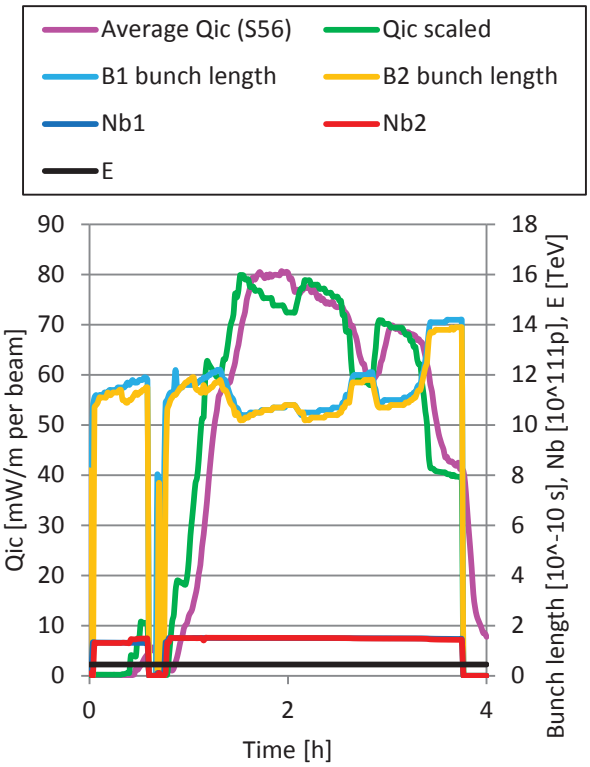

Figure 2: *Qic* evolution in the arcs for run3345

Bunch length dependence in the standalone and semi-standalone magnets

Using the same method, the beam-induced heating on the beam screens of the standalone (SAM) and semi-standalone (Semi-SAM) magnets can be assessed. Figure 3 shows the corresponding Qic evolution for the specific run (run3345).

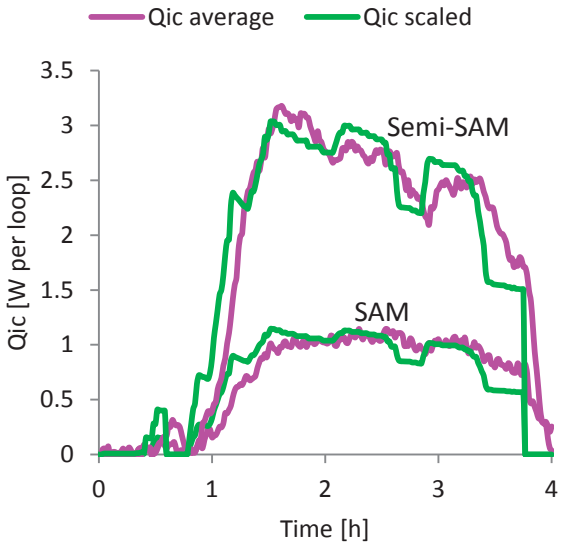

Figure 3: *Qic* evolution in standalone and semi-SAM (run3345)

As for the arc, the best fit corresponds to the scaling law (Equation 2) with:

- p= -2 (to be compared with -1.5 in the DR)
- Qic_{nom}= 0.135 W/m per beam (to be compared with the DR value of 0.180 W/m per beam, i.e. 25 % lower than expected).

Bunch length dependence in the Inner Triplets

Using the same method, the beam-induced heating on the beam screens of the Inner Triplets can be assessed. Figure 4 shows the corresponding Qic evolution for the specific run (run3345).

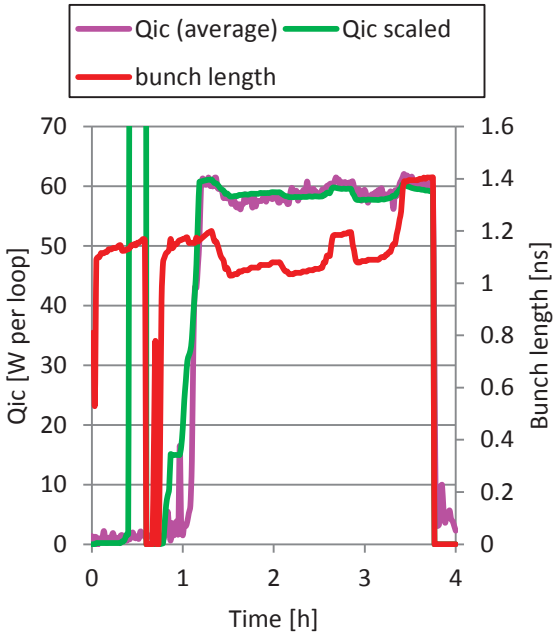

Figure 4: *Qic* evolution in Inner Triplets (run3345)

For Inner Triplets, the best fit corresponds to the scaling law (Equation 2) with:

- p= +0.3 (to be compared with -1.5 in the DR)
- Qic_{nom}= 1.17 W/m per beam (to be compared with the DR value of 0.180 W/m per beam, i.e. a factor 6.5 higher than expected).

Beam-induced heating *Qic* due to image current follows definitely another law in the Inner Triplet than in the rest of the machine. Additional investigation is required to explain this specific behaviour.

Beam-induced heating in the arcs

Beam-induced heating *Qdbs* on the beam screens of the arc half-cells is measured for a typical run (run3134: 4 TeV and 50-ns bunch spacing). Figure 5 shows the evolution of *Qdbs* on a typical sector (S56). The green line corresponds to the scaled evolution with the parameter defined here above (Qic_{nom}= 0.135 W/m per beam and p= -2). As a steady-state cannot be established (beams are continuously loosing protons), an area (see Figure 5) is defined to perform a proofer analysis.

Figure 6 shows the distribution of the Qdbs load on the 8-sector half-cells. The scaled value (green line) is in good agreement with the average value of the distribution.

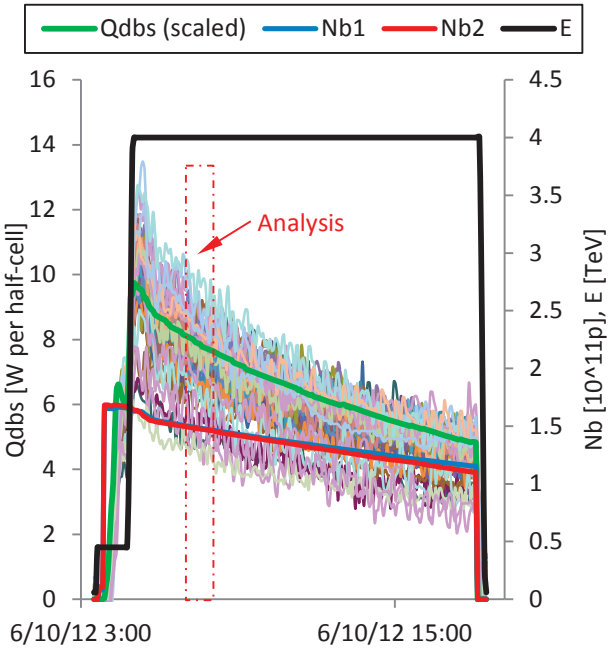

Figure 5: Qdbs evolution in S56 arc half-cells (run3134)

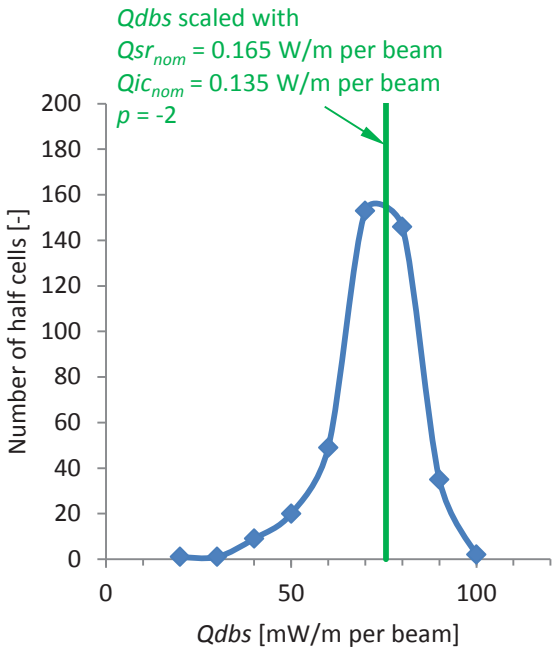

Figure 6: Distribution of Qdbs in the arc half-cells (run3134).

Beam-induced heating in standalone and semi-standalone magnets

Table 1 gives the inventory of standalone (SAM) and semi-standalone (semi-SAM) magnets.

Beam-induced heating *Qdbs* on the beam screens of the SAM and semi-SAM is measured for a typical run

(run3134). Figure 7 shows the distribution of the Qdbs load on the SAM and semi-SAM (data corresponding to the same analysis area than for the arc half-cells). The scaled value (green line) is in good agreement with the average value of the distribution for the semi-SAM. For the SAM the distribution is more erratic and the scaled value slightly over-estimates the average value for SAM. An outlier SAM (Q6R5) has very high beam-induced heating (factor 4.5 higher than the average value). The proximity of the TOTEM detector could be the reason of this overheating (issue under investigation).

Table 1: Inventory of SAM and semi-SAM

Inventory			Length [m]	CV Kvmax [m3/h]
SAM Type 1	Q5R1 Q5R5 Q6L5 Q6L1	Q6R1 Q6R5 Q5L5 Q5L1	8.2	0.02
SAM Type 2	Q6L4 Q4L6 Q5L6	Q6R4 Q4R6 Q5R6	6.9	0.03
	D3L4	D3R4	11.2	
	Q6L2 Q6L7 Q6L3 Q6L8	Q6R2 Q6R7 Q6R3 Q6R8	12.0	
	Q5L2 Q5L8	Q5R2 Q5R8	13.0	
Semi-SAM	Q5D4L4	D4Q5R4	16.7	0.05
	D2Q4R1 D2Q4R5	Q4D2L5 Q4D2L1	19.4	
	Q4D2L2 Q4D2L8	D2Q4R2 Q4D2R8	22.8	

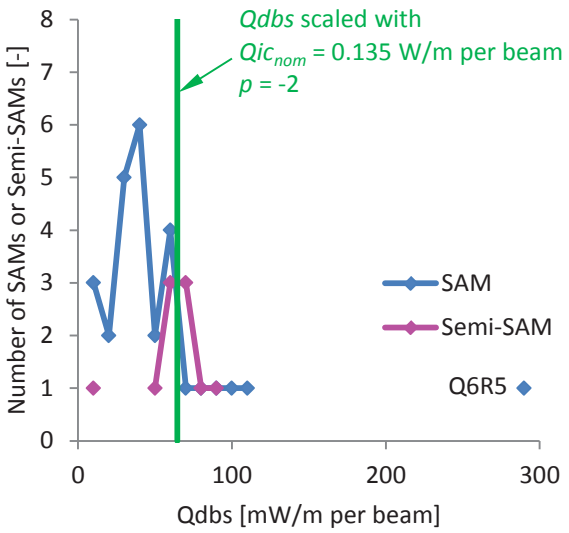

Figure 7: Distribution of Qdbs in SAM and semi-SAM (run3134)

Beam-induced heating in Inner Triplets

Table 2 gives the inventory of Inner Triplets (including the D1 magnets when cold).

Beam-induced heating *Qdbs* on the beam screens of the Inner Triplets is measured for a typical run (run3134). Figure 8 shows the evolution of Qdbs for the Inner Triplets. Figure 9 shows the distribution of the Qdbs load on the Inner Triplets (data corresponding to the analysis area). The scaled value (green line) is in good agreement with the high-luminosity Inner Triplets (IT1 and IT5). Low-luminosity Inner Triplets are significantly lower (up to a factor 1.6 for IT2).

Table 2: Inventory of Inner Triplets

Inventory				Length [m]
ITL1	ITR1	ITL5	ITR5	40
ITL2	ITR2	ITL8	ITR8	50

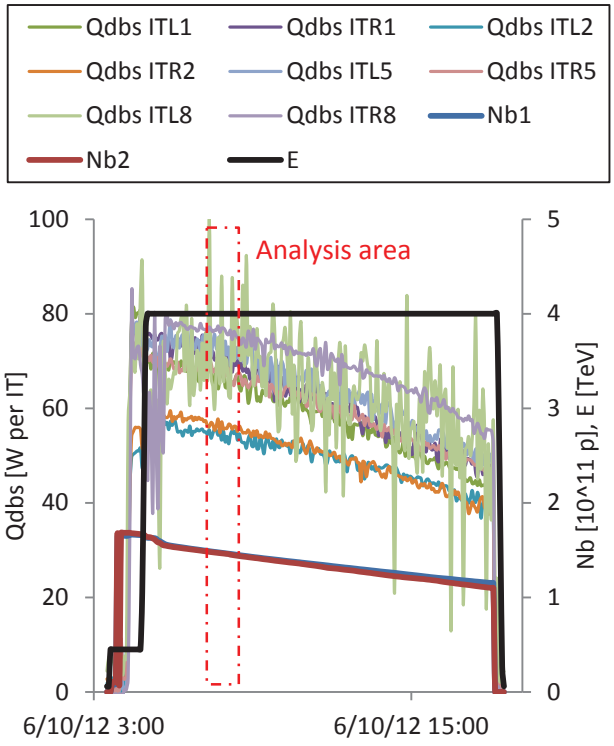

Figure 8: Qdbs evolution in Inner Triplets (run3134)

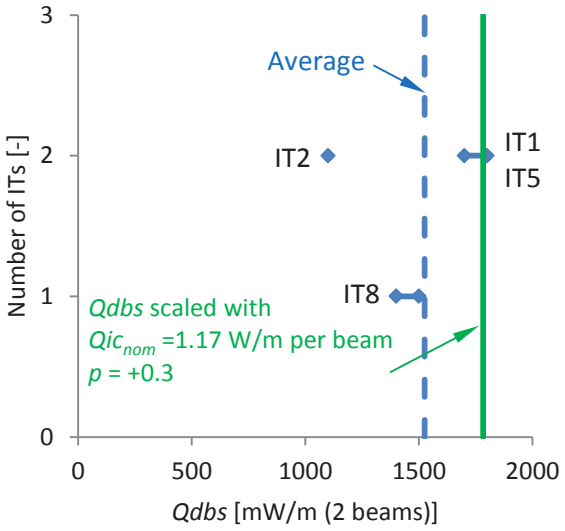

Figure 9: Distribution of Qdbs in Inner Triplets (run3134)

Bunch population dependence

According to the Qic scaling law given by Equation 2, the beam-induced heating due to image current goes with the square of the bunch population *Nb*. Figures 10 and 11 show the measured *Qic* as a function of *Nb* during a typical run for the arc half-cells and for the Inner triplets. The power factor 2 is confirmed for the arc half-cells but is not in accordance with the Inner Triplet for which a power factor of 1.3 is measured.

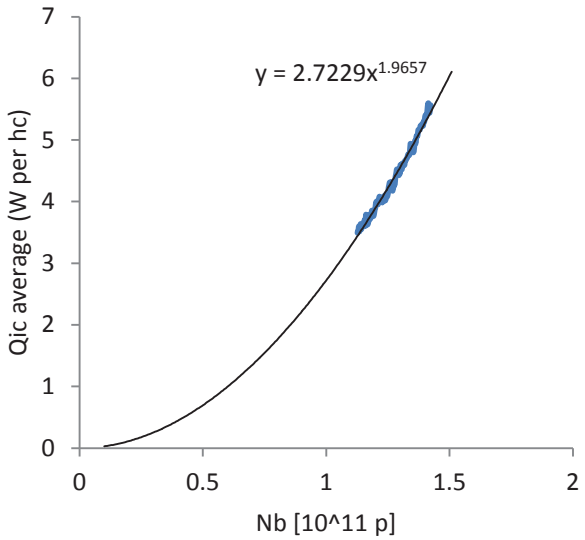

Figure 10: Bunch population dependence of *Qic* for the arc half-cells (run3134)

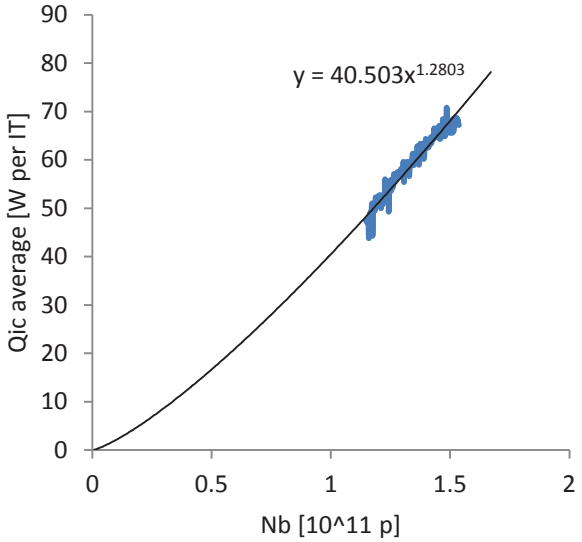

Figure 11: bunch population dependence of *Qic* for the Inner Triplets (run3134)

Scaling for 2015 operation

Two operating scenarios corresponding to bunch spacing of 25 and 50 ns are foreseen during the second physics campaign which will start in 2015. Table 3 gives the corresponding main beam parameters. Beam parameter for the run3134 is also given for comparison.

Table 3: Main beam parameters for 2015

	Run3134	25 ns 2015	50 ns 2015
Nb [p per bunch]	1.49E11	1.15E11	1.6E11
nb [-]	1374	2760	1380
E [TeV]	4	6.5	6.5
σ [ns]	1.29	1.06	1.06
L [Hz/cm^2]	$6.7 \cdot 10^{33}$	10^{34}	10^{34}

Scaling laws with corrected parameter (Qic_{nom} and *p*) can be applied to assess the expected power to be extracted in 2015 for the two 2015 operating scenarios. Table 4 gives the present measured values. Table 5 gives the corresponding total *Qbs* scaled values (including the static heat inleaks *Qsbs*) and the locally installed capacity which is mainly due to the control valve located at the loop outlet. For the arc half-cells of sector S34, the valve poppets were change in 2009 in order to test on a sector the loop controls with a smaller valve, reducing consequently the locally installed capacity in the corresponding arc.

Except for the SAM Q6R5 for which the present capacity is already at the limit, some margins are existing.

Theses margins could be partially or totally used for photo-electron impingement which is present during the beam scrubbing process. Table 6 gives the maximum photo-electron impingement locally acceptable with respect to the present margins.

Table 4: Run3134 measured values [W]

	Qsbs	Qsr	Qic	Total Qbs
Arc half-cell	7.5	1.2	6.9	15.6
SAM type 1	4	0	1.1	5.1
SAM type 2	4	0	1.7	5.7
Semi-SAM	5	0.5	2.9	8.4
SAM Q6R5	10	0	4.8	14.8
IT	5	0.5	71	76

Table 5: *Qbs* scaled values [W]

	25 ns 2015	50 ns 2015	Locally installed
Arc half-cell	34	30	255 (140*)
SAM type 1	6	6	16
SAM type 2	7	7	24
Semi-SAM	16	15	40
SAM Q6R5	20	19	16
IT	114	89	200

*: Data for S34

Table 6: Locally acceptable photo-electron impingement in [W/m per aperture]

	25 ns 2015	50 ns 2015
Arc half-cell	2.1 (1.0*)	2.1 (1.0*)
SAM type 1	0.6	0.6
SAM type 2	0.6	0.6
Semi-SAM	0.6	0.7
SAM Q6R5	N/A	N/A
IT	1.7	2.2

*: Data for S34

25-ns beam scrubbing

A beam scrubbing campaign was scheduled in December 2012 with 25-ns bunch-spacing beams. Figures 12 and 13 show the evolution of the maximum and average photo-electron impingement *Qec* during this campaign.

With respect to the existing margins (given in Table 6 and plotted on the right of the Figures), some limitations are existing for SAM and semi-SAM for which valve poppets and seats have to be changed during the LS1. Concerning the arc of the S34, the maximum values are at the limit and original poppets will be reinstalled in order to recover the same margin present in the other arcs.

The identified limitations seen during this beam-scrubbing campaign are corroborated with the control valve openings which reached 100 % for some of them. Figure 14 shows, as example, the evolution of the Type 1 SAM valve openings.

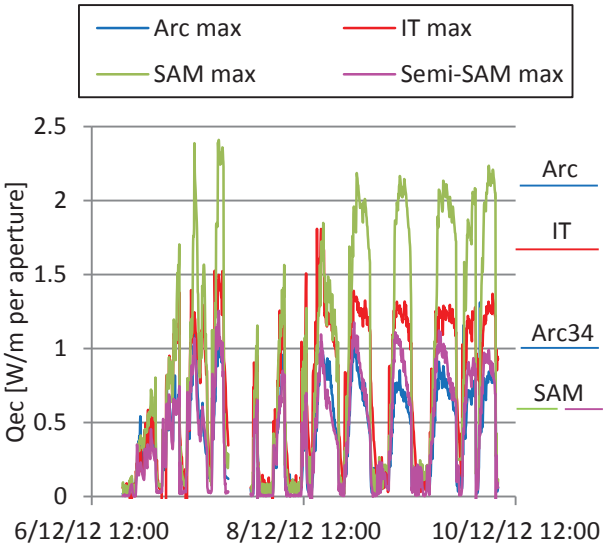

Figure 12: Maximum *Qec* deposition

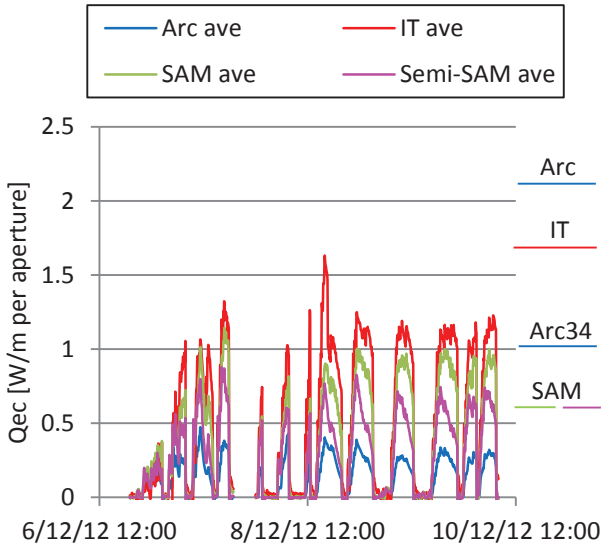

Figure 13: Average *Qec* deposition

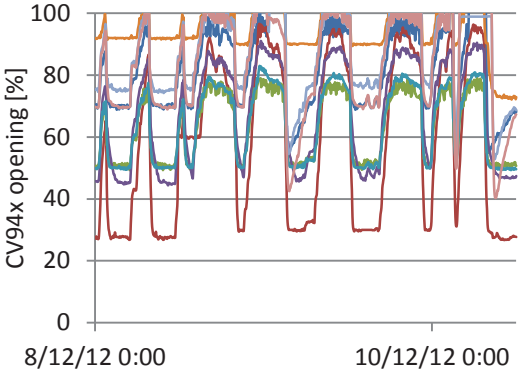

Figure 14: Type 1 SAM valve openings

MEASURMENT OF DYNAMIC HEAT LOAD ON COLD MASSES

Loss of secondary particles in Inner Triplets

The measurement method of the losses of secondary particles in the cold masses of the Inner Triplets is based on the calibration of the extra-opening of the valves controlling the Inner Triplet temperature versus a known electrical heating deposition. Figure 15 shows the calibration of the eight valves. Figure 16 shows the evolution of the losses of secondary particles during the typical run 3134.

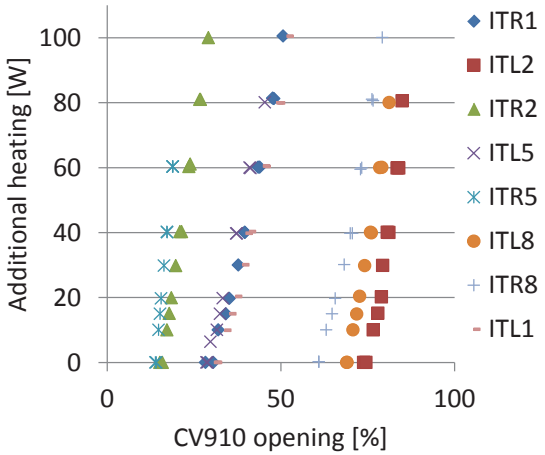

Figure 15: calibration of the IT control valves

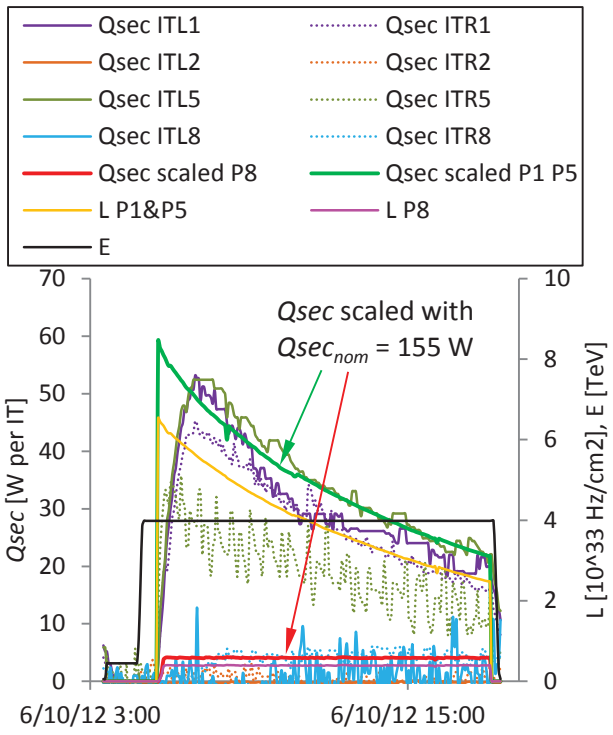

Figure 16: Evolution of secondary particle losses (run3134)

As expected, the losses in the P2 Inner Triplets are negligible (very low luminosity). The secondary particle losses in Inner Triplet at P1 and P5 are significant and show a maximum value around 50 W per IT. In order to scale this evolution according to Equation 5, $Qsec_{nom}$ has to be set at 155 W, i.e. 15 % below the DR value of 180 W. The secondary particle losses at P8 are smaller (~4 W per IT) but are in accordance with the scaled value with a $Qsec_{nom}$ of 155 W.

Dynamic heat load on arc cold masses

The total dynamic heat loads *Qdcm* (loss of secondary particles, beam-gas scattering and resistive heating) can be measured by the variation of the cold compressor pumping flow (S12, S56 & S67) or return module heating (S23). This measurement was only made on the sector equipped with Air Liquide cold compressors given more exploitable data. Figure 17 shows the *Qdcm* evolution for the 4 sectors. At point 6, the same cryoplant is cooling the 2 adjacent sectors (S56 and S67). Consequently, the measured variations correspond to 2-sector heat loads.

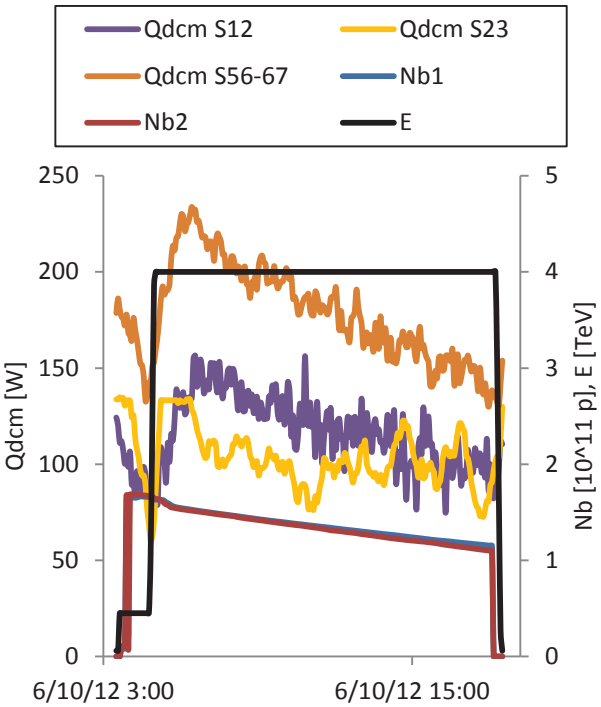

Figure 17: Qdcm evolution for sectors S12, S23, S56 & S67 (run3134)

By subtracting the secondary particle losses measured previously, and by taking into account the length of the concerned cold masses, Figure 18 shows the specific dynamic heat loads in the arc cold masses.

Since the calorimetry [2] performed in 2009 to detect bad splices in the machine, it was shown than the average splice resistance is better than the expected DR data (Qrh_{nom}= 0.10 W/m). The 2009 measured value [3] corresponding to Qrh_{nom}= 0.056 W/m is used in the

scaled evolution (green line in Figure 18) which fits the evolution of the 4 measured sectors.

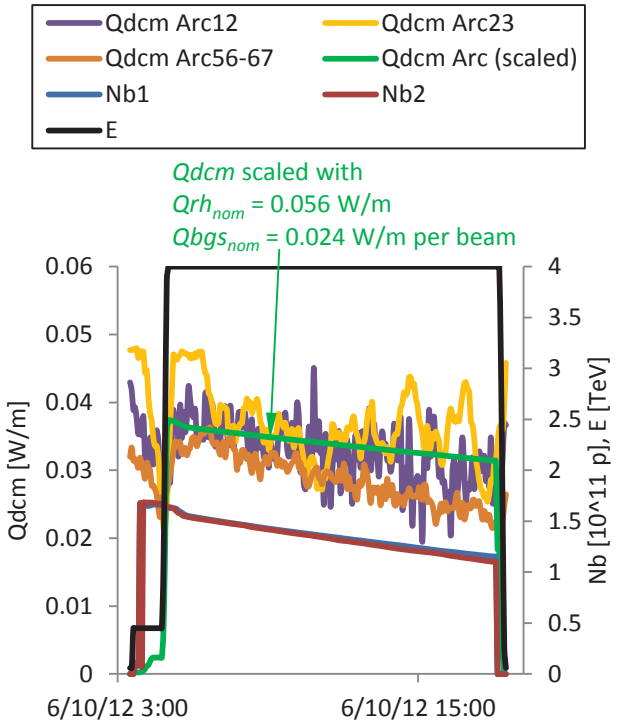

Figure 18: specific *Qdcm* evolution in arc cold masses (run3134)

Scaling for 2015 operation

Scaling laws with corrected parameter ($Qsec_{nom}$ and Qrh_{nom}) can be applied to assess the expected power to be extracted in 2015 for the two 2015 operating scenarios. Table 7 gives the present measured values. Table 8 gives the corresponding total *Qcm* scaled values (including the static heat inleaks *Qscm*) and the locally installed capacity which is mainly due to subcooling heat exchangers capacity or to bayonet heat exchangers (for P1 and P5 Inner Triplets). Table 8 gives also the remaining margins with respect to the local limitations.

Table 7: Run3134 measured values [W]

	Qscm	Qrh	Qbgs	Qsec	Total *Qcm*
Arc cell	18	2.3	2	0.0	22
DS cell	25	1.9	2	0.0	29
ITL1	60	0.5	0.7	60	121
ITR1	52	0.5	0.7	60	113
ITL2	110	0.5	0.9	0.0	111
ITR2	50	0.5	0.9	0.0	51
ITL5	50	0.5	0.7	60	111
ITR5	47	0.5	0.7	60	108
ITL8	80	0.5	0.9	3.6	85
ITR8	46	0.5	0.9	3.6	51

Table 8: *Qcm* Scaled values and remaining margins [W]

	2015 scaled values		Locally installed	2015 remaining margins	
	25 ns	50 ns		25 ns	50 ns
Arc cell	27	26	90(1)	63	64
DS cell	33	32	140(1)	107	108
ITL1	208	208	320(2)	112(3)	112(3)
ITR1	200	200	320(2)	120	120
ITL2	113	112	140(1)	27(3)	28(3)
ITR2	53	52	140(1)	87(3)	88(3)
ITL5	198	198	320(2)	122	122
ITR5	195	195	320(2)	125(3)	125(3)
ITL8	86	86	140(1)	54(3)	54(3)
ITR8	52	52	140(1)	88(3)	88(3)

(1): limited by sub-cooling heat exchanger
(2): limited by bayonet heat exchanger (IT)
(3): could be jeopardized by NC copper braid

Significant margins are existing for arc and DS cells. The identified margins for the Inner Triplet could be jeopardized by non-conformed copper braids on 6 ITs. It is recommended to consolidate these copper braids to fully profit of these extra capacities (Planned for the LS1). Once consolidated, the remaining margins (112 W in ITL1) could be used for higher luminosity production up to $1.75 \cdot 10^{34}$ Hz/cm^2 (scaled from Equation 5).

CRYOPLANT OUTLOOK AND GLOBAL MARGINS

Table 9 recalls the installed refrigeration capacity of the LHC sector cryogenic plants.

Table 9: Installed refrigeration capacity of cryoplants

Temperature level		Installed capacity High-load sectors (S12, S45, S56, S81)	Low-load sectors (S23, S34, S67, S78)
50-75 K	[W]	33000	31000
4.6-20 K (BS)	[W]	7700	7600
4.5 K	[W]	300	150
1.9 K LHe (CM)	[W]	2400	2100
4 K VLP	[W]	430	380
20-280 K	[g/s]	41	27

Figure 19 shows the scaled capacity *Qbs* (25-ns 2015 scenario) required for the beam screen cooling between 4.6 and 20 K. The *Qec* values correspond to the measurements of the December'12 beam scrubbing campaign. The total cooling requirements remain below the installed capacity with margin of about 50 %. A factor 10 is existing between static (only *Qsbs*) and the total cooling requirements. This important factor will certainly create tricky transients both for local and global controls.

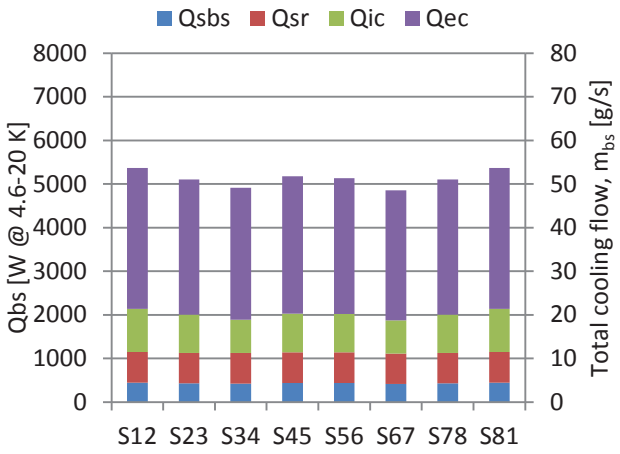

Figure 19: Beam-screen cooling requirement (25-ns 2015 scenario)

Figure 20 shows the scaled capacity *Qcm* (25-ns 2015 scenario) required for the cold-mass cooling at 1.9 K. The total cooling requirements remain below the installed capacity with a large global margin (factor ~2).

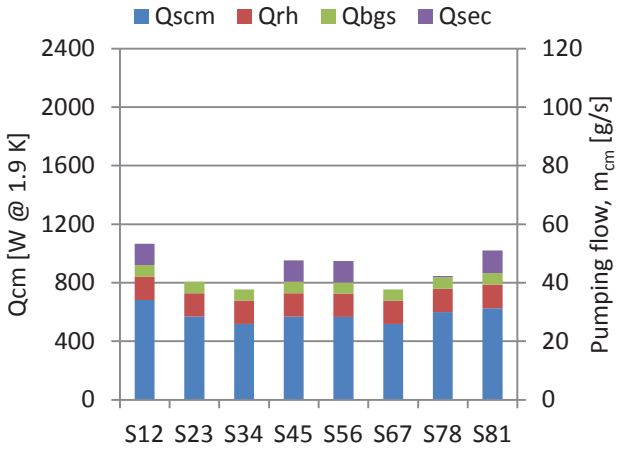

Figure 20: Cold-mass cooling requirement (25-ns 2015 scenario)

Figure 21 shows the arrangement of a cryogenic plant with the two cooling loops for beam screens (BS) and cold masses (CM). These two loop loads are seen by the 4.5-K cryoplant as non-isothermal refrigeration between 4.6 and 20 K. Consequently some capacity sharing is possible. Therefore, the global limitation is when the total flow m_{tot} (= m_{bs} + m_{cm}) reaches the installed flow (197 g/s for high-load sectors and 180 g/s for the low-load sectors). Figure 22 shows the total flow m_{tot} for the different sectors. A cooling margin equivalent to about 90 g/s is existing and corresponds to about 9000 W between 4.6 and 20 K, i.e. about 1.5 W/m per beam for additional dissipation like impingement of photo-electrons, i.e. about 2 W/m per beam available in total for photo-electron impingement (~0.5 W/m per beam already included in the 25-ns 2015 scenario).

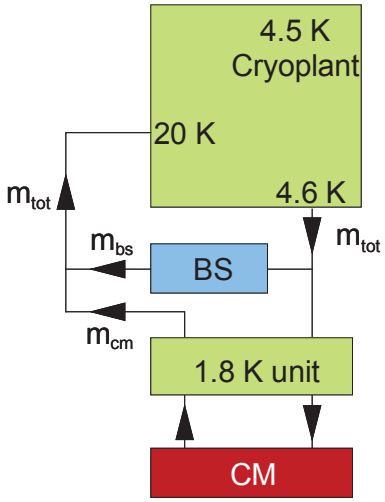

Figure 21: Sector cryoplant arrangement

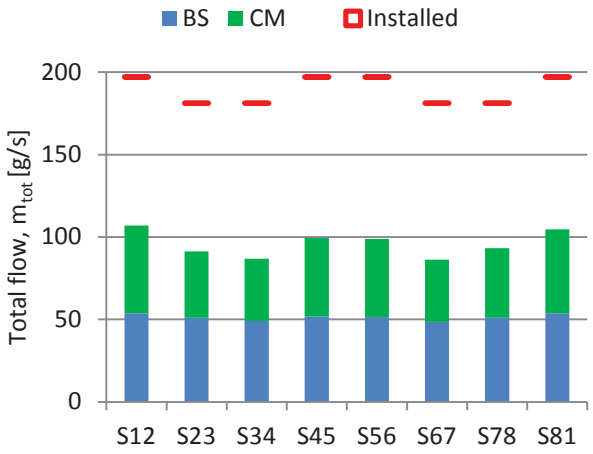

Figure 22: m_{tot} requirement (25-ns 2015 scenario)

CONCLUSION

LHC physics runs have been analysed and dynamic loads have been measured on the beam-screen and 1.9-K cold-mass circuits. Globally dynamic heat loads are below expectation with respect to the Design Report scaling laws except for IT and Q6R5 beam-screen circuits. The scaling laws of dynamic heat loads due to beam-induced heating and splice resistive heating have been refined. Table 10 gives the new working parameters.

A large discrepancy has been identified concerning the resistive dissipation *Qic* of the image current in the Inner Triplets, with:

- a bunch length dependence to the power p= +0.3 (to be compared with p= -2 measured for the rest of the machine and p= -1.5 from the DR).
- a bunch population dependence to the power 1.3 (to be compared with a power factor 2 for the rest of the machine)
- a nominal dissipation of Qic_{nom}= 1.17 W/m per beam (to be compared with 0.135 W/m par beam

measured for the rest of the machine and 0.180 W/m per beam from the DR).

Additional investigation is required to understand this discrepancy. Concerning Q6R5, the proximity of TOTEM roman pots is under investigation.

Table 10: New working data for scaling laws

		DR data	New working data	Delta%
Beam screens	Qsr_{nom} [mW/m per beam]	165	165	0%
	Qic_{nom} (1) [mW/m per beam]	180	135	- 25%
	p (1) [-]	- 1.5	- 2	- 33%
Cold masses	$Qbgs_{nom}$ [mW/m per beam]	24	24	0%
	Qrh_{nom} [mW/m]	100	56	- 44%
	$Qsec_{nom}$ [W per IT]	182	155	- 15%

(1): Not applicable for Inner Triplets

Scaling with 2015 beam parameters shows sufficient margin with respect to local and global cooling limitations by implementing the following consolidations:

- consolidation of the copper braid configuration on 6 over 8 Inner Triplets (planned for LS1). This will allow to efficiently use the 1.9-K cooling margin for luminosity production. However, the maximum luminosity of $1.75 \cdot 10^{34}$ Hz/cm^2 limited today by the consolidated bayonet heat exchanger of the Inner-Triplet cryo-magnets is not in accordance with some simulations showing higher luminosity peak values (up to $2.3 \cdot 10^{34}$ Hz/cm^2).
- increase of the maximum flow coefficient of the beam-screen control valves of the standalone and semi-standalone magnets by exchanging the seat and poppet in order to be compatible with photo-electron impingement of 2 W/m per beam.
- re-installation of the original poppets of the arc34 beam-screen control valves in order to recover the same margin than for the other arcs (to be planned for LS1).

25-ns beam scrubbing run in December 2012 has identified or confirmed:

- a tricky transient to be controlled due to the large dynamic range seen by the 500 local control loops and by the 6 cryoplants. A new control principle is under investigation.
- a discrepancy (about a factor 2) between the cryogenic dynamic heat load measurement (typically 20 kW for the whole machine) and the RF power supply to the beams (typically 40 kW for the two beams). This discrepancy is under investigation by assessing the power dissipated in the warm sections (~3 km) and by assessing the extra capacity supplied by the cryogenic plants during the beam scrubbing run.

ACKNOWLEDGEMENTS

Many thanks to the Cryo-operation team for the tuning of the loops and to Serge Claudet for useful discussions.

REFERENCES

[1] K. Brodzinski and L. Tavian, “First measurements of beam-induced heating on the LHC cryogenic system”, Proc. ICEC24, 2012, pp. 665-668. (CERN-ATS-2013-009)

[2] L. Tavian, “Helium II calorimetry for the detection of abnormal resistive zones in LHC sectors, Proc. PAC’09 Vancouver (2009). (CERN-ATS-2009-006)

[3] G. Ferlin *et al*, “1.9 K heat inleak and resistive heating measurements on LHC cryomagnets” AIP Conf. Proc. 1218 (2010) pp. 1275-1282. (CERN-ATS-2010-016)

LHC VACUUM SYSTEM: 2012 REVIEW AND 2014 OUTLOOK*

G.Lanza*, V.Baglin, G.Bregliozzi, J.M.Jimenez, CERN, Geneva, Switzerland

Abstract

During 2012 only a few beam dumps were attributed to vacuum sector valve closures and the vacuum surface and coating group was involved in only two urgent interventions that kept the beam off for less than two days each. In this paper the pressure threshold policy adopted since the beginning of the LHC running is examined in terms of beam vacuum performances and beam dumps. The so-called "pressure spikes" detected during these years are treated and correlated with the cryogenic temperature, the beam pipe dimensions and non-conformities. A review of the standard and special interventions performed on the beam pipe during technical stops and shutdowns is given, with a list of the main characteristics and foreseen outcomes. Finally, the vacuum expectations during LHC nominal runs, that will follow the LHC consolidations during the Long Shutdown 1 (LS1), are discussed.

INTRODUCTION

The 50 ns scrubbing run and the five 25 ns (Machine Development) MDs performed in 2011 made the 2012 LHC dynamic vacuum negligible compared to the previous years. The reduction of the secondary electron yield well below the buildup threshold for 50 ns was observed all around the machine except where the sectors were opened to air during the winter technical stop. In 2012, 17 beam dumps were attributed to vacuum sector valve closures and this gave a total turnaround time (the time to get back to injection) of 52 hours. The 2012 LHC operation challenged the vacuum surface and coating group with two urgent interventions that made it necessary to stop the beam, however it was only for less than two days each time: the removal of the Longitudinal and Transverse Synchrotron Light Monitors (BSRT) and Wire Scanner Profile Monitor (BWS) in point 4.

In the context of the LHC operation request to reduce the beam downtime during urgent intervention and to minimize the number of technical stops that cause subsequent long recovery time, this paper focuses on the impact that the vacuum interlocks and interventions may have on the beam operation.

The strategy used by the vacuum, surface and coating group to protect the vacuum integrity of the LHC is described. A detailed description of the vacuum recovery after mechanical intervention and the procedure adopted during the years to minimize the beam downtime is given.

Based on the experience acquired during three years of LHC operation (2010-2012), this paper discusses the vacuum expectations and the major concerns for the 2015 LHC operation that will follow its consolidation during the Long Shutdown 1.

VACUUM INTEGRITY PROTECTION

The LHC beam vacuum system is divided into 230 sectors of varying length. The sectorisation strategy focused first on the arcs and standalone magnets, then the experimental areas and delicate equipment. The sector definition was a compromise between the safety and operational requirements, the costs and the ring complexity. The power limitation for bake-out and the reduction of potential intervention in high radiation area was taken into account in order to determine the sector valve position [1,2].

To protect the beam pipe from any possible sudden air venting, to minimize the propagation of the effect of a leak and finally to reduce the beam downtime, the 353 vacuum sector valves installed in the LHC are triggered to closure, by gauges and ion pumps, when the detected pressure rises above the interlock pressure limit.

The vacuum interlocks are set with different purpose for the warm and cold vacuum system.

On warm vacuum system, where the leak opening can saturate several NEG chambers, the vacuum interlocks are set to reduce the recovery time determined by the bake-out and NEG vacuum activation procedure.

On the cold vacuum system, the valve closure in case of pressure rises, minimizes the gas contamination of the beam screen and it avoids the need of a magnet warm-up.

The valve closing time varies from 0.5 to 1.1 s. This doesn't include the 300 ms integration time of a penning gauge due to its controller Pfeiffer TPG300 [3].

The pressure interlock threshold value, valid for most of the sector valves in the LHC is $4x10^{-7}$ mbar (N_2 equivalent).

This value is lower than the pressure value corresponding to $1.7x10^{17}$ He molec./m^3 that is the estimated gas density over 1m to induce a quench at 7TeV in the LHC superconducting magnet ($7x10^8$ protons/m/s lost in the cold mass).

The interlock threshold is obviously higher than $1x10^{15}$ H_2 molec/m^3 that is the maximum gas density allowed in the arcs to grant 100h beam lifetime.

Below this limit the vacuum beam lifetime remains always negligible compared to other beam lifetime factors. That is why the 100 hour limit was chosen.

The sector valve opening is interlocked as well and a lower threshold has been set to $1x10^{-7}$ mbar. When the pressure goes below this value on both sides of the sector valve, it is possible to open it and connect the two sectors. The lower threshold is set to avoid mistakenly connecting a baked sector with an unbaked or open one and to let the pressure recover during operation after any possible sector valve closure due to pressure rise.

The sector valve interlock is triggered by a logic combination of signals and it applies a redundancy N=3 or 4 vacuum components: two gauges and one or two ion pumps. The redundancy N increases the reliability of the interlock system and eliminates the possibility of valves closure due to a single component failure.

The only condition while the beam is dumped due to vacuum is when N-1 of the N equipment reach the limit. In that case the signal for beam dump is sent to the sector valves for closure. The loss of the sector valves open status triggers the beam dump.

A general rule applied almost to the entire machine for sector valves closure is that once the interlock is triggered, the valve of the concerned sector and the valves of the two adjacent sectors close.

The experiment central beam pipes have a different rule regarding interlock valve closure: to protect the fragile beryllium central beam pipe from overpressure, the sector doesn't close in case of pressure rise. Instead, the Interaction Point (IP) sector valves stay open to keep the chambers connected with the two adjacent sectors. Those two sectors are the only warm sectors equipped with a rupture disk that opens at 500 mbar over the atmospheric pressure.

Finally there are pressure gauges and ion pump signals that are used by clients to monitor their vacuum status equipment. Those signals are used also as interlocks and each equipment owner decides the threshold and chooses how to use it. The table below summarizes the upper and lower vacuum interlock thresholds required and defined by the vacuum clients: Transverse Damper (ADT) by the clients.

Equipment	Lower threshold	Upper threshold
ADT	$5x10^{-7}$ mbar	$1x10^{-7}$ mbar
MKB	$2x10^{-5}$ mbar	$1x10^{-5}$ mbar
MKI	$2x10^{-8}$ mbar	$1x10^{-8}$ mbar
RF Cavities	$4x10^{-7}$ mbar	$1x10^{-7}$ mbar

Impact of the Pressure Threshold on Recovery Time

6 km of the LHC Long Straight Section are NEG coated. The NEG coating, after vacuum activation, enables a distributed pumping speed all along the beam pipes with a secondary electron yield close to unity and extremely low photon and ion induced desorption yield.

The NEG dissolves into the bulk, in the form of solid solutions, all main gases present in the air (Oxygen, Nitrogen, Carbon Dioxide, and Carbon Monoxide) except Argon [4]. After the NEG activation, an ultra-high vacuum pressure is granted in the warm straight section but, in case of leak, all the air is pumped by the NEG. This means the detection of a pressure increase in the gauge of the sector might not be as rapid as required.

The following example shows, seeing as each vacuum gauge indicates a local pressure value [5], how a pressure rise due to an air leak opening is masked by several meters of fully vacuum activated and NEG coated beam pipe.

In Figure 1 the pressure distribution time development in a simplified NEG coated system is described. The 114 m NEG coated sector is vacuum activated. At its extremities and every 28m there is a vacuum module with an ion pump. There is only one gauge positioned at 28m from the left end. In the unfortunate event that a leak opens at 7m from the gauge, the entire system would be affected by a distributed pressure increase.

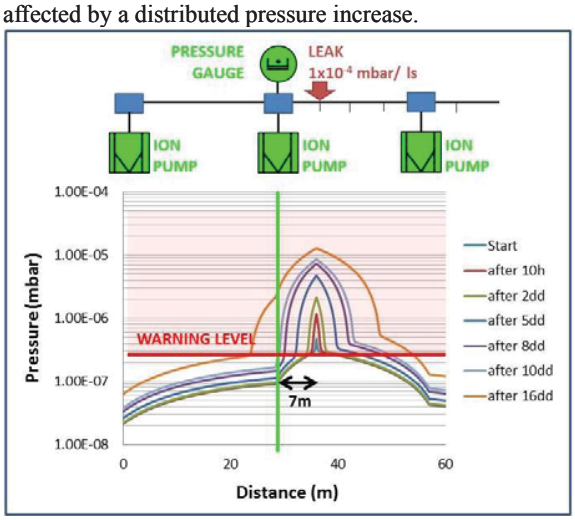

Figure 1: Pressure profile time evolution of a vacuum activated NEG vacuum sector when a leak of $1.4x10^{-4}$ mbar/ls opens at 7m far from the gauge. The pressure increase is proportional to the NEG saturated length.

In Figure 1 the case of a $1.4x10^{-4}$ mbar/ls leak is used to describe the pressure evolution along the system. After 10 hours the gauge still registers a pressure of $8x10^{-8}$ mbar while at the position of the leak the pressure is $1x10^{-6}$ mbar. It takes between 8 and 10 days and about 12 m of saturated NEG chamber to reach the interlock level ($4x10^{-7}$ mbar) on the gauge.

The NEG saturation length is linear with the time the NEG is exposed to air. An increased interlock threshold level of one order of magnitude would require 10 times more time to be detected. Once the NEG coating in the sector is widely saturated, it takes a complete bake out and NEG activation intervention for the initial condition to be restored – the recovery time is consequently severely affected.

Dealing with pressure spikes

Pressure gauge controllers and ion pump power supplies have "no intrinsic intelligence". The interlock crate that receives the signal from the gauges and pumps is only "logic"-based *i.e.* there is no signal treatment.

With the actual system of vacuum interlocks, it is impossible to distinguish a pressure spike from a pressure rise due to a leak before the pressure starts decreasing again. Pressure spikes exceeding the high interlock limit will always trigger the sector valve fast closure, as requested after the incident in the arc 3-4.

Mainly during 2011, some non–conformities present at the level of the RF inserts in LHC sectors like the A4L2,

A4R2, A4L8 and A4R8 [6] caused six beam dumps. The number of dumps due to RF finger non-conformities was reduced after the 2011-2012 winter technical stop where most of the critical non–conformities were exchanged (e.g. CMS and vacuum module VMTSA, in Figure 2). In some more severe cases the interlock level was increased up to $1x10^{-6}$ mbar to let the beam circulate without interruption. Protecting the machine is always the priority, so each case of interlock level increase was and has to be evaluated with the owners of the surrounding equipment and endorsed by the LHC operators.

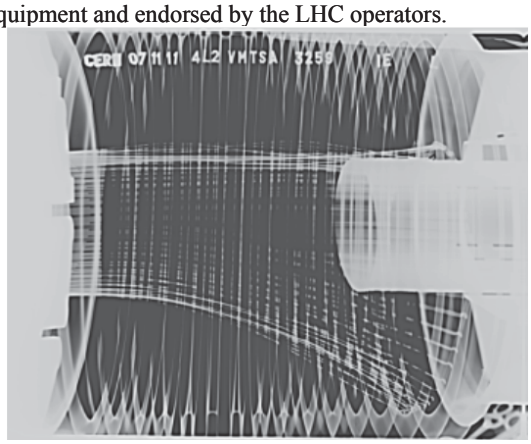

Figure 2: X-ray image of the non-conform RF fingers detected in a VMTSA vacuum module.

During periods like the scrubbing runs or the MDs, to allow for the conditioning of the machine, the interlock can be temporarily increased. In these cases a vacuum operator is always present in the control room to monitor the pressure rises around the ring. As the beam lifetime during scrubbing is shorter, a smaller vacuum beam lifetime remains negligible compared to the beam lifetime.

Beam dumps related to vacuum

During 2012, 17 beam dumps were attributed to vacuum sector valve closures (Figure 3) and this gave a total turnaround time (*i.e.* the time to get back to injection) of 52 hours.

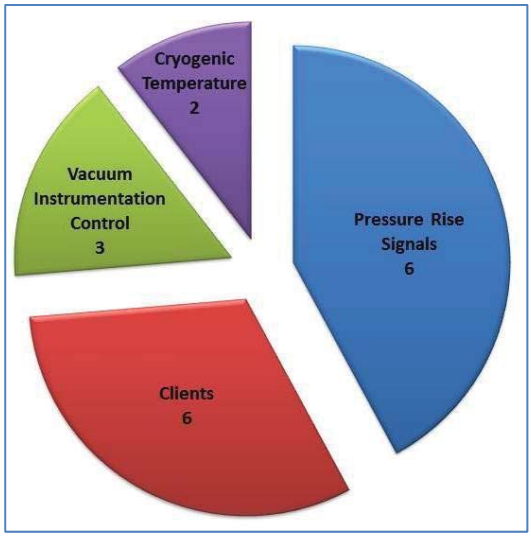

Figure 3: The type distribution of beam dumps attributed to vacuum sector valve closures during 2012.

The following paragraph summarizes the five reasons that caused the sector valve closure and induced the beam dumps in 2012.

Three vacuum beam dumps were related to vacuum instrumentation control: vacuum gauges, ion pumps or PLC which switched off or went to undefined status. During the LS1 the vacuum surface and coating group will implement all the Radiation to Equipment (R2E) recommendation to reduce the number of possible electronic fault.

Two pressure rise and beam dumps were connected to cryogenic temperature oscillations. One example is presented in Figure 4: after 10 hours of continuous neon injection in the LHCb beam pipe (SMOG – System for Measuring the Overlap with Gas injection) a beam dump was registered on the inner triplets on the right of IP 8 during beam injection. The beam screen equilibrium surface coverage depends on parameters such as the beam parameter and the beam screen temperature and is perturbed by gas load coming from the beam screen (BS) warm-up or quench or, like in this case, unusual high gas density in the beam pipe due to neon accumulation.

If the surface coverage exceeds its equilibrium value, pressure excursion or transient could appear during the beam injection due to cryogenics temperature oscillation [7,8].

Another type of vacuum beam dump was a pressure rise signal observed in the vicinity of the collimators. Unfortunately in this area it is tricky to distinguish the real pressure signal, when the gas desorption is induced by proton hitting the beam pipe walls from the “false” signals produced by a possible ionization of the cables (phenomena already observed in ISRs).

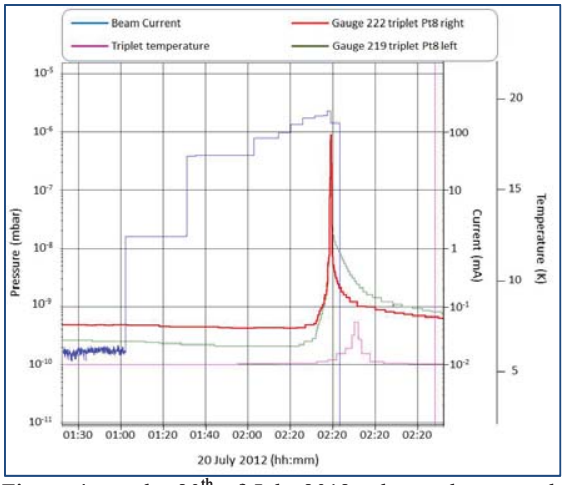

Figure 4: on the 20th of July 2012 a beam dump on the inner triplets on the right of IP 8 was registered during beam injection.

The final causes for beam dump were the mechanical non-conformities [6] of the vacuum beam pipes. At the moment all non-conformities have been detected and their reparation is foreseen during the LS1.

Finally the machine equipment like MKI, RF cavities, MKB and ADT that use vacuum gauges or pumps to monitor their equipment vacuum status, have directly or indirectly hardware-connected their vacuum alarm to the beam dump. The absence of any redundancy was the cause of four beam dumps during 2012.

VACUUM INTERVENTIONS

The standard vacuum intervention on the beam pipe restores the previous pressure in the concerned sector. This intervention has no impact on the LHC operation, beam lifetime and on the background of the experiments.

The vacuum intervention baseline is the bake out of each component of the beam pipe and the vacuum activation of the NEG coated components.

The intervention time schedule for venting and bake out for a typical LHC vacuum sector is two weeks. This time can vary, depending on the sector and the mechanical intervention complexity. This intervention includes the activities listed in Table 1. For each activity the average timescale is also given.

Table 1: Average timescale of the standard bake out and NEG vacuum activation intervention

Activity	Time (h)
Preparation and sector venting	0.5
Mechanical intervention	-
Pumping	1
Bakeout installation	24
Bakeout and NEG activation	120
Bakeout removal	12

The interventions performed with nitrogen venting, bake out and activation in 2012 are: the Zero Degree Calorimeter (ZDC) upgrade in point 2 left and right, the VMTSA reparation in point 8 left and right, the warm transition of the Q5 left of IP1 RF insert exchange, the Ionization Profile Monitor (BGI) opening in point 4 on the left and the BSRT removal in point 4 on the left.

One exceptional intervention performed during the technical stop 4 on the LHC was the MKI exchange. This intervention was characterized by three peculiarities:

- 5 days of Technical Stop: continuous day and night shifts.
- Additional manpower
- 3 weeks of preparation of the kicker on the surface where the kicker was pumped and baked and kept under vacuum between its two sector valves until its installation in the machine.
- a complete week was dedicated to scrubbing the new component after its installation.

An exceptional, alternative solution is the intervention under neon flux [10]. This choice has to be made by the vacuum surface and coating group experts together with the LHC committee in order to evaluate possible consequences. This modus operandi reduces the intervention, avoids a major NEG saturation but a local saturation close to the exchanged piece is inevitable. The intervention consists of overpressurizing (100-300 mbar over the atmospheric pressure) the beam pipe with neon, exchanging or removing the damaged piece, closing the sector and pumping it down.

For the neon gas option and the neon intervention modus operandi cf. reference [9]. The concerned sector and its equipment must be able to stand the overpressurisation. A careful a priori preparation of the activities is important to minimize the mechanical intervention time.

The Neon venting without bake out is a five-day intervention that includes:

- compulsory bakeout of the neon trolley,
- neon venting and overpressurization of the vacuum sector,
- mechanical intervention and sector closure,
- neon pump down with a baked pumping group,
- neon pump down with the vacuum sector ion pumps.

Depending on the available time, the sector may just be pumped down or a partial bakeout of the saturated area may be added to the procedure.

The new uncoated installed piece or chamber would require beam conditioning, and temporary local pressure rises in its vicinity are expected during the restart of the LHC operation.

Three examples of neon intervention effectuated in 2012 are: the RF insert exchange in CMS, the BSRT and the BWS removal in point 4 right and left respectively.

2014 OUTLOOK

The LS1 vacuum consolidation includes:

- the reparation of all non-conformities,

• all the actions on the electronics to fulfill the R2E recommendations,

• the NEG coating of the 150 inter-modules in the experimental zone for e-cloud mitigation purpose,

• The insertion of NEG coated liners inside the 800 mm vacuum chambers to reduce the background in ALICE,

• the NEG coating of 150 module in the LSS for e-cloud mitigation purpose,

• the optimization of the pumping layout all around the machine where it was considered a potential limitation for the machine nominal operation: MKI, collimators and TDI where having a built-in operational contingency would grant more pumping speed.

More than 90% of the beam pipe will be opened to air during the LS1 and, as a consequence, the secondary electron yield and the electron stimulated gas desorption will be reset for almost the entire machine. Since previously scrubbed and air exposed surface scrubs about ten times faster than an "as-received" surface, the conditioning of "old" chambers and components will be faster [10]. Moreover the new components installed during the LS1 will need a complete conditioning.

The two major concerns, related to the vacuum activity after the LS1 are:

- the proton stimulated gas desorption at 6.5 TeV from collimators will be larger than what we had at 4TeV,

- the possible pressure excursion related to beam screen temperature regulation following operation with 25 ns beams.

Finally, after the LS1, the beam energy will approach its nominal value, leading to an increase of the synchrotron radiation critical energy, that is proportional to the photon stimulated desorption yield, and the augmentation of the photon flux. The expected desorption due to synchrotron radiation is one order of magnitude higher than the one experienced in 2012. This source of gas will decrease with the beam pipe conditioning. [11]

SUMMARY

The vacuum interlock system was designed to protect the integrity of the vacuum system from sudden pressure rise. The interlock limit is 4×10^{-7} mbar; it has been relaxed during scrubbing runs and MDs and in special cases where the presence of non-conformity in the beam pipe was detected.

The standard vacuum intervention includes the bakeout and NEG activation of the beam pipe that may take from 5 days with shifts, additional manpower and increased control of safety aspects, to 2/3 weeks depending on the sector complexity. The neon venting interventions may be carried out in special cases and require at least 5 complete days.

The operation experience from the 2012 run confirmed that the scrubbing and beam pipe conditioning approach is a valid option for the future beam operation.

*giulia.lanza@cern.ch

ACKNOWLEDGMENT

Many thanks to Paolo Chiggiato and Gregory Pigny for their patience, fruitful discussions and comments.

REFERENCES

[1] J. M. Jimenez, document EDMS 382884, *Vacuum Sectorisation of the LHC long straight sections and experimental areas*.

[2] LHC design report

[3] J. Chauré, document EDMS 1254417, *ECR: Sector Valves Upgrade.*

[4] P. Chiggiato et al, Thin Solid Film 2006; 515, 2: 382-388

[5] G. Bregliozzi et al, IPAC 2012, New Orleans, USA

[6] G. Bregliozzi et al, LHC Beam Operation workshop, Evian 2012

[7] V. Baglin, LHC Project Workshop – Chamonix XIV

[8] V. Baglin, LHC Project Workshop – Chamonix XIII

[9] G. Bregliozzi et al, PAC 2009, Vancouver, Canada

[10] J.M. Jimenez et al., CERN LHC Project Report 632 (2003), *Electron Cloud with LHC-Type Beams in the SPS: A Review of Three Years of Measurements*

[11] V. Baglin et al, IPAC 2011, San Sebastian, Spain

UFOs: OBSERVATIONS, STATISTICS AND EXTRAPOLATIONS

T. Baer* (CERN, Switzerland and University of Hamburg, Germany), M.J. Barnes, F. Cerutti, B. Dehning, E. Effinger, B. Goddard, A. Lechner, V. Mertens, E. Nebot del Busto, M. Sapinski, R. Schmidt, J. Uythoven, J. Wenninger, F. Zimmermann (CERN, Switzerland), M. Hempel (DESY-Zeuthen, Germany)

Abstract

Unidentified falling objects (UFOs) could be a major limitation for nominal LHC operation. Therefore, in 2011/12, the diagnostics for UFO events were significantly improved, dedicated measurements, MDs and laboratory tests were performed and complemented by simulations (FLUKA & MadX) and theoretical studies.

In this talk the state of knowledge is summarized and extrapolations for LHC operation with 25 ns bunch spacing and at higher energy are presented. An overview of the mitigation strategies (in particular BLM redistribution and MKI modifications) is given and a first evaluation is shown.

OBSERVATIONS AND STATISTICS

In 2012/13 UFOs led to 22 premature protection beam dumps of LHC fills (in total 58 since 2010). UFOs are presumably micrometer sized dust particles that lead to beam losses with a duration of about 10 turns when they interact with the beam. Such events were observed in the whole machine and for both beams, for proton as well as for lead ion operation. From mid 2011 onwards, their impact on LHC availability was mitigated by increasing and optimizing the BLM thresholds. Figure 1a and 1b show the spatial and temporal loss profile of a typical UFO event. An introduction to the topic is given in [1, 2, 3].

Most of the UFO events lead to beam losses far below the BLM dump thresholds. These events are detected in real time by the *UFO Buster* application [1]. In 2012 more than 17'000 candidate UFO events have been detected (16'000 in 2011).

In 2012 the diagnostics for UFO events were significantly improved: additional BLMs are installed in the arc cell 19R3 [3] and the BLM Study Buffer allows the measurement of the temporal loss profile with 80 μs time resolution also for UFO events below the BLM dump thresholds [3]. Since May 2012, dedicated diamond BLMs in IR7 are used to further improve the temporal resolution for UFO events to ns time-scales [4]. Figure 1c and 1d show the temporal loss profile measured with the beam 2 diamond BLM in IR7. Figure 1d shows that the bunches contribute equally to the beam losses, as expected for a macro particle interaction.

The evolution of the arc UFO rate is shown in Fig. 2. Throughout 2011 and 2012 a clear conditioning effect is observable, which leads to a decrease of the UFO rate by about 80% per year. Over the winter technical stop 2011/12 a deconditioning was observed, resulting in a $\approx$ 2.5 times

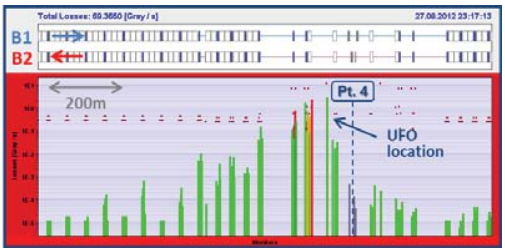

(a) Spatial loss profile (ring BLMs).

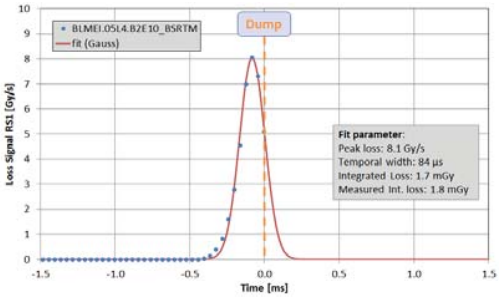

(b) Temporal loss profile (ring BLM).

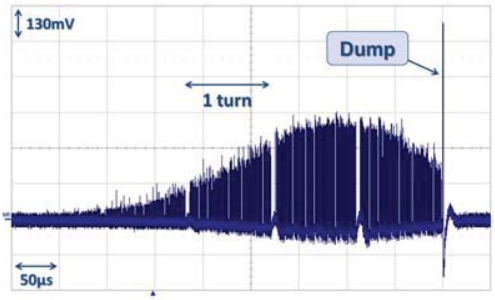

(c) Temporal loss profile (IR7 diamond BLM, 50 μs/div).

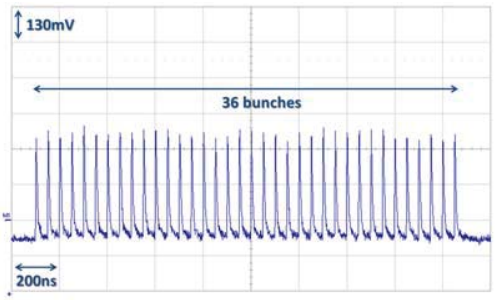

(d) Temporal loss profile (IR7 diamond BLM, 200 ns/div).

Figure 1: Spatial (a) and temporal (b, c, d) loss profile of an UFO event around the beam 2 synchrotron light monitor during stable beams, measured with the ring BLMs (a, b) and the beam 2 diamond BLM in IR7 (c, d). The beam losses reach up to 219% of the BLM dump thresholds. The losses start $\approx$ 5 turns before the beam dump (b, c). All bunches contribute equally to the beam losses (d).

* contact: Tobias.Baer@cern.ch

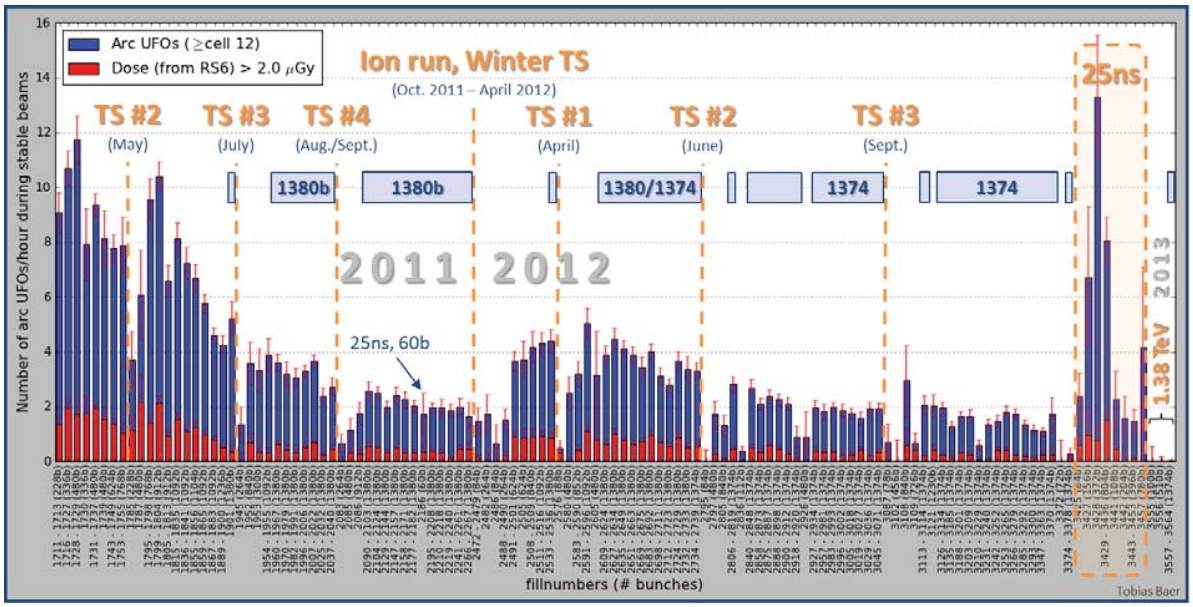

Figure 2: The arc UFO ($\geq$ cell 12) rate during stable beams. The rate is decreased in the intermediate intensity fills after the technical stops (TS). 9406 UFOs in all proton-proton fills with at least one hour of stable beams since 14.04.2011 until the end of the 2012/13 run are taken into account. Up to 5 consecutive fills with the same number of bunches are grouped. Only UFOs with a signal in 640 μs running-sum $> 2 \cdot 10^{-4}$ Gy/s and with a signal in 320 μs running-sum / signal in 80 μs running-sum ≥ 0.45 are considered.

increased arc UFO rate in the beginning of 2012. In the fills with 25 ns bunch spacing, the UFO activity is significantly increased (initially by over a factor 10 [5]). During the intermediate energy run in February 2013, not a single UFO was observed in about 17.5 hours at 1.38 TeV with 1374 bunches.

The dependence of the UFO rate on the beam intensity could be observed during the fast intensity ramp up in 2012 without being biased by the conditioning effect (Fig. 3). In agreement with previous studies [6] the rate of detectable UFO events increases proportionally to the beam intensity for small intensities. Above a few hundred bunches the effect saturates.

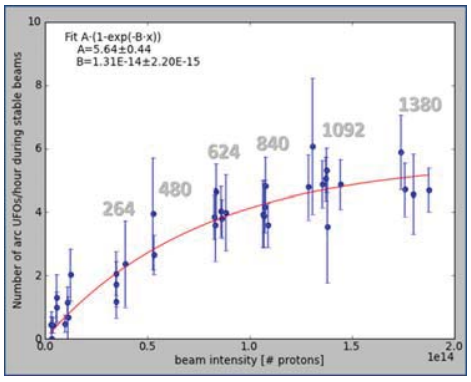

Figure 3: The arc UFO ($\geq$ cell 12) rate as a function of the beam intensity. The gray numbers indicate the number of bunches. 667 UFOs in 37 fills with at least 1 hour of stable beams during the intensity ramp up between 05.04.2012 and 10.05.2012 are taken into account. Signal in 640 μs running-sum $> 2 \cdot 10^{-4}$ Gy/s.

Based on the different running-sums of the BLM data, the temporal structure of the UFO events can be determined. Figure 4 shows the distribution of the temporal width of UFO events assuming a Gaussian loss profile. For many UFOs the temporal width is in the order of the LHC revolution period (89 μs), or even faster. It is expected that the temporal loss profile becomes even faster for operation at higher energies due to the smaller transverse emittance. This implies that some UFOs may be too fast for active quench protection by a beam dump[1].

To identify potential UFO locations, FLUKA [7, 8] simulations of (inelastic) proton-UFO interactions and the in-

[1] Up to three turns are needed until the full beam is extracted after the detection of an abnormal beam loss.

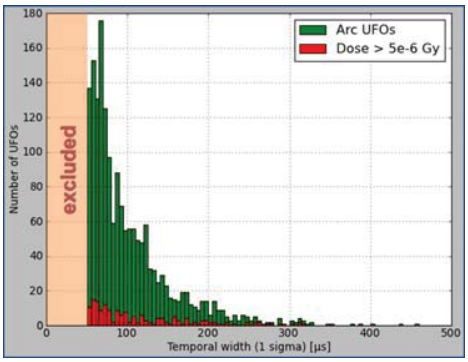

Figure 4: Distribution of temporal width from Gaussian fit of UFO events. 1753 arc UFOs ($\geq$ cell 12) at 4 TeV operation with 1374/1380 bunches are taken into account. UFO events with a temporal width < 50 μs or a peak loss rate of the fit $< 1 \cdot 10^{-3}$ Gy/s are excluded from the analysis.

duced particle showers were performed [9]. The simulations reveal that with standard quadrupole BLMs a precise loss location cannot be identified. To improve the spatial resolution, additional BLMs were installed at the three dipole magnets in cell 19R3 in early 2012. UFO events observed in cell 19R3 in 2012 indeed exhibit different loss patterns, suggesting that UFOs originate from various positions across the arc cell [10]. In particular, loss patterns suggesting UFO locations close to the magnet interconnections have been observed as well as loss patterns suggesting UFO locations inside dipole magnets [11].

MKI UFOS

Four injection kicker magnets (MKIs) are installed in each injection region (Pt. 2 for injection of beam 1, Pt. 8 for injection of beam 2). The MKIs in Pt. 2 and Pt. 8 are labeled MKI.A - MKI.D with MKI.D being the magnet seen first by the injected beam.

With 21 beam dumps since 2010 (8 in 2012), the UFOs at the MKIs had the largest impact on LHC operation. 16 of these events occurred at top energy, but only 5 during stable beams. 17 events occurred at the MKI.D in Pt. 2.

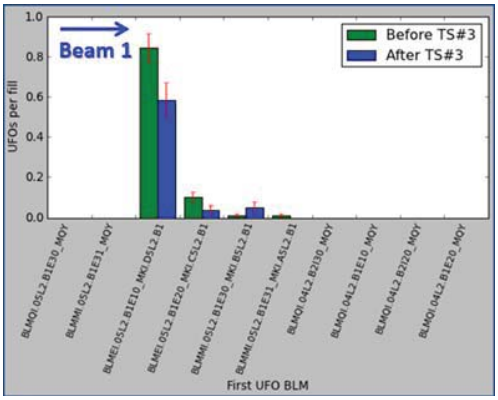

(a) Pt. 2.

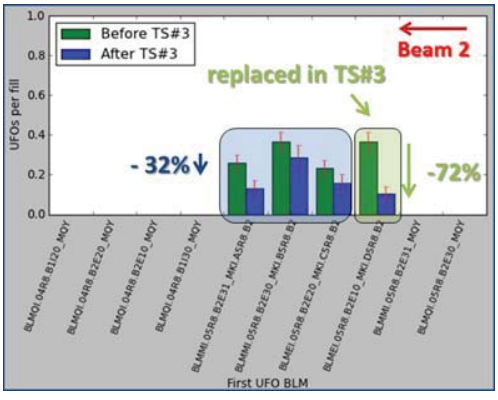

(b) Pt. 8.

Figure 5: Distribution of UFOs among the individual MKI magnets in Pt. 2 (a) and Pt. 8 (b) before and after TS#3 in 2012. The BLMs at the MKIs indicate in which magnet an UFO occurs. 145/52 UFOs (a) and 194/52 UFOs (b) in 159/77 fills with stable beams and at least 1000 bunches before/after TS#3 are taken into account. Signal in 640 μs running-sum $> 5 \cdot 10^{-4}$ Gy/s.

After a comprehensive study program in 2011 the MKI UFOs have been identified as macro particles originating from the ceramic tube inside the MKI magnets [12]. In the technical stop in September 2012 (TS#3), the MKI.D in Pt. 8 was replaced by an improved version, which includes UFO-mitigation measures[2].

Figure 5 shows the distribution of UFOs among the different MKIs in Pt. 2 and Pt. 8 before and after TS#3. Whereas in Pt. 2, the UFO activity in MKI.D is dominant, the distribution is more equal among the four MKIs in Pt. 8. Notably, before TS#3, MKI.D had the highest UFO activity of the MKIs in Pt. 8; after the replacement MKI.D has the lowest UFO activity. The number of UFOs per fill at MKI.D is reduced by $(72 \pm 11)\%$ compared to an average reduction (due to the general conditioning effect) of $(32 \pm 12)\%$ at the other MKIs. This shows that the modifications of MKI.D in Pt. 8 indeed significantly mitigated the UFO activity.

MID-TERM EXTRAPOLATION

As shown in Fig. 3 there is no significant increase of the UFO activity expected for operation with design intensity.

As shown in Fig. 2 the UFO rate is significantly increased with 25 ns operation (initially over a factor 10 [5]). Nevertheless, with higher UFO activity, also a faster conditioning effect is expected [5].

The beam losses due to UFOs are expected to increase with beam energy. Figure 6 shows the peak energy density per inelastic proton-UFO interaction (at the interconnection between two arc dipole magnets) in the downstream dipole magnets. The highest energy density is caused by the neutral collision products of the proton-UFO interac-

[2] In particular, an improved cleaning procedure was applied and the electrical field during most of the MKI pulse is reduced by four additional screen conductors.

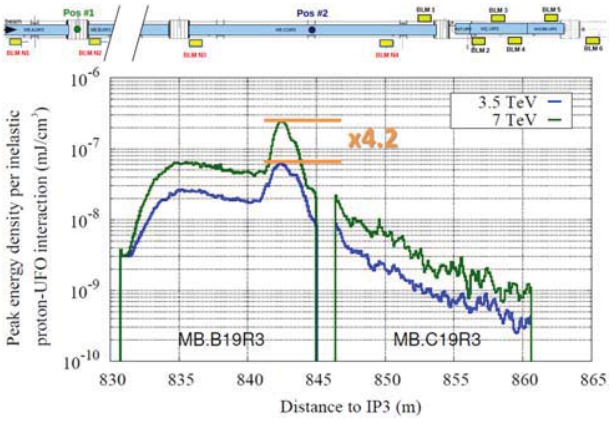

Figure 6: Peak energy density per (inelastic) proton-UFO interaction at *Pos #1* (dipole-dipole interconnect) in the downstream dipole magnets simulated with FLUKA (courtesy of A. Lechner and the FLUKA team [9]).

tions, which impact the magnet ≈ 11 m downstream of the UFO location due to the geometrical bending of the magnet [9]. Fig. 6 shows that the peak energy density per inelastic proton-UFO interaction is about a factor 4.2 higher for 7 TeV operation compared to 3.5 TeV operation[3].

Based on the FLUKA simulations [9], about $1.3 \cdot 10^8$ inelastic proton-UFO interactions are needed to explain the observed beam losses for the largest arc UFO which was observed in 2012[4]. An UFO event at *Pos #1* with the same number of inelastic proton-UFO interactions would accoring to Fig. 6 imply a peak energy density in the dipole magnet of $\approx 7.8 \frac{\text{mJ}}{\text{cm}^3}$ for 3.5 TeV operation and $\approx 32.5 \frac{\text{mJ}}{\text{cm}^3}$ for 7 TeV operation.

These values are compared in Fig. 7 to the expected quench margin for the LHC arc dipole magnets. For 3.5 TeV operation, the beam losses are at about 30% of the QP3 quench margin, for 7 TeV about a factor 5 above the QP3 quench margin.

The expected scaling of BLM signal/BLM threshold for UFO events is shown in Figure 8. Applying the scaling to the BLM signals and thresholds of all 2012 arc UFOs, they would have caused 91 beam dumps, if the LHC would have been operated at 7 TeV instead of 4 TeV (112 beam dumps from 2011 arc UFOs). An additional 21 beam dumps would have been caused by MKI UFOs (27 beam dumps from 2011 MKI UFOs)[5]. These numbers have to be compared to one actual dumps by arc UFOs and 8 dumps by MKI UFOs in 2012 (2011: 2 dumps by arc UFOs, 11 dumps by MKI UFOs).

In February 2013, a dedicated magnet quench test with beam losses on UFO-timescales was performed. The initial analysis indicates that the quench level is significantly above the expected level, which would allow for large-scale increases of the arc BLM thresholds and significantly mitigate the extrapolation shown in Fig. 8 [5]. A detailed analysis of the quench test is ongoing.

[3]The scaling is geometry dependent. A scaling of a factor 3 was found from wire scanner measurements at different energies [6] and FLUKA simulations for MKI UFOs [13].

[4]The event occurred on 05.10.2012 at 06:19:41. Beam losses of 0.67 mGy were measured at *BLM 2* (cp. Fig. 6). It is assumed that the UFO occurred at *Pos #2*, i.e. close to the quadrupole magnet. The FLUKA simulations for 3.5 TeV are used for the analysis.

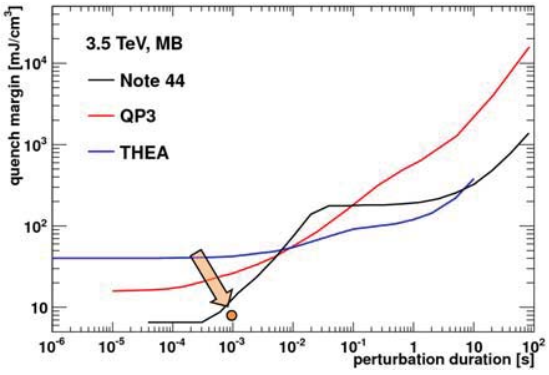

(a) Quench margin at 3.5 TeV.

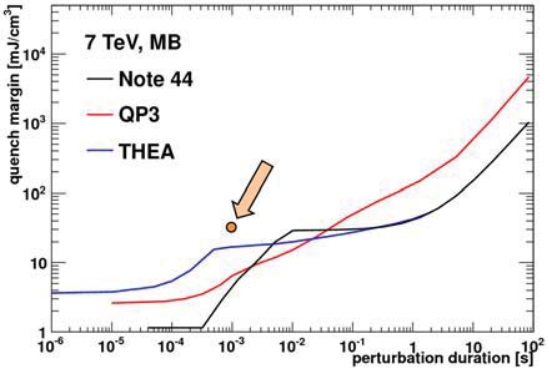

(b) Quench margin at 7 TeV.

Figure 7: The estimated quench margin of the LHC main dipole magnets as function of the beam loss duration from LHC Project Note 44 [14], the QP3 model and the THEA model [15] for operation at 3.5 TeV (a) and 7 TeV (b). The orange point indicates the estimated peak energy density in the magnet for $1.3 \cdot 10^8$ inelastic nuclear proton-UFO interactions at *Pos #1* (cp. Fig. 6).

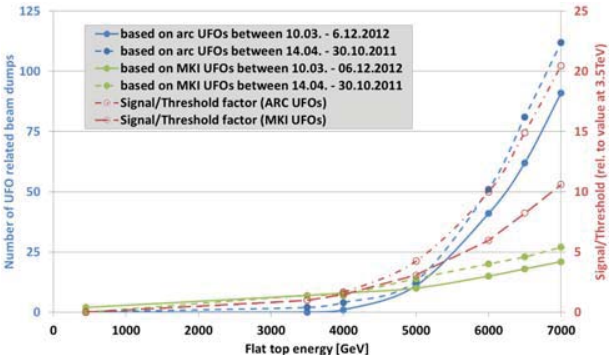

Figure 8: The expected number of beam dumps by arc and MKI UFOs and the expected scaling of BLM signal/BLM threshold as function of the beam energy (based on [6, 9, 13]).

MITIGATION AND OUTLOOK

The energy dependence indicates that UFOs could be a major performance limitation for LHC operation after the long shutdown in 2013/14 (LS1).

Concerning the MKIs, the source of the UFOs is identified and many mitigation measures are in preparation for after LS1:

- All MKI magnets will be equipped with 24 screen conductors. This reduces the electric field during the majority of the MKI pulse. The electric field is thought to be responsible for causing the detachment of macro particles from the ceramic tube [12].

[5]The extrapolation assumes (apart from the beam energy) identical running conditions as in 2011/12. Excluded are potential increases of the BLM thresholds, the conditioning effect, the increased UFO rate at 25 ns operation and changes in beam intensity and beam size. Concerning the MKI UFOs, only the BLM thresholds at the superconducting elements are assumed to be limiting.

- An improved cleaning procedure will be applied to all MKIs. This is expected to reduce the initial macro particle contamination by a factor 5-7 [12].
- The MKI interconnect, bypass-tubes and close-by equipment will be NEG coated. This mitigates electron-cloud and improves the vacuum in the MKIs. Electron-cloud and high vacuum pressure were observed to enhance the UFO activity.
- A coating of the ceramic tube, possibly with carbon or Cr_2O_3, is under investigation. This would reduce electron-cloud activity and the risk of surface flashovers in the MKIs and could seal the surface of the ceramic tube.

In particular the successful reduction of the UFO activity with the replacement of the MKI.D in Pt. 8 demonstrates the effectiveness of the mitigation measures.

The main mitigation strategy for arc UFOs is to increase the BLM thresholds towards the magnet quench limit and to profit from the conditioning effect.

Nevertheless, the arc FLUKA simulations and the additional instrumentation in cell 19R3 show that the current BLM distribution (six BLMs per half-cell, all at the quadrupole) is highly inefficient for protection against beam losses due to UFOs at the dipole magnets [16]. Furthermore, the current BLM distribution implies an over-redundancy for protection against beam losses at the quadrupole magnet. Thus, a systematic relocation of the arc BLMs is proposed: Two BLMs of each half-cell will be moved from the quadrupole and be positioned vertically above the dipole-dipole interconnects as illustrated in Fig. 9.

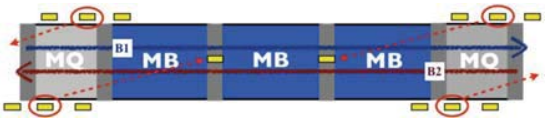

Figure 9: Proposed relocation of BLMs during LS1, seen from the top (courtesy of E. Nebot del Busto [16]).

Moreover, during LS1, several magnets will be replaced, which allows an endoscopic inspection of three locations with particularly high UFO activity (16L3.B2, 25R3.B2, 28R7.B2).

CONCLUSION

Since 2010 in total 54 LHC fills were terminated above injection energy due to UFOs. Thus, between 2011 and 2013 intensive studies were made, which include improvements of the diagnostics, dedicated experiments in the LHC (including a magnet quench test) and in the laboratory, FLUKA and MadX simulations and theoretical studies. As a result, fundamental correlations were found, the macro particle dynamics are characterized, the response of the BLM system is understood and the source of the UFO events at the MKIs has been identified. This allows for mid-term extrapolations.

In particular the energy and bunch-spacing dependence imply that UFOs could be a major performance limitation for LHC operation after LS1. Thus, various mitigation measures for MKI UFOs are ongoing and a large-scale relocation of the arc BLMs during LS1 is proposed to allow a better protection against arc UFO events.

REFERENCES

[1] T. Baer et al., "UFOs in the LHC", IPAC'11, TUPC137, Sep. 2011.

[2] T. Baer et al., "UFOs in the LHC after LS1", Chamonix Workshop 2012, Feb. 2012.

[3] T. Baer et al., "UFOs in the LHC: Observations, Studies and Extrapolations", IPAC'12, THPPP086, May 2012.

[4] M. Hempel, "Application of Diamond Based Beam Loss Monitors at LHC", Master thesis, DESY Zeuthen/Brandenburg University of Technology/CERN, Nov. 2012.

[5] T. Baer et al., "UFOs - Observations, statistics and Extrapolations", 7th meeting of the CERN Machine Advisory Committee, Mar. 2013.

[6] E. Nebot del Busto et al., "Analysis of fast Losses in the LHC with the BLM System", IPAC'11, TUPC136, Sep. 2011.

[7] G. Battistoni et al., "The FLUKA Code: Description and Benchmarking", HSS'06, Mar. 2007.

[8] A. Ferrari et al., "FLUKA: a Multi-Particle Transport Code", CERN-2005-10, Oct. 2005.

[9] A. Lechner et al., "FLUKA Simulations of UFO-induced Losses in the LHC Arc", 2nd Quench Test Strategy Working Group Meeting, CERN, May 2012.

[10] T. Baer et al., "UFO Statistics and Extrapolations", 6th meeting of the CERN Machine Advisory Committee, Aug. 2011.

[11] A. Lechner et al., "Analysis of 2012 UFO Events in 19R3", 4th LHC UFO Study Group Meeting, CERN, Aug. 2012.

[12] B. Goddard et al., "Transient Beam Losses in the LHC Injection Kickers from Micron Scale Dust Particles", IPAC'12, TUPPR092, May 2012.

[13] A. Lechner, "FLUKA Simulations of UFO-Induced Losses in IR2", 3rd LHC UFO Study Group Meeting, CERN, Sep. 2011.

[14] J.B. Jeanneret et al., "Quench Levels and Transient Beam Losses in the LHC Magnets", LHC Project Report 44, May 1996.

[15] L. Bottura et al., "A General model for Thermal, Hydraulic and Electric Analysis of Superconducting Cables", LHC Project Report 456, Dec 2000.

[16] E. Nebot del Busto et al., "Beam Losses and Thresholds", MPP Workshop 2013, Mar. 2013.

BLM THRESHOLDS. PAST EXPERIENCE AND STRATEGY AFTER LS1.

E. Nebot del Busto, T. Baer, G. Bellodi, C. Bracco, B. Dehning, J. Jowett, E.B. Holzer, A. Lechner, B. Salvachua, R. Schmidt, S. Redaeli, A. Priebe, M. Sapinski, J. Wenninger, D. Wollmann, C. Zamantzas, M. Zerlauth, CERN, Geneva, Switzerland

Abstract

The history and motivation of dump threshold changes for the Beam Loss Monitoring (BLM) system throughout the 2012 run are described here. Also discussed are several dedicated beam experiments to probe the quench levels at different time scales foreseen for the end of the current run. The implications of these results to the threshold strategy are outlined. Moreover, the noise inherent to the BLM system may become an operational limitation in 2014 if running with the current dump thresholds. The most critical locations are discussed and revised thresholds are proposed that would mitigate the problem. Finally, the installation of new BLMs or the relocation of existing ones will require modifications that are explained in this document.

RECALL OF THRESHOLD CALCULATION

The main goal of the BLM system is to protect the LHC superconducting magnets against quench and any other equipment against damage induced by beam losses. The beam dump thresholds must be chosen carefully in order to not only protect the LHC equipment but also maximize the machine availability. In the most limiting case, i.e. BLMs protecting superconducting magnets, the dump thresholds may be written as:

$$T(t,E) = 3 \cdot \frac{E_{BLM}(t,E)}{E_{COIL}(t,E)} \cdot Q_L(t,E) \cdot C(t,E) \quad (1)$$

where t is the beam loss duration and E the beam energy. The values of E_{BLM} and E_{COIL} represent the energy deposited in the BLM and in the magnetic coil respectively. Note that this two quantities are typically extracted from Monte Carlo simulations. The energy dependence in both terms accounts for the fact that the energy density increases with the energy of the primary particle. The quench margin, $Q_L(t,E)$, is an intrinsic property of the protected magnet and it is computed via the algorithms derived from Note 44 [1] or by means of simulation codes such as QP3 [2]. Moreover, several corrections ($C(t,E)$) may be applied in order to account for various effects: electronic saturation, filter delays, margin for injection, etc. By convention, the thresholds are set to a factor three higher than the best estimation of the quench margin. Hence, a multiplicative factor three is present in the equation above. Note that the thresholds are technically implemented as a table of 12x32 (12 running sums and 32 energy levels).

To take into account potential uncertainties on Monte Carlo simulations and for operational flexibility an applied Thresholds Table is defined as:

$$t(t,E) = MF \times T(t,E) \quad (2)$$

where the monitor factor, MF, is enforced to be lower (or equal) than one. The Applied Thresholds are the tables sent to the electronics and they are independent for each BLM. Typically calculated with $MF = 0.1$, the dump thresholds are set to roughly a factor three below the quench limit estimation.

HISTORY OF CHANGES AND MOTIVATION DURING 2012

A set of 221 modifications for the BLM thresholds of individual detectors have been implemented for the operation of the LHC in 2012 (note that modifications for special running such as Machine Developments, MDs, are not accounted here). The full list of changes is summarized in Table 1. Most of the modifications were driven by Instabilities while Squeezing-Colliding (ISC) the LHC beams. The first set of threshold changes were implemented during the first intensity ramp-up of the year (50 BLMs protecting 2 TCLA collimators and 48 warm quadrupoles in IR3 and IR7) as the thresholds at the time were not able to sustain losses with beams of 824 nominal bunches. The second main modification corresponds to tuning of the dump threshold to allow the collimation system to clean losses of up to 200kW as explained in a subsequent section. After the extensive threshold tuning before the start of the 2011 run to allow UFO losses, only one increase of thresholds was required during 2012. Four BLMs protecting Q4L2 and Q4R8 had their thresholds increased in order to allow losses produced by UFOs generated in the injection kickers. Finally, minor changes in the Roman Pots in IP5, monitor factor increase by a factor 3, were implemented.

Table 1: Summary of BLM threshold changes throughout the 2012 run.

Date	BLMs	Location	Comment
Mar 12th	15	L2,L8	new BLMs
Apr 13th	50	IR3,IR7	ISC
Apr 19th	4	4R2,4R8	MKI UFOs
May 4th	2	L7	ISC
May 8th	4	R6,L6	ISC
Jun 28th	41	IR3,IR7	200kW IR7
Jul 13th	72	IR3,IR7,IR6	ISC
Oct 25th	1	6R5	correc
Nov 8th	2	IR5	Margin RP
Nov 30th	30	IR3,IR7	200 kW IR3

Note that despite the large number of BLMs that required modification, there is a reduction of more than a factor 20 with respect to 2011, where about 90% of the roughly 4000 BLMs had their thresholds changed. The number of interventions has also been reduced by a factor 2 with respect to the previous year. Note also that only a 20% (44) of the changes affected the protection of cold elements, while 44% (98) affected warm elements (roman pots and normal conducting quadrupoles) and 36% affected collimators.

UFO RELOCATION

The BLM system in the LHC arcs equips the Main Quadrupoles (MQ) with three Ionization Chambers (IC) per beam separated by 3 and 4 m respectively. This provides both redundancy and spacial resolution to distinguish between beam losses originated at different points within an MQ, but it prevents from determining the original location of the beam loss if it happens anywhere within the three Main Bending (MB) dipoles located in between. During the beginning of the 2011 LHC run, four ICs were situated at the MB magnets of cell 19R3[1] as shown in Figure 1. Comparison of data collected during the 2012 run with FLUKA simulations [3] demonstrated that UFO losses can originate anywhere within the LHC FODO cell. Therefore, the BLM system in its current configuration does not protect MB magnets against potential quenches generated by UFO losses.

Several new configurations of the BLMs have been discussed, all of them based on the relocation of the second BLM at the MQ to a certain position along the arc cell. The first proposal consists of moving the IC to either immediately after the interconnection MB.A-MB.B (BLM N2) or immediately after the interconnection MB.B-MB.C (BLM N3). Table 2 summarizes simulation results [4] for three different UFO locations and the two proposed BLM positions. The numbers indicate the threshold reduction that would be required at the BLMs in their current position in order to protect against the various UFO losses. Note that, even though the signal gain is quite significant in all cases, some of the configurations do not protect for all the UFO scenarios. The possibility of locating the BLMs at the interconnect between MB.A and MB.B (and MB.B and MB.C) has been found as a better solution. This proposal presents the advantages (with the proper choice of transverse position) of covering UFO losses originated anywhere along the arc cell. Note that dedicated simulations will be required in order to estimate the BLM signals necessary to calculate specific BLM threshold.

QUENCH TESTS

A period of 48 hours has been allocated at the end of the 2013 run in order to perform dedicated exercises to probe the quench limits in different time scales. In this section

[1]Cell 19R3 is one of the LHC locations where a larger fraction of UFOs has been systematically observed.

Table 2: Signal gain factor for several BLM relocation and UFO scenarios.

UFO location	BLM N2	BLM N3
MB.A end	80	13
MB.B beginning	–	50
MB.B end	–	7

are described the expectations of those test as well as the impact on the threshold strategy for LS1.

Possibly the test that could have a biggest impact will be the test trying to probe the Quench level in the ms scale, where the current calculation (based on Note 44) seems to underestimate the quench margin. In previous MDs, it has been demonstrated that the tranverse damper (ADT) and kicker for tune and aperture measurements (MKQ) can be used to generate losses in the ms scale. The QP3 code predicts a quench margin which at 3.5 TeV is on the order of $30\ \mathrm{mJ \cdot cm^3}$. However, extrapolations from data collected during 2012 [5] indicate that the maximum energy deposited in the coils is at the level of 10% of the estimated quench margin. Geant 4 simulations with geometries equivalent to that in cell 12L6, are used to estimate the energy depositions in the magnetic coils within the conditions of the proposed experiment. Comparing those energy depositions with the estimated quench levels with the QP3 code [2], a quench is expected to occur for total beam losses in the order of 10^8 protons. This, if confirmed, will have a severe impact on the BLM thresholds as corrections would be required in all BLMs protecting cold elements.

Two independent exercises are foreseen to test if magnets MQ8R7 or MQR9R7 could be quenched due to collimation cleaning losses. In previous tests [6], losses of 500 kW at the primary collimator were achieved while reaching 70% of the assumed quench level in Q8. In this case the beam was excited by tune resonance crossing, generating beam losses of about one second. The proposed test will apply an ADT excitation to generate losses of a longer scale. The BLM threshold for Q8 and Q9 are calculated based on a different (direct impact of protons in the beam screen) loss scenario. Therefore, a quench may occur for signals that exceed the current estimated quench level. If this is confirmed, it may have an impact on the BLM thresholds for the cold elements in the Dispersion Suppressor (DS). The same exercise is scheduled with an ion beam. The previous attempt [7] achieved BLM signals at the estimated quench level for losses in a shorter time scale. The expected impact on BLM thresholds is a potential increase for cold elements in the DS as well as possible specific loss locations for the ion operation.

Another experiment will be conducted to explore the quench level in the steady-state limit. In this case, an orbital bump and an ADT excitation will be produced to generate losses at the center of Q12L6. In previous tests the estimation of the quench level for losses of 5 seconds was found to be a factor 3 too high and the BLM thresholds

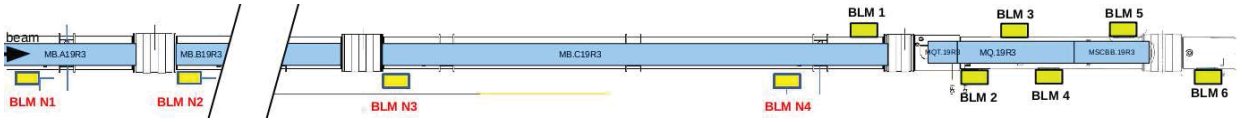

Figure 1: Schematic view of the BLM location in cell 19R3.

were accordingly corrected. The goal of the exercise is to achieve longer losses that approximate better to the steady-state case. The results of this test may impact the dump threshold for all the BLMs protecting cold elements.

The last proposed test consists of injecting probe bunches onto a closed TCLIB in order to produce showers that may quench Q6. The current of Q6 will be increased to study the energy behaviour of the quench level. No quench was achieved in previous attempts [8].

NOISE

In order to study the performance of the BLM system in terms of noise, the signals observed in the detectors are analyzed during periods without beam. The noise of a BLM is defined as the maximum signal (integrated over 40 μs) recorded in a period of 9 h. As an example, Figure 2 shows the noise versus threshold for 7 TeV operation with data collected on December 11th starting at 17:00 local time. The aim of this analysis is to identify potential locations where the BLM system could trigger a beam dump as a consequence of its intrinsic noise. The red line corresponds to the case in which the noise would reach the dump thresholds while the blue line represents a noise level at 10% of the dump threshold. The later is choosen as level for comfortable operation. The analysis showed no signals higher than 50% of the threhold but about 40 BLMs were found above the operational limit. The list includes BLMs protecting MQM and MQML magnets in the long straight section and Dispersion Suppressor (DS), MB magnets in the DS, several quadrupoles in the arc and injection septa magnets MSI.

Several mitigation strategies have been applied in the past. During the previous shut down period, about 3 km of standard BNC read-out cable (affecting 90 monitors) were replaced by a new NES-18 cable with a double copper shielding in order to minimize the effect of noise. Further cable replacements (6 km affecting 22 BLMs) are foreseen during LS1.

Typically, a correction that allows at least 10 times the noise level (i.e operational margin) has been applied, by imposing a minimum threshold of 0.15 Gy/s in the 40 μs integration window and decaying exponentially to simulate the signal collection time. This value, as shown in Figure 2, is above the dump threshold for several monitors. However, note that there is some margin in the dump thresholds as they are typically set well below (factor 3.3) the estimated quench limit. In case of this level being above the estimated quench levels, redundancy of the BLM system would need to be considered.

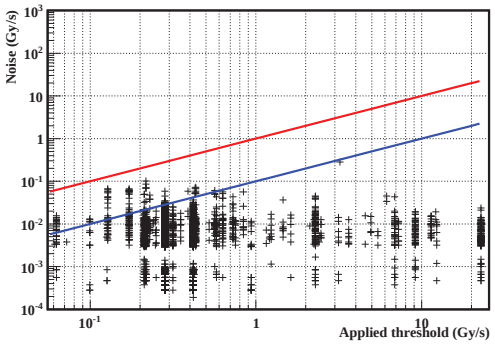

Figure 2: Noise vs thresholds for all ionization chambers. Data collected during December 11th 2012.

TRIPLET MAGNETS

Initial thresholds settings for triplet magnets were calculated according to the Note 44 quench level estimations [1] and dedicated FLUKA simulations [9] of three different failure scenarios (at 7 TeV), namely:

- Beam loss at TAS. The obtained energy depositions in the coil were on the order of $2-3\cdot10^{-9}\mathrm{mJ}\cdot\mathrm{cm}^{-3}$ per lost proton.
- Proton direct impact at the center of a triplet magnet as a consequence of misalignment of primary and secondary collimators (or accidental retraction of tertiaries). For the so-call Q2B loss scenario, the estimated maximum energy depositions in the coil were in the order of $159\cdot10^{-9}\mathrm{mJ}\cdot\mathrm{cm}^{-3}$ per lost proton.
- Particle debris originated in the interaction point due to p-p collisions. In this case, $5\cdot10^{-9}\mathrm{mJ/cm}^3$ per proton-proton interaction was computed.

As the most limiting case (by two orders of magnitude), the Q2B loss scenario was the selected case for the calculation of the original thresholds. However, several changes were introduced to the original settings during the 2011 run. Moreover, the dump thresholds in the long integration windows (5.3 seconds and above) were increased in order to allow for extra luminosity induced losses [10].

During high luminosity fills at 4 TeV, the signals observed in BLMs protecting triplet magnets systematically reached 50-80% of the dump threshold due to signals induced by particle debris. The current thresholds decrease by a factor 4.5 when going from 4 TeV to 7 TeV operation. Moreover, the signals observed in the BLMs are

expected to increase by a factor 1-3.3 depending on the considered magnet and the BLM position. Hence, it is expected that the BLMs would get signals a factor 2.25-7.42 over the dump threshold, making operation not possible with the current settings. However, it is believed that the current quench levels are very conservative and the situation will be revised. As an example, when comparing the estimated quench levels for MQ magnets ($24\,\mathrm{mW \cdot cm^{-3}}$ at 450 GeV and $5\,\mathrm{mW \cdot cm^{-3}}$ at 7 TeV) and triplet magnets ($50\,\mathrm{mW \cdot cm^{-3}}$ at 450 GeV and $12\,\mathrm{mW \cdot cm^{-3}}$ at 7 TeV) only a factor 2-2.5 difference is found. This is in contradiction with the fact that the triplet magnets were designed to sustain significantly more radiation than the standard quadrupoles. Moreover, the loss scenario used to set thresholds in the steady-state case (currently Q2B in the full time range) may be revisited. Finally, note that the long term plan (foreseen for LS2) is to provide a more direct measurement of the energy depositions in the magnetic coil by locating diamond detectors in the cold mass [11].

OPTIMIZATION OF COLLIMATION THRESHOLDS

Several changes were introduced to the original threshold settings [12] for the BLMs protecting LHC collimators during the 2012 run. The dump thresholds for BLMs at TCP, TCSG and TCLA collimators in IR7 [13] were increased to allow (collimation design) 500 kW[2] power loss at primary collimators by scaling the beam losses observed during betatron loss maps. This was possible as such beam losses have been measured during MDs [6] without the observation of any magnet quench. In a subsequent step, a similar change was introduced for IP3 collimators in order to avoid limiting losses due to off-momentum particles [14]. Further threshold increases at collimators are foreseen at the beginning of the 2014 run. In particular, tertiary collimators in IP1/5 have been observed to exceed the warning level (30% of threshold) during high luminosity fills.

SUMMARY AND CONCLUSIONS

A large campaign of threshold changes is expected during LS1. Potentially all the BLMs protecting cryogenic magnets and several monitors protecting collimators will require a modification. Two ionization chambers per quadrupole will be moved to a different location for better protection of MB magnets against UFO losses, and this monitors will require specific thresholds. The result of several dedicated experiments to probe the quench level in different time scales will be taken as input for the BLM thresholds. An intensive effort will be necessary for understanding the different measurements. The signals observed in the BLMs will be taken as input and Monte Carlo simulations will provide the energy depositions in the magnetic coil. Furthermore, the energy deposition in the coils needs to be compared with the quench levels predicted by the Note 44 model as well as the QP3 program. The BLMs at locations affected by Noise may need to be increased in the short running sums in order to overcome false dumps. Finally, monitors protecting triplet magnets will also have their thresholds revisited. The loss scenarios as well as the quench level predictions that determine the original BLM threshold calculation need to be investigated.

[2]Note that the thresholds are reduced to sustain a power loss of 200 kW, as mentioned in previous sections, via the monitor factor.

REFERENCES

[1] “Quench levels and transient losses in LHC magnets”, J.B Jeanneret et al. LHC-Project-Note-44 (1996).

[2] “QP3: users manual”, A. Verweij, CERN/EDMS 1150045.

[3] “Analysis of 2012 UFO events in 19R3”, A. Lechner. August 9th 2012, UFO study Working group.

[4] “FLUKA simulations of UFO-induced losses in the LHC ARCs”, A. Lechner, Apri 5th 2012 . UFO study Working group.

[5] “UFOs: Observations, statistics and extrapolations”, T. Baer, this proceedings.

[6] “Quench test at the hadron collider with collimation losses at 3.5 Z TeV”, S.Redaelli, MOP240, September 2012, HB2012.

[7] “Pb ions collimator losses in IR7 DS and quench test at 3.5 Z TeV”, G.Bellodi, CERN-ATS-Note-2012-81.

[8] . “Experiments on the margin of beam induced quenches a superconducting quadrupole magnet in the LHC.”, C. Bracco, MOPPC004, May 2012, IPAC2012.

[9] “Estimation of BLM thresholds on the LHC insertion superconducting magnets”, F Cerutti et al, CERN/EDMS 1049072.

[10] “BLM thresholds for the 2011 start up”, E. B. Holzer et al, CERN/EDMS 1133965.

[11] “Investigation of the use of Silicon, Diamond and liquid Helium detectors for beam loss measurements at 2 K”, C. Kurfuerst, TUOAB02, May 2012, IPAC 2012.

[12] “Initial settings of Beam Loss Monitors thresholds on LHC collimators”, A.Gomez Alonso et al, CERN/EDMS 995569.

[13] “Increase of BLM thresholds for collimators in IP7”, E. Nebot, CERN/EDMS 1227009.

[14] “Increase of BLM thresholds for collimators in IP3”, E. Nebot, CERN/EDMS 1251530.

LHC COLLIMATION CLEANING AND OPERATION OUTLOOK

B.Salvachua*, R.W.Assmann†, R.Bruce, M.Cauchi, D.Deboy, L.Lari,
A.Marsili, D.Mirarchi, E.Quaranta, S.Redaelli, A.Rossi, G.Valentino,
CERN, Geneva, Switzerland

Abstract

An overview of the collimation system performance during 2012 is described. The collimator "tight" settings for the 60 cm $\beta^\star$ reach are introduced and the evolution of the cleaning inefficiency achieved throughout the year with one single collimator alignment is presented. The performance of the semi-automatic collimator alignment tools is discussed. We investigate the beam losses through the cycle with emphasis on the yearly evolution of the measured instantaneous beam lifetime in critical phases of the operational cycle.

The concept of collimators with integrated beam positions monitors (BPM) is presented here and their effect on the $\beta^\star$ reach after the long shutdown I is analyzed. The baseline settings strategy for the startup in 2015 is discussed based on the expected performance of the collimators with BPMs. New values of $\beta^\star$ reach are discussed.

THE LHC COLLIMATION SYSTEM

The LHC collimation system provides a multi-stage cleaning in the two warm cleaning insertions, IR3 for momentum cleaning and IR7 for betatron cleaning. The primary collimators (TCPs) are the closest to the beam in transverse normalized space, cutting the primary halo. The secondary collimators (TCSGs) cut the particles scattered by the primaries (secondary halo) and the absorbers (TCLAs) stop the showers from upstream collimators [1]. The tertiary collimators (TCT) protect directly the triplets at the colliding IRs. Together with the passive absorbers, the physics debris absorbers, transfer line collimators, injection and dump protection makes a total of 108 collimators, hundred of them movable that need to be aligned within $10-50$ μm precision to achieve the required cleaning.

During 2012 running period with 4 TeV beam energy the collimator system was setup with the so-called "tight" collimator settings [2], illustrated in Fig. 1. The primary collimators are set to the nominal 7 TeV gap in mm which corresponds to 4.3 σ at 4 TeV, where σ is the transverse beam size assuming transverse normalized emittance of $\epsilon_{norm} = 3.5$ μm rad. We will assume in all the document the same normalized emittance unless explicitly quoted. The secondaries and absorbers in IR7 are placed at 6.3 σ and 8.3 σ respectively. The secondary collimator in IR6 (part of the dump protection system) is at 7.1 σ and TCTs at 9 σ, protecting the tripet aperture of 10.5 σ and allowing a $\beta^\star$ of 60 cm. These settings were validated during MD's in 2011 [2] [3] [4]. In particular, it was verified that the proposed hierarchy could be achieved without additional alignment campaigns, indicating that the orbit and collimator settings are stable enough to ensure a good hierarchy with 2 σ retraction between TCP's and TCSG's. Optimization of TCT settings and measurement of the aperture that can be protected are detailed in [5] [6] [7].

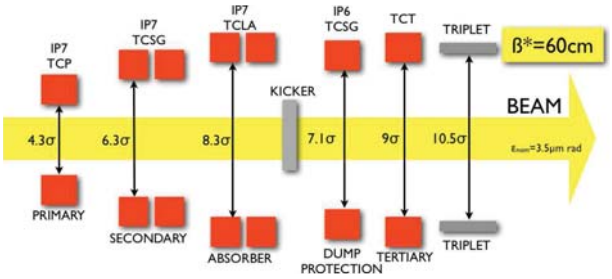

Figure 1: Tight collimator settings for 4 TeV beam energy and $\beta^\star = 60$ cm.

SYSTEM PERFORMANCE

All collimators are setup symmetrically around the beam orbit for each machine configuration (*i.e.* injection, flat top, squeeze and collisions) with full gap as small as 2 mm. The alignment procedure aligns each collimator jaw independently based on the beam loss monitor (BLM) spike observed when touching the beam halo produced with the primary collimators. This is done only in dedicated low intensity fills with up to 3 nominal bunches in order to avoid any machine damage.

The operational strategy during 2011 and 2012 run periods was to perform one full alignment of the main cleaning insertions (IR3 and IR7) and monitor regularly the losses along the ring to validate if a new alignment was needed by looking at the cleaning and the collimator hierarchy. For new physics configurations only the 16 TCTs collimators at the colliding IRs need to be re-aligned.

Since 2010 several improvements have been implemented in the alignment software towards a faster and more reproducible alignment [8] [9] [10]. The main improvement on the alignment speed was the use of the 12.5 Hz BLM data, available from the start of 2012 run. This allowed to use the maximum collimator movement rate of 8 Hz that before was limited by the 1 Hz BLM data. In

* belen.salvachua@cern.ch
† Present address: DESY, Germany

addition, currently, it is possible to align in parallel several collimators and the algorithm routine automatically identifies the loss spike and decides if the collimator is completely aligned. Fig. 2 shows the setup time per collimator as function of time. Nowadays, all collimators in IR7 (19 collimators per beam) and IR6 (2 collimators per beam), a total of 42 collimators, can be re-aligned in about 50 min. Ever since the semi-automatic alignment was set in place, no more beam dumps at top energy happened during alignments [10].

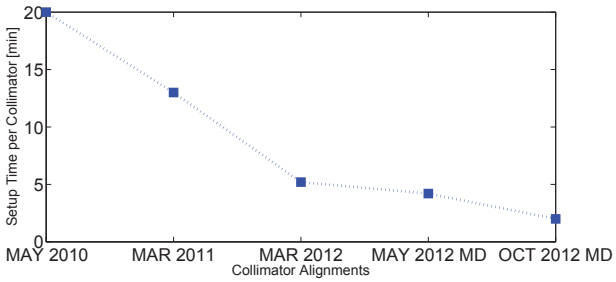

Figure 2: Setup time per collimator versus alignment date.

Losses along the ring

In order to validate the cleaning hierarchy and study the performance of the collimator system, loss maps are performed. Beam losses are recorded along the ring while exciting the beam with the transverse damper (ADT) [11] and are compared with the peak losses at the primary collimators to compute the cleaning inefficiency. The ADT introduces white noise in vertical or horizontal plane that can be gated to selected bunches. When the ADT is working on this mode the excited bunch is blown up and interacts with the collimators producing beam losses along the ring. Fig. 3 shows the losses, noise subtracted and normalized to the highest loss, for beam 1 (beam is going from left to right) blown up in the horizontal plane. The highest peak occurs at the betatron cleaning insertion (IR7). The minimum cleaning inefficiency is defined as the highest leakage at the cold magnets, which is in the dispersion suppressor region of IR7. Fig. 4 shows a zoom into IR7, the cleaning hierarchy appears as decreasing losses from the primary collimators (left IR7) to the absorbers (right IR7). The local cleaning inefficiency is measured at Q8 magnet, in this case right of IR7.

The local cleaning inefficiency from 2010 to 2013 is provided in Fig. 5. In 2010 and 2011 the beam energy was 3.5 TeV and the relaxed collimator settings were used [12] while in 2012 the beam energy was increased to 4 TeV and the tighter collimators settings described in previous section were used. The figure shows an excellent stability of the cleaning performance which was achieved with only one alignment campaign per year at the beginning of each run period. In 2012, with the "tight" settings the cleaning improved from 99.97 % to 99.993 %. This was observed also during a machine development test in 2011 [3]

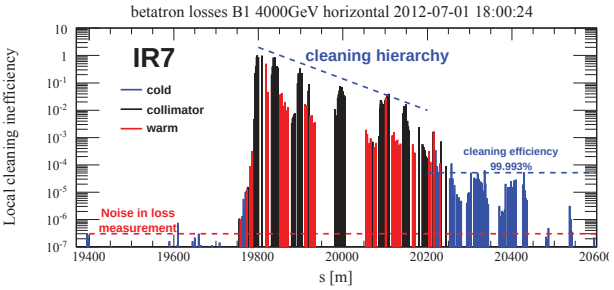

Figure 4: Distribution of the losses in the betatron cleaning insertion (IR7) while exciting beam 1 in the horizontal plane.

which is included in Fig. 5. The performance shown in the plot has been calculated taking into a account all top energy cycles, and no significant differences on the cleaning in IR7 were found. This confirms that the IR7 cleaning is not much affected by changes in the colliding IRs [13].

Lifetime through the cycle

The maximum number of charges that can be injected in the machine without risk of quenching a magnet is determined by

$$N_{\max} = \tau_{\text{beam}} \cdot \frac{dN}{dt} \approx \tau_{\text{beam}} \cdot R_{\max}^{\text{TCP}} = \tau_{\text{beam}} \cdot \frac{R_{\text{q}}}{\eta_c}$$

where τ_{beam} is the minimum beam lifetime, dN/dt is the particle loss rate which is approximated to the particle loss per second at the primary collimator $R_{\max}^{\text{TCP}}$. R_{q} is the quench limit and η_c is the collimation cleaning inefficiency [14]. We have studied the beam lifetime through the LHC cycles by analyzing the measured beam intensity from the BCT signal (LHC.BCTFR.A6R4.B1 and LHC.BCTFR.4R6.B2). For each cycle and fill the BCT signal was smoothed using a running average of 5 s. Afterwards the beam intensity lifetime was calculated by performing linear fits to the smoothed intensity signal. As an example, the intensity and lifetime distribution of a random fill (#2469) during ADJUST [1] beam mode are shown in Fig. 6.

The minimum beam lifetime is shown in Figs. 7 and 8 for every fill and cycle of 2012 run period during SQUEEZE and ADJUST beam modes respectively. The plots include all the fills that were setup for physics, with a filter on the total injected intensity of $\text{I}_{\text{tot}} > 10^{13}$ protons to exclude low intensity fills not relevant for the performance reach. The fills with lifetime below 0.2 h were dumped. The vertical red dashed lines show changes of running periods or significant machine configurations. TS1 and TS2 are the first and second technical stops of 2012. On August 7th, 2012, the octupoles polarity was changed and seemed to improved the beam lifetime. However on August 18th,

[1] ADJUST is the beam mode that follows SQUEEZE, used when the beams are collapsed to produce collisions.

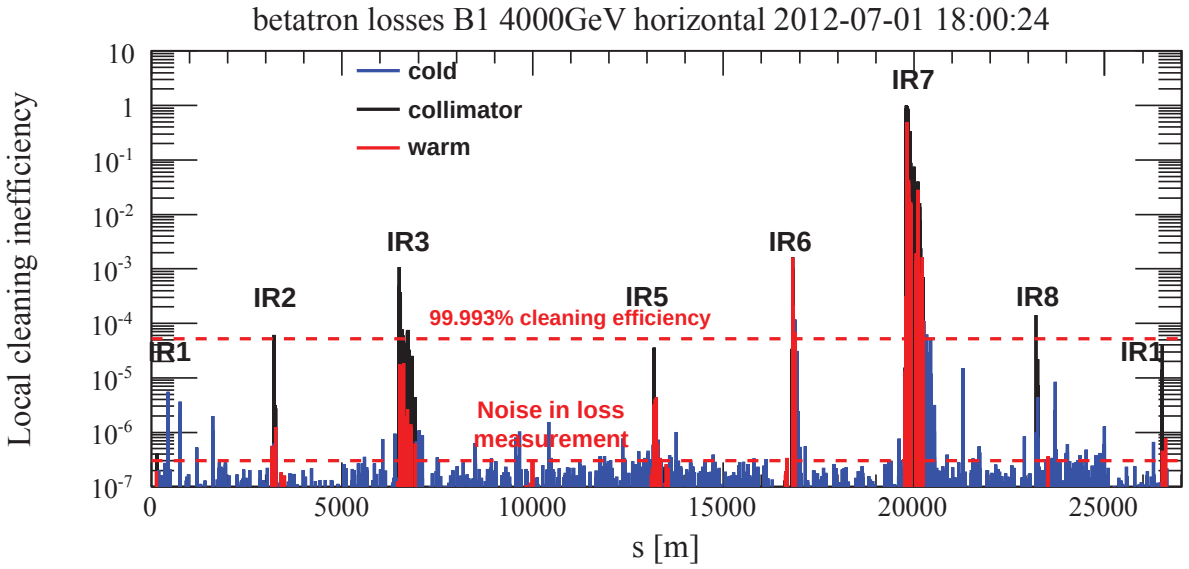

Figure 3: Distribution of the losses in the LHC ring while exciting beam 1 in the horizontal plane.

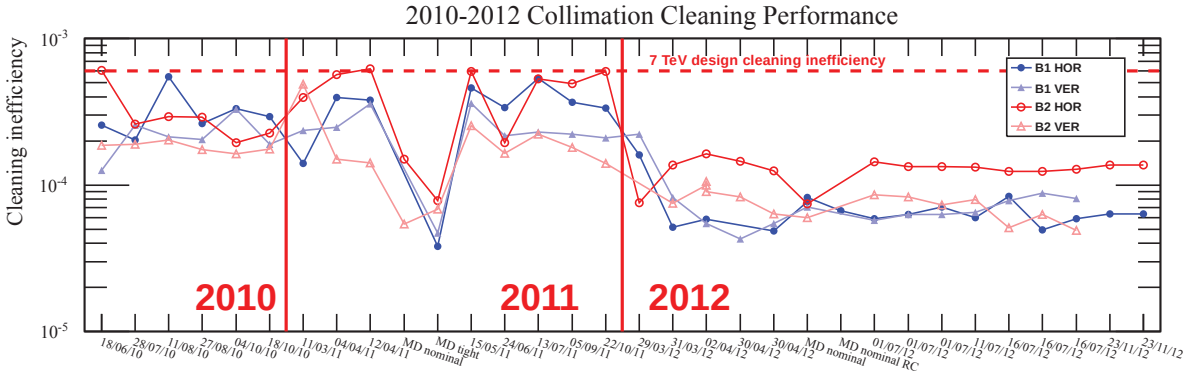

Figure 5: Collimation cleaning inefficiency as function of time since 2010 until end of 2012 run.

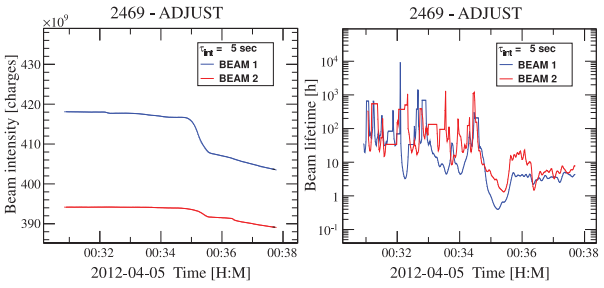

Figure 6: Measured beam intensity (left) and calculated beam lifetime (right) for fill 2469 during ADJUST beam mode.

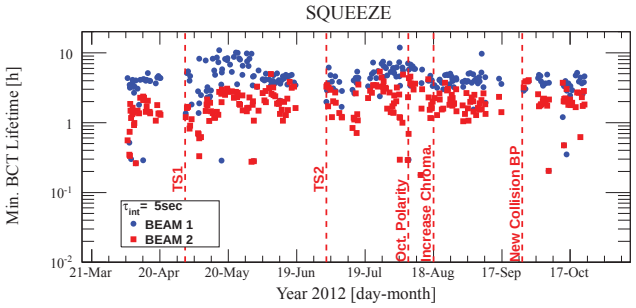

Figure 7: Minimum beam lifetime over 5 seconds during SQUEEZE beam mode.

the chromaticity was increased and the lifetime came decreased again. On September 26th, the collision beam process was changed to bring collisions in IP8 after IP1 and IP5, this seems to improve the lifetime during ADJUST beam mode.

The most critical phase is when the beams are going to collide, the average minimum lifetime along the year is found to be between 0.5 and 10 h, worse than during the ramp of energy or squeeze. Contrary to the operation in 2011 when the losses are starting only from collisions, in 2012 the instability occurred during the full adjust mode.

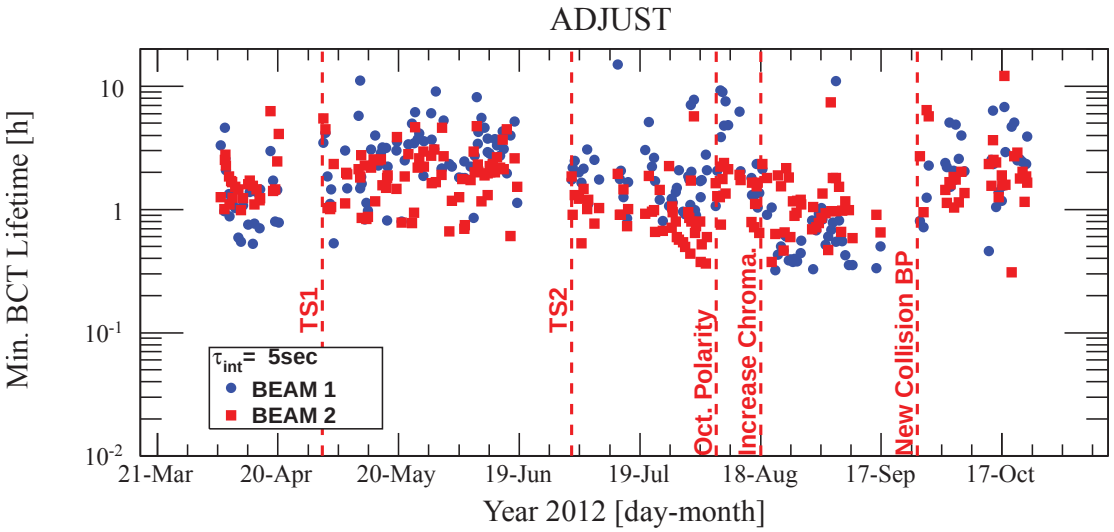

Figure 8: Minimum beam lifetime over 5 seconds during ADJUST beam mode.

COLLIMATOR HARDWARE: IMPROVEMENTS FOR LS1

During the LHC long shutdown I , 16 Tungsten tertiary collimators in all colliding interaction regions and 2 Carbon secondary collimators in IR6 will be replaced by new collimators with integrated beam positions monitors buttons. The layout will not be changed, the collimators will stay in the same positions along the ring (with the exception of IR8 where the 2-beam design TCTVB will be replaced with 1-beam design collimators) but with the gain of

- alignment without touching the beam,
- reducing orbit margins allowing more room to squeeze and
- allowing regular monitoring during operation at high intensity (with possibility to improve interlocking strategy).

Fig. 9 shows the schematic view of a collimator with integrated BPM buttons in the jaws. Since 2010, several tests on the CERN SPS accelerator were performed in order to validate this concept [15]. The beam orbit was measured with the BPM buttons with an accuracy of up to 10 μm and a fully automatic alignment algorithm was tested achieving a 10 s alignment (centering both jaws with respect to the beam) without touching the beam core [16]. Fig. 10 shows the measured beam orbit with respect to the collimator jaws (for upstream and downstream BPMs) as a function of time during one the alignment tests. The figure shows how in about 10 s the beam is centered with respect to the collimator, this corresponds to beam position equal to 0 mm.

Proposed collimator settings

The evolution of collimator settings followed the improved knowledge of the machine: tighter and tighter settings for improved β^* were achieved every year. A similar

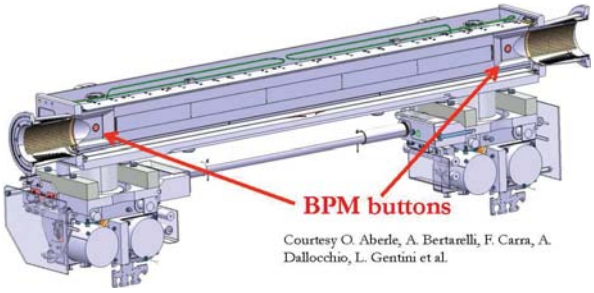

Figure 9: Schematic view of a collimator with integrated BPM buttons.

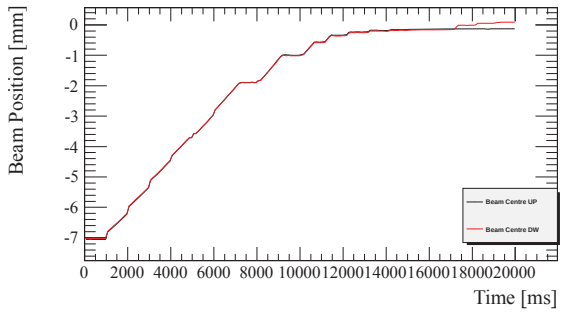

Figure 10: Measured beam position with respect to the collimator jaws with embedded beam position monitor buttons as a function of time during an alignment test on the CERN SPS.

evolution is expected for the recommissioning at higher energy after LS1. Fig. 11 shows the evolution of the collimator settings from 2010 until now extrapolated to 6.5 TeV in beam sigma size with normalized emittance of 3.5 μm rad. The solid black line represents the collimator relaxed settings used in 2011 in mm. The solid blue line represents the achieved tight collimator settings in 2012 without BPMs in

mm. The solid red line represents the nominal collimator settings. The dashed lines represent 2 proposals of collimator settings without exploiting the collimators with integrated BPM potential. Option black-dashed is the relaxed approach, with collimator gaps around 20% larger than the current tight settings in mm, while option blue-dashed, tighter than the 2012 "tight" settings, proposes 5.5 σ opening for the primary collimators (the same as the nominal settings) and 2 σ retraction for secondaries.

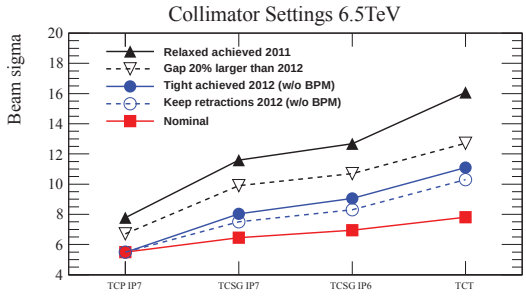

Figure 11: Proposed collimator settings in beam sigma size with normalized emittance ($\epsilon_{\text{norm}} = 3.5$ μm rad).

The last point of each line identifies the setting in sigma of the TCTs at the main colliding IRs, in order to push the $\beta^\star$ limit the opening of the TCTs need to be reduced to protect the triplet aperture. However, this imposes tighter tolerances which may require frequent alignments. The cleaning hierarchy must be respected in order to guarantee the required cleaning, this is illustrated in the line trend that should be always positive. With collimator gaps as small as few mm, this can be only achieved if collimators are precisely aligned around the correct orbit.

Table 1 compares the 2012 "tight" settings with the 2 proposed approaches. The relaxed approach of gaps about 20 % larger than in 2012 and the tighter approach of nominal settings at the primary and 2 σ retraction at the secondaries. The collimator settings in beam sigma as well as the allowed apertures at the triplets are listened for the case of using and not using the integrated BPMs information. The use of collimators with BPMs allows smaller apertures at the triplets and thus smaller $\beta^\star$. The more ambitious approach of keeping the 2 σ retraction at the secondaries allows almost 1 σ larger aperture at the triplet than the 2012 "tight" settings.

Beta-star reach after LS1

One of the limitations when going to smaller $\beta^\star$ is the aperture limit at the triplet, which is the fact that the margins at the triplet aperture decreases when decreasing $\beta^\star$. The assumptions for calculating new $\beta^\star$ reach and aperture after LS1 are:

- same excellent apertures, orbit and beta-beat as in 2012,
- primary collimator in betatron cleaning insertion at the same position in mm,

Table 1: Proposed collimator settings expressed in beam sigma size at 6.5 TeV [17].

Collimator	**Gap 20% larger than 2012**	**Tight 2012 in mm**		**Keeping retractions in σ**	
TCP 7	6.7	5.5		5.5	
TCSG 7	9.9	8.0		7.5	
TCLA 7	12.5	10.6		9.5	
TCSG 6	10.7	9.1		8.3	
TCDQ 6	11.2	9.6		8.8	
BPM	no	no	yes	no	yes
TCT	12.7	11.1	10.0	10.3	9.1
Aperture	14.3	12.6	11.2	11.7	10.3

- and BPM buttons with collimators providing orbit measurement with 50 μm precision at the TCTs in the colliding IRs and TCSG in IR6.

The last item on the list do not fully exploit the potential of the BPMs, since the results on the SPS showed better precision. However this scenario represents already a big improvement from the present orbit precision of 0.5 to 1 mm and we assume that for the start up we will start with a more relaxed approach on the use of the BPMs until we gain enough operational experience to fully exploit them.

Figure 12 shows the beta-star reach for 5 different collimator settings and 4 different scenarios [17] :

- **case 1**: 25 ns bunch spacing, 12 σ beam-beam separation and normalized emittance of 3.75 μm rad,
- **case 2**: 25 ns bunch spacing, 12 σ beam-beam separation and normalized emittance of 1.9 μm rad,
- **case 3**: 50 ns bunch spacing, 9.3 σ beam-beam separation and normalized emittance of 2.5 μm rad and
- **case 4**: 50 ns bunch spacing, 9.3 σ beam-beam separation and normalized emittance of 1.6 μm rad.

On one hand, the more pessimistic scenario corresponds of collimator settings with gap 20% larger than in 2012 and no use of BPM buttons, this will allow $\beta^\star \geq 70$ cm at 25 ns or $\beta^\star \geq 57$ cm at 50 ns. On the other hand, the more optimistic scenario of keeping same retractions in sigma as in 2012 and using the BPM buttons will allow $\beta^\star \geq 37$ cm at 25 ns or $\beta^\star \geq 30$ cm at 50 ns. The final choice of collimator settings should take into account also the impedance constrains. This might require larger collimator gaps than the proposed here and thus worse $\beta^\star$.

Clearly, we will only exploit the full potential of the BPMs after we gain the needed operational experience with them. Thus, at the start-up after LS1 we propose to start with the 2012 "tight" settings, assuming the machine impedance is still under control, and move towards the tighter approach of keeping 2 σ retraction at the secondaries at 6.5 TeV.

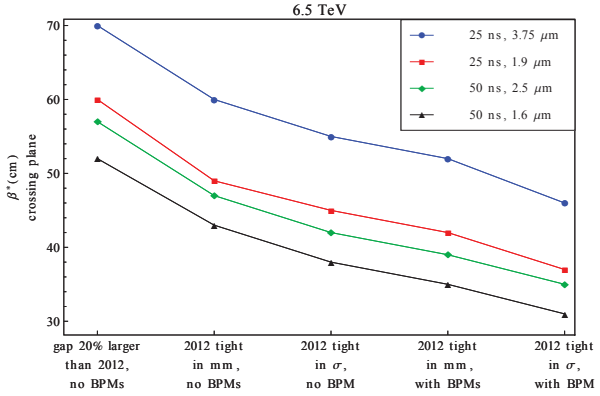

Figure 12: $\beta^\star$ reach in the crossing plane at 6.5 TeV as a function of collimator settings.

SUMMARY

The performance of the collimation system was discussed. The improvements on the alignment tool decreased the collimation setup time from 20 min to few minutes per collimator. The cleaning stability in the dispersion suppressor region of IR7 along the LHC running periods was analyzed and was shown to be excellent. In 2012, with the "tight" collimator settings the average leakage at Q8 cell in IR7 was about $\eta_c = 7 \cdot 10^{-5}$ for beam 1 (both horizontal and vertical halo cleaning) and beam 2 vertical and around $\eta_c = 10^{-4}$ for beam 2 horizontal. No quenches with circulating beams were experienced with up to 140 MJ at 4 TeV. The minimum beam lifetimes, that is one of the required parameters to estimate the intensity reach was also discussed. It was found that the most critical phase is when the beams are collapsed to collide, with minimum lifetimes along the year between 0.5 and 10 h depending on the fill conditions. Unlike what was experienced in the "loss-free" operation in 2011, some 45 fills were lost in 2012 due to losses before putting the beams in collision (due to instabilities during squeeze and adjust). This analysis must be continued to understand better the implications for the operation after LS1.

The concept of collimators with integrated BPM buttons is introduced and we showed the expected $\beta^\star$ reach after LS1 for different proposed collimator settings at 6.5 TeV, with special emphasis on the $\beta^\star$ limit if we exploit the potential of the collimators with BPMs. Assuming 50 ns bunch spacing and normalized emittance of 1.6 μm rad the $\beta^\star$ limit with BPMs is $\beta^\star \geq 30$ cm. However, this will only come after gaining some experience with the embedded BPMs, until then we propose to start with the 2012 "tight" collimator settings as baseline and approach to the 2 σ retraction settings and full use of the BPMs after improving the knowledge of the machine at higher energy.

ACKNOWLEDGMENT

The authors would like to acknowledge the LHC operations team, injection and dump protection team and beam loss monitor team for all the good collaboration during the first running period of the LHC. We would like mention specially the ADT team, in particular D.Valuch and W.Hofle for all the help in the setup of the ADT for the loss maps and many other tests. And finally, many thanks also to M.Gasior, A.Masi and the CERN STI team for the engineering support.

REFERENCES

[1] The LHC Design Report, Vol. I, The LHC Main Ring, CERN-2004-003 (2004).

[2] R.Assmann *et al*, "Tests of tight collimator settings in the LHC", CERN-ATS-Note-2012-022 MD.

[3] R. Assmann *et al.*, "Summary of MD on nominal collimator settings", CERN-ATS-Note-2011-036 MD.

[4] R. Assmann *et al.*, "End-of-fill study on collimator tight settings", CERN-ATS-Note-2011-125 MD.

[5] R. Bruce and R. Assmann, "LHC beta*-reach in 2012, Proceedings of the LHC Beam Operation workshop", Evian 2011.

[6] R. Bruce *et al.*, "Collimator settings and performance in 2011 and 2012", Proceedings of Chamonix 2012 workshop

[7] S. Redaelli *et al.*, "IR1 and IR5 aperture at 3.5 TeV"

[8] R.Assmann *et al*, "Improving LHC Collimator Setup Efficiency at 3.5TeV", CERN-ATS-Note-2011-062 MD.

[9] G.Valentino *et al.*. "Semiautomatic beam-based LHC collimator alignment",*Phys. Rev. ST Accel. Beams* 15, 5 (2012) pp.051002.

[10] R.Assmann *et al.*, "Beam-based collimator alignment MD", CERN-ATS-Note-2012-046 MD.

[11] W.Hofle *et al.*, "Controlled transverse blow-up of high-energy proton beams for aperture measurements and loss maps", Proceedings of IPAC2012, New Orleans, Louisiana, USA, THPPR039, p.4059 (2012)

[12] R.Assmann *et al.* "Tight collimator settings with beta* = 1.0 m", CERN-ATS-Note-2011-079 MD.

[13] B.Salvachua *et al.*, "Results on nominal collimator settings MD at 4 TeV", CERN-ATS-Note-2012-092 MD.

[14] C.Bracco, "Commissioning Scenarios and Tests for the LHC Collimation System", CERN-THESIS-2009-031, EuCARD-DIS-2009-004.

[15] D.Wollmann *et al.*, "First beam results for a collimator with in-jaw beam positions monitors", Proceedings of IPAC2011, San Sebastian, Spain, THPZ027, p. 3747 (2011).

[16] G.Valentino *et al.*, "Preliminary results from the SPS BPM prototype collimator MDs", talk on the Collimation Working Group, Nov 26th, (2012) `http://indico.cern.ch/conferenceOtherViews.py?view=standard&confId=218177`, note on preparation.

[17] R.Bruce *et al.*, "Collimation after LS1: cleaning and $\beta^\star$ reach", talk on the LHC Beam Operation Committee, Dec 11th, (2012) `http://lhc-beam-operation-committee.web.cern.ch/lhc-beam-operation-committee/`

LHC EMITTANCE PRESERVATION DURING THE 2012 RUN

M. Kuhn (University of Hamburg, Germany), G. Arduini, J. Emery, A. Guerrero, W. Hofle, V. Kain, F. Roncarolo, M. Sapinski, M. Schaumann, R. Steinhagen, CERN, Geneva, Switzerland.

Abstract

Emittance measurements through the 2012 LHC proton cycle examined possible major sources for the large blow-up through the LHC cycle already seen in 2011. The behavior of single bunch and 50 ns beams from LHC injection to collisions has been investigated. Accuracy and limitations of the LHC transverse profile monitors will be discussed. The effect of 50 Hz noise on the emittance growth and the influence of different transverse damper gains are presented. Intra beam scattering is one of the major sources of blow-up in the horizontal plane at injection. RF batch-by-batch blow-up has been put into operation towards the end of the year to counteract this effect. The impact of these measures on specific luminosity will be presented. The creation of tails through the LHC cycle will also be briefly discussed and an outlook for future LHC upgrade scenarios with low emittance beams will be given.

INTRODUCTION

Measurement campaigns during the 2011 proton run revealed substantial transverse emittance blow-up through the LHC cycle. The emittances at collision - typically 2.5 μm for 1.5×10^{11} ppb - were still below the LHC design values of 3.5 μm, but about 30 % larger than at the end of LHC injector chain. The blow-up during the different phases in the LHC cycle was evaluated with the following main results [1]:

- No measurable blow-up from injection into the LHC
- Blow-up during injection plateau: consistent with Intra-Beam Scattering (IBS), causes batch-by-batch differences, 0 - 10 % blow-up depending on injection time of batch
- Significant blow-up during the ramp: more than 20 % for 1.6 μm emittances
- Beam 1, horizontal plane, blow-up by about 20 % during the squeeze
- Absolute emittance growth seems to be independent of bunch intensity and initial emittance: $\Delta\varepsilon \sim 0.5 - 0.6$ μm, convolution of beam 1 and beam 2.

In 2012 the protons were ramped to 4 TeV instead of 3.5 TeV as in 2011 and β* was squeezed down to 0.6 m in point 1 and point 5 instead of 1 m as in 2011. The main parameters of the 2012 run are summarized in Table 1. Fig. 1 shows the evolution of the emittances in collision (green) and after injection (yellow) throughout the 2012 proton run. The emittances from the high performing injectors were as small as 1.5 μm for bunch intensities of up to 1.7×10^{11} ppb. The emittances of the beams were, however, blown up by up to 40 % in the LHC until collision during the 2012 high intensity proton run.

Table 1: LHC proton run configuration in 2012

Total number bunches for fill	1374
Max number bunches injected	144
Bunch spacing [ns]	50
Intensity/bunch	$1.1 - 1.7 \times10^{11}$
Intermediate intensity [bunches]	12
Number of injections per fill and beam	12 (+1 pilot)
Filling time	~ 30 min
Number collisions (ATLAS+CMS/ALICE/LHCb)	1368/0/1262
Collision energy per beam	4 TeV
Max. luminosity achieved [$cm^{-2}s^{-1}$]	7.7×10^{33}

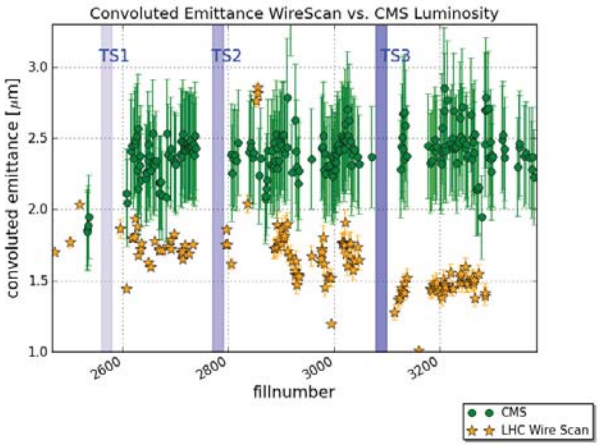

Figure 1: Convoluted, average emittance of the first 144 bunch batch measured with wire scanners at LHC injection (yellow stars) compared to the convoluted emittance calculated from CMS peak luminosity (green dots). The periods of the technical stops are marked with TS. With the introduction of the Q20 optics in the SPS [2] (after TS3) the emittances from the injectors were even smaller (improvement from 1.8 to 1.5 μm), but the emittance at collision in the LHC stayed the same.

EMITTANCE MEASUREMENT

Three types of instruments are installed in the LHC to measure the transverse beam size: the wire scanner, the Beam Synchrotron Radiation Telescope (BSRT) and the Beam-Gas Ionization Monitor (BGI). Still none of the instruments could be used to measure the high intensity physics beams throughout the whole cycle due to the systems limitations. For physics beams the emittances were measured at two points of the cycle: wire scans were performed after the first 144 bunch batch injection and indirect measurements of the convoluted emittance were obtained through luminosity and luminous region measurements at the end of the cycle, see Eq. 1.

$$\varepsilon_{conv} = \sqrt{\varepsilon_{1x} + \varepsilon_{2x}}\sqrt{\varepsilon_{1y} + \varepsilon_{2y}} \quad (1)$$

The uncertainties on emittances from luminosity presented in this paper assume 15 % error on β* and 5 % error on the crossing angle.

Low intensity test cycles were used to measure the emittances through the cycle with wire scanners. The cores of the transverse profiles of in and out scans were fitted with Gauss Functions to obtain beam sizes. All emittance values from wire scanners in this paper were calculated with beta functions measured with k-modulation. K-modulation values for 2012 are available at injection, end of ramp and after the squeeze. For measurements through the ramp, the beta functions were obtained through linear interpolation between the beta value at injection and at flattop.

Towards the end of the proton run, the wire scanners became partly unavailable. Issues occurred with the maximum number of measurement cycles and robustness of the wires. During technical stop (TS) 3 all wires were switched to the spare system and the maximum allowed intensity for scans was even further reduced due to the still thicker wires. The wire scanner intensity limit at 4 TeV flattop energy was decreased from 30 to 20 nominal bunches. After a wire had broken with beam no more scans were done with physics beam at injection (from Fill 3287 onwards). Another issue with the wire scanners in 2012 concerned the accuracy of the beam size measurement. This topic will be treated in more detail later on in this paper.

The LHC BSRTs became the workhorse for physics beam measurements during the injection plateau and at 4 TeV. Due to the improved speed of the scans (3 to 4 bunches per second) since May 2012 the bunch-by-bunch emittance evolution during injection and squeeze can be studied with sufficient statistics for the full machine. However, only the beam 1 system was available from August 2012 due to a damaged mirror on the beam 2 systems.

The BGI - the only system which is able to measure physics beams through the ramp – could not be used in 2012. Only the beam 2 system was operational, but the energy dependent calibration was not satisfying. There are signs of beam space charge driven distortion of the beam profile in the BGI.

EMITTANCE EVOLUTION THROUGH THE CYCLE

Fig. 2 shows the emittance evolution through the cycle for beam 1, horizontal plane, measured with wire scanners during a test fill with 6 + 6 bunches per ring, 50 ns bunch spacing and bunch intensities of about 1.6 x 10^{11} ppb (Fill 3217). Beam 2 horizontal looks qualitatively similar: the emittances grow mainly during the injection plateau and the ramp. Some growth is also seen towards the end of the squeeze, especially for fills later in the 2012 run.

The total emittance growth measured by wire scanners for the fill in Fig. 2 is about 0.48 ± 0.06 μm (35 %), convoluted emittance. Yet the peak luminosity for ATLAS and CMS measured at the end of the cycle corresponded to a growth of the convoluted emittance of about 0.72 ± 0.34 μm (50 %). This discrepancy between wire scanner measurements and emittance from luminosity were seen throughout the 2012 run. More details on this topic will be discussed later in the paper. In the following the emittance growth of the different parts of the LHC cycle will be presented.

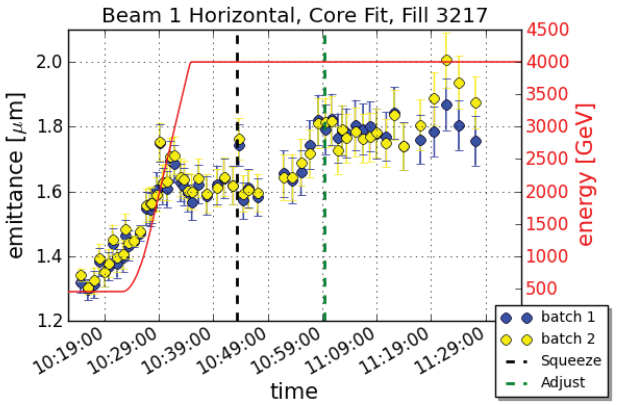

Figure 2: Average emittance of 6 bunches per batch through the whole LHC cycle for beam 1 horizontal measured with wire scanner, Fill 3217. Batch 1 is colliding at LHCb, batch 2 in ATLAS and CMS.

The LHC injection process

As was already the case in 2011, the emittances in the vertical and horizontal plane are conserved within the measurement precision at injection from the SPS into the LHC (measurement precision ± 10 %). The LHC matching monitors are not operational yet. Wire scans at SPS flattop and right after LHC injection are used instead. Fig. 3 shows an example of measurements in the SPS and in the LHC. The measurements in the LHC are bunch-by-bunch, whereas in the SPS an average for all bunches is given. The wire scanners in the SPS are at locations with small beta functions and the wire speed cannot be reduced due to issues with saturation. Only a few points are available per scan to obtain the Gaussian fit. Overlaying profiles of several scans increases the accuracy significantly, see Fig. 4. This method was used to obtain the SPS numbers in Fig. 3 and 4.

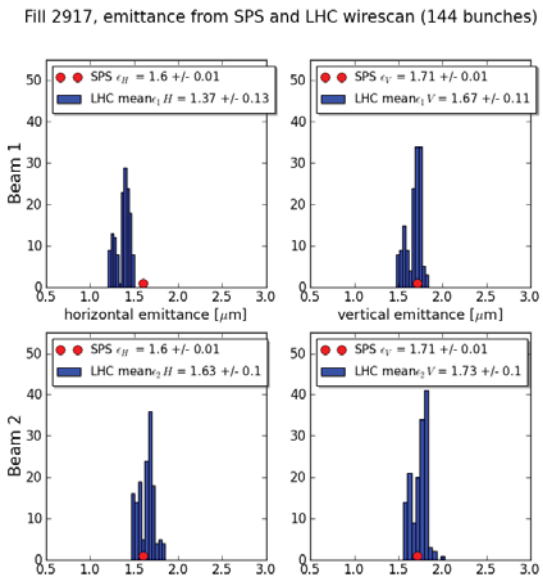

Figure 3: Emittances at SPS and LHC. Wire scan histograms of bunch-by-bunch emittances at LHC injection (blue bars) compared to average emittances of 144 bunches at SPS extraction (red dot).

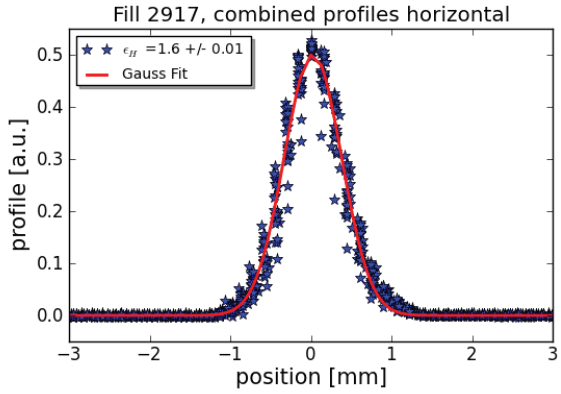

Figure 4: SPS combined profiles from wire scans of 144 bunches in the horizontal plane at SPS extraction energy of 450 GeV.

The LHC injection plateau

In 2012 many dedicated fills at injection energy were compared to IBS simulations. Fig. 5 and 6 show 6 nominal (1.6 x 10^{11} ppb) 50 ns bunches measured with wire scanners and the matching IBS simulations for every bunch of beam 1 horizontal and vertical. The emittance growth in the horizontal plane is well predicted with IBS, but slightly faster than the simulation. A possible explanation is 50 Hz noise. The results were cross checked with measurements from BSRT and also different initial emittances, which give similar agreement. As a solution for the effects from IBS the longitudinal RF batch-by-batch blow-up was tested. The effects at injection introduce batch-by-batch differences in the specific luminosity. Batches that stay longer at injection have a larger emittance blow-up and therefore their specific luminosity is smaller than batches that spend less

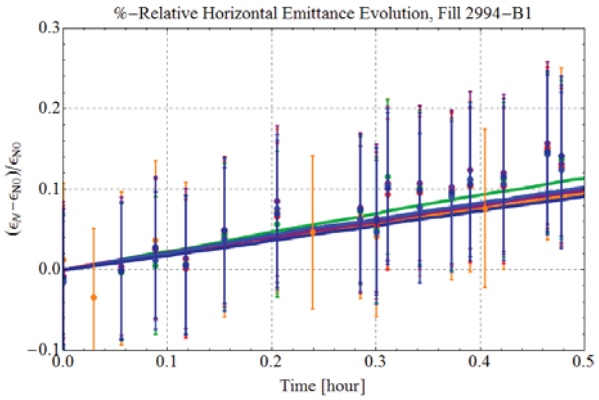

Figure 5: Relative emittance growth at the injection plateau for 6 bunches of beam 1 horizontal measured with wire scanner (dots) and compared to IBS simulations with same initial conditions (lines), Fill 2994.

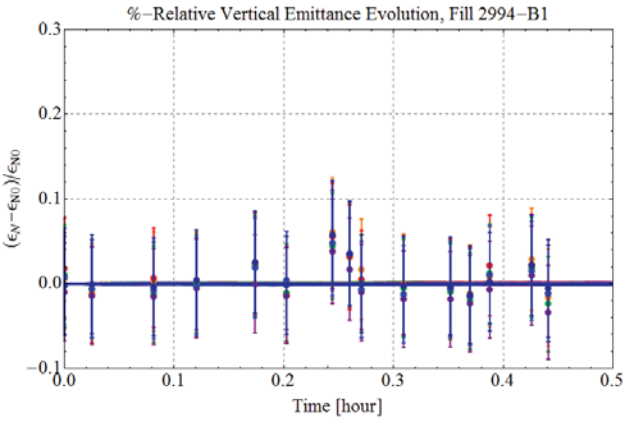

Figure 6: Relative emittance growth at the injection plateau for 6 bunches of beam 1 vertical measured with wire scanner (dots) and compared to IBS simulations with same initial conditions (lines), Fill 2994.

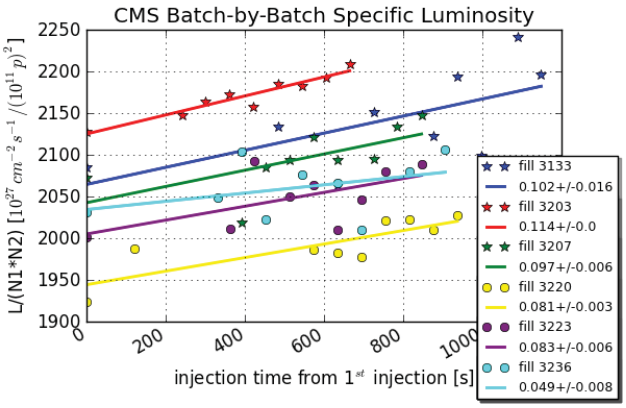

Figure 7: Specific CMS luminosity calculated from CMS peak luminosity and bunch intensity at collision, averaged per batch and plotted as a function of injection time from the first injection for fills with (dots) and without RF batch-by-batch blow-up (stars). A linear interpolation is displayed. The fitted slopes can be found in the legend.

time at the injection plateau. Fig. 7 shows the specific luminosity for the different batches as function of the injection time for fills with and without RF batch-by-batch blow-up. Fills 3133, 3203 and 3207 are left to natural blow-up. Fills 3220, 3223 and 3236 are longitudinally blown up to a target bunch length of 1.4 ns. The data points are fitted linearly. The average slope is slightly smaller for fills with longer bunches but there is no clear improvement. Another source of the batch-by-batch differences could be 50 Hz noise.

Noise Studies at 450 GeV

The LHC horizontal injection tune sits on top of a 50 Hz line and the beam is slightly excited by this noise. Fig. 8 shows the influence of the 50 Hz noise on the emittances of 6 nominal (1.3 x 10^{11} ppb) 50 ns bunches measured with wire scanners. The bunches were injected and kept at the nominal fractional tune of 0.28 for a period of 10 min. Then the horizontal tune was moved to 0.283 to avoid the 50 Hz noise. After 10 min the tune was moved back to nominal. Changing the horizontal tune clearly had an effect on the emittances in both planes. The effect coupled into the vertical plane as the betatron coupling was about a factor 2 above the typical physics fill values for this fill. In the horizontal plane IBS and 50 Hz noise cause emittance growth and the effect of the tune changes was only a small change of the slope of the emittance growth. The effect was, however, more visible in the vertical plane where the blow-up almost vanished with a tune far away from the 50 Hz line and then increased again when changing back to the nominal tune.

In view of these results a test ramp was carried out with a horizontal tune off the 50 Hz line. No evident improvement of the emittances at the end of the ramp was measured. The test ramp will have to be repeated under controlled conditions.

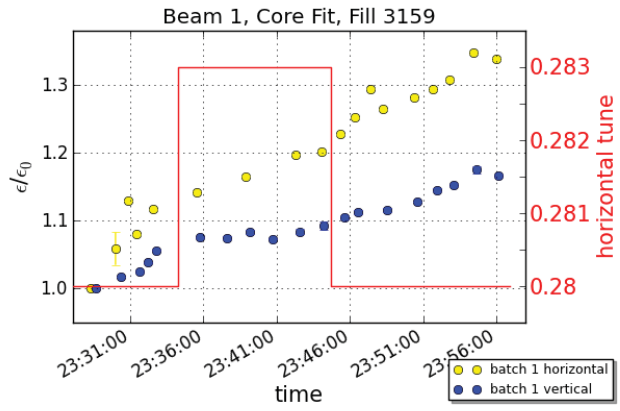

Figure 8: Relative average emittance growth of 6 bunches at injection energy for beam 1 horizontal and vertical measured with wire scanners, Fill 3159. ε_0 is the emittance at injection into the LHC. The horizontal fractional tune during the measurement period is displayed as well.

Transverse Damper Gain at 450 GeV

At injection, the LHC transverse damper is operated with a very high gain to keep emittances small after injection due to injection oscillations and possible other effects. At the start of the ramp the gain is reduced to allow for a sufficient tune signal to switch on the tune feedback during the ramp [3]. The tune measurement of the feedback system comes from the LHC Base-Band-Tune (BBQ) monitors. Fig. 9 and 10 display BSRT emittance measurements at injection energy with varying transverse damper gain in both planes for beam 1. One nominal bunch with an intensity of 1.4 x 10^{11} protons was injected with high injection gain. Then the gain was reduced to the original 2012 low ramp gain and after 10 min back to high gain. The slope of the fit for the vertical plane clearly increases when moving to lower damper gain. The higher damper gain reduces or even removes the emittance growth. In the horizontal plane the blow-up mainly originates from IBS, on which the damper has no effect and the slope of the growth only changes slightly between the different gains.

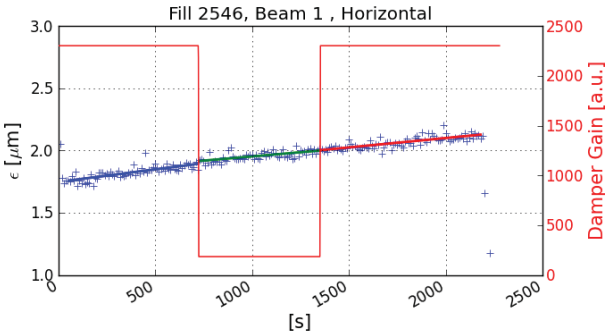

Figure 9: BSRT measurements on 1 nominal bunch for beam 1 horizontal at injection energy with changing horizontal ADT gain from nominal high injection gain to low ramp gain and back to high gain. The emittance growth in the different segments is fitted linearly, Fill 2546.

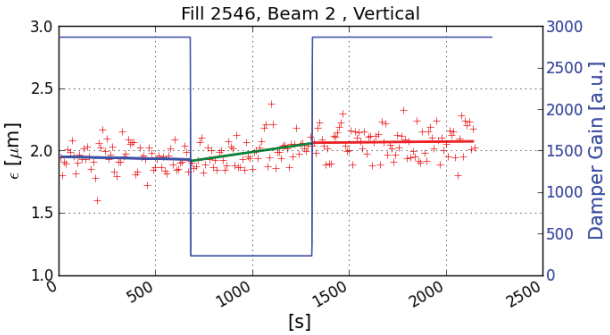

Figure 10: BSRT measurements on 1 nominal bunch for beam 2 vertical at injection energy with changing vertical ADT gain from nominal high injection gain to low ramp gain and back to high gain. The emittance growth in the different segments is fitted linearly, Fill 2546.

The LHC ramp

All beams and planes show an emittance blow-up through the ramp. Generally it is larger in the horizontal plane than the vertical plane and more pronounced for beam 2 than for beam 1 in 2012. In Fig. 11 a test ramp measured with wire scanner for beam 1 horizontal is shown. For Fill 3217 the total average emittance growth during the ramp is about 20 % for beam 2 horizontal, about 15 % for beam 1 horizontal, and approximately 5 % in the vertical plane for both beams. The ramp has been studied thoroughly. The observed growth is unlikely to be a measurement artifact. The measured beta functions are used at injection and flattop and a linear interpolation between these values for energies during the ramp is applied. Dispersion is not taken into account as it has been measured to be small (< 10 cm at injection, < 30 cm at flattop). The absolute emittance blow-up through the ramp is roughly the same, independent of the emittance value at the start of the ramp.

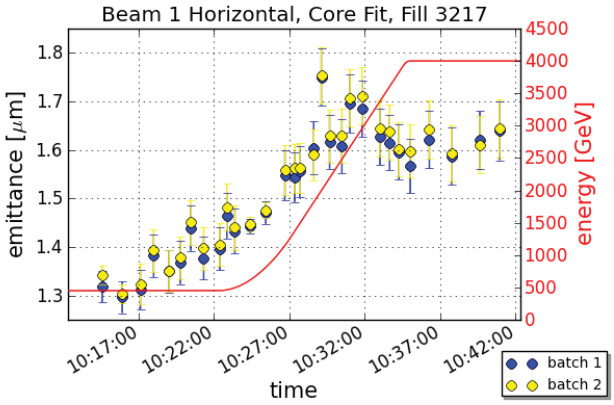

Figure 11: Wire scans of beam 1 horizontal during the ramp with emittances averaged over 6 bunches in one batch, Fill 3217.

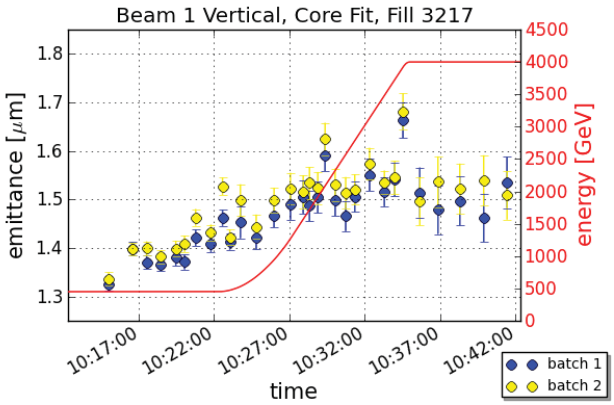

Figure 12: Wire scans of beam 1 vertical during the ramp with emittances averaged over 6 bunches in one batch, Fill 3217.

Transverse Damper Gain during the Ramp

The encouraging results on emittance growth from increased damper gain during the injection plateau triggered a test with increased damper gain during the ramp. To be able to compare batches with and without increased gain, the damper gain was modulated around the LHC circumference. Fig. 13 and Table 2 summarize the ADT gain modulation for the 4 batches used during the test. Each batch contained 6 nominal (1.3×10^{11} ppb) 50 ns bunches. The emittance measurement results of the different batches are shown in Fig. 14 and 15. The emittance growth in the vertical plane is small, see Fig. 15. Table 3 summarizes the emittance growth of the different batches of beam 1, horizontal. For all batches the growth during the ramp was about 0.26 ± 0.07 μm (25 %). There was no significant difference of blow-up for different transverse damper gains.

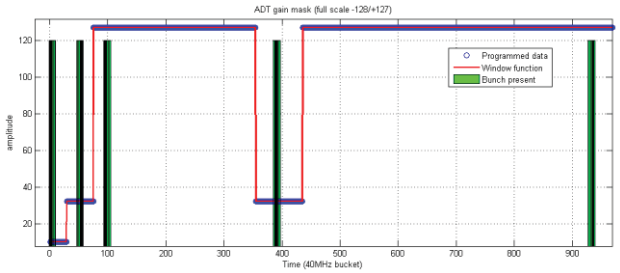

Figure 13: ADT ramp gain modulation for Fill 3160, beam 1. Batch number 4 was not injected. The function was applied before starting the ramp.

Table 2: ADT ramp gain modulation for Fill 3160

Batch 1	Very low gain bunches, sacrificial (lower than operational gains)
Batch 2	Low gain bunches (~ nominal low prepare ramp gain)
Batch 3 Batch 4	Very high transverse damper gain (~ nominal injection gain)

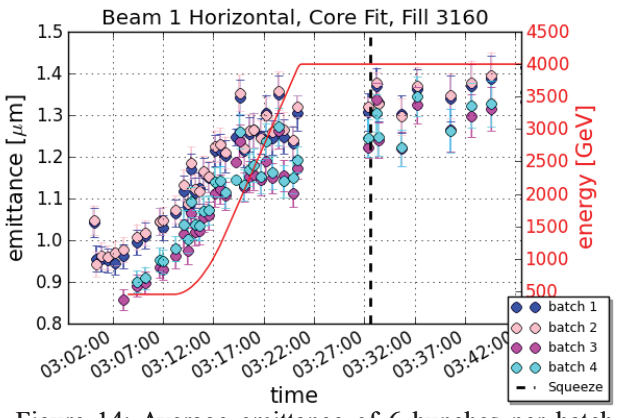

Figure 14: Average emittance of 6 bunches per batch through the ramp and the squeeze for beam 1 horizontal measured with wire scanner, Fill 3160. The bunches have different transverse damper gains at the start of the ramp, see Table 2.

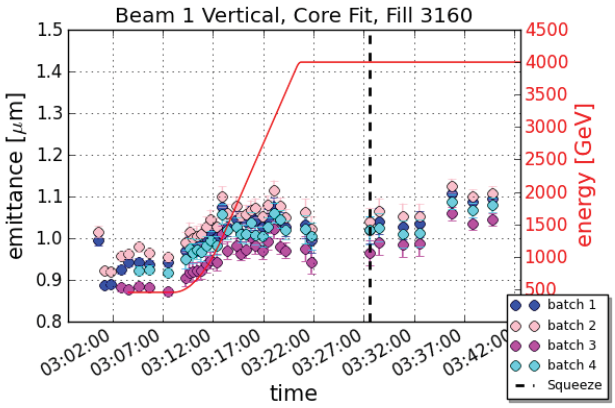

Figure 15: Average emittance of 6 bunches per batch through the ramp and the squeeze for beam 1 vertical measured with wire scanner, Fill 3160. The bunches have different transverse damper gains at the start of the ramp, see Table 2.

Table 3: Emittance growth of beam 1 horizontal, Fill 3160

	Growth during ramp [μm]
Batch 1	0.24 ± 0.08 (23 %)
Batch 2	0.25 ± 0.06 (23 %)
Batch 3	0.26 ± 0.05 (27 %)
Batch 4	0.27 ± 0.07 (27 %)

The LHC squeeze

Towards the end of the 2012 proton run a small blow-up at the end of the squeeze for beam 1 horizontal was observed, but not always by the same amount. The emittances in the vertical planes and beam 2 horizontal were conserved (caveat: beam 2 was only measured with wire scanners for low intensity fills). Examples are given in Fig. 16 - 19.

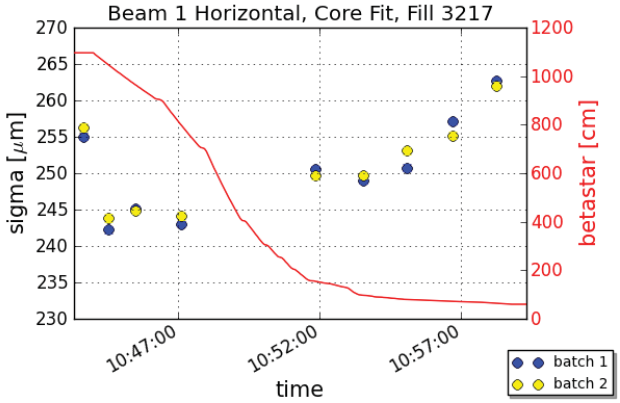

Figure 16: Beam sizes averaged over 6 bunches in one batch for beam 1 horizontal during the squeeze of Fill 3217 measured with wire scanner.

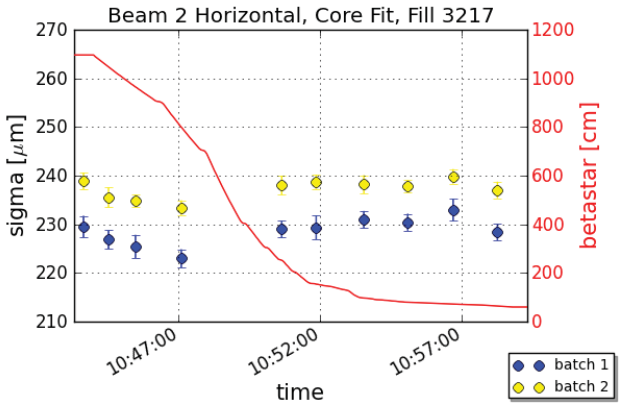

Figure 17: Beam sizes averaged over 6 bunches in one batch for beam 2 horizontal during the squeeze of Fill 3217 measured with wire scanner.

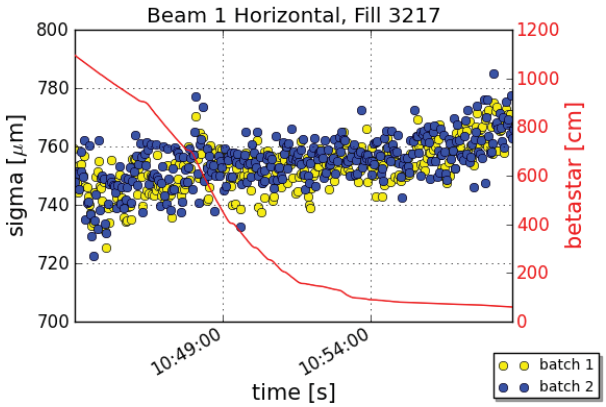

Figure 18: Beam sizes for beam 1 horizontal during the squeeze of Fill 3217 measured with BSRT. Beam sizes are averaged over 6 bunches in one batch.

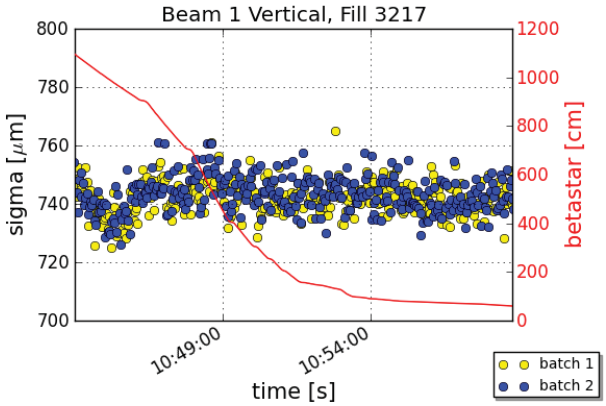

Figure 19: Beam sizes for beam 1 vertical during the squeeze of Fill 3217 measured with BSRT. Beam sizes are averaged over 6 bunches in one batch.

MEASURES AGAINST EMITTANCE GROWTH

After Technical Stop 3 (TS3) several potential measures against emittance growth during the LHC cycle became operational. A summary can be found in Fig. 20. Since Fill 3220 the RF batch-by-batch blow-up was used for physics fills. Because the gated BBQ system became operational after Fill 3286 it was possible to have fills

with higher ADT gain for the ramp. Also higher ADT bandwidth was used from flattop to the start of stable beams. Fig. 20 shows the influence of the different measures on the emittance at LHC collision. The emittances at injection are plotted as well for comparison. The emittances from peak luminosity vary slightly but within the error bars they are constant.

There is a short period around Fill 3280 where the emittances at collision were reduced when only the high ADT bandwidth was used. Due to the small number of fills during this period it is, however, not clear whether this is not just a statistical fluctuation. In conclusion, there is no obvious improvement of the average emittance at collision for any measures taken so far. But it seems the peak bunch-by-bunch specific luminosity can be increased with higher transverse damper gain during the ramp [4].

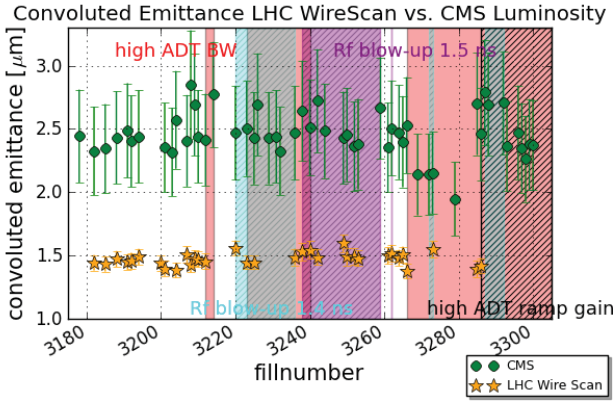

Figure 20: Convoluted averaged emittance of the first 144 bunch batch measured with wire scanners at injection in the LHC and compared to the convoluted emittance obtained from peak luminosity at CMS. Periods with different measures as RF batch-by-batch blow-up, high ADT bandwidth (BW) and high ADT ramp gain are highlighted.

COMPARISON OF EMITTANCE FROM EXPERIMENTS AND WIRE SCANNERS

For MD Fill 3160, 6 nominal (1.3 x 10^{11} ppb) 50 ns bunches were colliding head on in ATLAS and CMS. Wire scan measurements were taken and could be compared to bunch-by-bunch data from luminosity and luminous region. Also the LHCb SMOG experiment was taking beam size data. In Fig. 21 and 22 the convoluted bunch emittances from ATLAS luminosity, luminous region, wire scanner and SMOG are shown at two different timestamps. For the emittance from the experiments the nominal beta functions were used (IP1&IP5 $\beta^* = 0.6$ m, IP8 $\beta^* = 3$ m). The error on emittance from SMOG data and ATLAS luminous region also include statistical errors and systematic errors in case of the SMOG experiment.

There is a large discrepancy between the different values from wire scanners and experiments, sometimes more pronounced (Fig. 21) and sometimes less (Fig. 22). There is also a systematic difference between SMOG data and emittances from ATLAS/CMS. In general the wire scan measurements always showed smaller emittances than obtained by the experiments.

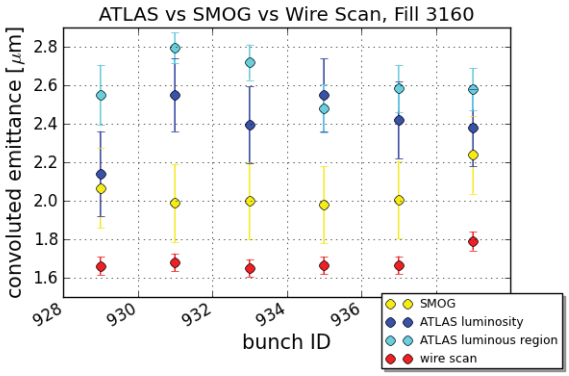

Figure 21: Convoluted emittance per bunch measured with SMOG and wire scanners and calculated from ATLAS luminosity and luminous region. Timestamp 12/10/2012 04:42, Fill 3160.

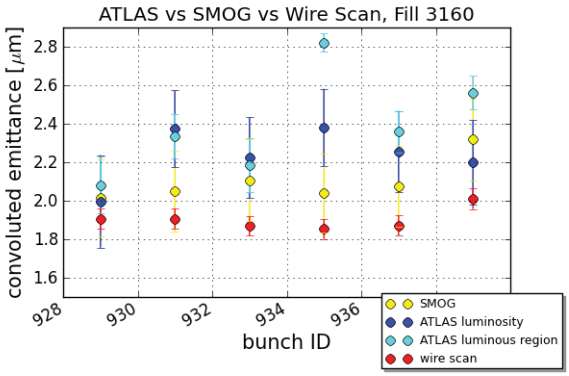

Figure 22: Convoluted emittance per bunch measured with SMOG and wire scanners and calculated from ATLAS luminosity and luminous region. Timestamp 12/10/2012 5:04, Fill 3160.

Accuracy of the Wire Scanners

The findings presented in the previous section led to investigations of the optimum wire scanner settings. For this purpose the beam size was measured with the wire scanners for different settings of photomultiplier voltage and transmission filter. Fig. 23 shows an example of the measurements at injection energy for beam 1 horizontal. Scans were performed for all beams and planes at injection and flattop energy and the results look all similar. The constant linear emittance growth in the plot is due to IBS at injection energy but clearly gain and filter change have a significant influence on the beam size. This is not ADC saturation, since all profiles still look Gaussian. The photomultipliers are saturating at certain settings and it is not clear which settings give the real beam size. The resulting uncertainty on the beam size measurement therefore has to be increased from originally 0.1 μm to 0.5 μm at 450 GeV and to 0.8 μm at 4 TeV. The optimum working point of the wire scanners needs further investigation.

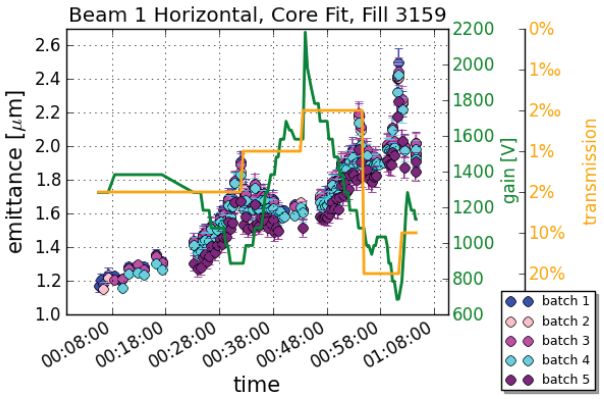

Figure 23: Average emittance of 6 bunches per batch during the injection plateau measured with wire scanner. Variations of wire scanner filter and voltage are displayed for beam 1 horizontal, Fill 3159.

EMITTANCE BLOW-UP VERSUS BUNCH INTENSITY

Fig. 24 shows the emittance blow-up from LHC injection to collision for all physics fills during the 2012 proton run as a function of the average bunch intensity. The intensity was obtained with the Fast Beam Current Transformer (FBCT) at peak luminosity. The high brightness test fills [5] (Fill 2994 and Fill 3372) are marked in green. Up to a bunch intensity of 1.5 x 10^{11} ppb the emittance blow-up is almost constant - about 0.7 μm. For bunch intensities beyond 1.5 x 10^{11} ppb the growth increases with bunch intensity. Whereas for the high brightness Fill 2994 the overall growth is similar as surrounding points in the plot, the growth for Fill 3372 is below 0.5 μm. Fill 3372, where the Batch Compression, Merging and Splitting (BCMS) [5] scheme in the PS was used, fell in a period where the higher damper gain during the ramp was already operational, which could be an explanation for the lower growth.

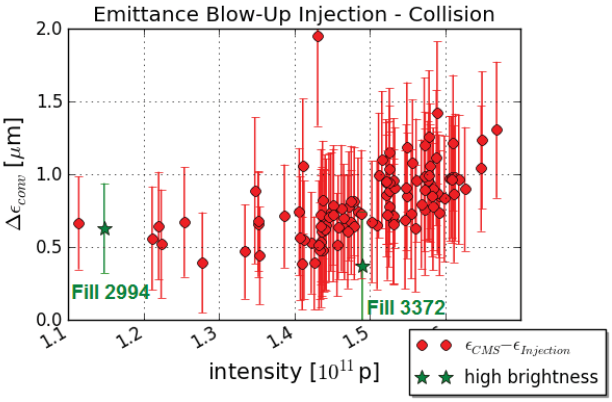

Figure 24: Convoluted average emittance growth from injection to collision as a function of average bunch intensity at collision. Δε is calculated from emittance from CMS peak luminosity and convoluted average emittance of the first 144 bunch batch measured with wire scanners at LHC injection. The high brightness fills (stars) are highlighted.

TAILS: CAN WE MEASURE THEM?

The evolution of transverse tails through the cycle has not been studied in 2012, but a way to indicate tails was found. The difference between the measurement signal and the Gauss fit of the transverse profile, see Fig. 25, was used to give an estimate of the tail population. In Fig. 26 the evolution of this difference is plotted for the wire sans at injection of beam 2 horizontal, for the period after TS2. Problems with tails right after TS2 are clearly visible.

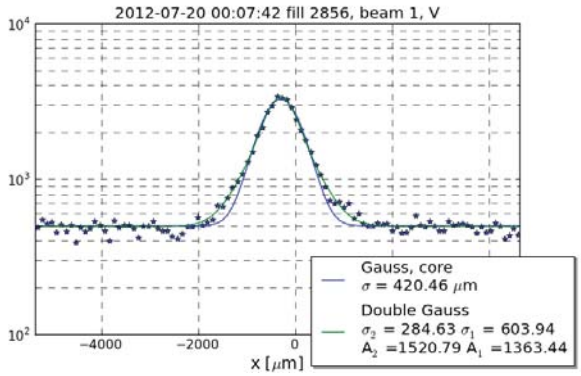

Figure 25: Transverse beam profile measured with wire scanner (dots). The core of the profile is fitted with a Gauss (blue line). Also a double Gauss fit is shown (green line). The corresponding beam sizes are given in the legend.

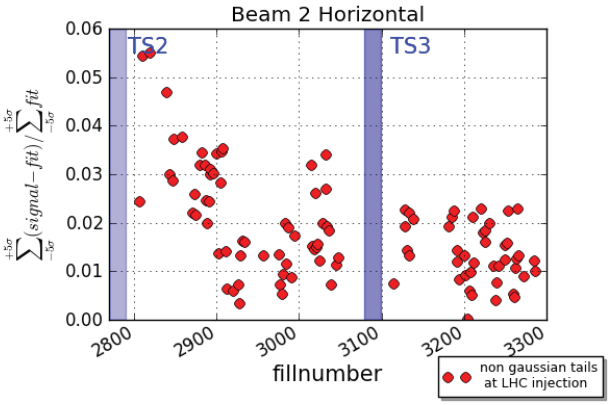

Figure 26: Tails calculated from the Gaussian fit of the transverse profiles measured with wire scanner and averaged over the first 144 bunch batch at LHC injection for the 2012 run after TS2.

INSTRUMENTATION WISH LIST FOR AFTER LS1

After the first long LHC shutdown (LS1) reliable emittance measurements through the whole cycle will be essential. The LHC wire scanners will have to be able to measure 288 bunches at injection. More time will have to be dedicated to understanding the wire scanner systematics to reliably calibrate the other instruments. Measurements through the cycle with physics beams would be highly desirable. For this the BSRT would need to be complemented with an operational BGI during the ramp. The installation of a Beam-Gas Imaging Vertex

Detector (BGV) following the principle of LHCb SMOG is under discussion. This device would greatly enhance the possibilities for understanding the LHC emittance evolution with physics beams.

CONCLUSIONS

At the end of LHC run 1, it is still very difficult to measure emittances and emittance blow-up. The wire scanner beam size measurements have large systematic errors due to issues with photomultiplier saturation. The emittances from luminosity still give the most trustable result. Emittance blow-up through the cycle in 2012 is similar to 2011. Most of the blow-up occurs during injection and ramp, occasionally also at the end of the squeeze. The sources of emittance growth at 450 GeV have been identified as IBS and 50 Hz noise. The cause for the blow-up during the ramp is still a mystery. The absolute emittance growth through the cycle is about 0.7 – 1 μm using the convoluted averaged emittance from luminosity. Any potential mitigation like RF batch-by-batch blow-up against IBS and higher transverse damper gain during the ramp have not lead to significant improvement of the emittance blow-up.

ACKNOWLEDGEMENTS

The authors would like to thank the colleagues from OP, CMS, ATLAS and LHCb for their cooperation and analysis during machine development periods.

REFERENCES

[1] V. Kain et al., "Emittance Preservation", LHC Operations Workshop, Evian, France 2011.

[2] H. Bartosik et al., Optics Considerations for Lowering Transition Energy in the SPS, IPAC 2011, San Sebastian, Spain, September 2011.

[3] R. Steinhagen, "Real-Time Beam Control at the LHC", PAC 2011, New York, USA, March 2011.

[4] M. Kuhn, "Emittance Preservation at the LHC", Master Thesis, University of Hamburg/CERN, Geneva, Switzerland 2012.

[5] H. Damerau et al., "Performance Potential of the Injectors after LS1", LHC Performance Workshop, Chamonix, France 2012.

OPTICS AND NON-LINEAR BEAM DYNAMICS AT 4 AND 6.5 TEV

R. Tomás, T. Bach, P. Hagen, A. Langner, Y.I. Levinsen, M.J. McAteer, E.H. Maclean, T.H.B. Persson, P. Skowronski and S. White

Abstract

2012 has been an extraordinary year for the control and understanding of the LHC optics. A record low β-beating of about 7% has been achieved during nominal operation. Consequently the luminosity imbalance between the two main experiments has also achieved a record low value. Magnet experts have found 1% gradient errors in some MQY quadrupoles, which are in good agreement with the beam-based optics corrections. A large effort has been put into probing the polarity of the non-linear correction circuits. So far more than 60 sextupolar and octupolar circuits have been probed revealing some inconsistencies. A large collection of new optics has been tested, including the post LS1 baseline β^*=0.4 m. Dedicated MDs have brought first time achievements in the LHC non-linear beam dynamics regime, namely: (i) measurement of DA at injection, (ii) chromatic coupling correction, (iii) IR non-linear corrections at β^*=0.6 m, and (iv) the direct measurement of amplitude detuning with AC dipoles. All of these accomplishments give a comfortable basis to make projections and recommendations towards 6.5 TeV.

RECORD LOW β-BEATING

High energy colliders have not traditionally required high precision control of their optics. The maximum relative deviation of the β-function with respect to the model (β-beating) is an appropriate figure of merit to compare different colliders. An illustration of the achieved peak β-beating in various high energy colliders is shown in Table 1 as collected during the "Optics Measurements, Corrections and Modeling for High-Performance Storage Rings" workshop [1]. References for the various machines on the table are: PEP II [2], LEP [3], KEKB [4], CESR [5], HERA-p [6], Tevatron [7] and RHIC [8]. The record low β-beating is held by CESR, the smallest of these colliders with a 768 m circumference. The achieved peak β-beating in these machines is far from the 1-2% in modern light sources such as DIAMOND [9], SOLEIL [10] and ALBA [11].

A 10% peak β-beating at top energy was already demonstrated in the LHC in 2010 [12]. However, owing to the change in the hysteresis branch of some quadrupoles involved in the correction, it was not possible to keep this 10% β-beating during regular operation. In 2011 this technical obstacle was solved [13] and a β-beating near 10% became operational [14, 15]. 2011 started with a β^*= 1.5 m and intensive optics corrections following the same strategies as in [12]. In August a beta squeeze down to β^*= 1 m was successfully commissioned [15], apparently without requiring further optics corrections, although precise β^* measurements were not performed. Between these two periods of different β^* the luminosity imbalance between the ATLAS and CMS experiments increased from roughly 5% to 10% [16] (providing more luminosity for CMS). Squeezing further down to 0.6 m in 2012 could have increased the luminosity imbalance to intolerable levels. It was therefore decided to place special attention to the optics commissioning following the procedure below:

1. Measure the machine in the absence of any beam-based corrections (*virgin* machine) throughout the entire magnetic cycle.
2. Reduce the measurement uncertainty compared to previous years by increasing the excitation amplitude of the AC dipole.
3. Compute new local IR corrections, which can remain constant throughout the beta squeeze process.
4. Compute global corrections to minimize β-beating and dispersion beating simultaneously.
5. Use of local β^* and IP waist knobs to equalize luminosities if required. These knobs must use independently powered quadrupoles excluding the triplet quadrupoles as these act on both beams.

All β-beating and coupling corrections prior to 2012 were removed all along the LHC magnetic cycle. The LHC AC dipoles [17] were used to measure the β-functions along the β^*-squeeze process. A peak β-beating of about 100% is reached for β^*= 0.6 m. The β-beating rms and peak values corresponding to all measurements during the β-squeeze are shown in Fig. 1. A monotonic increase of the peak and rms values is observed while reducing β^*, suggesting the need for local optics corrections in the Interaction Regions (IRs).

Local corrections are best suited for the IRs where the β functions are large and there are independently powered quadrupoles. However, the small phase advance between quadrupoles introduces some degeneracy in the possible corrections. To minimize the level of degeneracy, multiple optics were corrected simultaneously for both beams in 2012. Figure 2 shows an illustration of a simultaneous correction for six different optics (three per beam) using the segment-by-segment technique [18] for IR5. The good quality of the corrections, as illustrated in Fig. 2, in this tightly constrained scenario provides confidence in this approach.

Global corrections are required to take care of the optics errors in the arcs and the residuals from the IR local corrections. All available singly powered quadrupoles were used

Lepton Collider	Circumference [km]	Peak $\Delta\beta/\beta$ [%]	Hadron Collider	Circumference [km]	Peak $\Delta\beta/\beta$ [%]
PEP II	2.2	30	HERA-p	6.3	20
LEP	27	20	Tevatron	6.3	20
KEKB	3	20	RHIC	3.8	20
CESR	0.8	7	LHC	27	7

Table 1: Peak β-beating of various high energy colliders as collected during the Optics Measurements, Corrections and Modeling for High Performance Storage Rings workshop [1].

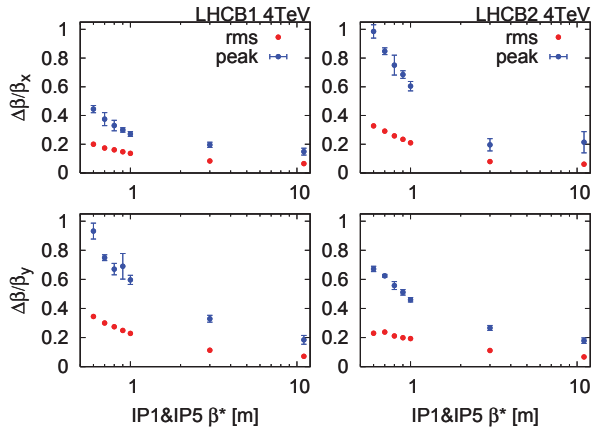

Figure 1: β-beating of the virgin machine along the squeeze. Beam 1 (left) and Beam 2 (right), horizontal (top) and vertical (bottom) plots showing the peak and rms β-beating values versus β^*.

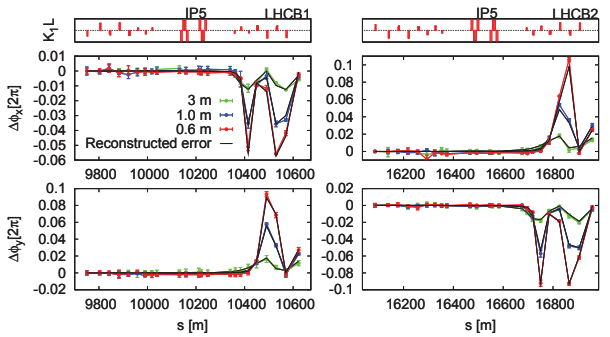

Figure 2: Illustration of the segment-by-segment technique applied to IR5 simultaneously to the two beams and three different β^*. The black lines show the reconstructed error model.

to minimize the β-beating and the normalized dispersion beating at all BPMs in an inverse response matrix approach. Figure 3 shows the evolution of the β-beating along the squeeze after local and global corrections. The record low β-beating of about 7% is reached for β^*= 0.6 m; see [18] for further details.

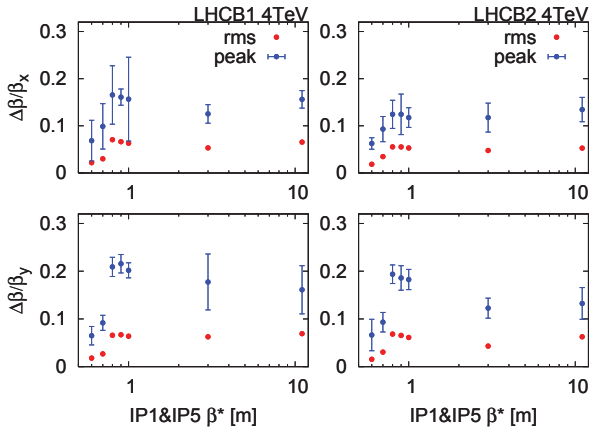

Figure 3: β-beating after local and global corrections along the squeeze. Beam 1 (left) and Beam 2 (right), horizontal (top) and vertical (bottom) plots showing the peak and rms β-beating values versus β^*.

COUPLING CORRECTION

The global coupling knobs for Beam 2 were improved before the 2012 run by optimizing their performance in computer simulations using their orthogonality and required skew quadrupole strength as figures of merit. The new knobs required substantially less strength of the skew quadrupole while providing a better orthogonality to the complex space of f_{1001} [19].

From the measurements of the the virgin machine new local coupling corrections were calculated for 2012. The local corrections have remained very constant throughout the magnetic cycle and very stable throughout the year. This is of big importance, for the use of the global knobs requires that the strong local sources are corrected.

The global knobs are used by the shift crew in an iterative manner to correct the coupling. The best setting is found by testing different settings of the global knobs while observing the $|C^-|$ in the TuneViewer [20]. This can be time consuming operation. The fact that the measurement is based on a pickup at a single location is also a limiting factor. This is because minimizing the coupling at this location might not be the same as minimize the coupling globally.

In 2012 a new software to measure the coupling from the

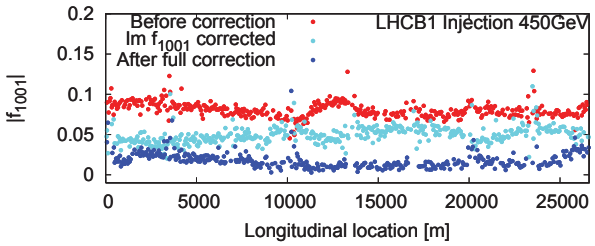

Figure 4: Coupling corrections using the turn-by-turn from the pilot injections in the LHC.

injections oscillations was developed. It uses the recorded turn-by-turn data for the first 1000 turns after an injection to calculate the f_{1001} at each individual BPM. It uses the undamped oscillations from the pilot bunches that are preceding every fill in the LHC. From the f_{1001} the optimum setting for the coupling knobs are calculated and presented in the software. This correction scheme has now been tested for both beams and proven itself successful in normal operation of the LHC. An example of a correction using this method is shown in Figure 4. In this case the correction was done in two steps, first correcting the imaginary part of the f_{1001}, and then later correcting the real as well as the imaginary part. However, in normal operation both parts of the f_{1001} can be corrected simultaneously. The corrections were successful and the results were in good agreement with the values received from the TuneViewer system. Hence, we can conclude that we were able to reduce the $|C^-|$ by about a factor 4. In 2011 there was a problem with large drifts of the coupling of Beam 2. In 2012 this problem seems to have disappeared and the need to change the coupling knobs is now less frequent.

MQY 1% CALIBRATION ERRORS

After revising the FiDeL existing magnetic measurements and the LHC LSA databases, inconsistencies of up to 1.5% where found in the transfer function of some MQY magnets. These errors seem in good agreement with those previously found from the optics measurement [18]. Table 2 compares the errors found from magnetic measurements (FiDeL) to the values from beam-based optics corrections. In most cases similar errors are found by both methods. The largest discrepancy (marked in red in the table) is for a rather strong error in IR8. The beam-based correction used a quadrupole right of IP8 while FiDeL finds an error in a quadrupole left of IP8.

In order to experimentally verify that the new FiDeL predictions are correct an MD was performed in November 2012. The magnet strength of the MQY quadrupoles was corrected according to the suggestions from FiDeL. The correction was performed via a knob in a virgin machine, without any other corrections, and starting from the pre-cycle up to the energy of 4 TeV to avoid any hysteresis effects. No beta-squeeze was performed during this MD.

Quad beam2	b-based [10^{-4}]	FiDeL [10^{-4}]	Quad beam1	b-based [10^{-4}]	FiDeL [10^{-4}]
q4.l1	13	0	q4.l1	0	0
q4.r1	0	0	q4.r1	0	0
q4.l2	0	0	q4.r2	0	0
q4.r2	0	0	q4.l2	0	0
q5.l2	0	36	q5.l2	0	41
q5.l4	0	0	q5.l4	0	0
q6.r4	0	0	q6.r4	0	0
q6.l4	0	61	q5.r4	0	21
q5.r4	0	10	q6.l4	0	72
q4.l5	100	153	q4.l5	0	32
q4.r5	0	0	q4.r5	0	0
q5.r6	10	0	q5.l6	60	72
q4.l6	0	0	q4.r6	0	0
q5.l6	70	73	q5.r6	10	0
q4.r6	0	0	q4.l6	0	0
q5.r8	80	95	q4.r8	0	0
q4.l8	0	119	q4.l8	100	122
q4.r8	240	0	q5.r8	270	99

Table 2: MQY errors as seen from beam-based optics corrections (b-based column) and FiDeL magnetic measurements. The largest discrepancy between these two approaches is marked in red.

Optics measurements with the AC dipole were carried out at flat-top. Figure 5 compares the resulting local phase-beating to measurements before the optics commissioning in 2012 for IR6 and IR8 of Beam 1. A clear improvement is achieved with the new calibrations. These improvements are also seen for other IRs and represent the experimental verification of the new MQY calibration.

POLARITY CHECKS

Polarities and strengths of the focusing and defocusing octupoles (MOF and MOD), spool piece octupole correctors (MCO), arc skew sextupole correctors (MSS), and interaction region sextupoles (MCSX and MCSSX) have been extensively checked. Table 3 summarizes the results of all the polarity checks.

Each arc contains between 8 and 13 octupoles of each of types MOF and MOD, and 77 type MCO. All octupoles of a type in each arc are powered as a group. More details about these magnets can be found in [21].The polarity of each octupole group in each arc was verified by trimming one group and measuring the resulting change in second order chromaticity. In each case the measured second order chromaticity agreed well with predicted value, indicating that all octupoles have the correct polarity.

Each arc contains four skew sextupoles MSS, powered as a group. The MSS polarities were checked by measuring the change to chromatic coupling when a magnet family was trimmed. A comparison of the measured chro-

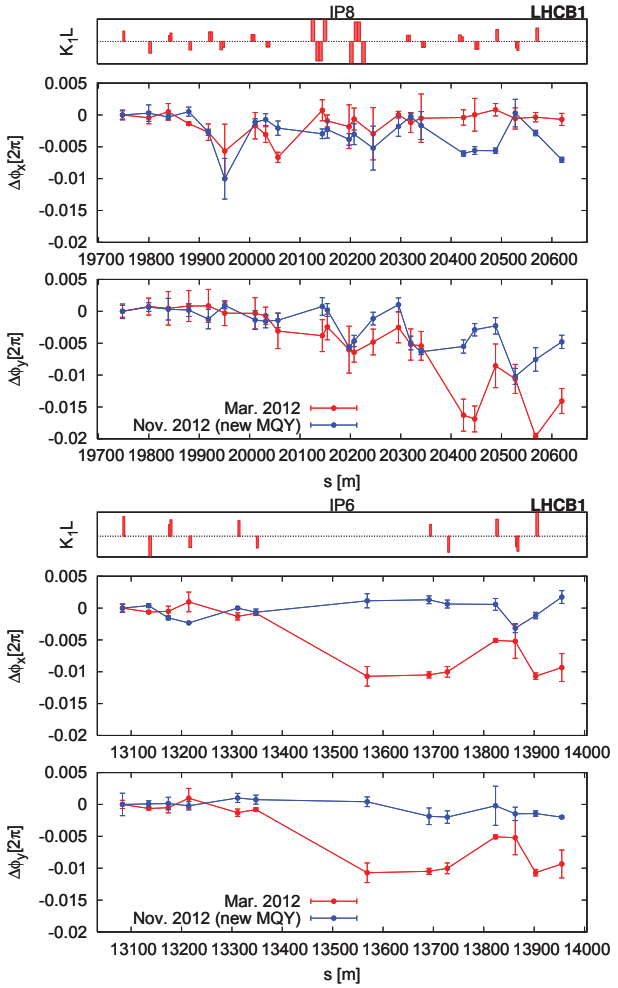

Figure 5: Phase beating with the old (red) and the new MQY calibrations (blue) for IR8 (top) and IR6 (bottom), showing a clear improvement with the new calibrations.

matic coupling with model predictions indicated that all measured MSS magnets have reversed polarity.

Each interaction region contains pairs of normal sextupole correctors MCSX and skew sextupole correctors MCSSX. The polarities of the skew sextupoles in IR1, where the crossing angle is vertical, and the normal sextupoles in IR5, where the crossing angle is horizontal, were verified by trimming the magnets and measuring the resulting tune shifts. Comparison of the measured tune shifts with model predictions shows that the polarities of MCSSX in IR1 and MCSX in IR5 are correct.

DA MEASUREMENT AT INJECTION

During the June 2012 MD block non-linear optics studies were performed on LHC Beam 2 at injection. The Aperture Kicker (MKQA) was used to excite high amplitude betatron oscillations for the measurement of the dynamic aperture (DA) and first and second order anharmonicities.

Type	Location	polarity	Location	polarity
MOF	A12 B1	Correct	A12 B2	Correct
MOF	A23 B1	Correct	A23 B2	Correct
MOF	A34 B1	Correct	A34 B2	Correct
MOF	A45 B1	Correct	A45 B2	Correct
MOF	A56 B1	Correct	A56 B2	Correct
MOF	A67 B1	Correct	A67 B2	Correct
MOF	A78 B1	Correct	A78 B2	Correct
MOF	A81 B1	Correct	A81 B2	Correct
MOD	A12 B1	Correct	A12 B2	Correct
MOD	A23 B1	Correct	A23 B2	Correct
MOD	A34 B1	Correct	A34 B2	Correct
MOD	A45 B1	Correct	A45 B2	Correct
MOD	A56 B1	Correct	A56 B2	Correct
MOD	A67 B1	Correct	A67 B2	Correct
MOD	A78 B1	Correct	A78 B2	Correct
MOD	A81 B1	Correct	A81 B2	Correct
MCO	A12 B1	NA	A12 B2	NA
MCO	A23 B1	Correct	A23 B2	Correct
MCO	A34 B1	Correct	A34 B2	Correct
MCO	A45 B1	Correct	A45 B2	Correct
MCO	A56 B1	Correct	A56 B2	Correct
MCO	A67 B1	Correct	A67 B2	Correct
MCO	A78 B1	Correct	A78 B2	NA
MCO	A81 B1	Correct	A81 B2	NA
MSS	A12 B1	Reversed	A12 B2	Reversed
MSS	A23 B1	Reversed	A23 B2	Reversed
MSS	A34 B1	Reversed	A34 B2	Reversed
MSS	A45 B1	-	A45 B2	Reversed
MSS	A56 B1	-	A56 B2	Reversed
MSS	A67 B1	-	A67 B2	Reversed
MSS	A78 B1	-	A78 B2	-
MSS	A81 B1	NA	A81 B2	-
MCSSX	L1	Correct	R1	Correct
MCSX	L5	Correct	R5	Correct
MQS	A23 B1	Reversed	R2 B2	Reversed
MQS	A45 B1	Reversed	R4 B2	Reversed
MQS	A67 B1	Reversed	R6 B2	Reversed
MQS	A81 B1	Reversed	R8 B2	Reversed
MQS	L2 B1	Reversed	L1 B2	Reversed
MQS	L6 B1	Reversed	L3 B2	Reversed
MQS	L8 B1	Reversed	L5 B2	Reversed
MQS	R1 B1	Reversed	L7 B2	Reversed
MQS	R5 B1	Reversed	A12 B2	Reversed
MQS	R7 B1	Reversed	A78 B2	Reversed
MQS			A56 B2	Reversed
MQSX	L1	Reversed	R1	Reversed
MQSX	L2	Reversed	R2	Reversed
MQSX	L5	Reversed	R5	Reversed
MQSX	L8	Reversed	R8	Reversed

Table 3: Polarities of arc octupoles, arc sextupoles, and interaction region sextupoles as resulting from beam-based comparisons between LSA and MAD. "NA" stands for not available and the sign "-" means that the corresponding circuit was not tested.

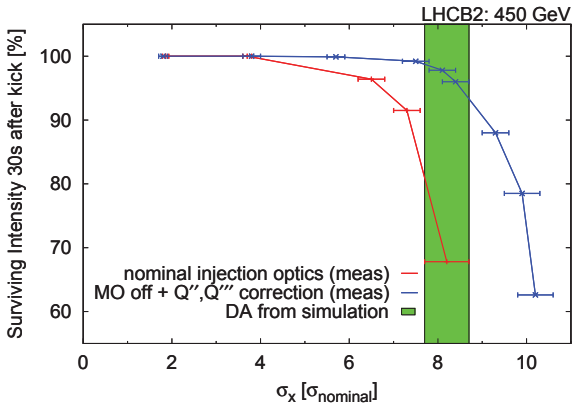

Figure 6: Surviving beam intensity 30 seconds after a transverse kick versus the amplitude of the kick for the nominal (red) and the corrected (blue) machines. The simulated dynamic aperture is also shown corresponding to the nominal machine during the first part of the year with the defocusing polarity in the MO Landau octupoles.

Measurements were performed on the nominal injection settings, and with the Landau octupoles (MO) depowered and Q'' and Q''' corrections applied to obtain as linear a machine as possible.

By examining how losses experienced by the beam varied with amplitude of excitation it is possible to determine the DA. In particular by linearising the machine in the second stage of the MD and repeating the measurement, the effect of the DA was clearly revealed. Figure 6 shows the surviving beam intensity following horizontal excitation with the MKQA versus the amplitude of excitation. Our best available model of the LHC (which well reproduces the measured detuning with amplitude) has been used to perform DA simulations with SIXTRACK. The result of this simulation was found to be $8.2 \pm 0.5\sigma_{nominal}$[1] and is also displayed in Figure 6. Our measurements and simulation are in excellent agreement.

Later in 2012 the polarity of the MO were reversed for operation. Figure 7 shows the results of SIXTRACK simulations with our best model for both polarities of MO, showing a clear improvement with the new polarity.

CHROMATIC COUPLING CORRECTION

The systematic skew sextupole components in the dipoles are known to cause significant chromatic coupling if left uncorrected. There are several skew sextupoles installed to compensate for this known systematic effect [22]. The spurious skew sextupole errors will produce additional chromatic coupling since the dispersion is largely horizontal. Normal sextupoles produce chromatic coupling in regions of vertical dispersion. Once linear coupling is well corrected, chromatic coupling should be corrected as well for optimal machine performance.

[1]By $\sigma_{nominal}$ we refer to the beam size with normalized emittance of $\epsilon = 3.75$ μm.

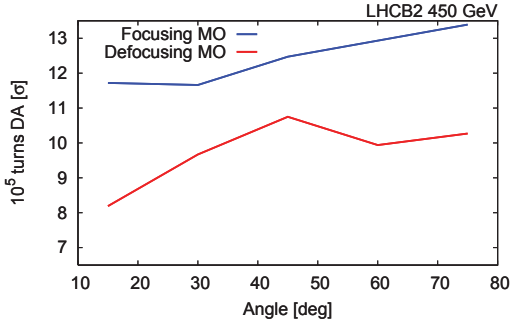

Figure 7: Dynamic aperture at injection with nominal tunes and for the two polarities of the Landau octupoles. The defocuing MO corresponds to the MO polarity during the first part of the year.

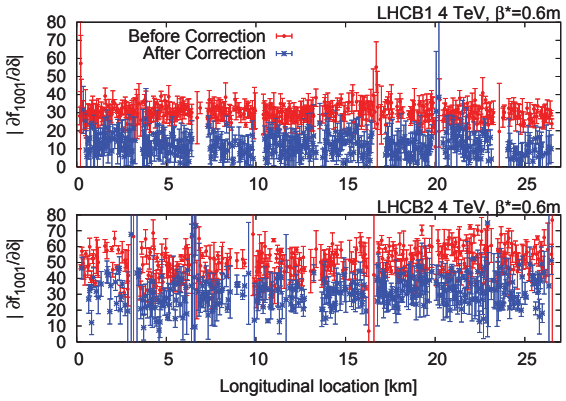

Figure 8: First chromatic coupling correction in the LHC for Beam 1 (top) and Beam 2 (bottom).

In 2012 the first beam based chromatic coupling correction was performed in the LHC. The correction was tested for the nominal 2012 optics, meaning a β^*= 0.6 m. Beam 2 had 9 independent skew sextupole circuits while Beam 1 had 8 available at this time. In Figure 8 the chromatic coupling before and after correction are presented. The weighted mean value of $\partial f_{1001}/\partial\delta$ was measured to be somewhat larger for Beam 2 than Beam 1, approximately 50 units for beam 2 and 30 units for Beam 1. The chromatic f_{1001} was decreased by about 20 units for both beams, proving that the corrections were successful.

IR NON-LINEAR CORRECTION

Non-linear errors in the the LHC IRs may have a significant detrimental impact on lifetime and dynamic aperture. By examining the feed down to tunes and free coupling while varying the crossing angles in IP1 and IP5, we have performed first attempts at the local correction of higher order magnetic errors in the LHC IRs.

Table 4 displays the feed down to tune and coupling from higher order multipoles for horizontal and vertical excursions.

Table 4: Tune (ΔQ) and Coupling (ΔC) feed down from non-linear Multipoles

	b_3	a_3	b_4	a_4	b_5	a_5	b_6
H bump	ΔQ	ΔC	ΔQ	ΔC	ΔQ	ΔC	ΔQ
V bump	ΔC	ΔQ	ΔQ	ΔC	ΔC	ΔQ	ΔQ

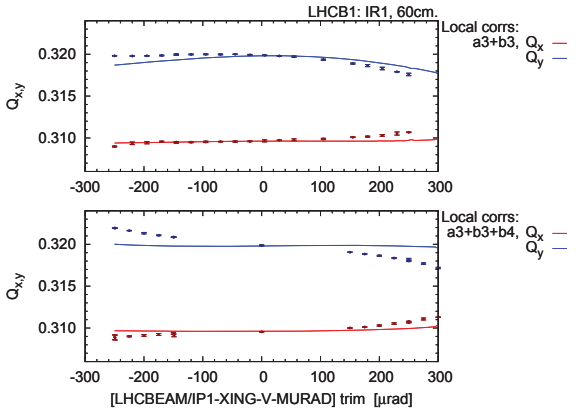

Figure 9: Beam 1 tunes vs IP1 crossing angle from measurement and simulation with $a_3 + b_3$ and $a_3 + b_3 + b_4$ correction applied.

Measurements performed on the uncorrected machine during the $\beta^* = 0.6$ m MD in November 2012 showed a good agreement with simulations incorporating magnetic measurements of the errors in the IRs. The magnetic measurements were therefore used for the calculation of local corrections of the b_3, a_3 and b_4 multipoles in IP1 and IP5.

During dedicated MD time the crossing angles in IP1 and 5 (vertical and horizontal respectively) were varied, firstly with $a_3 + b_3$ corrections applied, then on further addition of the b_4 correction. The tunes as measured by the LHC BBQ system and found in simulation, are plotted versus the IP1 crossing angle in Figures 9 and 10 for Beam 1 and 2 respectively.

The coupling data was of too low quality to draw any conclusions; however the method has previously been successful observing feed down from errors in IP2. Analysis of IP5 data is ongoing.

Measurement and simulation with $a_3 + b_3$ corrections applied show a good agreement for both beams (note however that this verifies only the a_3 correction in IP1: the b_3 feeds down to coupling for a vertical excursion). On applying the b_4 correction, measurement and simulation remain in good agreement for Beam 2; however Beam 1 displays a large linear discrepancy in the variation of tune with crossing angle. This may be explained by a $\sim$ 5mm vertical misalignment of the b_4 corrector with respect to the b_4 sources. Results of simulation incorporating such a misalignment are shown in Figure 11, which is seen to be in good agreement with the measurements.

The additional a_3 component resulting from feed-down

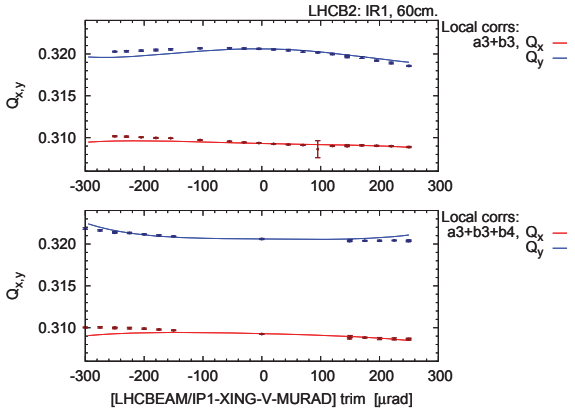

Figure 10: Beam 2 tunes vs IP1 crossing angle from measurement and simulation with $a_3 + b_3$ and $a_3 + b_3 + b_4$ correction applied.

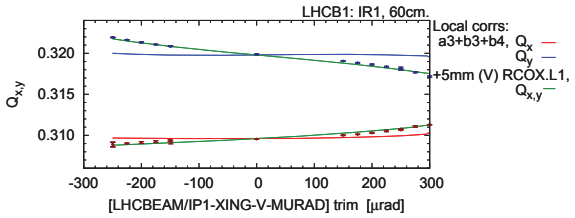

Figure 11: Beam 1 tunes vs IP1 crossing angle from measurement and simulation with $a_3 + b_3 + b_4$ corrections applied and a 5mm vertical misalignment of the b_4 corrector.

from the b_4 corrector must be incorporated in any final correction scheme, however these results demonstrate the feasibility of applying this method to the LHC.

MEASUREMENT OF AMPLITUDE DETUNING

The amplitude detuning is a critical parameter for the understanding and control of beam instabilities. Yet, measuring the amplitude detuning at top energy represents a real challenge as the only available exciters that can provide a few sigmas oscillation are the AC dipoles. Furthermore, the AC dipoles force oscillations at frequencies different from the natural tunes of the machine and, ideally, the machine tunes should not be excited during the flat-top. We relied on the residual non-adiabaticity of the AC dipole ramping process to measure the tunes during a dedicated MD in 2012. The actual observation of the machine tunes required aggressive cleaning using SVD techniques. The measured horizontal and vertical tunes are shown in Fig. 12 versus the horizontal oscillation amplitude for Beam 2. This represents the first successful direct measurement of amplitude detuning with AC dipoles. The comparison to model predictions is under study [23].

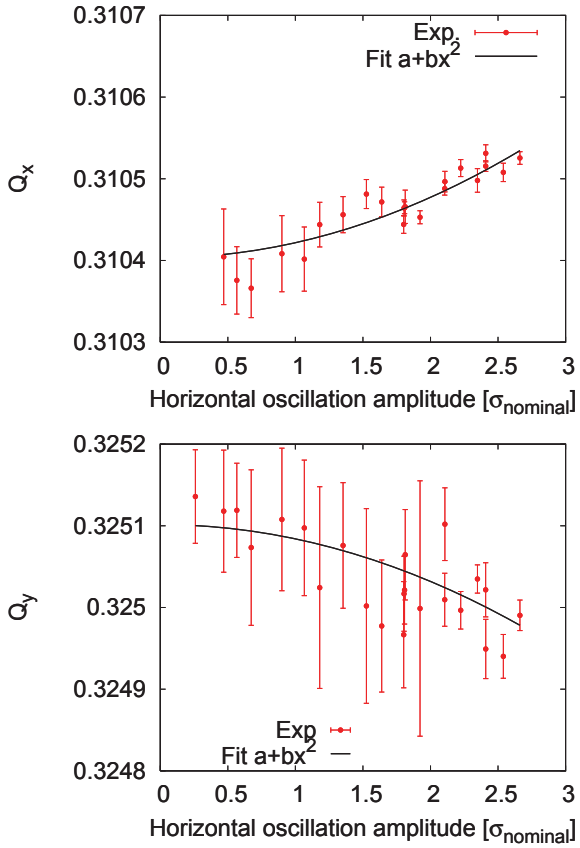

Figure 12: Beam 2 horizontal (top) and vertical (bottom) amplitude detuning versus the horizontal oscillation amplitude as measured during 2012 MDs at β^*=0.6 m together with quadratic fits.

OPTICS MEASUREMENTS AT β^*=0.4 M

During the 2012 MDs two different optics featuring β^*=0.4 m were tested and measured in the LHC. One optics corresponds to the continuation of the nominal squeeze and the other uses the ATS [24]. In both cases IR local corrections were implemented while global corrections were considered less critical and, consequently, they were not applied. The β-beating from these optics is compared in Fig. 13, both showing similarly acceptable levels of β-beating.

The off-momentum optics aberrations have been a concern for the LHC machine protection at low β^* values since these could degrade the collimation performance. A direct measurement of the off-momentum β-beating for the nominal optics at β^*=0.4 m is shown in Fig. 14. Measurement and model predictions are in very good agreement.

INJECTION TUNES AND β^* AFTER LS1

The first step of the LHC beta-squeeze at top energy consists in shifting the fractional tunes between the injection (0.28, 0.31) and collision (0.31, 0.32) working points. Figure 15 shows the tune jump crossing 7th and 10th order resonances. This was decided to reduce the effects from transverse coupling at injection and during the energy ramp, and to profit from the larger Dynamic Aperture at the injection tunes [25, 26]. However, nowadays this tune jump is found to be too violent for the orbit feedback and, furthermore, in the scenario of a smaller β^* at injection and/or at flat-top the tune jump would be seen as even more violent (not only for the orbit feedback but also for beam losses due to stronger resonances). A possible way to avoid losing the orbit feedback during the tune jump would be to lengthen the time used for the jump. This would cause softer changes in the orbit but, on the other hand, it would increase the time that the beams sit on the 7th and 10th order resonances.

The feasibility of injecting and ramping with collision tunes was already demonstrated during the MDs of 2011 [27]. Figure 16 shows how after correcting the transverse coupling along the energy ramp the collision tunes

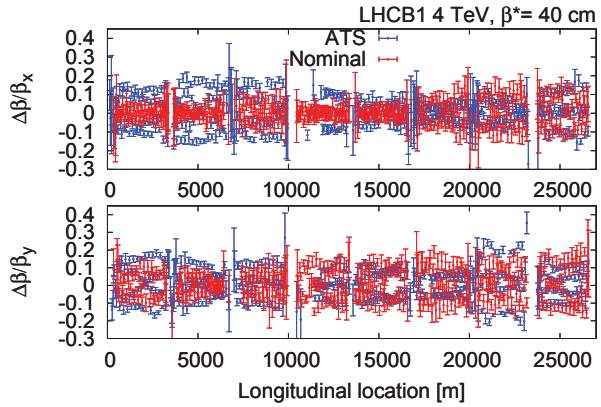

Figure 13: Horizontal (top) and vertical (bottom) β-beating as measured during 2012 MDs for two different optics at β^*=0.4 m.

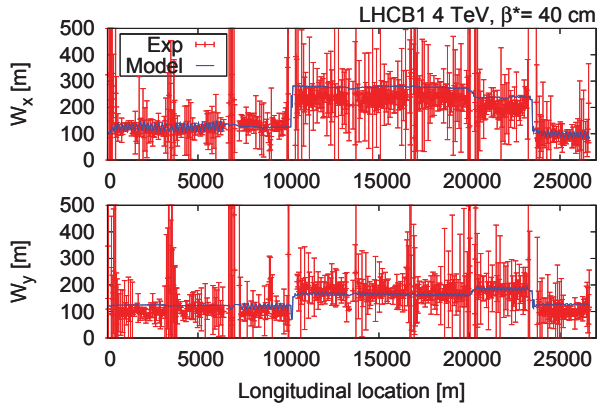

Figure 14: Chromatic β-beating (Montague function) for the nominal LHC optics at β^*=0.4 m compared to the model prediction (blue line).

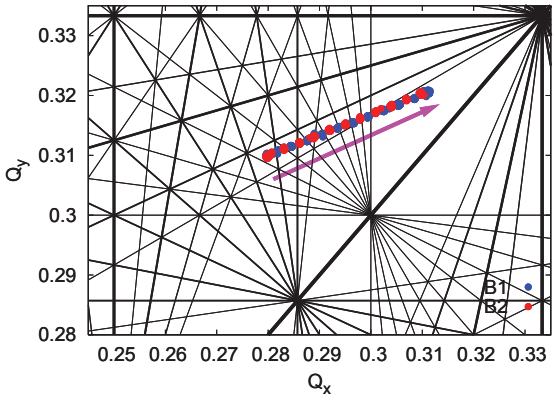

Figure 15: Tune jump between injection and collision tunes together with the relevant resonances.

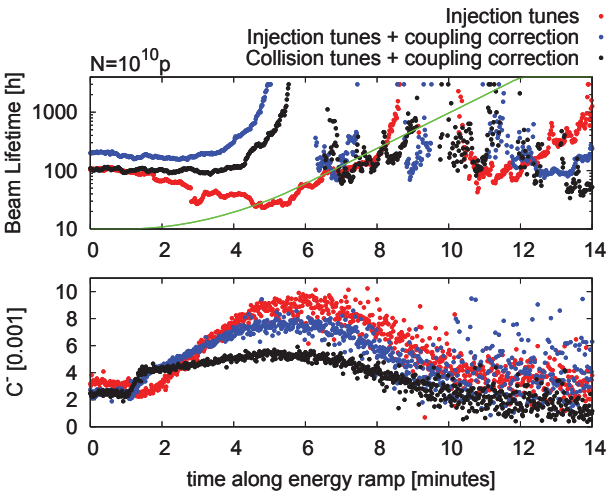

Figure 16: Comparison of lifetime and coupling along 3 energy ramps with injection tunes (2 successive coupling corrections) and collision tunes.

performed as well as the injection tunes in terms of lifetime.

As shown in Section "DA measurement at injection" Landau octupoles have an impact on dynamic aperture. Figure 17 shows the DA using collision tunes at injection for the two 2012 octupole settings. This is to be compared to Fig. 7 with nominal injection tunes. For the defocusing octupole polarity (used during the first months of 2012) a DA increase of about 4σ is observed moving to the collision tunes. For the focusing octupole polarity (used towards the end of 2012) a reduction of about 1σ is observed. In the scenario of using collision tunes and the octupole focusing polarity a reduction of the octupole strength should be investigated in order not to lose this 1σ in the DA. As a matter of fact the strength of the octupoles at injection was not optimized during 2012.

In [28] it was already proposed to use collision tunes at injection and reduce a couple of meters the β^* in IP1 and

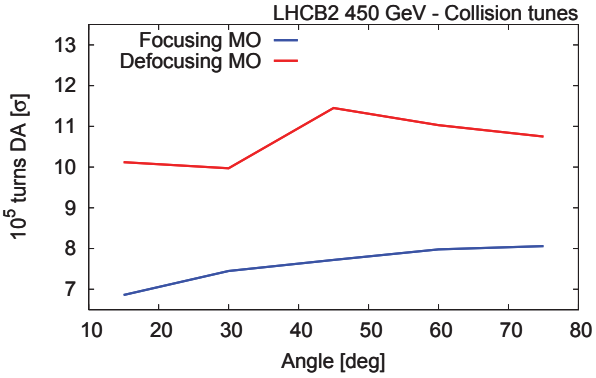

Figure 17: Dynamic aperture at injection with collision tunes and for the two polarities of the Landau octupoles.

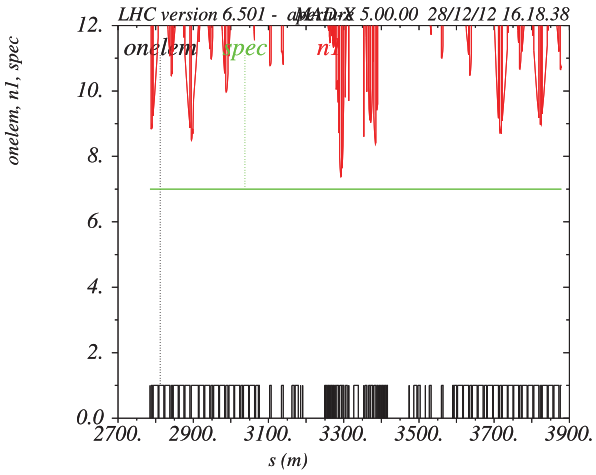

Figure 18: Aperture in terms of N1 for Beam 1 and IR5. The used parameters are: $\epsilon_{x,y} = 3\mu$m, c.o.= 3mm, $\frac{dp}{p} = 0.5‰$, $\theta = 190\mu$m.

IP5. The minimum β^* at injection is limited by the available aperture in the IR and by the minimum current allowed in the MQY magnets, which is nominally 120 A. This limit is just above the 116 A needed for the β^* =5 m; however, magnet experts would consider acceptable to reduce the 120 A nominal limit to 116 A. The available aperture puts tighter constraints in the β^*. The half crossing angle scales as $\theta[\mu\text{m}] = 170\sqrt{11\epsilon/(\beta^*3.75)}$, where ϵ is the emittance in μm. The largest emittance expected in 2015 at injection is $\epsilon = 3\mu$m. This sets a β^*=7 m as an absolute minimum as shown in Fig. 18. However, it might not be needed to push so much the β^* since there will be the possibility to squeeze the β^* during the energy ramp.

RAMP & SQUEEZE AND COLLIDE & SQUEEZE

The IR2 and IR8 triplets in their injection optics configuration can only be ramped up to 6.45 TeV. Therefore to reach the planned 6.5 TeV after LS1, the optics has to be

	Beam 1	Beam 2
Maximum focusing in MO, MCO & MCOX		
∂Qx/∂2Jx [Amps (MO equiv.)]	1191	-1012
∂Qy/∂2Jy [Amps (MO equiv.)]	619	-1319
∂Qx/∂2Jy [Amps (MO equiv.)]	650	-2638
Maximum defocusing in MO, MCO & MCOX		
∂Qx/∂2Jx [Amps (MO equiv.)]	-586	1540
∂Qy/∂2Jy [Amps (MO equiv.)]	-1086	1082
∂Qx/∂2Jy [Amps (MO equiv.)]	-1482	1976

Table 5: Amplitude detunings for two configurations of the available octupoles in the LHC at 7 TeV yielding a maximum focusing for Beam 1 and a maximum defocusing for Beam 1 at β^*=0.4 m.

modified during the energy ramp. This qualitative step in optics control and commissioning should be used to start the beta-squeeze during the ramp and save time for luminosity production. This is known as Ramp & Squeeze [29].

It has been proposed to put the beams in collision before the end of the beta-squeeze. This could help to suppress instabilities and/or to increase integrated luminosity via β^* leveling.

The challenge being faced by both Ramp & Squeeze and Collide & Squeeze is the optics measurement resolution with just a single AC dipole shot (since it has to be run while magnets ramp). Some test measurements during the energy ramp in 2012 revealed about a 10% resolution on the β-functions. Doubling the length of the AC dipole flattop excitation from 200 ms to 400 ms might be the only way to improve the measurement resolution. Currently it would not be straight forward to reconstruct the optics status of the machine at any given time, e.g. between two matching points during the squeeze. Some tools will need to be developed to address this point.

DA AND OCTUPOLE REACH AT β^*=0.4 M

Since MO octupoles were used close to their maximum strength at 4 TeV it is feared that they will not be strong enough for 6.5 or 7 TeV. However it is possible to resort to the inner triplet octupoles to provide extra amplitude detuning. This has the inconvenience that the the inner triplet octupoles affect both beams with opposite effects in the amplitude detuning. Therefore when using these octupoles the maximum amplitude detuning will need to have opposite signs for the two beams. Table 5 shows the maximum amplitude detunings in terms of MO equivalent current for both beams in the two possible configurations. The direct term of the amplitude detuning can be doubled with respect to using only the arc MO octupoles.

In these extreme octupolar configurations a reduction of the single particle dynamic aperture is expected. Figure 19 shows DA calculations in four configurations at 7 TeV and at β^*=0.4 m corresponding to: IR correction, No IR correction, Maximum octupole focusing and Maximum octupole defocusing. The ideal configuration is with IR correction,

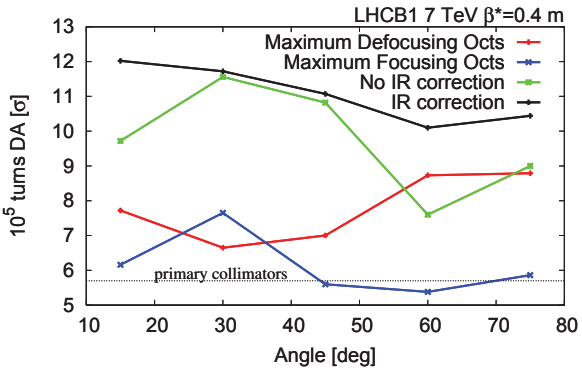

Figure 19: Dynamic aperture at 7 TeV and β^*=0.4 m for the bare machine (No IR correction), including IR correction and using the octupolar IR correctors to generate maximum focusing or maximum defocusing amplitude detuning.

	Minimum DA [σ]
IR correction	10
No IR correction	7.5
Maximum octupole focusing	5.5
Maximum octupole defocusing	6.5

Table 6: Minimum DA for two configurations of the available octupoles for Beam 1 at 7 TeV and β^*=0.4 m.

feature the largest DA. Removing the IR non-linear correction reduces the DA by almost 3σ. This is a strong reason to make available all inner triplet correctors after LS1. Using all octupoles with the above extreme configurations cause a significant loss of DA even below the settings of the primary collimators. The minimum DA is summarized in Table 6.

LUMINOSITY PROJECTIONS AT 6.5 TEV

Table 7 shows peak luminosities for various β^* and crossing angles at 6.5 TeV with the 50 ns bunch spacing configuration and assuming normalized emittances of $\epsilon = 1.6$ μm. The crossing angle is chosen to provide a separation of 9.3 σ in the horizontal plane. The upper part of the table shows luminosities for round beams yielding up to 2.4 10^{34}cm^{-2}s^{-1} with the lowest foreseen β^* of 0.3 m. The lower part of the table shows flat optics with tentative β^*s that might be achievable if the lowest β^* is set in the plane where the beam chamber has the largest aperture in the triplets. A 23% increase in luminosity might be avhievable with flat optics if the corresponding minimum β^* were avhievable.

Table 8 shows peak luminosities for various β^* and crossing angles at 6.5 TeV with the 25 ns bunch spacing configuration and assuming normalized emittances of $\epsilon = 1.9$ μm. The crossing angle is chosen to provide a separation of 12 σ in the horizontal plane. The upper part of the table shows luminosities for almost round beams yielding up to 1.9 10^{34}cm^{-2}s^{-1} with the lowest foreseen β^* of

β_x^* [m]	β_y^* [m]	θ [μrad]	Pile-up	Luminosity [10^{34}cm^{-2}s^{-1}]	Δ [%]
0.5	0.5	201	110	1.90	
0.4	0.4	225	130	2.14	13
0.3	0.3	260	150	2.41	13
0.6	0.4	184	130	2.08	
0.6	0.3	184	140	2.40	15
0.6	0.2	184	180	2.94	23

Table 7: Luminosity projections for various β^* and crossing angles at 6.5 TeV with the 50 ns configuration and assuming normalized emittances of $\epsilon = 1.6$ μm. The last column shows the relative differential luminosity with respect to the previous row.

β_x^* [m]	β_y^* [m]	θ [μrad]	Pile-up	Luminosity [10^{34}cm^{-2}s^{-1}]	Δ [%]
0.5	0.5	282	47	1.60	
0.45	0.43	298	50	1.71	7
0.37	0.33	326	56	1.92	12
0.5	0.33	282	58	1.97	
0.5	0.23	282	69	2.36	20

Table 8: Luminosity projections for various β^* and crossing angles at 6.5 TeV with the 25 ns configuration and assuming normalized emittances of $\epsilon = 1.9$ μm. The last column shows the relative differential luminosity with respect to the previous row.

0.33 m. The lower part of the table shows flat optics with tentative β^*s that might be achievable if the lowest β^* is set in the plane where the beam chamber has the largest aperture in the triplets. A 20% increase in luminosity might be avhievable with flat optics if the corresponding minimum β^* were avhievable. The 25 ns configuration gives about 20% lower luminosity than the 50% for similar β^* settings. It is important to note that the peak luminosity is almost insensitive to the β^* in the crossing plane between β^* =0.37 m and β^* =0.6 m since a reduction of β^* implies an increase in the crossing angle.

SUMMARY & OUTLOOK

2012 has been an extraordinary year for the LHC Optics Measurement and Corrections. A long list of first time achievements has been accomplished:

1. Record low beta-beating of 7% for hadron colliders
2. First LHC Dynamic Aperture measurement at injection benchmarking simulations
3. First LHC beam-based chromatic coupling correction improving existing model-based corrections
4. First demonstration of triplet non-linear corrections in LHC
5. First direct measurement of amplitude detuning using AC dipoles.

Furthermore, probably all the quadrupole errors in the 1% level have been identified and the databases will be fixed for 2015. All these accomplishments give a comfortable basis to make projections and recommendations for the post LS1 era. Starting from injection the tunes should be already set to the collision tunes to avoid tune jumps at low β^* since it is foreseen to squeeze during the energy ramp. If the squeeze during the energy ramp needed to be boosted the IP1 and IP5 β^* at injection could be reduced to some value above 7 m. The Landau octupoles have a significant impact on the dynamic aperture at injection. The lowest strength needed to suppress instabilities from collective effects should be used. The optics measurements during the ramp and squeeze with the 2012 performance would not be good enough to guarantee corrections at β^* values close to 1 m. In order to reach a β^*=1 m in the ramp and squeeze it is recommended to extend the AC dipole plateau and to provide tools to reconstruct the machine status at any given time.

A β^*=0.4 m was already demonstrated in 2012 with two different optics concepts. Achieving β^*=0.3 m should be equally feasible. It is recommended to make available all IR non-linear correctors as they can significantly improve the DA at these low β^* values. If the arc MO octupoles were not strong enough to suppress instabilities the IR octupoles could be used to considerably enhance the amplitude detuning. However the DA could also be severely reduced and therefore compromises should be adopted. The two bunch spacing configurations of 25 ns and 50 ns have been considered for luminosity evaluations. The 25 ns bunch spacing tends to give a 20% lower peak luminosity than the equivalent β^* setting at 50 ns.

ACKNOWLEDGMENTS

We would like to thank the following people for their contributions and discussions: O.E. Berrig, R. Bruce, S. Fartoukh, M. Giovannozzi, B. Goddard, W. Herr, D. Jacquet, V. Kain, A. Macpherson, N. Magnin, R. de Maria, R. Miyamoto, N. Mounet, T. Pieloni, M. Pojer, S. Redaelli, F. Schmidt, M. Solfaroli, E. Todesco and J. Wenninger.

REFERENCES

[1] Optics Measurements, Corrections and Modeling for High-Performance Storage Rings, June 2011, CERN. https://indico.cern.ch/conferenceDisplay.py?confId=132526

[2] Y.T. Yan, Y. Cai, F-J. Decker, J. Irwin, J. Seeman, S. Ecklund, M. Sullivan, J. Turner, U. Wienands, "PEP-II Beta Beat Fixes with MIA", SLAC-PUB-10369, 2004.

[3] P. Castro, "Applications of the 1000-turns Orbit Measurement System at LEP", Proceedings of the 1999 Particle Accelerator Conference, New York, 1999.

[4] A. Morita, H. Koiso, Y. Ohnishi and K. Oide, "Measurement and correction of on- and off-momentum beta functions at KEKB", Phys. Rev. ST Accel. Beams **10**, 072801 (2007).

[5] D. Sagan, R. Meller, R. Littauer, and D. Rubin, "Betatron phase and coupling measurements at the Cornell Electron/Positron Storage Ring", Phys. Rev. ST Accel. Beams **3**, 092801 (2000).

[6] F. Brinker, H. Burkhardt, W. Decking, K. Ehert, W. Fischer, M. Funcke, E. Gianfelice, S. Herb, G.H. Hoffstaetter (editor), U. Hurdelbrink, W. Kriens, C. Montag, F. Schmidt, F. Stulle, R. Tomás, E. Vogel, M. Werner, A. Xiao, "HERA Accelerator studies 2000", DESY HERA 00-07.

[7] A. Jansson, P. Lebrun, J.T. Volk, "Beta function measurement in the Tevatron using quadrupole gradient modulation", Proceedings of PAC 2005, Knoxville, Tennessee.

[8] G. Vanbavinckhove, M. Bai, G. Robert-Demolaize, "Optics corrections at RHIC", Proceedings of IPAC 2011, San Sebastián, Spain.

[9] I.P.S. Martin, R. Bartolini, R. Fielder, E. Longhi, B. Singh, "Electron beam dynamics studies during commissioning of the DIAMOND storage ring", Proceedings of PAC07, Albuquerque, New Mexico, USA. "Further advances in understanding and optimising beam dynamics in the DIAMOND storage ring", Proceedings of EPAC08, Genoa, Italy.

[10] L.S. Nadolski, "Use of LOCO at synchrotron SOLEIL", Proceedings of EPAC08, Genoa, Italy.

[11] G. Benedetti, D. Einfeld, Z. Martí, M. Muñoz, "LOCO in the ALBA storage ring", Proceedings of IPAC 2011, San Sebastián, Spain.

[12] R. Tomás, M. Aiba, C. Alabau, O. Brüning, R. Calaga, M. Giovannozzi, V. Kain, P. Hagen, M. Lamont, R. Miyamoto, F. Schmidt, M. Strzelczyk and G. Vanbavinckhove, "The LHC Optics in Practice", 2nd Evian 2010 Workshop on LHC Beam Operation, Evian, 7-9 Dec. 2010, CERN-ATS-2011-017.

[13] L. Deniau, N. Aquilina, L. Fiscarelli, M. Giovannozzi, P. Hagen, M. Lamont, G. Montenero, R. Steinhagen, M. Strzelczyk, E. Todesco, R. Tomás, W. Venturini Delsolaro and J. Wenninger, "The magnetic model of the LHC during commissioning to higher beam intensities in 2010-2011", Proceedings of IPAC 2011, San Sebastián, Spain.

[14] G. Vanbavinckhove, M. Aiba, R. Calaga, R. Miyamoto and R. Tomás, "Record low β-beat of 10% in the LHC", Proceedings of IPAC 2011, San Sebastián, Spain.

[15] R. Assmann, R. Bruce, M. Giovannozzi, M. Lamont, E. Maclean, R. Miyamoto, G. Mueller, G. Papotti, L. Ponce, S. Redaelli, R. Tomás, G. Vanbavinckhove and J. Wenninger, "Commissioning of the betatron squeeze to 1 m in IR1 and IR5", CERN-ATS-Note-2012-005 MD

[16] E. Meschi, "Luminosity comparison for ATLAS and CMS" 129th LHC Machine Committee meeting held on 18 April 2012.

[17] J. Serrano and M. Cattin, "The LHC AC Dipole system: an introduction", CERN-BE-Note-2010-014 (CO).

[18] R. Tomás, T. Bach, R. Calaga, A. Langner, Y.I. Levinsen, E.H. Maclean, R. Miyamoto, T.H.B. Persson, P.K. Skowronski, M. Strzelczyk and G. Vanbavinckhove, "Record low β-beating in the LHC", Phys. Rev. ST Accel. Beams **15**, 091001 (2012).

[19] R. Tomás, "Optimizing the global coupling knobs for the LHC", CERN-ATS-Note-2012-019 MD.

[20] A. Boccardi, M. Gasior, O. R. Jones, P. Karlsson, R. J. Steinhagen, "First Results from the LHC BBQ Tune and Chromaticity Systems", CERN LHC-Performance-Note-007 (2008)

[21] O. Brüning, P. Collier, P. Lebrun, S. Myers, R. Ostojic, J. Poole and P. Proudlock, "LHC design report", CERN-2004-003-V-1.

[22] S. Fartoukh, "Chromatic Coupling Induced by Skew Sextupolar Field Errors in the LHC Main Dipoles and its Correction", CERN-LHC-Project-Report-278, 1999.

[23] S. White, E.H. Maclean and R. Tomás, "Direct measurement of amplitude detuning with AC dipoles", to be published.

[24] S. Fartoukh, V. Kain, Y. Levinsen, E. Maclean, R. de Maria, T. Person, M. Pojer, L. Ponce, P. Skowronski, M. Solfaroli, R. Tomás and J. Wenninger, "The 10 cm beta* ATS MD", CERN-ATS-Note-2013-004 MD.

[25] L. Jin and F. Schmidt, "Dynamic Aperture tune scan for LHC version 5 at injection energy", LHC Project Note 182 (1998).

[26] S. Fartoukh, M. Giovannozzi, "Dynamic aperture computation for the as-built CERN Large Hadron Collider and impact of main dipoles sorting" NIM-A, **671**, 2012.

[27] R. Calaga, D. Jacquet, E. Metral, R. Miyamoto, N. Mounet, L. Ponce, S. Redaelli, B. Salvant, F. Schmidt, R. Steinhagen, R. Tomás, G. Vanbavinckhove and F. Zimmermann, "Collision tunes at injection and ramp", CERN-ATS-Note-2011-034 MD (LHC).

[28] M. Giovannozzi, "OPTICS OPTIONS FOR THE 2012 PROTON RUN", Proceedings of Chamonix 2012 workshop on LHC Performance.

[29] S. Redaelli, M. Lamont, G. Müller, N. Ryckx, R. Tomás and J. Wenninger, "Combined ramp and squeeze at the Large Hadron Collider", CERN-ATS-2012-102.

EXPERIMENTS REQUIREMENTS AND LIMITATIONS FOR POST-LS1 OPERATION

B. Gorini, E. Meschi, CERN, Geneva, Switzerland

Abstract

The LHC will resume operation for physics in 2015, after a two year long shutdown, with an energy target of 13 TeV and a peak luminosity target of ~10^{34} $cm^{-2}s^{-1}$. The physics goals will be rich, with difficult precision measurements of the properties of the newly found Higgs boson, as well as of other equally important phenomena predicted by the standard model. With the higher energy, the experiment communities will also be looking for physics beyond the standard model. The two programs, which sometimes have diverging demands on the accelerator, need to be reconciled to guarantee the highest scientific output of the LHC. In this talk, we review the running scenarios for the Proton-Proton and Heavy Ion collider runs after LS1, in particular with respect to the issues related to bunch spacing (pile-up, triggers and reconstruction efficiency), but also to other aspects like bunch length, filling schemes, leveling, etc., as well as the experimental and technical challenges in the different scenarios.

PHYSICS GOALS

2012 has been a crucial year for all LHC experiments, in particular considering the subsequent long shutdown. Big scientific achievements were attained, starting from the discovery, by the ATLAS and CMS collaborations, of a new fundamental boson of mass of approximately 126 GeV, which is now understood to be the long sought after Standard Model Higgs boson [1], to major results on CP violation and rare decays in the b sector by LHCb [2]. These achievements turn into a rich set of new physics goals for after LS1.

Difficult precision measurements of the properties, in particular mass, spin and coupling constants, of the newly found boson are ahead of us (e.g. see Fig. 1 for the boson mass). Precision measurements of other important phenomena predicted by the standard model (or deviations thereof), will require even more efficient detectors and triggers.

The higher energy might open the way to the possibility of detecting new physics beyond the standard model (see Fig. 2).

These different goals pose many, sometimes diverging demands on the experiments and the accelerator. The running scenarios for the pp collider run after LS1 may become even more important in guaranteeing the best physics results. In particular, the bunch spacing and related issues (pile-up, trigger and reconstruction efficiency) may well prove a crucial choice in terms of exploiting the LHC potential at best. Decision on the bunch length, filling schemes, the use of β* leveling or otherwise, also require careful analysis with respect to the physics goals.

Many experimental and technical challenges are ahead of us in any of the different scenarios.

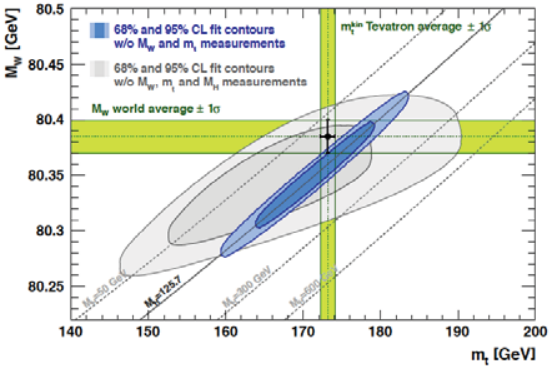

Figure 1: The direct measurent of M_H, together with the world average W and Top mass values (M_W and M_t), are remarkably consistent with the SM predictions.

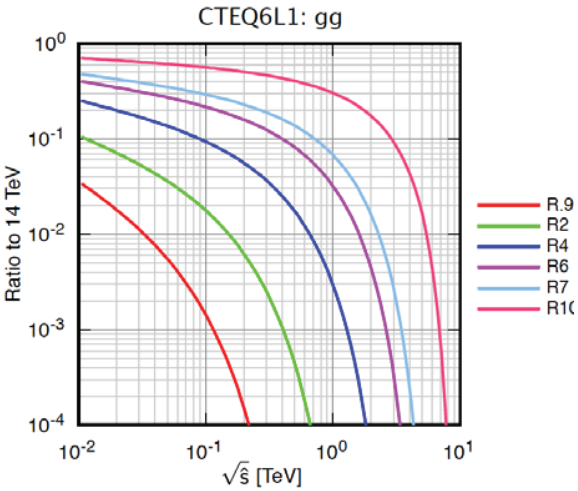

Figure 2: Ratio of parton luminosity for various center of mass energies relative to 14 TeV. For an object of mass 1 TeV, the parton luminosity is 10 times higher at 13 TeV than at 8 TeV.

CONSIDERATIONS ABOUT P-P BEAM PARAMETERS

Bunch Spacing. A bunch spacing of 50ns will produce twice the in-time pileup for the same instantaneous luminosity, e.g. for 10^{34} $cm^{-2}s^{-1}$ at 14 TeV, we expect μ=27 at 25ns and μ=54 at 50ns.

The study of the newly discovered fundamental boson is going to be the highest priority after LS1. Even with higher pile-up, the H->γγ and ZZ* decay modes would be "relatively" straightforward to trigger and study. Other modes would require good resolution and small systematic uncertainties for jets and τ-leptons. These will be much more difficult to achieve with high in-time pileup: for example, H->ττ: requires low-threshold ττ-triggers, which get spoilt by higher pile-up. ZH->ννbb relies on a trigger on missing transverse energy, whose thresholds will need to be increased with higher pile-up. On the other hand, to meet the physics goals, we would need to maximize the acceptance, which would imply to maintain or even lower those thresholds,. It is thus clear that from a physics perspective, operating at 25ns is strongly preferred.

Besides the general physics arguments, both ATLAS and CMS indicate that the current pile-up figures are close to the limit of what the detectors and the data processing chain can deal with. Inner detectors (Pixels and strips) occupancy increase with pileup is confronted with the limit on the total readout bandwidth. At 50ns and with increased luminosity, leveling will become necessary while, with 25ns, limits will only be hit above 10^{34} $cm^{-2}s^{-1}$. CMS also has estimated that 50ns would require about twice the CPU capabilities of the high-level trigger farm (Fig. 3), and a very significant increase of offline CPU and disk resources in comparison to 25ns, for the same amount of integrated luminosity.

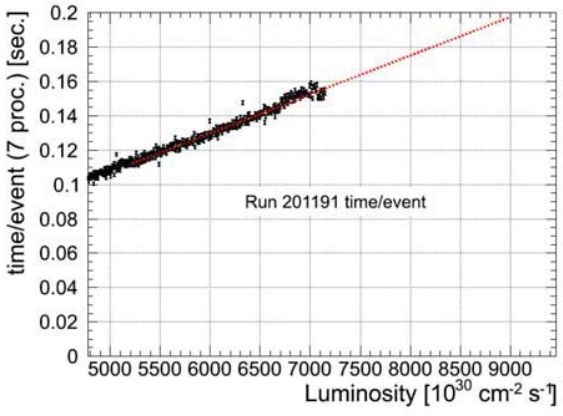

Figure 3: CPU time per event for the execution of the HLT in CMS. The current limit of the CMS farm is 0.19 s per event.

Effects on reconstruction and analysis become dramatic above 10^{34} $cm^{-2}s^{-1}$ at 50ns. These would require fundamental changes to the code and the selection cuts, e.g. raising track reconstruction p_T cut, and rethinking the primary vertex determination strategy.

Some studies also show [3] that the rate for certain inclusive triggers, especially those selecting on the total transverse and missing transverse energy, would not be controllable for pile-up higher than 50.

A special case must be made for LHCb. This experiment performs precision measurements in charm and beauty physics, looking for complex, fully reconstructed decay chains. At both trigger and offline level, high pileup means not only an increase of processing time, but also more ambiguities and ghost tracks, worse vertex, momentum, and mass resolution and, ultimately, a degradation of the signal to background ratio. The situation is exemplified in Figure 4 where the trigger yield for various b-signatures is shows as a function of instantaneous luminosity. The hadronic triggers rapidly saturate above $3 \cdot 10^{32}$ providing no additional signal for the increased triggrer rate.

Squeeze and leveling. In the 25ns bunch spacing scenario, the two high luminosity experiments will be squeezed to smallest β* possible. The result of tests of the low emittance option beams from the SPS promise peak luminosities in excess of 10^{34} $cm^{-2}s^{-1}$, in IP1 and IP4, from beams with nominal or higher intensity ($1.15 \cdot 10^{11}$ ppb) and an emittance in collision as low as of 1.9 μm.

For IP8 the peak luminosity with β*=10m and tilted crossing (resulting expected angle = 340 μrad) will be $9 \cdot 10^{32}$ $cm^{-2}s^{-1}$ and thus leveling will be required, both for luminosity control and physics optimization (maximizing integrated luminosity, trigger stability). LHCb has tested at the end of the 2012 run the running scenario for 2015: 4×10^{32} $cm^{-2}s^{-1}$ at 13 TeV and μ ~ 1.0. At 25ns bunch spacing and with 2200 LHCb bunches (high brightness, no private bunches), multiplicity will increase by about ~20% in going from 8 TeV to 13 TeV.

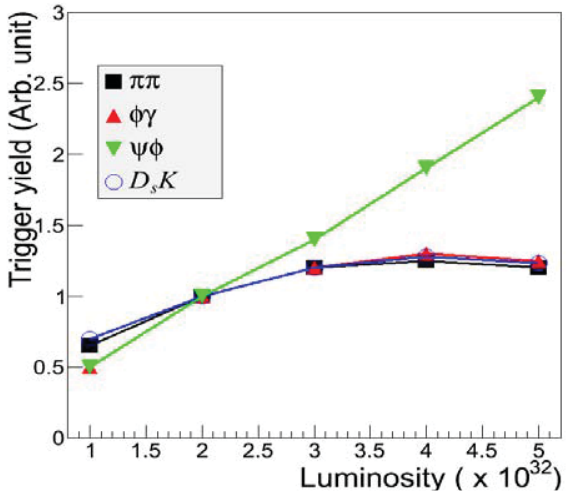

Figure 4: LHCb trigger yield for different B triggers. The yield for the non-muon triggers saturates at about $3 \cdot 10^{32}$ $cm^{-2}s^{-1}$.

The maximum acceptable detector particle flux will be equivalent to 5.5×10^{32} $cm^{-2}s^{-1}$ [1] at 8 TeV. Assuming a luminosity lifetime of about 10h, as today, luminosity will reach that level after 8.5 hours, compared to ~14 hours in 2012. A $\beta^* < 10$ m (or at least the square root of the product of β^*_x and β^*_y) would at that point become desirable. LHCb deems therefore important to commission a dynamic β^* leveling option for 2015. One proposed solution involves defocusing LHCb in the vertical plane and dynamically reducing β^*_y.

Bunch and luminous region length. The critical parameter for experiments is the luminous region rather than the bunch length, therefore, longer bunches could be partially compensated by larger crossing angles. As a general rule, a shorter luminous region gives more 'merged vertices', thus making it more difficult to reconstruct the primary event vertex. In fact, a moderate increase of the luminous region would probably benefit ATLAS and CMS (not LHCb) tracking and vertex reconstruction at high pile up, but this would come at a price. For example, in CMS, it would also worsen the mass resolution in the H->γγ analysis (benefits vs drawbacks are under study – they will also depend on the pile up conditions). In general, for both ATLAS and CMS, due to the limited acceptance of the inner tracking system, a longer luminous region can cause acceptance and efficiency losses for tracking and photons.

Again, a special case must be made for LHCb: the limited acceptance of the VELO causes some loss of efficiency for "long-lived" B decays, contributing 1/3 of the systematic error in lifetime measurements. So for LHCb a longer luminous region seems not to be an option.

Crossing angles. LHCb will require a vertical external crossing angle to maintain the tilted crossing scheme that was successfully used in 2012. This scheme guarantees the same boost vector amplitude in both polarities, thus simplifying the analysis of systematics. Polarity swaps of the LHCb spectrometer will also be required.

In general, an increase of the crossing angles (for 25ns) will have no other effect on the experiments and is therefore left to the machine to decide.

ALICE operation in proton-proton. ALICE goal for the proton-proton operations after LS1 will be to work at a (leveled) luminosity between 10^{30} and 10^{31} $cm^{-2}s^{-1}$. ALICE operated in 2012 using main-satellite collisions instead of offset main-main collisions as in 2011. Following a discussion in Chamonix 2012 "natural" satellites were used. These were expected to provide sufficient luminosity and were attractive to avoid big separations in IP2 and to optimize the filling schemes. Several problems, including vacuum conditions around IP2 and unpredictable satellite population, resulted in some difficulty for ALICE to collect the desired statistics. Enhancing the satellites during the final phase provided peak luminosities of up to 18Hz/ub, which allowed ALICE to level the luminosity to the desired value. These mode of operation turned out to have several drawbacks: monitoring of the satellite population in the injectors was not possible, hence the quality of the beams was not known until injection in the LHC; also, the luminosity decayed very steeply. Artificially enhancing the satellites resulted as well in several occasional operational issues like high losses at injection. In the (remote) case of a 50ns beam, ALICE has therefore no interest in continuing with the main-satellite scheme after LS1, and would prefer of order 45 main-main collisions with leveling, and a β^* as large as possible. With 25ns separation ALICE will naturally get ~2000 main-main collisions and a β^* of at least 10m will be required. Larger values (18-30) have been investigated [3] and may not be beneficial (because of an interplay of beam-beam effects and separation with broader beams), such that leveling by large separation seems the only available option. Further analysis will be needed.

SPECIAL RUNS

In addition to the low-beta program for proton-proton physics, very high β^* measurements have a potentially very interesting program, the main goal being the study of low-|t| Elastic Scattering at 13 TeV and the measurement of the total p-p cross section. For the success of the high β^* program, it is assumed that additional magnet cables will be installed during the 2015-2016 winter technical stop at the latest. In the initial phase, without these cables the focus will be on commissioning the injection and ramp at $\beta^* = 90$m, with the goal of increasing the number of bunches using crossing angles.

Both TOTEM and ALFA have a long list of interventions and commissioning, to consolidate and expand the current capabilities. In particular, ALFA has plans to address RF-heating aiming at a factor 10 reduction. Active liquid cooling is under consideration.

TOTEM plans to pursue the study of diffractive physics with squeezed beams, leveraging the experience acquired in 2012 with approaching the RPs to 12-14 σ during standard physics runs. Investigations are planned to identify the source of high UFO rate induced by the movement of the horizontal pots.

The LHCf detector will be upgraded with radiation hard GSO scintillators capable of withstanding doses up to 1kGy. The goal is to collect at least 500 nb-1 at $\sqrt{s}$=13-14TeV with more than 2μs event-to-event interval. This would require an extended initial phase of operation with less than 43 bunch and μ<=0.01. LHCf is also requesting an energy scan for extrapolation to cosmic ray energies (7, 3.5 and 2.2TeV if possible) with a $\beta^* = 11$m, and instantaneous luminosity less than 10^{29} cm^{-2} s^{-1}. This second part of the running plan will be discussed in the near future.

HEAVY ION PHYSICS

Many important results on heavy ion data have been produced by the ALICE collaboration [4], as well as ATLAS and CMS. For 2015 (and after) only Pb-Pb operation at 13Z TeV is requested. There is a potential for reaching peak luminosities of order 1-2 10^{27}, while ALICE working point after LS1 will be at 10^{27} $cm^{-2}s^{-1}$. For this and other reasons, leveling options in one or more IPs might have to be studied.

CONCLUSIONS

During LS1 some detector will undergo non-minor modifications: e.g. CMS will install new muon and calorimeter triggers and additional endcap muon chambers; ATLAS will install an additional innermost pixel layer. The intensity ramp-up at 25ns period can be used, in general, to commission the triggers and the new hardware and study the detector performance at a new energy. As usual establishing the Standard Model Physics candles at 13 TeV will provide an excellent testing ground for the upgraded components.

If an initial period at 50ns and 13 TeV should be deemed absolutely necessary, it will require an extra luminosity and trigger optimization. All the collaborations agree that this possible period should be kept as short as possible as it will unavoidably affect the physics yield.

In conclusion, 25 ns pp operation is a strong request of all the experiments, as it provides a much cleaner environment for precision physics and is less demanding in terms of computing resources. A bunch spacing of 50 ns should be considered an option only in case of major showstoppers. Optimization of other beam parameters (bunch length, crossing angles) should be carried out during commissioning as needed, as there is a clear demand for stable conditions for data taking.

Experiments accept that the commissioning period for 25ns operation may be longer than usual.

ALICE pp operation at 25ns will require further studies and discussion, as will the special runs program (ALFA, TOTEM and LHCf).

Only Pb-Pb operation at 13Z TeV is envisaged for Heavy Ions in 2015.

AKNOWLEDGEMENTS

Many thanks to the experiments Spokespersons and Run Coordinators for withstanding the endless discussions that they have been forced to have with us.

A special thanks goes to our LHC colleagues for their collaborative spirit, their patience, and their professionalism.

REFERENCES

[1] ATLAS Collaboration, Physics Letters B, **716**, 1, 1-29 (2012)
CMS Collaboration, Physics Letters B, **716**, 1, 30-61 (2012)

[2] LHCb Collaboration, arXiv:1211.2674

[3] P.D. Hermes, R.Schicker ATS note, in preparation

[4] see for example Y.Kharlov, arXiv:1203.2420v1 [nucl-ex]

POST LS1 25 NS AND 50 NS OPTIONS FROM THE INJECTORS

R. Steerenberg, G. Arduini, T. Argyropoulos, H. Bartosik, T. Bohl, K. Cornelis, H. Damerau, A. Findlay, R. Garoby, S. Gilardoni, B. Goddard, S. Hancock, K. Hanke, W. Höfle, G. Iadarola, E. Métral, B. Mikulec, Y. Papaphilippou, G. Rumulo, E. Shaposhnikova.

CERN, Geneva, Switzerland

Abstract

Pre-LS1, the parameters of the 50 ns and 25 ns LHC-type beams in the LHC injector chain have considerably improved with respect to their initial specifications. In addition significant and rather successful effort has gone into the development and testing of several alternative LHC beam production schemes in the injectors with the aim of providing high brightness beams to the LHC.

These schemes will be outlined together with their performance potential, possible challenges and additional requirements for their use by the LHC in the post-LS1 era.

2012 LHC 50 NS AND 25 NS EVOLUTION

The initial LHC multi-bunch beam characteristics, as given in Table 1 have evolved significantly since they were documented in 2004 [1]. During the Chamonix workshop on LHC performance, in January 2012, the performance reach of the injectors for 2012 was discussed [2] and a set of tentative beam characteristics for the 2012 run was extrapolated from results obtained during the 2011 run, exploring possible margins and taking into account known limitations in the different accelerators of the LHC injector chain. In the final days of the 2011 proton run, the SPS routinely delivered the 50 ns beam with an average transverse emittance of 1.9 μm and a bunch intensity of 1.5×10^{11} protons. All transverse emittances in this publication are the average of the horizontal and vertical emittances and are defined at 1 σ normalised. The tentative beam characteristics for the 2012 LHC run are summarized in Table 2 and foresaw a marginal increase in the average transverse emittance to 2 μm for a bunch intensity increase to 1.6×10^{11} protons, providing roughly the same brightness for a slightly higher intensity.

However, further improvements made during the 2012 run lead to a slightly higher bunch intensity of 1.65×10^{11} and a decrease of the average transverse emittances to 1.65 μm. The beam parameters obtained for the whole LHC injector chain in 2012 are summarised in Table 3.

Although the 25 ns beam was not used by the LHC during the physics run, it was regularly used for machine development studies. It should be noted that also the performance of this beam was enhanced, as for the first time the 25ns beam could be delivered well within specifications, with an average transverse emittance that was decreased from 3.6 μm to 2.6 μm out of the SPS for a nominal bunch intensity of 1.15×10^{11} protons.

Reminder of the classical 25 ns and 50 ns LHC beam production scheme

Both the 25 ns and 50 ns beams in the PS are produced, using the same well-established principles [3] that are based on different variants of longitudinal bunch splitting.

Table 1: Specified beam characteristics for the principal multi-bunch LHC beams in the injectors [1].

	PSB extraction				PS extraction			SPS extraction			
Beam	**Ip/ring [×10¹¹]**	**$\varepsilon_{h/v}$ [μm]**	**nb batch**	**nb bunch**	**Ip/bunch [×10¹¹]**	**$\varepsilon_{h/v}$ [μm]**	**nb bunch**	**Ip/bunch [×10¹¹]**	**$\varepsilon_{h/v}$ [μm]**	**$\varepsilon_{long.}$ [eVs]**	**nb bunch**
25 ns	2.4 – 13.8	≤ 2.5	2	4 + 2	0.2 – 1.15	≤ 3	72	0.2 – 1.15	≤ 3.5	≤ 0.8	1 - 4×72
50 ns	1.2 – 6.9	≤ 2.5	2	4 + 2	0.2 – 1.15	≤ 3	36	0.2 – 1.15	≤ 3.5	≤ 0.8	1 – 4×36

Table 2: Proposed beam characteristics for the principal multi-bunch LHC beams in the injectors for the 2012 run [2].

	PSB extraction				PS extraction			SPS extraction			
Beam	**Ip/ring [×10¹¹]**	**$\varepsilon_{h/v}$ [μm]**	**nb batch**	**nb bunch**	**Ip/bunch [×10¹¹]**	**$\varepsilon_{h/v}$ [μm]**	**nb bunch**	**Ip/bunch [×10¹¹]**	**$\varepsilon_{h/v}$ [μm]**	**$\varepsilon_{long.}$ [eVs]**	**nb bunch**
25 ns	16	2.5	2	4 + 2	1.3	2.5	72	**1.15**	**3.5**	0.7	1 - 4×72
50 ns	8	1.6	2	4 + 2	1.8	1.9	36	**1.6**	**2**	≤ 0.8	1 – 4×36

Table 3: Achieved beam characteristics for principal multi-bunch LHC beams in the injectors at the end of the 2012 run.

	PSB extraction				PS extraction			SPS extraction			
Beam	**Ip/ring [×10^{11}]**	**$\varepsilon_{h/v}$ [μm]**	**nb batch**	**nb bunch**	**Ip/bunch [×10^{11}]**	**$\varepsilon_{h/v}$ [μm]**	**nb bunch**	**Ip/bunch [×10^{11}]**	**$\varepsilon_{h/v}$ [μm]**	**$\varepsilon_{long.}$ [eVs]**	**nb bunch**
25 ns	16	2	2	4 + 2	1.3	2.4	72	**1.15**	**2.6**	0.7	1 - 4×72
50 ns	12	1.35	2	4 + 2	1.9	1.5	36	**1.65**	**1.65**	≤ 0.8	1 – 4×36

The PS Booster provides the beam in 2 batches of respectively 4 and 2 bunches. Special care is taken to provide the required longitudinal emittance, but also the transverse emittance blow up is kept as low as possible. The SPS will then receive up to 4 batches from the PS with each 36 or 72 bunches per batch for the 50 ns and 25 ns beams respectively.

The detailed PS production scheme for the 50 ns beam is illustrated in Fig 1. The production of the 25 ns bunch spacing beam is identical, apart from an additional longitudinal bunch splitting on the 26 GeV/c flattop. In order to maintain the extracted nominal bunch intensity and longitudinal emittance at PS extraction equal for the 50 ns and the 25 ns versions, the PS Booster bunch intensity for the 25 ns version is twice the intensity of the 50 ns version. In addition the 25 ns beam undergoes a controlled longitudinal blow up at PS injection to increase the longitudinal emittance by nearly a factor 2 in order to compensate for the extra longitudinal splitting.

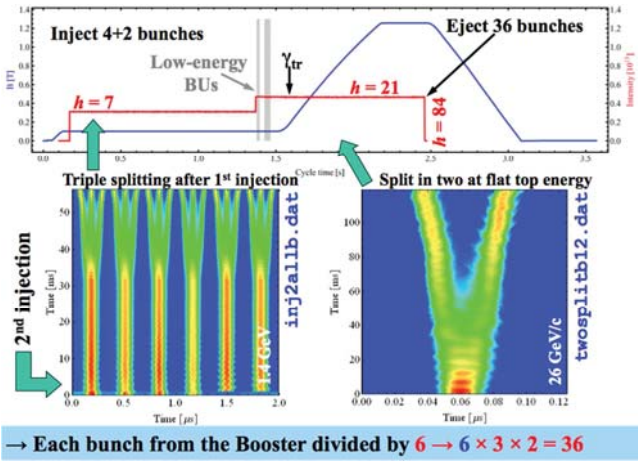

Figure 1: LHC 50 ns double batch beam production scheme.

For the first injection into the PS, the PS Booster provides 4 bunches, 1 bunch per ring. The second PS injection of 2 bunches takes place 1.2 seconds later. As a result 6 bunches are injected in the PS that uses the 7th harmonic, leaving 1 RF bucket unpopulated, to be used as PS extraction kicker gap. Towards the end of the long flat bottom each bunch is split in 3 by changing the RF harmonic of the 10 MHz cavities from h=7 to h=21. This results in 18 bunches that are then accelerated up to the 26 GeV/c flattop, where another harmonic change from h=21 to h=42 takes places, using the 20 MHz cavity. This final splitting provides a beam of 36 bunches followed by 6 empty buckets, all spaced by 50 ns that are handed over to the 40 MHz cavity running at h=84. The final step, just before extracting the beam, consists of shortening the bunch length to the required ~ 4 ns at 4σ, by increasing the 40 MHz cavity voltage, first adiabatically and later non-adiabatically. Once the rotated bunches have become sufficiently short to fit in the 80 MHz bucket, the 80 MHz cavities are added.

The transverse emittance established by the PS Booster multi-turn injection scheme is reasonably well preserved along the remainder of the injector chain and also explains the larger transverse emittance for the 25 ns beam at the extraction of each of the machines, starting at the PS Booster. For the 25 ns beam the bunch intensity per ring needs to be a factor 2 higher than for the 50 ns beam. In the PS Booster the transverse emittance increases linearly with the intensity per ring and thus per bunch.

LHC injectors 2012 performance improvement

During the 2012 run, much emphasis was put on the identification and reduction of transverse blow up sources in the PS Booster, PS and SPS, hence the transverse emittance reduction at SPS extraction from 2 μm in 2011 to 1.65 μm in 2012 for a slight increase in intensity per bunch, as given in Table 2 and Table 3.

In order to monitor the beam brightness evolution in the different machines, systematic measurements and logging of the measurement results was put in place in July. Fig. 2 shows an example of the beam brightness evolution in the PS. The red crosses represent the bunch intensity at PS extraction, while the blue squares represent the brightness of the extracted beam. These plots were regularly updated for the different machines in order to follow the trend and to identify possible beam brightness degradation. For example, early August an improvement on the PS Booster injection matching was identified and implemented. As a result the beam brightness increased and the PS working point had to be adapted in order for the LHC to profit from this improvement. In Fig. 2 this is visible by a step increase of the beam brightness, while the intensity per bunch remained constant.

In September another important improvement was introduced, but this time in the SPS, when the Q26 working point made place for the newly developed Q20 working point, lowering the transition energy and thus moving it away from the injection energy. The aim is to

remove or at least ease the intensity limitations in the SPS with minimal cost and no hardware changes [4]. The new optics was thoroughly and successfully tested before being used to fill the LHC.

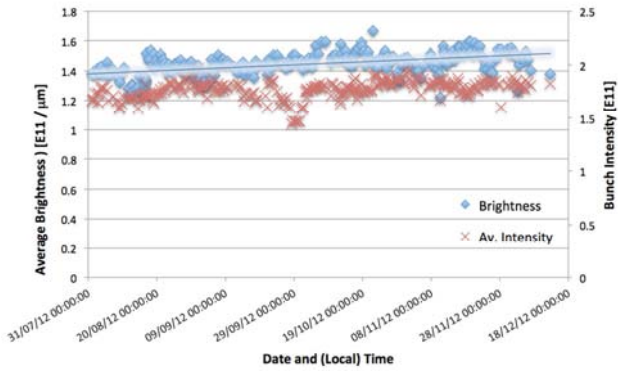

Figure 2: PS flattop beam brightness and bunch intensity evolution from the end of July until the end of the 2012 proton run.

Fig. 3 illustrates this improvement by indicating the beam brightness measurements on the SPS flattop, the LHC flat bottom and the LHC flattop over about 300 fills, during which the Q20 working point was introduced.

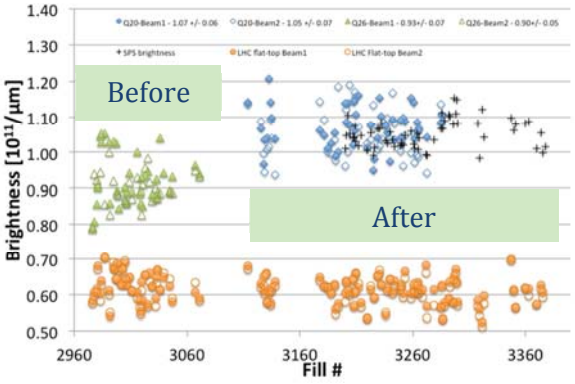

Figure 3: SPS and LHC beam brightness before and after the Q20 deployment.

With the Q26 working point the beam brightness, as measured on the LHC flat bottom, lies around 0.9×10^{11} p/µm with a spread of about 0.12×10^{11} p/µm. After the deployment of the Q20 working point the beam brightness increased by nearly 20% to an average of 1.05×10^{11} p/µm with approximately the same spread of 0.12×10^{11} p/µm. However, as a result of transverse emittance blow up during the LHC ramp and/or squeeze the beam brightness on the flattop in the LHC could not yet benefit from this injector performance improvement.

The continuous optimisation resulted in considerably brighter beams from the LHC injectors. Table 4 summarises the initial beam parameters available to the LHC in April, when the SPS started producing the 50 ns beam in 2012, and the beam parameters at the end of the 2012 run, together with the relative improvements.

Table 4. Summary of beam parameter out of the SPS start and end 2012 run.

	April	November	Relative change
Intensity [×10]	1.4	1.65	+ 18%
$\varepsilon_{h/v}$ [µm]	1.8	1.65	- 10%

Some limitations and difficulties encountered

The reduction of the transverse beam size in the PS Booster also means that beam alignment errors in the recombination process will result in larger relative transverse emittance blow up in the PS, as the injection oscillations of the individual bunches cannot be corrected. The transverse damper, which was tested in 2012 and will be made operational for 2014, will alleviate this situation.

The increase of the beam brightness intensifies the PS injection space charge effects with the danger of transverse emittance blow up, especially during the 1.2 second long flat bottom. In order to avoid this, the working point needs to be controlled precisely.

Another issue encountered does not lie in the production of the high brightness beams, but in measuring its transverse emittance. The PS Booster and the PS do not contain non-dispersive regions. Therefore the dispersion contribution needs to be subtracted from the measured beam size. Errors in the determination of the dp/p and the dispersion value at the wire scanner position will make the precise determination of the transverse emittances more difficult for the low emittance beams. In the SPS the small beam sizes result in only about 15 measurement points per wire scan. Accumulating measurements during multiple cycles enhances the precision of the measurement and thus the fit, but it will also average the difference between the batches. In addition the combination of the beam intensity and brightness on the SPS flattop provides beam conditions that are beyond the breakage limit of the wire, excluding transverse emittance measurements at high energy in the SPS.

THE MENU FOR POST-LS1

The classical 50 ns and 25 ns beams

The classical 25 ns and 50 ns beams should remain available for the LHC after LS1 with the beam characteristics as presented previously. However some of the LS1 activities, in particular the exposure to air of the SPS vacuum chambers, can potentially compromise the performance temporarily as a result of an increase of the secondary emission yield for electrons, possibly resulting in electron cloud issues.

The high-brightness 50 ns and 25 ns beams

In parallel to the continuous optimisation of the classical 50 ns beam the new 50 ns and 25 ns beam production schemes, developed in the framework of the LIU project [5] were tested successfully in the injectors.

These beams were also occasionally provided to the LHC for tests.

The roots for this new scheme reside in the fact that the PS Booster transverse emittance increases linearly with intensity. Therefore, lowering the intensity per ring and making use of all rings, with 1 bunch each, for both batches to the PS, in combination with a longitudinal bunch-merging scheme in the PS, the bunch intensity can be increased while the transverse emittance is preserved, provided space charge effects are managed correctly. As a result the so-called Batch Compression, Merging and Splitting (BCMS) scheme has been developed, which is illustrated in Fig. 4.

The PS Booster will produce two batches of 4 bunches each, still injected 1.2 seconds apart into the PS, which has the 10 MHz RF system working on h=9. On an intermediate flattop of 2.5 GeV, where longitudinal acceptance is increased and space charge effects are reduced, a batch compression will take place, inserting empty buckets along the PS circumference, by increasing the RF harmonic number in steps from h=9 through h=10, h=11, h=12, h=13 to h=14, resulting in 8 bunches and 6 empty buckets. The second stage consists of merging 2 bunches into 1 bucket by changing the harmonic from h=14 to h=7. The merged bunches contain twice the intensity, for the same transverse emittance. The 4 bunches obtained are then each split in 3 going from h=7 to h=21, resulting in 12 bunches and 9 empty buckets. The beam is then accelerated up to the 26 GeV/c flattop, where another harmonic change from h=21 to h=42 takes places, using the 20 MHz cavity and splitting the bunches. A final bunch rotation will then provide 24 bunches spaced a 50 ns. However, for the 25 ns bunch spacing version, before performing the final bunch rotation, an additional bunch splitting, increasing the harmonic from h=42 to h=84, will produce 48 bunches spaced at 25 ns.

The intensity required from the PS Booster per ring for 24 bunches at 50 ns on the BCMS scheme is a factor 2 lower than for the 36 bunch 50 ns classical beam, hence the increase of beam brightness, at the expense of a reduced number of bunches. Optimising the LHC filling scheme can for the major part compensate the later.

Table 5 summarises the performances achieved in 2012 with both the classical and the BCMS production schemes, which will also be the expected performance available after LS1.

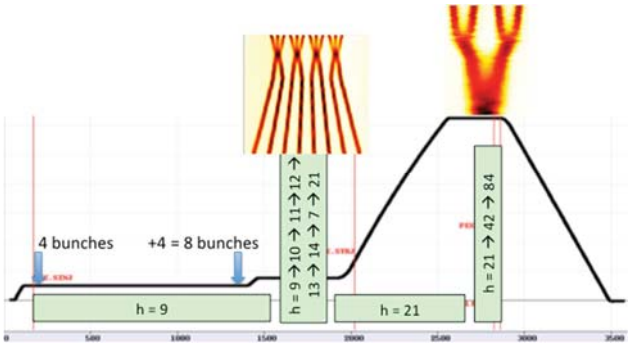

Figure 4: LHC 25 ns BCMS beam production scheme.

The number of bunches per PS batch from the BCMS beams is 50% lower than for the classical scheme. However, injecting 5 batches instead of 4 in the SPS and optimizing the LHC filling scheme will only result in a 10% reduction of the number of bunches in the LHC.

In order to evaluate the potential increase in luminosity for the BCMS scheme the luminosity is calculated using eq. 1, assuming that all geometrical parameters, such as crossing angle etc. remain constant.

$$L \propto \frac{N^2}{\varepsilon} M \qquad (1)$$

N represents the number of protons per bunch, M the number of bunches and ε the average transverse emittance.

In Fig. 5 the classical 50 ns beam, as produced at the end of the 2012 proton run is taken as a reference, normalised with the number of bunches that can be stored per beam in the LHC. The other beam variants with each their maximum number of bunches in the LHC per beam are then compared to the classical 50 ns version. From this it is clear that the newly developed BCMS production scheme will provide substantially higher luminosity than the classical scheme.

Table 5: Beam characteristics overview for the classical and batch compression, merging and splitting (BCMS) scheme achieved in 2012 and expected for after LS1.

	PSB extraction				PS extraction			SPS extraction			
Beam	**Ip/ring [×10^{11}]**	**$\varepsilon_{h/v}$ [μm]**	**nb batch**	**nb bunch**	**Ip/bunch [×10^{11}]**	**$\varepsilon_{h/v}$ [μm]**	**nb bunch**	**Ip/bunch [×10^{11}]**	**$\varepsilon_{h/v}$ [μm]**	**$\varepsilon_{long.}$ [eVs]**	**nb bunch**
25 ns	16	2.3	2	4 + 2	1.3	2.5	72	**1.35**	**~3**	0.7	1 - 4×72
50 ns	12	1.35	2	4 + 2	1.9	1.5	36	**1.65**	**1.65**	≤ 0.8	1 – 4×36
25 ns BCMS	7.5	1	2	4 + 4	1.2	1.2	48	**1.15**	**1.4**	0.7	1 - 4×48
50 ns BCMS	6	0.9	2	4 + 4	1.9	1.1	24	**1.6**	**1.2**	≤ 0.8	1 – 4×24

The 50 ns BCMS beam produces about 20% more luminosity, but will also increase the pile-up in the experiments, which is already considered being high. The 25 ns BCMS provides close to 30% more luminosity than the classical version and about 5% more than the classical 50 ns beam. The latter means that with the 25 ns BCMS a slightly higher luminosity can be produced, but with twice the amount of bunches, therefore reducing the pile-up by 50%.

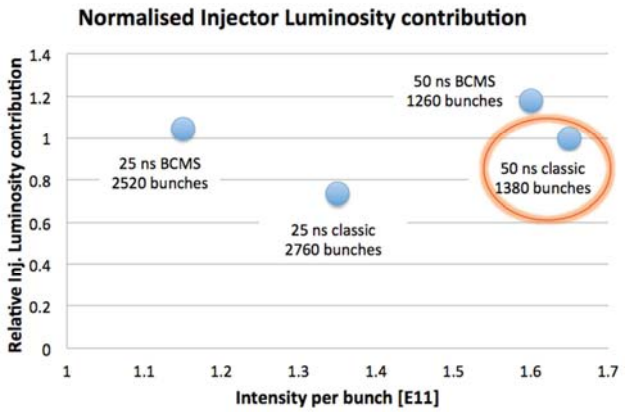

Figure 5: Relative luminosity contribution by the injectors for the different production schemes.

Although the BCMS beams have been successfully tested and have proven to provide good performance, these beams are new and were only commissioned during the autumn of 2012. Since then these beams were produced in a machine development context, providing little, but nevertheless some operational experience. During the 2014 injector run these beams will undergo further development and will need to be made fully operational, while exploring their performance limitations.

LS1 WORK POTENTIALLY IMPACTING THE BEAM PERFORMANCE

During LS1 many machine improvements are foreseen. However some of these can also form potential issues or challenges during the restart in 2014.

In the PS Booster the magnet stacks will be realigned with the aim to improve the uncorrected closed orbit. In addition the orbit correctors will be powered making it possible to correct the closed orbit, using also new beam position monitors. A new transverse damper will also be installed and commissioned, in parallel to the existing transverse feedback.

The PS magnets will be realigned, followed by a beam-based realignment during the 2014 restart. The transverse damper will be made operational in both planes, making the PS less dependent on the residual PS booster recombination errors. The longitudinal beam control will also be upgraded with a new 1-turn delay feedback, an increase of voltage available per 10 MHz cavity tuning group and a new longitudinal feedback kicker, for which no experience exists in the PS.

The SPS machine will also be partly realigned, mainly in sector 6. The ungrounded vacuum chambers that caused orbit perturbation in 2012 will be grounded and the loose shims will be consolidated. The MKE kicker that presently presents a limitation due to heating will be equipped with improved shielding, using serigraphy. The entire 800 MHz RF system will undergo a complete overhaul and the transverse damper will be upgraded and a high bandwidth system will be developed. The beam-based realignment during the 2014 start up will focus on the high-energy orbit for the Q20 optics. The SPS vacuum chambers will be opened in many places, risking an increase in the electron secondary emission yield. This means that substantial scrubbing will be required during the 2014 run in order to retrieved the good conditions of 2012, obtained after "years" of scrubbing.

In addition to these machine-specific changes and consolidation a general and major timing and controls renovation will take place. All these changes need to be commissioned and made operational at start up in 2014.

CONCLUSIONS

The operational beam performance in the LHC injector chain has evolved considerably during the 2012 run, mainly by identifying and reducing transverse emittance blow up sources. The new high-brightness LHC beams have been developed within the LIU project and were tested successfully toward the end of 2012, using a scheme of batch compression, merging and splitting. As a major result the 25 ns BCMS beam will provide a slightly higher luminosity in the LHC than the classical 50 ns beam, with the advantage that the event pileup in the detectors will be reduced by a factor 2.

The LS1 activities will potentially improve the machines status and should contribute to a better beam performance. However, the new and/or consolidated systems will need to be commissioned and made fully operational in order to be able to fully benefit from their potential.

REFERENCES

[1] M. Benedikt, "LHC Operational Beam Definitions for the Proton Injector Chain", November 2004.

[2] R. Steerenberg *et al.*, "Performance Reach of the Injectors in 2011", Chamonix 2011, p 331-338 CERN-2011-005

[3] R. Garoby, "LHC Proton Beams in the PS: Status of Preparation and Capabilities", Chamonix XII, p 34-37, CERN-AB-2003-008-ADM.

[4] H. Bartosik, *et al.*, "Increasing instability thresholds in the SPS by lowering transition energy", CERN-ATS-2012-177.

[5] H. Damerau *et al.*, "Performance potential of the injectors after LS1", Chamonix 2012, p 268-274, CERN-2012-006.

FIRST LOOK AT THE RE-COMMISSIONING PLANS AFTER LS1: HWC- DRY RUNS - SYSTEMS COMMISSIONING

M. Pojer, CERN, Geneva, Switzerland

Abstract

In 2015 the LHC will enter a new era. The energy of the machine will be increased by more than 50%; the beam stored energy will increase maybe by a factor 2 or even more. A thorough re-commissioning of all systems will be fundamental for a safe operation with beam. The experience gained in the last three years will be as well critical in defining the needed commissioning steps.

PREAMBLE

In the preparation for this work, some of the relevant systems experts have been contacted, to enquire on the major modifications that will be done during the Long Shut-down 1 (LS1): all hardware which will be replaced or repaired and all software implementations could demand for new qualifications and additional time need. The "delivery" date for all equipment and the guessed time needed for the re-commissioning were demanded. Special stress was put on the interdependency between the different systems, and the necessity for dry runs was also investigated as an important commissioning step. Finally everybody was asked whether the 2015 re-commissioning would more look like the one of 2008 or 2010.

Some implications of the tight scheduling are already clear if we take a look at the general LS1 planning:

- the R2E activities are finishing late, and they will delay the powering of the superconducting circuits at point 5 and 7;
- sector 45 and 56 are among the last sectors to be tested, which means that the LBDS energy tracking tests will be performed in ideal conditions only at the very end of the powering test period;
- the powering tests and the dry runs of the machine checkout will have to be done mostly in parallel.

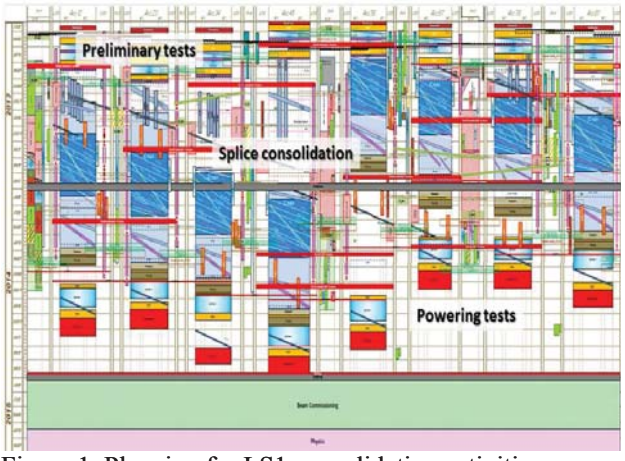

Figure 1. Planning for LS1 consolidation activities.

THE SUPERCONDUCTING CIRCUITS

The Copper Stabilizer Continuity Measurement

Among the powering tests to be performed on the superconducting circuits, the CSCM (aka, thermal amplifier) will be the first one to be executed.

The CSCM is a technique initially proposed by H. Pfeffer and later developed by H. Thiesen, which could be used to investigate the thermal runaway of faulty splices of an entire 13 kA line, including the current leads to pigtails, the splices between magnets and the diode connections.

The procedure consists in powering a main (dipole or quadrupole) circuit while it is kept at 20 K: the diodes are all closed by a voltage pulse, so that the magnets are taken out from the loop; a 12 kA current is then circulated inside the busbar/diode circuit, to check whether faulty splices are detected, which would lead to a thermal runaway.

The CSCM will be executed as a type test on a sector at the beginning of LS1, before the consolidation. If qualified, the method will be possibly applied to the rest of the machine at the end of LS1.

Superconducting circuits commissioning

Many interventions will be performed on the superconducting circuits during LS1, either maintenance activities or system upgrade. Just to give some examples:

- the QPS will be upgraded on many aspects, like additional systems for the diagnostics of the quench heater circuits (measure of the resistance of the heater circuit with high precision, in order to see precursors of eventual faults), specific transducers for precision measurement of the power pulse during heater discharge and in general detectors change and firmware upgrade;
- the power converters will undergo major modifications, including active filters and auxiliary power supplies replacement;
- following R2E relocations, many electronic equipment will be removed from areas close to the tunnel and put far away
- cables will be re-routed (mainly at point 5, due to R2E) and the sheaths of many of them replaced.

Following the numerous modifications and upgrades of the superconducting circuits, a massive campaign of individual system tests will be performed by the equipment owners; in particular, for the superconducting circuits, the tests will have to check for the protection functionalities and for the efficient interface between all powering and protection systems, apart for their

reliability. Also, all cable activities will require for short circuit tests and heat runs.

As for all machine protection elements, the most critical part will be the interface between the different systems, because of the delayed delivery of one with respect to the other and their non-synchronized commissioning.

For the commissioning of the superconducting circuits, new powering procedures will be needed, to keep into account all hardware and software modifications. What will follow is a brand new commissioning, where sector 67 will be the pilot and longer one, hopefully with a fast learning curve on the others.

Time needed and strategy

In terms of time required to commissioning the superconducting circuits and the strategy to be adopted, not much should change with respect to what done in the past campaigns. The main difference will be of course in the commissioning current, which should aim at being the one corresponding to 7 TeV, but some limitations might apply: some 600 A circuits could be limited according to their known weakness and operation need; some other parameters could be relaxed, to improve flexibility and increase the performance. No surprises should be expected after the splice consolidation and the powering tests to be performed at the beginning of LS1.

Automation should play a fundamental role, not only in speeding up the test execution, but also in ensuring a safer commissioning, of which QPS would certainly profit. Also the traceability of tests execution and results would be improved.

More than 6 months in total will be needed, along which the manpower (above all at the beginning) could be an issue, being the operation team deeply involved in the splice consolidation. About 3-4 weeks per sectors have been allocated to the commissioning, but the real length will mostly depend on the time needed to train the main circuits. We know, in fact, from 2008 that the training could be long and we will be obliged to start from an initial energy of about 6.5 TeV (with a slightly higher commissioning energy, to allow a comfortable operation), if we don't want to experience too many quenches. If we suppose to perform 2-3 quenches per day on each sector, in about 1 week the main circuits could be ready to operate at 6.5 TeV.

SYSTEM RE-COMMISSIONING

LBDS

Three main consolidation activities are foreseen on the LHC Beam Dumping System:

- the consolidation of all HV generators for 7 TeV operation;
- the installation of the missing diluters (2 per side), needed for the intensity increase;
- the solution of the 12V problem, with the installation of new synchronization unit from the Beam Interlock to the kickers.

For the commissioning of the LBDS, the experts have foreseen the test of the generators directly underground and not in the lab. This will lead to possible interference with the powering tests in the nearby sectors.

A reliability run will be needed, to validate the system for operation at 7 TeV: this will be done in local during the 1st semester of 2014. Starting from late summer '14, the dry run phase will start, which includes the sequencer use, with arming sequences, ramp and dump; this will lead to the verification of possible faults. The BIS loop will be in local for this testing phase.

The dry run part will require solid software already available from early summer; no change is foreseen on the LBDS software, but there will be changes at the level of the FESA classes which could be an issue.

Finally, time will be needed before beam to test the whole system in the final configuration.

Others from ABT

A new 3m-long TCDQ will be installed, for which an extensive control validation will be carried out. The delivery of the whole system is foreseen for the end of the 1st semester of 2014, which means that there might be some conflict with the powering tests and time issue for its qualification.

Concerning the kickers, all magnets will be replaced. A long conditioning will be needed, after which the dry run could be performed, starting from end of summer '14.

Also, for the MKQA, a modification of the internal electrical distribution will be done, which will not affect the commissioning. A request was as well made to change the length and amplitude of the modulation.

RF

The first big intervention done on the RF system will be the modification of the klystron cooling (8 klystron over 16 will have to be changed). This implies the re-test from the end of summer '14, with short circuits on the wave guides to allow powering without closing the area. In fact interventions in the tunnel will be still ongoing and also some conflict might appear with the powering tests. The full testing will be nevertheless difficult, due to the absence of BIS connection till very late; electrical power and demineralized water will be needed.

The second important intervention will be the replacement of one module, containing the sick cavity 3B2. A long conditioning (between 1.5 and 2 weeks) will be needed and the RF zone will have to be closed, which implies a possible interference with the powering tests and other activities in the area.

Software-wise, the major modification will be the migration to the new versions (e.g., FESA3). All RF VMI front-ends will be moved to Linux, for which part of the drivers will be re-written.

ADT

A complete new system is being planned by the owners, which will require a lot of work for cabling, front-end, twice the number of pick-ups, a new signal

processing unit and a new algorithm. Unfortunately not much can be done without beam and the re-commissioning will not take less time than in the past, even if experts are planning for some automatic systems to speed up the tests.

Collimators

Between 22 and 26 new collimators will be installed in LS1, mostly BPM collimators as TCTs at all interaction points and 2 TCSs at point 6, plus 1 or 2 new TCLs per side/beam at IP1 and 5. All these new collimators will require for calibration and a full re-commissioning for machine protection.

In addition, a plan is foreseen to move periodically all collimators to avoid some get stuck, and to put protections in place around the collimators to avoid damages during the LS1 activities.

From the software point of view, no radical change will be done, but the new BPM collimators will require new control software, which has nevertheless already been tested in SPS in a prototypal form.

In the baseline, no systematic replacement of LVDT or step motor is foreseen, since no problem of ageing has been observed nor problem of radiation. Some acoustic check will however be performed.

Beam instrumentation

Many interventions will be carried out in LS1: the BPM and BLM cooling, the modifications on the HW of the orbit feedback, the attenuators on the interlocked BPMs, additional HW on the tune system, new optics of the light monitors and thinner wires for the wire scanners. Most of them will only be tested with beam. What will be tested beforehand is the cooling system on the racks of the BPM and BLM, which will require a reliability run, to be performed well in advance with respect to the beam. The BLMs will be also tested with a radioactive source before beam.

Vacuum

New "transparent" ultra-fast valves are under study by the vacuum group and could be installed close to the RF cavities to avoid pollution in case of an incident like the one occurred in sector 34. They would close in about 20 ms and need to be interlocked not with the vacuum system, but (most presumably) with some powering signal.

From the software point of view, a new tool should be available which would ease the check of all interlocks at the beginning of machine checkout.

Beam Interlock System

Several issues affect the BIS in view of LS1:

- the electronic interfaces which pilot the CIBUs will be touched or moved in many places;
- the optical fibers are subject to ageing and they are fragile and could be damaged easily, plus new fibers will be pulled after moving the equipment from UJ56 to USC55;
- all BIC processors in the Front-End will be changed due to the change in software and technology no more supported.

All this would demand for a conservative re-qualification of all user inputs, that is all CIBUs for all users. Such a re-qualification should be done in the real conditions, which is with all users TRUE, and would require 6 months for the 250 connections: this is unfeasible. That's why a more pragmatic approach has been chosen: all users moving their electronic interface will have to declare their intervention (awareness raising campaign). For these changes, re-commissioning will be done and about 3months before restart, BIS experts will need to enter in test mode on all CIBUs for loop A and B; in addition, 1 week will be needed for attenuation measurements (budget is between 3 and 6 dB and the BIS experts will have to pass after intervention completion, to clean the connections).

Powering Interlock Controller

The most important changes are those related to R2E, namely the displacement of 9 PIC units (for UJ14/16/56) and new cables pulled, which will have to be qualified. A complete re-commissioning of those systems is needed, which will happen just before the powering tests.

More generally, all units will have to be individually tested, plus the PIC1 and PIC2 tests will have to be performed on the superconducting circuits.

A change will be applied in PVSS for the global protection mechanism (which prevents from powering any circuit in a powering subsector when the big circuits are in fault): it could be switched ON and OFF, allowing for more flexibility during the powering tests.

Also, a new solution will be deployed for the PIC-LASS interface. This is presently based on software (Laurette's interlock); a new PLC will be connected with the access system and a new FESA class will be created in SIS for the access conditions.

Finally, a singularity has to be reminded on the temperature interlock of the top part of the current leads: everywhere connected to the power converter, it will be connected to the PIC in RR53 (cabling issue) and will have to be tested.

Fast Magnet Current Monitor

The FMCM will not be changed in the LHC, but the displacement in UJ56, following the R2E works, will demand for the re-commissioning of the system in that location.

Cryogenics

All machines for cryogenics will be dismantled and then remounted during LS1; all valves and attenuators as well. The control software will be rewritten.

After all interventions, 2 months will be needed for the re-commissioning of the production, 4-5 weeks for the cool-down of all magnets and 1 week for the cryo-tuning. In addition, the cryogenics experts request for some time to tune their system for frequent ramps.

Manpower could be an issue, since only one third of people are left from the first commissioning in 2008.

Controls

All the interventions performed at control level (hardware and software) will require for dry runs as a fundamental re-validation.

MACHINE CHECKOUT

The objectives of the machine checkout, as defined in 2008, are:

- drive all relevant systems in a synchronized way through the standard operational sequence
- check functionality of the control system from the control room high level applications
- check the beam instrumentation acquisition chain
- check low synchronization
- check all equipment control functionality
- check machine protection and interlock systems.

The differences from 2008 are various, since the infrastructure is already present and the software tools are available and well developed. On the other side, a lot of changes will be done in LS1 and the planning of restart is compressed, with a late delivery of many systems.

Preliminary, regular meetings should be organized with the equipment owners by the machine checkout responsible, starting from spring ’14; individual system tests (equipment tests toward operational condition) should be performed by the equipment responsible and reported at these meetings.

On a later phase, functional tests will be performed depending on the advancement of the hardware commissioning and dry runs should be coordinated by OP with the equipment responsible starting from late summer ’14.

Powering tests and machine checkout will cohabit for the last period. BIS checks should be done one week before the end of powering tests and the real machine checkout test can only take place at the final phase when the powering tests will be completed and should last about 2-3 weeks.

CONCLUSIONS

It is a common believe that the one of 2014 will be a brand new commissioning. A lot of experience has been gained in the past years, but there will be two years without running the machine and a lot of changes will be done to hardware and software; in addition, there will be new people to train and the members of the operation team will be busy till the end on the consolidation activities.

The software will have to be ready from mid-2014.

Equipment tests and dry runs will be important to revalidate all systems, but they will be possible only from end of summer ’14 and will have to be well coordinated.

At least 3 weeks of real machine checkout will be needed once the powering tests are over.

ACKNOWLEDGMENT

The author would like to thank the following persons for the information and useful material provided for this paper: V. Baggiolini , V. Baglin, E. Carlier, S. Claudet , K. Fuchsberger, C. Garion , R. Giachino, R. Jones, P. Maesen, C. Martin, T. Mastoridis, B. Puccio, S. Redaelli, I. Romera, R. Schmidt, M. Solfaroli, H. Thiesen, J. Uythoven, D. Valuch, A. Verweij.

Wrap-up and prospects for post LS1 operations

M. Lamont, CERN, Geneva, Switzerland

Abstract

A terse summary of the workshop is presented in which an attempt is made to highlight issues with direct bearing on post LS1 operation. A preliminary attempt is made to estimate the potential post LS1 performance, outline the commissioning strategy and the potential limitations for run II.

INTRODUCTION

The 3 day workshop attempted a survey of the following areas with the emphasis very much on identifying issues pertinent to operations in the post LS1 era.

The sessions covered:

- Availability during 2012 : review of the year; availability; R2E; and machine protection.
- Performance of the nominal cycle and potential performance improvements for post-LS1. This section considers the implications of 7 TeV, possibly squeezing colliding beams, and the operation of LHCb and ALICE's spectrometers after LS1. Also included under this heading below are consideration of the presentations on: optics measurement and corrections; emittance growth through the cycle, and beam loss through the cycle.
- System performance was considered in a number of sessions and included critical reviews of:
  - beam instrumentation;
  - RF;
  - transverse damper system;
  - injection and beam dump systems;
  - vacuum;
  - cryogenics;
  - collimation;
  - beam loss monitors.
- Limitations: beam induced heating, electron cloud, instabilities, UFOs, and cryogenics.
- A look forward to 2015 and the experiments requirements; beams from injectors; the plans for restart; and the potential performance.

AVAILABILITY

Review of 2012 [1]

2012 was a production year at an increased beam energy of 4 TeV. The choice was made to continue to exploit 50 ns and run with a total number of bunches of around 1380. Based on the experience of 2011, the decision was taken to operate with tight collimator settings. The tighter collimator hierarchy shadows the inner triplet magnets more effectively allowing a more aggressive squeeze to a β^* of 0.6 m. The price to pay was increased sensitivity to orbit movements, particularly in the squeeze, and increased impedance. The latter having a clear effect on beam stability as expected.

2012 was a very long operational year and included the extension of the proton-proton run until December resulting in the shift of the proton-lead run to 2013. Integrated rates were healthy at around the 1 fb^{-1} per week level and this allowed a total for the year of about 23 fb^{-1} to be delivered to both ATLAS and CMS.

The 257 day run included around 200.5 days dedicated to proton-proton physics. 36.5% of the time was spent in Stable Beams with an overall Hübner factor of around 0.18. Cryogenics availability improved to 94.4 % during proton-proton operation. In terms of beam dumps above 450 GeV, QPS leads in occurrence and recovery time and in the number of SEUs suffered.

Table 1: LHC availability 2012

Mode	% of scheduled time
Access	14%
Setup	28%
Beam in	15%
Ramp and squeeze	8%
Stable beams	36%

Of note:

- Technical stops still disturb the flow, and we lose highly optimized conditions across the complex. This is less due to technical problems (although they do figure), and rather more due configuration changes (PS extraction modifications, ALICE etc.)
- Peak luminosity got up close to its peak pretty quickly. This was followed by a determined and long running attempts to improve peak performance. This was successful to a certain extent, but with little effect on integrated rates. Instabilities, discussed below, although never debilitating, were a reoccurring problem and

there were phases when they cut into operational efficiency. Essentially the 1.5e11 ppb per bunch limit was passed by a switch in octupole polarity and, perhaps, more importantly a large increase in chromaticity which at least partially negated the instability problems that had dogged the end of the squeeze and going into collisions.

Availability [2]

LHC is a critical asset with a CHF 5-6 billion capital cost and around 300 MCHF/year operating costs. Effective fault tracking and analysis for targeting weak points and system improvements could be considered mandatory. There are some short coming in this area and **a team needs to be give a mandate and resources to put in place an effective, robust solution for the re-start**. Note other initiatives with operational issue management being considered as part of the Maintenance Management project.

Although fault tracking maybe less than ideal it should be noted that the major issue up to now (R2E) has seen a coordinated approach and the individual system teams have targeted improvements based on their own experience (e.g. power converters, RF, QPS) with some success.

Radiation to Electronics (R2E) [3]

The success of this campaign is impressive. There were several shielding campaigns prior to the 2011 run including relocations on the fly and equipment upgrades. The 2011/12 Christmas stop saw some Early relocation and additional shielding and further equipment upgrades. This has resulted in the reduction of premature dumps from 12/fb^{-1} to 3/fb^{-1} in 2012, going a long way to helping the efficiency of integrated luminosity delivery.

The R2E-Project is aiming post LS1 for 0.3 premature dumps per fb^{-1} via a combination of: equipment relocations at 4 LHC Points; additional shielding; and critical system upgrades (QPS, FGC).

Machine Protection [4]

The machine protection system as a ensemble has worked well. There were around 1000 clean beam dumps performed in 2012 with 585 beam dumps above 450 GeV. There were some interesting probes of problem space in 2012 even with the system in its present state of maturity. Issues included: problem with the orbit feedback survey unit (OFSU); 12 V supply issues to the TSU of the LBDS; BSRT mirror deformation following beam induced heating; trasfer line collimator settings not tracking an optics change; and timing issues injecting the H9 low emittance beam; MD safety could do with some re-enforcement.

Full analysis and follow-up to be present at the MPP workshop in Annecy [5].

OPERATIONAL CYCLE

The present operational cycle, after a lot of effort, is well optimized and transfers reasonably well to 7 TeV [6]. The magnetic machine is well established and there is excellent understanding of linear and non-linear optics. Methods for the necessary optics measurement and correction have demonstrated excellent results.

Further optimization of the cycle are possible and those highlighted at the workshop include the following.

- A **combined ramp and squeeze** which would allow certainly allow time saving, but the proposal is not without operational risks and implications for systems such as orbit feedback and collimation.
- A partial **squeeze with colliding beams** which would provide Laudau damping and certainly help the instability issue that dogged the end of the squeeze in 2012.
- β^* **levelling** could also be important, particularly if 50 ns is needed as a long term operational solution. **Possible implementations have been/need to be explored further and an effective solution should be in place for post LS1.**
- The use of a lower β^* at injection.
- The possible used of Achromatic Telescope Scheme (ATS) optics.
- Squeezing more in one plane than the other (flat beams).
- Start with a lower ramp rate to ease the impact of heat load transients on the cryogenics system.
- Keep the collimators out for as long as possible in the ramp and squeeze avoiding the increased impedance until absolutely necessary.
- Non-synchronized collisions to avoid potential dangerous cancellation of beam-beam tune spread and effect of Landau octupoles.

2012 issues

Despite the impressive final integrated luminosity total there were a number of issues that hampered smooth operation in 2012, and lessons certainly deserved to be drawn from the experience.

- Enhanced satellites got blamed for a lot, perhaps unfairly. Improved diagnostics should be provided.
- Frequent re-steering of transfer lines was required. See the section on Injection below.
- The use of a tilted crossing angle in LHCb caused problems initially. Bringing all experiments into collisions at the same time did not help matters, and things fully stabilized when going into collisions in 1 & 5 was separated from that in 8.

- The **handling of all orbit corrector settings at the round in and round out at the matched points in the squeeze** requires a consistent approach.

- We were clearly sensitive to beam conditions from injectors with tight collimator settings, particularly during the squeeze. **Improved tail and scraping diagnostics are needed in the injectors.** There are systematic losses at end of the ramp as we transition to tight collimator settings. The extrapolation of this to 7 TeV needs further study and the exploration of possible strategies to alleviate potential limitations at higher energies.

Spectrometers

The switch of the IR8 crossing angle to the vertical plane at injection, while being elegant solution (for 25 ns operation), implies global change of aperture limit to point 8 [7]. The implications are to be fully explored. The lack of a possibility to rotate the beam screen during LS1 has been confirmed.

Emittance blow-up [8]

- It is still very difficult to measure emittances and emittance blow-up. **Details of required improvements to beam diagnostics were detailed - need reliable and accurate transverse profile measurement systems after LS1.** We still not sure about the wire scanner results - issues with calibration; emittances from luminosity results are the most reliable.

- Overall the emittance blow-up situation in 2012 was similar to 2011 with significant blow-up from injection and through the ramp. It is also observed, sometimes, at the end of squeeze.

- Among the clear sources are IBS and 50 Hz noise - one should be able to quantify these effects. We are sitting on the 50 hZ line with the horizontal tune at injection and in the ramp.

- Absolute emittance growth through cycle is between 0.7 and 1 microns based on the convoluted, averaged emittance from luminosity.

- Any potential mitigation like RF batch-by-batch blow-up and higher transverse damper gain have not yet lead to significant improvement of emittance blow-up on the normal injection timescale.

- It is curious that the low emittances delivered by the Q20 optics end up at the same values as the Q26 optics going into collisions.

Optics and dynamic aperture[9]

LHC achieved record low β-beating for hadron colliders and many other first achievements in 2012:

- dynamic aperture measurement at injection;

- chromatic coupling correction;

- triplet non-linear correction;

- measurement of amplitude detuning with AC dipoles.

The linear and non-linear dynamics is now very well understood.

Suggested modifications to the cycle included: injecting into a β^* of 7 m with collisions tunes. The combined ramp and squeeze and squeezing with colliding beams will come with a price and dynamic measurements in these configurations will need improved tools. The final β^* has yet to be decided but triplet non-linear correctors are needed for dynamic aperture and/or Landau damping (but watch the dynamic aperture in the latter case).

SYSTEM PERFORMANCE

Analysis of systems issues from an OP perspective [10]

In general we have seen good to very good performance across the board. System are now mature. Outstanding issues have been identified, and improvements and upgrades are planned. One can imagine these coming back post LS1 in good shape with appropriate time dedicated to recommissioning and tests.

Outstanding issues of note include:

- **The need for fully reliable tune measurement and feedback**

- **Orbit feedback system issues to be resolved.** Clearly a critical system and instrumental in the successful commissioning, however 21 dumps were assigned to OFC/OFSU problem in 2012. Besides the obvious requirements of stability, staying on through the cycle etc. better release management and testing and better information flow is requested.

- **Interlocked BPMs** All sorts of problem here related to their sensitivity to different bunch currents. Situation has to be resolved post LS1.

- Beam size measurement systems (BSRT, BGI) deserved fully operational applications in the CCC.

- Improved instability observation tools are required.

- Reduce the time spent steering the lines and address the cause of the problem: orbit variations in the SPS, ripple in the SPS extraction septa.

- Injection kickers and associated systems often need expert counselling and input. This related to vacuum activity, electron cloud, breakdown etc. Clear need to be attentive but difficult to track changes in limits etc.

- RF: interlock diagnostics; phase acquisition per batch; faster BQM; phase/amplitude noise for each klystron
- ADT settings management: less dependency on experts is to be encouraged. But again, this is a sensitive system with potential damage potential, any shift of functionality to operations has to be accompanied by appropriate safe guards.

Regarding Control System and data management, 4 pages of issues, requirements and proposed improvements were presented. Full follow-up is required.

ADT [11]

The transverse damper system has reached maturity with impressive performance through the cycle and a host of novel functionality. This has included resolution of outstanding issues related to the interplay with the BBQ by the use of gating out a few bunch.

For settings management the ADT team worries about operational rigour and the safety of their equipment!

There are lot more plans for improved and additional functionality and ADT2 post LS2 will require some concerted re-commissioning.

Will we keep the gated bunches? The consensus at the workshop was yes we will. The requirements of tune control etc. will only become more rigorous as the total beam intensity increases and this approach certainly has proved its utility.

Beam instrumentation [12]

- DOROS looking very encouraging and would certainly address the IR requirements. The triplet BPMs thus equipped could certainly help luminosity stability with β^* levelling.
- The interlocked BPMS system should really improve its intensity dependence behaviour.
- There were a number of issues with the orbit feedback system and a full orbit feedback review is incoming.
- Abort gap monitoring needs to be revisited from a machine protection perspective.
- Analysis of the source of 50 Hz lines and potential mitigation needs to be pursued.
- Beam size measurements: follow-up is required across the board.

RF [13]

The key issues here is the preparation for higher beam currents post LS1. At least 200 kW forward power will be required at nominal intensity, and to deal with this the importance of cavity voltage set-point modulation for 25 ns operation was stressed.

Module 1B2 to be replaced because of an underperforming cavity.

The importance of longitudinal bunch distribution when considering beam induced heating was stressed.

Injection [14]

- Reproducibility of transfer lines compromised by: MSE current ripple and flat-top orbit variation in SPS. To be addressed.
- A certain amount of intellectual rigour is required by operations. Conclusions from surmise are to be avoided. It wasnt always the satellites; correct for the right problem; could be helped by improved diagnostics.
- The sunglasses scheme and the use of LICs is to be followed-up.
- There were many well documented issues with the injection kickers heating and flash-overs - new chambers across the board post LS1.
- The TDI has also experienced a number of well documented problems. Even after refurbishment during LS1, will they remain a risk in the medium term?

Beam dump system [14]

- New TCDQs to be installed.
- Common mode failure on 12V line has been addressed, but one might worry about increasing probability of asynchronous dump with the additional interlocks.
- There will be higher voltages on the switches at 6.5 TeV and thus an increased risk of erratics.

Controls [15]

Major infrastructure upgrades are planned and commissioning time will be required. Upgrade team should remember the requirements of ongoing TI monitoring etc.

- Timing/cycle management improvements required and incoming with coherent approach across the complex required.
- Improved data analysis tools are required.
- We have learnt a lot, we know how to operate the machine, and the question beggedis : can we do it better? Operations should consider the coherency of the high level approach after 5 years of sometimes ad hoc development. A review should be organized.

LIMITATIONS

Instabilities [16]

Instabilities were an interesting problem that dogged operations through 2012. Although never debilitating there were phases when they cut into operational efficiency. Although it should be noted that these problems paralleled a gentle push in bunch intensity with the peak going into stable beams reaching around 1.7e11 ppb i.e. ultimate bunch intensity. Cofactors included increased impedance from tight collimator settings; smaller than nominal emittance; and operation with low chromaticity during the first half of the run.

Of note:

- The first period was dogged by occassional beam loss provoked by instabilities that occured at the end of the squeeze and while going into collision.
- Switch of octupole polarity at start of August. To stabilize the beam during the squeeze, it proved necessary to push the chromaticity to the order 15, and increase the Landau damping octupoles to near their maximum value. Even this didn't fully solve the problem and instabilities were still observed (B1V) on certain bunches at the end of the squeeze with associated emittance blow-up.

Three main classes of instabilities were observed:

- The so-called snowflakes phenomenon, individual bunch drop-out - extremely bad lifetime for some seconds, stabilizing at much reduced bunch intensity. This was seen on the so-called IP8 private bunches which experienced luminosity levelling motivated offset collisions.
- During the collapse of separation bumps. One cause was ending with too large residual separation which provoked coherent beam-beam instabilites. Another possibility was interference between long range beam-beam tune spread and octupole detuning resulting in the loss of Landau damping.
- Instabilites at the end of squeeze were generally on a few bunches of one beam. The bunches affected tended to be a the end of batches. Folling the flip of the octupole sign, the instability moved to beam 1 vertical. This appeared to be a two beam effects and long-range beam-beam and electron cloud have been proposed as co-factors.

Impedance [17]

This is still a bit of a mystery, we observe ≈3 times more impedance than expected at 450 GeV and ≈2 times more than expected at 4 TeV. For post LS1 operation, performance can be sacrificed if required by drawing on impedance dependence on collimators settings: nominal gives a +50% increase in impedance tight settings +10%; with relaxed settings buying a 25% reduction.

Beam induced heating [18]

Beam induced heating will remain an issue, and the possible guilty parties were clearly enumerated. In particular the upgrade of TDI should be pursued - this foreseen for post-LS2. The maximum bunch length should be pursued compatible with maximum extension of the luminous region - 1.35/1.4 ns seems to be within reach.

Scrubbing [19]

There were 3.5 days of scrubbing with 25 ns beams at 450 GeV between 6 - 9 Dec. 2012. The tests saw regular filling of the ring with up to 2748 bunches with a total intensity per beam of up to 2.7×10^{14}. Overall there was very good efficiency with the injection rate determined by MKI vacuum interlocks (in the beginning) and by time required by the cryogenic system to adapt to the increasing heat load (mainly in stand-alone magnets).

Scrubbing effects in the arcs saw quite rapid conditioning observed in the first stages. The SEY evolution significantly slows down during the last scrubbing fills (more than expected by estimates from lab. measurements and simulations).

There is a potential change of mode of operation with 25 ns. An electron cloud free environment after scrubbing at 450 GeV seem not be reachable in acceptable time. Operation with high heat load and electron cloud density (with blow-up) seems to be unavoidable with a corresponding slow intensity ramp-up. In 2015 following the warm-up and opening of the entire ring to atmosphere, the SEY and vacuum conditions will be reset and initial re-conditioning will be required. **It is anticipated that we will need to start with 50 ns and only later to move to 25 ns to recover vacuum, cryogenics, UFOs conditions were used in 2012.**

Cryogenics [20]

Scaling with the 2015 beam parameters shows sufficient margin with respect to local and global cooling limitations by implementing the following consolidations:

- consolidation of the copper braid configuration on 6/8 IT (planned for LS1);
- increase of the maximum flow coefficient of the BS control valve of the standalone magnets (seat and poppet exchange) - compatible with e-cloud deposition of 1.6 W/m per aperture - to be planned for LS1;
- however, a triplet cryogenic limit on luminosity of around 1.7e34 $cm^{-1}s^{-2}$ ($\pm$20%) is noted. This due to the reduced diameter heat exchanger pipes installed following the first triplet incident during installation.

The 25 ns beam scrubbing run in December 2012 has identified or confirmed: a tricky transient at the start of the energy ramp; and a discrepancy (factor 2) between the cryogenic heat load measurement (typically 20 kW) and the RF power (typically 40 kW).

Vacuum[21]

Subjects covered include the integrity of the protection functionality; beam dumps in 2012; interventions in 2012; and the outlook for 2015.

Of note:

- all RF non-conformities to be repaired during LS1;
- vacuum interlocks required for integrity of the vacuum system (e.g. NEG coating) have been relaxed (classed as a non-conformity);
- vacuum interventions need a lot of care to minimize unacceptable conditions after the interventions;
- no particular issues for scrubbing, again it is noted than the SEY and vacuum conditions in general will be reset during LS1.

Initial conditioning will be required post LS1. It was argued that it would be better to start with 50 ns.

BLM thresholds [22]

- Modified BLM layout is essential, otherwise thresholds to prevent quenches from UFOs in the dipole magnets are too low
- Risk of magnet quenching must be accepted at the start. We need to plan for beam induced quenches! BLM thresholds in arc to be set above expected quench threshold (as proposed in Chamonix 2012 for 2012, but not done)
- Can we use different algorithms to detect UFOs from BLMs? E.g. validation time as for QPS? Quench tests gave more insight and will be important for establishing thresholds.
- Noise: optimistic that BI will solve this issue.
- Triplets: IR8 will be in the shadow of 1 and 5.

Cleaning and collimation operation [23]

We now have excellent performance and fast setting up and validation. The TCL collimators have proved to reduce the effects of luminosity debris. Further improvement is expected with button equipped TCTs.

Different scenarios for collimation settings were proposed - see Belen's talk for details [23].

- Pessimistic scenario (larger emittance): β^* = 70 cm at 25 ns or β^* = 57 cm at 50 ns
- Optimistic scenario (H9 emittance) β^* = 37 cm at 25 ns or β^* = 30 cm at 50 ns

Quench tests will provide more input. We are encouraged to start with a relaxed approach in 2015.

UFOs [24]

UFOs were presented as a potential show-stopper for 25 ns at 6.5 TeV. There will be a tenfold increase in rate and the UFOs will be harder. However it is noted that there was no increase in low total intensity 25 ns fills following the scrubbing run.

- UFO "scrubbing": how does it work? What are the relevant parameters?
- 91 arc UFOs in 2012 would have lead to a dump at 7 TeV.
- De-conditioning to be expected after LS1 and an operational scenario is to be developed. For example do we: start with lower energy and/or 50 ns beam for UFO conditioning?
- Other options include increasing BLM thresholds and optimizing the BLM spatial distribution. There were interesting results from the quench tests in this regard.

POST LS1

Physics requirements

- **25 ns proton-proton operation is a strong request of all the experiments.** In fact, they would prefer not to have any significant luminosity with 50 ns (different triggers, out of time pile-up, Monte Carlos etc.). Significant here is of the order 1 fb^{-1}. 25 ns provides a cleaner environment for precision physics (trigger and reconstruction efficiencies, resolution) and is less demanding in terms of resources (online and offline computing).
- The experiments accept that the commissioning period for 25 ns operation may be longer than usual if 50 ns not used as a stepping stone but are prepared to accept the overhead.
- **Extended 50 ns running is only an option in case of major show-stoppers.**
- Optimization of other parameters (bunch length, crossing angles) is accepted as needed, but with a clear demand for stable conditions.
- ALICE proton-proton operation with 25 ns needs further studies.
- Special runs program (TOTEM, ALFA, high β^*, LHCf) will be similar to 2012.
- A heavy ion run at 13Z TeV is foreseen in 2015.

Table 2: Beam parameters for various bunch spacings at exit of SPS.

Scheme	Nb	ppb 10^{11}	emittance exit SPS [μm]	emittance into collisions [μm]
25 ns nominal	2760	1.15	2.8	3.75
25 ns BCMS	2760	1.15	1.4	1.9
50 ns	1380	1.65	1.7	2.3
50 ns BCMS	2760	1.6	1.2	1.6

Beam from the injectors LS1 to LS2 [25]

The bunch spacings and associated performance on offer from the injectors between LS1 and LS2 are shown in table 2. 50 ns proved a good choice in 2011 and 2012 opening the way to an increased number of bunches and the excellent performance in terms of emittance and bunch intensity. The best that was taken into collisions in 2012 was around 1.7 $\times 10^{11}$ protons per bunch with an emittance of around 2.5 μm.

Further imaginative developments on the PS side have lead to the creation of the so-called BCMS (Batch Compression and (bunch) Merging and (bunch) Splittings) scheme. This scheme opens the way to above nominal performance in the post LS1 era.

Table 3: Approximate breakdown of LHC's 2015 schedule.

Activity	Time assigned
Recovery, machine check-out etc.	32
Commissioning with beam	56
Machine development	22
Technical stops	15
Scrubbing run	14
Technical stop recovery	6
Proton physics running inc. ramp-up	160
Special physics runs	7
Ion run setup	4
Ion physics run	24
Christmas 2015 technical stop	14
Contingency	7

Post LS1 operations

β^* reach at 6.5 TeV As discussed above different scenarios for collimation settings were proposed: pessimistic scenario (larger emittance): β^* = 70 cm at 25 ns or β^* = 57 cm at 50 ns; optimistic scenario (BCMS) β^* = 37 cm at 25 ns β^* = 30 cm at 50 ns. Further optimization via the use of flat beams were also considered. An average of around 40 cm is assumed in the performance estimates presented below.

Schedule 2015 2015 will be a re-commissioning, re-conditioning year. Following initial commissioning with beam, the intensity and performance ramp-up will take longer than it did in 2011 and 2012. It will also take some time to flush out inevitable issues and we should foresee availability also taking a hit.

In the estimates presented below, 160 days for proton physics are assumed including the ramp-up in beam intensity.

The potential performance for four scenarios are shown in table 4. Assumptions therein are: Assumptions:

- 6.5 TeV
- 1.1 ns bunch length
- 150 days proton physics, HF = 0.2
- 85 mb visible cross-section

It should be noted that the 50 ns options necessitate the use of a levelling scheme of some sort, as yet unproven operationally.

Summarizing the contents of table 4:

- Nominal 25 ns gives more-or-less nominal luminosity as one might expect.
- BCMS 25 ns gives a healthy 1.6e34 cm^{-2}s^{-1}, peak mean mu of around 50 with about 83% nominal intensity
- What has become nominal 50 ns gives a virtual luminosity of 1.6e34 cm^{-2}s^{-1} with a pile-up of over 70 levelling mandatory
- BCM 50 ns gives a virtual luminosity of 2.3e34 cm^{-2}s^{-1} with a pile-up of over 100 levelling even more mandatory

Cryogenics: cool-down and availability [26] We know now how to operate the LHC cryogenic system with a correct availability for beams of 95%. All identified repairs-maintenance-consolidations are being prepared to be done in 2013. It should help! Complete cryogenics re-commissioning is foreseen before scheduled date for cool-down of corresponding sector This will help the (two thirds of the team new) cryogenics operation team to get up its new learning curve while preparing for energies greater

Table 4: Post LS1 performance estimates - usual warnings apply

Scheme	Nb	ppb 10^{11}	beta *	emittance [μm]	peak	pile-up	Int.
25 ns nominal	2760	1.15	55/43/189	3.75	9.3e33	25	≈24
25 ns BCMS	2760	1.15	45/43/149	1.9	1.7e34	52	≈45
50 ns	1380	1.65	42/43/136	2.3	1.6e34	87	≈40
50 ns BCMS	2760	1.6	38/43/115	1.6	2.3e34	138	≈40

than 6 TeV. Target availability for next physics run is in the nineties.

2015 strategy The following outline schedule was presented for discussion.

- 2015 starts with system tests in parallel with hardware commissioning. Dry runs in parallel.
- Machine checkout
- Low intensity commissioning of full cycle for about 2 months, including first pass machine protection commissioning and validation in parallel with system commissioning.
- First stable beams, low number of bunches, low luminosity.
- Scrubbing for 6 to 8 days will be required early on (partially with 25 ns).
- Intensity ramp-up for 1 to 2 months. Commissioning with higher intensity continued: system commissioning (instrumentation, RF, TFB etc.), injection, machine protection, instrumentation Variables at this stage: bunch intensity, number of bunches, emittance. Would imagine passing straight to 50 ns and then stepping up in number of batches as previously.
- 50 ns operation (at pile-up limit): characterize vacuum, heat load, electron cloud, losses, instabilities, UFOs, impedance Nominal bunch intensity, 40 cm, 2.3 microns gives 9e33 $cm^{-2}s^{-1}$ and a pile-up of around 40.
- Thereafter: 1 week scrubbing for 25 ns, say 1 week to get 25 ns operational (if beta* and crossing angles are changed), intensity ramp up with 25 ns with further scrubbing as required. 50 ns held in reserve in case of serious problems with 25 ns.

CONCLUSIONS

Good year. Availability pretty good considering. We're enjoying the fruits of targeted improvements. Fault tracking could be better. Machine now magnetically, optically, operationally well understood. 6.5 TeV sequence shouldnt pose too many problems. Some new functionality to be developed, options to be explored. System performance has been generally good to excellent with issues identified and being addressed. Limitations well studied, well understood and quantified with still some potential implications for post LS1 operation. Imagine restarting post LS1 with 50 ns before moving to 25 ns. A non e-cloud free environment to be accepted at least initially, the strategy to be fully defined.

ACKNOWLEDGEMENTS

Organization: major credit to Malika Meddahi, Sylvia Dubourg, Brennan Goddard, Pierre Charrue for all their efforts. Session chairs: Jan Uythoven, Jorg Wenninger, Rhodri Jones, Gianluigi Arduini, Rudiger Schmidt and their scientific secretaries.

Brilliant job by the speakers, and excellent set of talks, for more details please see the originals at the workshop indico page.

And a big, big, big thank you for joining us on Wednesday evening: Fabiola Gianotti Paolo Giubellino Joao Varela Si-mone Giani Pierluigi Campana.

REFERENCES

[1] A. Macpherson, Introduction and review of the year, these proceedings.

[2] B. Todd, Step back on availability , these proceedings.

[3] G. Spiezia ,R2E Experience and Outlook, these proceedings.

[4] D. Wollmann, Machine protection issues, these proceedings.

[5] MPP Workshop March 2013, Annecy: indico.cern.ch confId=227895.

[6] M. Solfaroli, Cycles at 4 TeV and 7 TeV, these proceedings.

[7] B. Holzer, Optimising spectrometers operation, these proceedings.

[8] M. Kuhn, Emittance preservation, these proceedings.

[9] R. Tomas Garcia, Optics and dynamic aperture at 4 at 6.5 TeV, these proceedings.

[10] D. Jacquet, Beam Based Systems and Control: what we want, these proceedings.

[11] D. Valuch, Transverse Damper system, these proceedings.

[12] T. Lefevre, Orbit and tune measurement and feedback, these proceedings.

[13] T. Mastoridis, RF system, these proceedings.

[14] C. Bracco, Injection & dump systems, these proceedings.

[15] S. Jensen, Controls Software, these proceedings.

[16] E. Metral, Review of the instabilities observed during the 2012 run and actions taken, these proceedings.

[17] N. Mounet, Beam stability with separated beams at 6.5 TeV , these proceedings.

[18] B. Salvant, Beam induced RF heating, these proceedings.

[19] G. Iadarola, Electron Cloud and Scrubbing, these proceedings.

[20] L. Tavian, Cryogenics, these proceedings.

[21] G. Lanza, Vacuum, these proceedings.

[22] E. Nebot Del Busto, BLM thresholds - past experience, these proceedings.

[23] B. Salvachua Ferrando, Cleaning and collimator operation - outlook, these proceedings.

[24] T. Baer, UFOs, these proceedings.

[25] R. Steerenberg, Post LS1 25 ns and 50 ns options from the injectors, these proceedings.

[26] Serge Claudet, Cool-down: cryogenics strategy, these proceedings.

Authors Index

V

W

Z